Thermo-responsive Surfaces

For Enzyme Free

Mammalian Cell Culture

By Sabrina Dey, MPharm (Hons)

A thesis submitted to the University of Nottingham for the

degree of Doctor of Philosophy

June 2010

The University of Nottingham

Table of Contents

Table of Figures

Chapter 1: General Introduction

Chapter 2: Generation of Variable Adhesion Surfaces

methycrylate-*co*-oligo(ethyleneglycol) methacrylate using a 'grafting from' ATRP approach.

Figure 2.5. Schematic diagram of plasma reactor used for these experiments.

Figure 2.6. Chemical structure for allyl alcohol.

Figure 2.7. XPS survey scan of a cleaned glass substrate.

Figure 2.8. XPS wide scan spectra of plasma polymerised (allyl-alcohol) deposited at power = 5W (in red) and after treatment with 2 bromoisobutyryl bromide (in black).

Figure 2.9. XPS wide scan spectra of plasma polymerised allyl-alcohol deposited at power = 10W (in red) and after treatment with 2 bromoisobutyryl bromide (in black).

Figure 2.10. XPS wide scan spectra of plasma polymerised poly (allyl-alcohol) deposited at power = 15W (in red) and after treatment with 2 bromoisobutyryl bromide (in black).

Figure 2.11. XPS wide scan spectra of plasma polymerised poly (allyl-alcohol) deposited at power = 20W (in red) and after treatment with 2 bromoisobutyryl bromide (in black).

Figure 2.12. XPS wide scan spectra of plasma polymerised poly (allyl-alcohol) deposited at power = 50W (in red) and after treatment with 2 bromoisobutyryl bromide (in black).

Figure 2.13. XPS wide scan spectra of plasma polymerised poly (allyl-alcohol) deposited at power = 75W (in red) and after treatment with 2 bromoisobutyryl bromide (in black).

Figure 2.14. XPS wide scan spectra of plasma polymerised poly (allyl-alcohol) deposited at power = 100W (in red) and after treatment with 2 bromoisobutyryl bromide (in black).

Figure 2.15. The elemental composition determined by XPS analysis of plasma polymerised ally alcohol versus plasma input power.

Figure 2.16. C1s core level high resolution spectra recorded for plasma polymerised allyl alcohol (**A.**5W, **B.**20W, **C.**50W, **D.**100W) representing the following main peaks; **C-C/C-H** (polymer backbone), **C-OH/R** (alcohol/ether), **O-C-O/C=O** and **C (=O) OX**.

Figure 2.17. A. The relationship of the C1s and Si2p intensities. **B.** The carbon overlayer calculated thickness (dc in nm) derived from equation 1 against the concentration of the Br 3d.

Figure 2.18. A. XPS wide scan of poly (MEO_2MA-co-OEGMA). **B.** C1s core level spectra recorded after growth from the surface of poly (MEO_2MA-co-OEGMA) brushes via ATRP.

Figure 2.19. Positive ion ToF-SIMS spectra of **A.** cleaned glass (control), **B.** ppAAl, **C.** ppAAl-2-bromo-isobutyrate surfaces and **D.** Poly (MEO_2MA-co-OEGMA) grafted surfaces.

Figure 2.20. Negative ion ToF-SIMS spectra of **A.** Cleaned glass (control), **B.** ppAAl coated glass, **C.** ppAAl-2-bromo-isobutyrate surfaces and **D.** Poly (MEO_2MA-co-OEGMA) grafted surfaces.

Figure 2.21. Topographical images for positive (top) and negative (bottom) ions of the cleaned glass.

Figure 2.22. Topographical images for positive (top) and negative (bottom) ions of the ppAAl substrates.

cells adhere and spread, and they detach when the temperature is lowered to 20°C (below LCST).

Figure 3.2. XPS wide scan of poly (MEO_2MA-co-OEGMA) before (purple) and after UV sterilisation (black).

Figure 3.3. Representative images of mouse 3T3 fibroblast cell adhesion and subsequent detachment when cultured poly (MEO_2MA-co-OEGMA) surfaces.

Figure 3.4. Surface area covered by cell, expressed as a percentage of the total surface area, following attachment (24, 48, 72, 96 hr at 37°C) and detachment (1 and 2 hr at 20°C).

Figure 3.5. WCA measurements of poly (MEO_2MA-co-OEGMA) surface after three temperature cycles.

Figure 3.6. Growth curve for mouse 3T3 fibroblasts which they were serially passaged, over 10 passages, using trypsin and temperature from TCPS or poly (MEO_2MA-co-OEGMA) respectively.

Figure 3.7. Representative images illustrating the cellular morphology of 3T3 fibroblasts on TCPS (left column) and on poly (MEO_2MA-co-OEGMA) following serial passaging over 10 passages.

Figure 3.8. Representative fluorescent images of Phalloidin stained Actin of 3T3 fibroblasts after passage 10 following culture on TCPS (right) and poly (MEO_2MA-co-OEGMA). Actin filaments are shown in red and the nuclei of cells are in blue.

Chapter 4: Culture and passage of mouse embryonic stem cells from thermo-reversible poly (MEO_2MA-co-OEGMA) surfaces

Figure 4.1. Schematic diagram of the different incubation conditions for fibronectin adsorption on poly (MEO_2MA-co-OEGMA) surfaces.

Figure 4.2. Representative images for mESC adhesion response studies on untreated poly (MEO_2MA-co-OEGMA) surfaces and after different pre-conditioning treatments to the surface following culture for 96 hr at 37°C.

Figure 4.3. Representative images of mESC attachment (37°C; 96 hr) and detachment (20°C; 2 hr) respectively on poly (MEO_2MA-co-OEGMA)/fibronectin (200 μg/mL) surfaces.

Figure 4.4. Surface area, expressed as a percentage of the total surface area, covered by cells at several time intervals over a total culture time of 96 hr at 37°C on poly (MEO_2MA-co-OEGMA) surfaces previously incubated with fibronectin using method 1, method 2 and method 3.

Figure 4.5. Representative images of mESCs on poly (MEO_2MA-co-OEGMA) (labelled as 'The surface' on the figure) surfaces previously incubated with different concentrations of fibronectin. Images are shown over a 72 hr culture period.

Figure 4.6. Percentage surface area covered by cells on poly (MEO_2MA-co-OEGMA) surfaces preincubated with various concentrations of fibroenctin (at 37°C for 18 hrs) compared with gelatine coated TCPS (control).

Figure 4.7. Representative images for detachment assay after 2 hr at 20°C of mESCs from poly (MEO_2MA-co-OEGMA) preincubated with different concentrations of fibronectin previously adsorbed at 37°C for 18 hr.

Figure 4.8. Representative images of mESCs cultured on poly (MEO_2MA-co-OEGMA) treated with 5 μg/ml fibronectin and gelatine coated TCPS as the control.

Figure 4.9. mESCs attachment to gelatine and poly (MEO_2MA-co-OEGMA) brushes preincubated with 5 μg/ml of fibronectin (FN) after 72 hrs at 37°C for 9 samples from 3 different batches.

Figure 4.10. A. Alamar blue fluorescence intensity at 560nm during the cell culture time up to 72hr. **B.** Cell number estimated from the calibration curve at the time point (24, 48 and 72 hrs) for cells cultured on gelatine coated TCPS and poly (MEO_2MA-co-OEGMA)/fibronectin.

Figure 4.11. Representative images of mESC detachment at different temperatures 4°C, 10°C and 20°C. Scale bars=**100 μm** for all images.

Figure 4.12. Percentage surface area covered by cells following detachment at different temperatures 4°C, 10°C and 20°C (2hr).

Figure 4.13. Representative images for the re-attachment studies after 24 hrs using detached cells from poly (MEO_2MA-co-OEGMA)/fibronectin at different temperatures (4°C, 10°C and 20°C).

Figure 4.14. Representative fluorescence microscopy images of surfaces immuno-stained with fluorescent antibodies to fibronectin after incubation of fibronectin with a poly (MEO_2MA-co-OEGMA) thermo-responsive surface at 37°C for 18 hrs and after detachment of cells at 10°C for 2 hrs.

Figure 4.15. Average fluorescence intensities of Poly (MEO_2MA-co-OEGMA) surfaces following incubation with fibronectin at 37°C for 18 hrs, washing with warm PBS and immuno-staining with a FITC-anti fibronectin antibody. Error bars represent standard deviation for three samples.

Figure 4.16. Wide scan of a representative poly (MEO_2MA-co-OEGMA) thermo-responsive surface preincubated with 5 μg/ml fibronectin.

Figure 4.17. Growth curve of mESCs which they were serially trypsin and temperature passaged from TCPS or poly (MEO_2MA-co-OEGMA) respectively.

Figure 4.18. Representative images illustrating morphology of mESCs on gelatine coated TCPS and on poly (MEO_2MA-co-OEGMA)/fibronectin surfaces over 10 passages. Black arrows show the fibroblast shape of mESC at passage 5 and 10 compared to the colonies grown on gelatine coated TCPS.

Figure 4.19. RT-PCR images data for mESCs cultured on gelatine (control) and on poly (MEO2MA-co-OEGMA)/fibronectin thermo-responsive surfaces. **1:** GAPDH. **2:** OCT-4. **3:** Brachyury (mesoderm). **4:** Nestin (ectoderm). **5:** GATA-4 (endoderm).

Figure 4.20. Representative images of Oct-3/4 immuno-staining (LHS;green) of mESCs at passage 1, 5 and 10. Blue staining (RHS) is DAPI staining to identify cell nuclei.

Figure 4.21. Representative images of immuno-staining for the three differentiation markers (green) at passage 5. Blue staining (RHS) is DAPI staining to identify cell nuclei.

Figure 4.22. Representative images for Immuno-stained (LHS; green) GATA4, Brachyury and Nestin for cells collected after passage 10. Blue staining (RHS) is DAPI staining to identify cell nuclei.

Figure 4.23. Representative images for Immuno-stained (LHS; green) GATA4, Brachyury and Nestin for cells collected after passage 1, 5 and 10 for gelatine (control).

Scheme 2.1. Mechanism of metal complex-mediated Atom Transfer Radical Polymerisation (ATRP). $\mathbf{M_t^n}$**:** transition metal; **L:** complexing ligand; **R:** Polymer chain; **X:** Br or Cl

Equation 2.1. dc: thickness, **Lc(Ec)**: the effective attenuation length at the energy of the C1s photoelectrons of energy **Ec** in the top layer (core level) (=3.6nm)(1), **θ**: take off angle, **Ic**: the intensity of the C1s core level, **Ic∞**: The intensity of carbon determined from the intercept with the y-axis of a plot of C1s (from overlayer of the polymer) against Si2p (from glass).

Chapter 5: The synthesis of 4-pentynoic acid- AGPRGEHyPG to promote embryonic stem cell adhesion to the thermo-responsive surfaces

Figure 5.1. Schematic representation of mESCs cultured on fibronectin coated polymer brushes through the interaction with the RGD motif to aid their cell adhesion (Chapter 4).

Figure 5.2. Schematic representation of the combined ATRP and click chemistry to attach the gelatine peptide to the thermo-responsive surface.

Figure 5.3. MALDI-TOF mass spectrum of the main peak of the purified component (AGPRGEHyPG) with a molecular weight of 836.5 m/z.

Figure 5.4. Reverse-phase HPLC analysis of 4-pentynoic acid modified AGPRGEHyPG following purification of the main component peak.

Figure 5.5. Wide XPS scans for different treatments to the surface. **1.** (green) PAAl-*g*-2-bromoisobutyrate. **2.** (blue) PAAl-*g*-poly (MEO_2MA-co-OEGMA)-Br. **3.** (purple) PAAl-*g*-poly (MEO_2MA-co-OEGMA)-N_3. **4.** (pink) Poly (MEO_2MA-co-OEGMA)-g-propargyl alcohol. **5.** (red) Poly (MEO_2MA-co-OEGMA)-g-4-pentynoic acid- AGPRGEHyPG.

Figure 5.6. XPS wide scan spectra for TCPS (control; black) and TCPS coated with AGPRGEHyPG peptide sequence.

Figure 5.7. Representative images of mESC cells cultured on A: gelatine (control) and B: AGPRGEHyPG coated TCPS.

Figure 5.6. Representative phase contrast images showing mESCs adherence to gelatine (**A**). **B** shows the phase contrast images for Poly (MEO_2MA-co-OEGMA)-g-4-pentynoic acid- AGPRGEHyPG.

Figure 5.7. The surface area estimated for cells covering the surface of TCPS coated gelatine; TCPS coated AGPRGEHyPG and Poly (MEO_2MA-co-OEGMA)-g-4-pentynoic acid- AGPRGEHyPG surfaces. N=4 (total of 4 samples).

List of tables

Chapter 2: Generation of Variable Adhesion Surfaces

Chapter 3: Evaluation of variable bio-adhesion surfaces using mouse 3T3 fibroblasts as a model mammalian cell type.

Chapter 4: Culture and passage of mouse embryonic stem cells from thermo-reversible poly (MEO_2MA-co-OEGMA) surfaces

Chapter 5: The synthesis of 4-pentynoic acid- AGPRGEHyPG to promote embryonic stem cell adhesion to the thermo-responsive surfaces

acid- AGPRGEHyPG (5). The mean and standard deviation represents three points on each surface.

Table 5.2. WCA shown for PAAl-*g*-2-bromoisobutyrate (control) and PAAl-*g*-poly (MEO_2MA-co-OEGMA) ATRP and after the click coupling with 4-pentynoic acid- AGPRGEHyPG above and below the LCST.

Table 5.3. Elemental composition determined by XPS for TCPS and TCPS coated AGPRGEHyPG.

Acknowledgments

I would like to sincerely thank my supervisors, Dr Felicity Rose, Professor Cameron Alexander, Dr Barrie Kellam for their constructive criticism and support during the course of this PhD. I also thank Dr Morgan Alexander for his useful discussions regarding plasma polymerisation and XPS analysis. Many thanks go to my internal examiner, Professor Kevin Shakesheff for his criticism during my first and second year viva. I am also grateful to the Algerian government for the funding of this project. Thanks to Turrill Carol for organising my meetings as well as her support.

Thanks to all members of the Tissue Engineering and Drug Delivery groups from 2006 to 2010 for being great teams, especially Mischa and Ruby for their training on plasma polymerisation and cell culture, George Pasparakis for his help with the polymerisation as well as long discussions and criticism. Many thanks go to the technical staff in the School of Pharmacy especially Mrs Teresa Marshall and Christine Grainger-Boultby. Thanks to Emily Smith for her XPS training and guidance throughout this project. I also thank Professor Chen for his training on AFM and useful discussions. Many thanks go to Dr David Scurr for his help with ToF-SIMS analysis. Thanks to Aram Omer, Johannes Magnusson for their friendship and support particularly for accompanying me in the laboratory at late hours of the day. Thanks to Dr Cristina Tufarelli for providing mESCs and Kevin Bailey for his help with the peptide synthesis.

I sincerely thank my dear friends for their great support during stressful times and the list is long, all the lovely and helpful people I met in The tissue Engineering and Drug Delivery groups. Special thanks go to Assia Merabet, Nahed Souadkia, Amina, Slimani, Ouannessa Rached, Rasha Cheikh, Nadjoua Maouche and Abdennour Bouhroum. A heartfelt thank you goes to Dr Abdelghafour Ouchene for his continuous support during the writing up period and stressful times.

Great support I received from my family especially my wonderful mother, lovely sisters (Hidaya, Chafia and Selma) and brothers (Salah and Abd-basset). Thanks to all of them for their continuous encouragement that enabled me to finish my PhD. To my wonderful father (Mohammed) who I am sure he would be proud of me if he was still alive.

I dedicate this PhD work to the best Mama and Papa in the whole world.

Publications and Presentations

Some of the work reported in this thesis has been presented in the following meetings:

Oral presentation: Surface Science of Biologically Important Interfaces, 9th Annual Meeting, 13th-14th September 2007. Responsive surfaces for mouse embryonic stem cell culture.

Poster presentation: Tissues and Cells Engineering Society, The University of Nottingham, Nottingham, 2nd to 4th of July 2008. Biocompatible responsive surfaces for embryonic stem cell culture.

Poster presentation: World Forum on Advanced materials, Rouen, France, 20th to 24th April, 2009. Culture of embryonic stem cells on thermo-responsive polymers.

Publications

Aram Omer Saeed, Sabrina Dey, Steven M. Howdle, Kristofer J. Thurecht and Cameron Alexander (2009). **One-pot controlled synthesis of biodegradable and biocompatible co-polymer micelles.** ***J. Mater. Chem.***, 2009, **19**, 4529 – 4535.

Dey S, Kellam B, Alexander MR, Alexander C, Rose F RAJ. **Culture of mouse embryonic stem cells on thermo-responsive polymers; eliminating the need for enzymatic passage.** Biomaterials (Submitted).

Abstract

Embryonic stem cells are of great interest to scientists as they can differentiate into any somatic cell lineage making them excellent candidates for tissue regeneration and cell based treatment therapies. Currently, human embryonic stem cells (hESCs) are cultured using feeder fibroblasts or protein substrates such as matrigel, fibronectin or laminin in conditioned media. hESCs are then sub-cultured using enzymes to detach them from the culture substrate. However, the use of the xenosupport systems makes the hESCs therapeutic applications difficult due to cross-contamination with animal pathogens from the animal derived feeders, matrix or conditioned media to the hESCs. Moreover, the use of enzymes to recover hESCs can damage these cells. For the mentioned reasons, development of completely synthetic surfaces is desirable for hESCs culture.

Thermo-responsive surfaces have been extensively studied for cell culture using the well know thermo-responsive polymer poly (N-isopropylacrylamide) (PNIPAAM) which has a switchable properties across its lower critical solution temperature (LCST) at 32°C. However, more biocompatible polymers that have similar thermo-responsive properties to PNIPAAM and biocompatible properties, such as PEG based materials, have been proposed for use as switchable surfaces. Within this thesis, thermo-responsive copolymer brushes composed of 2-(2-methoxyethoxy) ethylmethacrylate (MEO_2MA) and oligo (ethylene glycol) methacrylate (OEGMA) that have LCST close to body temperature (37°C) were investigated for use as a cell culture surface for temperature sensitive passaging.

Poly (MEO_2MA-co-OEGMA) brushes were grafted from the surface using atom transfer radical polymerisation (ATRP). Hydroxyl plasma-polymer functionalised glass slides were prepared using plasma polymerisation and then an ATRP

initiator was reacted to these surfaces. ATRP of the copolymers was then performed from these initiation sites. These surfaces were characterised using X-ray photoelectron spectroscopy (XPS), Time of Flight Secondary Ion Mass Spectroscopy (ToF-SIMS), atomic force microscopy (AFM) and water contact angle (WCA).

Using 3T3 fibroblasts as a model cell type for initial studies, it was demonstrated that these cells adhered and proliferated on the poly (MEO_2MA-co-OEGMA) thermo-responsive surfaces at 37°C when the polymer brushes are in their hydrophobic state. Subsequent detachment assays were conducted when the temperature was lowered to 20°C i.e. the hydrated conformation of the copolymer brushes.

Mouse embryonic stem cells (mESCs) were then cultured on these surfaces following adsorption of fibronectin (to encourage cell attachment) and cultured for 3 days. Passaging experiments were performed for 10 passage cycles and the cells analysed for retention of the undifferentiated stem cell status. These thermo-responsive polymer/fibronectin surfaces are found to be suitable for mESCs culture but evidence of differentiation was observed.

Attachment of a novel gelatine based peptide to the poly (MEO_2MA-co-OEGMA) was also investigated for mESCs culture to avoid the use of fibronectin (which was thought to be a contributing factor to the stem cell differentiation seen). mESCs adhesion was observed both to the peptide adsorbed on TCPS and on the peptide coupled to the thermo-responsive poly (MEO_2MA-co-OEGMA) surface. This research indicates that these smart stimuli biomaterials have promise as a new generation of culture surfaces for enzyme free cell culture and passage suitable for generating cell populations for clinical applications.

Abbreviations

PNIPAAm	Poly (N-isopropyl acrylamide)
OEGMA	Oligo (ethylene glycol) methacrylate
MEO_2MA	2-(2-methoxyethoxy)ethylmethacrylate
AFM	Atomic Force Microscopy
XPS	X-ray Photoelectron Spectroscopy
ToF-SIMS	Time of Flight Secondary Ion Mass Spectroscopy
LCST	Lower Critical Solution Temperature
ppAAl	Plasma Polymerised allyl alcohol
WCA	Water Contact Angle
ATRP	Atom Transfer Radical Polymerisation
W	Watts
ESC(s)	Embryonic Stem Cell (s)
LIF	Leukaemia Inhibitory Factor
mESC(s)	Mouse embryonic stem cell (s)
hESC (s)	Human embryonic stem cell (s)
hrs	Hour
μL	Microlitre
mL	Millimetre
nm	nanometer
PBS	Phosphate buffered saline

CHAPTER 1

General Introduction

Stem cells have the ability to extensively self-renew to provide fully functional differentiated and/or undifferentiated daughter cells. They are classified according to either their origin i.e. embryonic, germinal or somatic (foetal or adult) or according to their ability to differentiate further to other cells i.e totipotent, pluripotent or multipotent.

This review aims at describing the recent literature reported with regard to differentiated and stem cells culture conditions and their potential for clinical therapy, leading to the main aims and objectives of this research project.

1.1 Adult stem cells

Adult stem cells are undifferentiated cells present in tissues which are characterised by their limited ability to differentiate in that they are solely restricted to the cell types of the tissue that they originate from. Bone marrow is the most common source of these cells which contains two stem cell types, haematopoietic stem cells which are capable of providing mature blood cells and

mesenchymal stem cells which have the ability to differentiate to bone, cartilage, adipose and muscle (1).

Umbilical cord blood cells also contains adult stem cells that are predominantly haematopoietic stem cells (HCs) which have a greater haematopoietic expansion capacity compared to mobilised adult blood cells (2). Additionally, it has been reported that these cells contain a more primitive sub-population of mesenchymal stem cells (MSCs) compared to the bone marrow (3).

Other adult stem cells are categorised according to their germ layer origin including pulmonary epithelial stem cells from the endoderm and neural stem cells from ectoderm. Figure 1.1 summarises adult stem cells categories according to their germ layer origin.

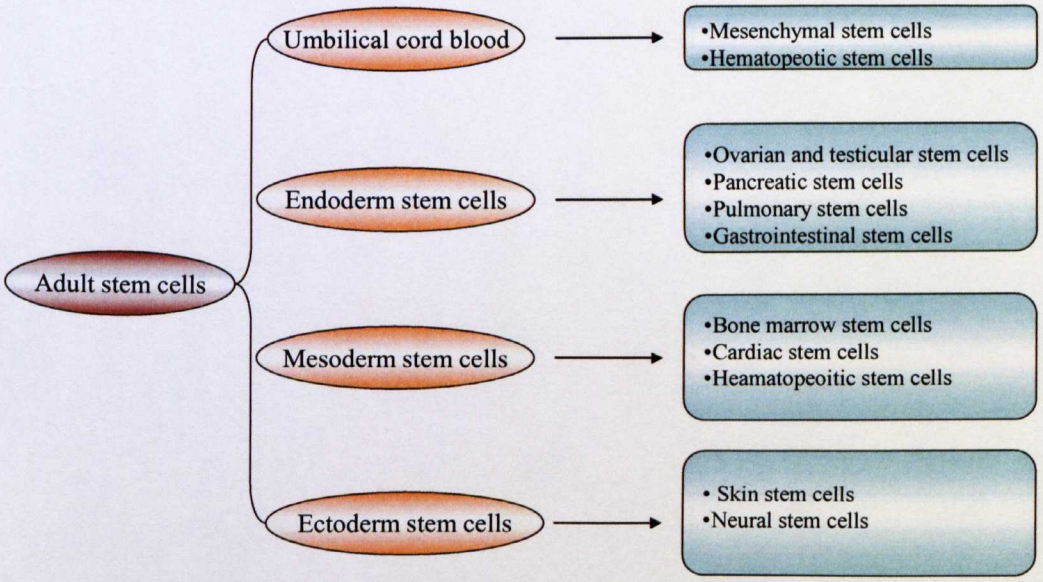

Figure 1.1. Representation of adult stem cells categorised according to their germ layer origin.

The lack of suitable donor organs and tissues is an urgent problem in transplantation medicine therefore cell replacement or transplantation based

therapies is can act as alternative to repair or replace diseased tissue. Despite the great amount of activity in the field of stem cell research, only a few reported therapies using adult stem cells have been approved to date for cell based therapies due to a reduced risk of immune rejection (4).

The most widespread adult stem cell therapies are for the treatment of malignancies, immuno-deficiency and leukaemia using stem cells from the bone marrow of the patient, which rebuild the haematopoietic system (5, 6). Other therapies reported include stimulating MSCs to differentiate to hepatocytes under suitable culture conditions and transplanting into the parenchyma of the liver; no immune rejection was observed (7). It has also been previously shown that human pancreatic islet transplantation to patients with type I diabetes resulted in reduced insulin requirements (8). Additionally, neural stem cells from ectodermal origin have been isolated and expanded in culture for the treatment of Parkinson's disease (9) as they can differentiate to oligodendrocytes and astrocytes for example.

Another example demonstrating adult stem cell therapies involved the use of MSCs, isolated from the bone marrow, and injected into the diseased tissue e.g. to treat damaged myocardium after a cardiac infarction has been reported (10). This study showed that transplanted bone marrow derived cells can significantly improve contractility and myocardial perfusion of the infarct region (10). Moreover, using similar principles, other therapies are being tested for their ability to treat autoimmune diseases such as rheumatoid arthitis (11).

In spite of the well characterised protocols for the use of differentiated adult stem cells (haematopoietic and mesenchymal) *in vivo* (HC) or *in vitro* (MSC), there are still concerns about the trans-differentiation potential of most adult

stem cells as a result of contamination or culture conditions (12) and cell fusion events (13, 14). In addition, the limited supply of a sufficient amount of adult stem cells is one of the problems encountered for use of adult stem cell therapies due to lack of donors as well as difficulties with isolation and *in vitro* expansion. These problems could be overcome using embryonic stem cell lines that could provide a variety of differentiated cells.

1.2. Embryonic stem cells

Embryonic stem cells retain the totipotency capacity found in the zygote up to the stage of the morula (Figure 1.2). Thereafter, the formation of the blastocyst results and this is composed of outer trophoblast cells and undifferentiated cells in the inner cell mass (ICM). Cells in the ICM are pluripotent cells which have the capacity to differentiate into a wide range of cell types *in vitro* (15, 16).

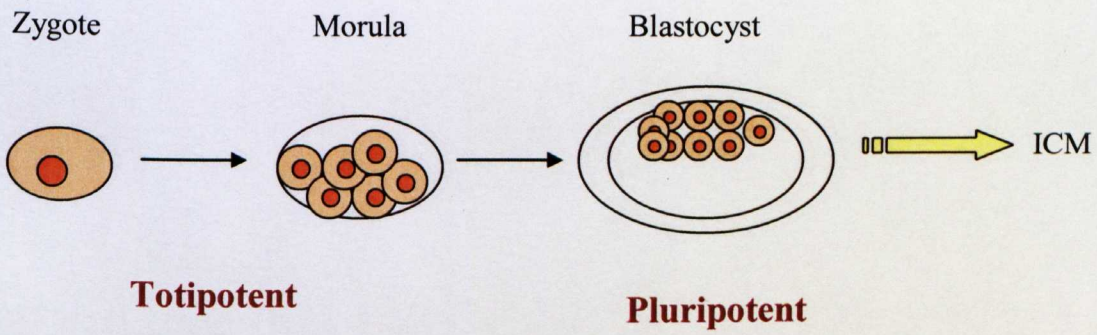

Figure 1.2. Pluripotent stem cells. Zygote and early cell division stages to the morula stage are defined as totipotent as they have the ability to generate a complex organism. At the blastocyst stage, only the cells of the inner cell mass retain the capacity to differentiate to the thee primary germ layers.

Embryonic stem cells (ESCs) derived from the ICM have the capacity to differentiate into cells of all somatic cell lineages i.e. endoderm, mesoderm and ectoderm. Subsequently, these thee germ layers generate a variety of cells and organized tissue structures as shown in Figure 1.3.

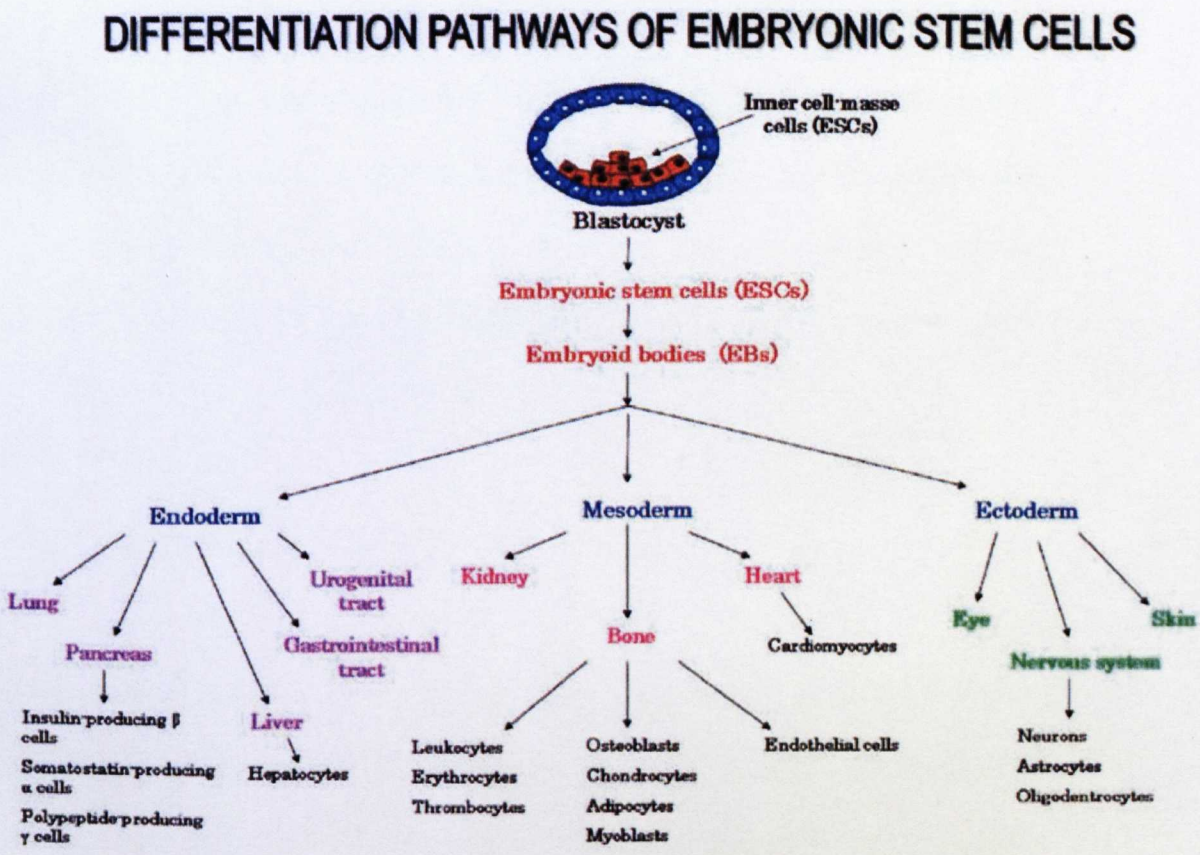

Figure 1.3. Representation of the differentiation of embryonic stem cells to the thee germ layers, endoderm, mesoderm and ectoderm, and into terminally differentiated tissue showing the capability of these cells to provide all cell types in the human body (17).

A variety of cell types have been generated from embryonic stem cells *in vitro*, including haematopoietic cells (18), hepatocytes (19), cardiomyocytes (20), neural tissue (21), endothelial cells (22), keratinocytes (23) and insulin-secreting cells (24). As discussed above, adult stem cells have been employed in human cell-grafting therapies; the best examples is bone marrow transplantations for the treatment of leukaemia. ESCs also hold a great potential for clinical use and may be able to address the issue of a limited supply of adult stem cells and provide an 'of-the-shelf' alternative. The main characteristics that render ESCs an attractive alternative to adult stem cells include their indefinite proliferation in culture and hence their seemingly unlimited supply. Moreover, numerous differentiation protocols are being established allowing the generation of almost any cell type in the human body.

1.3. Embryonic Stem Cell-based therapies

It has been previously reported that purified cardiomyocytes, derived from mouse embryonic stem cells (mESCs), were injected into the ventricular myocardium of adult dystrophic mice. The study showed that ES-derived cardiomyocyte grafts were present for as long as 7 weeks after implantation (25). In addition, this study demonstrated that using ES cell-derived cardiomyocytes for cardiac therapy is possible as the generated cardiomyocytes proved to be suitable for the formation of intra-cardiac grafts (27).

The potential use of ES derived neural cells has also been described where dissociated neural progenitors were introduced into dopaminergic neurons which promoted partial recovery in a rat model of Parkinson's disease (26). ES

also demonstrated their potential use for the treatment of Alzheimer's disease (27) and spinal cord injuries (28).

In addition, ESCs have also used for the treatment of diabetes. Insulin secreting cells were derived from ESCs and proved to normalise glycemia in Streptozotocin-induced diabetic mice (29, 30).

Despite the published literature describing the use of mESCs as models for the treatment of diseases in animal models, there is limited literature that has reported the use of human embryonic stem cells (hESCs) for cell therapies in man. This is due to the ethical issues regarding the isolation of these cells from *in vitro* fertilised human embryos as well as their tumour forming potential. In addition to ESCs based therapies, ESCs (human or mouse) could be a useful tool to study human diseases where insertion of genetic mutations could be used to generate cellular models for various diseases (31).

1.4 Embryonic Stem Culture Conditions

mESCs culture *in vitro* was established in the 1980s which required their cultivation on feeder layers of mitotically inactivated mouse embryonic fibroblasts (MEFs), that provide essential factors e.g. Leukemia inhibitory factor (LIF) to promote self-renewal and reduce their differentiation *in vitro* (32). Likewise the hESCs, isolated later in 1998 by Thompson *et al.*, also required subsequent culture on MEFs to maintain their pluripotency and prevent spontaneous differentiation (33). An alternative method is to culture hESCs on extracellular matrices including laminin and matrigel, without the use of feeder cells, in the presence of a conditioned medium obtained from fibroblast cultures

as reported previously (34) or in the presence of Leukaemia Inhibitory Factor (LIF) (Figure 1.4). However, the use of xenosupport systems hold a great risks of cross-contamination with animal pathogens from the animal derived feeders, matrix or conditioned media (to the hESCs) and hence are inappropriate for use for therapeutic purposes. In addition, the use of animal serum in the culture medium may result in cross-specied contamination with pathogens and hence compromise use in clinical applications (35). To eliminate this potential xenogenic contamination discussed above, it has been reported that human foetal and adult fibroblast feeders supported the prolonged undifferentiated hESCs growth (36).

It has also been proposed that combining serum-free culture media with ECM coated culture substrates could be a potential synthetically defined culture system for hESCs that is pathogen free. One study has reported that hESCs maintained their ESCs characteristics of both pluripotency and differentiation in such a culture system (37). This involved the culture of hESCs on a fibronectin matrix in a medium supplemented with 15% serum replacement that is composed of transforming growth factor β_1 (TGFβ_1), Leukaemia Inhibitory Factor (LIF) and basic fibroblast growth factor (37).

The maintenance of the undifferentiated state of ESCs is a necessary step which is usually achieved by adding LIF to the culture medium. LIF belongs to IL-6 cytokine family (38-40); the biological mechanism of preventing ESC differentiation is thought to be mediated via the heterodimerization of two members of the class I cytokine receptors gp130 protein and the low-affinity LIF receptor (LIF-R) (41, 42). This results in activation of the signal transducers and Activator of Transcription 3 protein (STAT3) signalling pathway though

janus kinases (JAK) which then induces transcription of self-renewal genes (43-46) including Oct-3/4 and Nanog. Expression of Oct3/4 and Nanog are essential for self-renewal of pluripotent ES cells (47-49). Oct3/4 is a POU domain-containing transcription factor[1] that is down-regulated if ESCs are differentiated (50) while Nanog sustain their pluripotency even in the absence of LIF (48). The minimum concentration of LIF reported to maintain the undifferentiated state of mESCs was 500 pM (39, 51). Figure 1.4 describes the pathways for embryonic stem cell pluripotency and self-renewal.

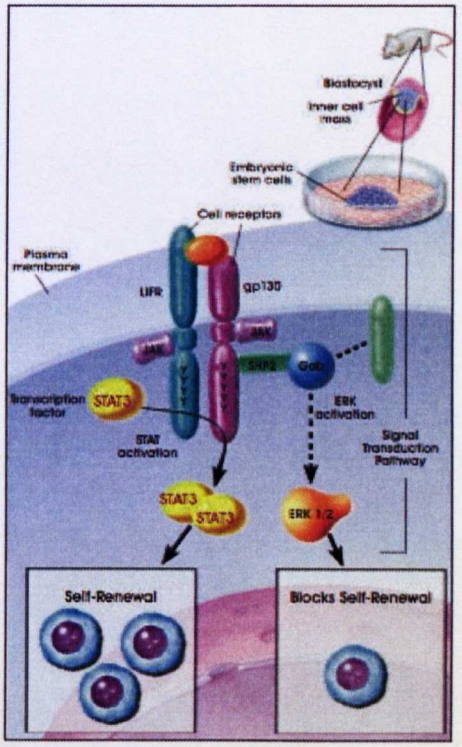

Figure 1.4. The LIF pathway maintains ESCs self-renewal though maintenance of the STAT3 signalling pathway via JAK pathway leading to induction of OCT3/4 and Nanog which are the main transcription factors reported to maintain stem cells self renewal (52).

[1] POU is derived from the names of thee mammalian transcription factors; **P**: The pituitary specific Pit-1, **O**: the Octamer transcription factor proteins OCT-1 and OCT-2, and **U**: the neural Unc-86 transcription factor from Caenorhabditis Elgans.

1.5 Disadvantages of Enzymatic Treatment of Cell Cultures

Generally, mammalian cells are cultured for a certain period of time and once they reach confluency they are detached from the culture substrate in a process called passaging. Efficient recovery of mammalian cell monolayers from the culture substrate is an essential process for their further utility which can be accomplished by the use of a cell scraper to physically peel them off the culture substrate and the cells are recovered as irregular in shape (53). Alternatively, proteolytic enzymes, e.g. trypsin, pronase or collagenase, are commonly used to fully recover the adherent cells from culture substrates as a single cell suspension (53). Enzymatic treatment is considered to be the most effective procedure for full cell recovery of individual cell populations with trypsin being the most frequently used dispersing agent in a mixture with EDTA (54).

Despite its widespread use in cell culture, proteases for tissue and cell dissociation can incur a wide variety of injuries on the cell. These include general damaging effects on cellular metabolism and cell viability and specific injury to the cell surface which will be the focus of this section (55). This is illustrated in a study, where the permeability and rupture of baby-hamster kidney cells (BHK 21-C13) was determined when harvesting adherent cells from glass using trypsin and EDTA. This was achieved by measuring the levels of (H^3) RNA and (^{14}C) DNA in the culture medium following trypsinisation. Cells harvested in this experiment from glass by trypsin lost 10.4% cellular RNA and 11.4% cellular DNA, consistent with lysis of about 11% of the cells (56). Besides surface damage to cells, trypsin has been found to induce internal damage including degradation of polyribosomes a net loss of ribosomes

recovered after dissociation of embryonic muscle cells with proteolytic enzymes (57).

In conclusion, proteolytic treatment can inflict damage to cells and therefore, prior to sub-culturing or passaging, cells must demonstrate sufficient resistance against proteolytic treatment for detachment from culture substrates. An alternative could be to fabricate surfaces whose surface properties can change leading to cell detachment by other physical processes (58).

As for most mammalian cells under consideration for use in tissue engineering constructs or cell based therapies, ESCs require a solid substrate or supporting scaffold upon which they can adhere and proliferate. These cells are anchorage dependent as they are normally adherent to ECM *in vivo*. Adherence to culture surfaces is important because the shape of the cell is tightly coupled to DNA synthesis; when cells are almost spherical and barely attached to the substratum, they fail to enter the synthesis phase. Therefore, the shape of cell is modulated by substrate adhesiveness and only when cells are spread to the appropriate degree can DNA synthesis proceed (59). Additionally, studies in a variety of cell culture systems have shown the importance of cell morphology changes in regulating tissue specific gene expression and in the maintenance of differentiated cell functions; particularly, cell-cell and cell-matrix interactions (60).

In order for hESC employment for clinical applications, these cells have to meet certain requirements. This includes their culture on substrates that are pathogen free (i.e. avoiding the use of mouse or human tissues or avoiding the use of cell culture matrices) and in serum-free culture medium to minimise the risk of

retrovirus infections being transmitted to these cells. In addition to culture substrate design, the recovery of these cells from the substrate without the use of proteolytic enzymes would be the ideal to ensure maintenance of the cell quality (61). Synthetic biomaterials could play a significant role in meeting the demands for the development of well-defined culture systems for the derivation and maintenance of ESCs.

1.6 Trends to Improve Culture Substrates for Mammalian Cell Culture

Biomaterials based expansion of mammalian cells has been achieved previously as a number of studies have been reported with respect to the use of synthetic substrates for the maintenance of mammalian cells including stem cells.

Different surface chemistries have been reported for this purpose including glass coated allyl amine (using plasma polymerisation) which promoted hepatocyte attachment (that usually require collagen coated substrates to adhere to) and maintenance of their differentiated phenotype (62). Moreover, 3T3 fibroblast cell attachment and maintenance of a fibroblastic morphology and metabolic activity on poly (D,L-Lactic acid) scaffolds was significantly improved when they were treated with plasma allyl amine which penetrated to the inner surfaces of the scaffold (63).

Substrates with modified surface chemistries following plasma polymer deposition using acrylic acid and allyl amine also improved the co-culture of melanocytes and keratinocytes compared with individual cultures (64).

Moreover, amine functionalisation of hydrogels significantly improved stromal and epithelial cell adhesion both in mono and co-culture (65). Another study showed that 3T3 fibroblast adhesion and proliferation is supported on plasma polymerised allyl amine in comparison to substrates coated with plasma polymerised hexane. This was thought to be due to the close correlation between the cell response and the wettability of the polymer films as the cells interact with the top 0.4 nm of the surface (66). Therefore, plasma polymerisation deposition to synthetic substrates could be used to support attachment and proliferation of mammalian cells to non-cell adhesive substrates.

Synthetic substrates using responsive polymers to an external stimulus (e.g. temperature, light and pH) could also be used as substrates for mammalian cell adhesion and their detachment. Such a culture system was described previously where mammalian cells were cultured on solely synthetic substrates and recovered from these responsive culture systems without using proteolytic treatment. The following section will describe a variety of synthetic substrates that has been reported to improve support cell adhesion and enzyme free detachment.

1.7 Responsive Surfaces for Mammalian Cell Culture

The observation that many eukaryotic cells adhere very differentially to hydrophobic compared to hydrophilic substrates has led to the development of responsive polymer surfaces designed for uses in cell culture (67, 68). These 'smart biomaterials' which change physical properties in response to applied

stimuli including temperature, light, pH and enzymes are being extensively studied as they could provide a new generation of materials to support cell adhesion, proliferation and detachment.

1.7.1 Enzyme-Responsive Systems

Bio-responsive systems are smart materials which change properties in response to a selective biological event i.e. after exposure to an enzyme or a growth factor; this in turn could trigger changes at the molecular interactions level and hence control cell behaviour on these surfaces (69). For example, cell attachment was achieved on an enzyme responsive surface after modification of the RGD cell adhesion peptide with a bulky blocking group that contained an enzyme recognition motif (70). In another study, synthetic poly (ethylene glycol) monolayers attached to epoxy silanes of glass functionalised with RGD sequence (cell binding ligand) that is attached to steric blocking groups were fabricated. These surfaces promoted the adhesion of osteoblasts after exposure of the surface to elastase which lead to the subsequent activation of the RGD motif (71).

1.7.2 Photo-responsive surfaces

It has been demonstrated that cells can adhere to photo-responsive surfaces following irradiation of the surface with UV (72). The fabrication of photo-responsive cell culture surfaces using nitrospirobenzopyran residues and poly (ethylene glycol) was demonstrated to promote BALB/3T3 fibroblasts adhesion after 12 h of culture. Cell adhesion was enhanced after UV light irradiation

(350-400 nm) for 5 minutes as it was observed that the number of adhered cells in irradiated region was 2.5 times greater than that in non-irradiated regions (73).

It is also possible to switch surfaces between hydrophilic and hydrophobic states via UV irradiation as was reported in another study. Such surfaces were prepared using the well know thermo-responsive poly (N-isopropyl acrylamide) (PNIPAAm) coupled with spiropyran chomophores as side chains, where cell adhesion was promoted by the irradiation of the surface with UV light. Cells remained adherent to the irradiated regions compared to the non-irradiated parts of the surface (74). Therefore, photo-responsive surfaces could also be used as smart substrates to control cell adhesion and detachment.

1.7.3 Thermo-Responsive Surfaces

Thermo-responsive behaviour of a polymer arises due to a change in chain conformation, which is manifested in a transformation from a hydrophilic to a hydrophobic state. The temperature at which this behaviour is observed is termed the lower critical solution temperature (LCST) for water-soluble polymers (75).

Thermo-responsive polymer films can exhibit a hydrophobic and hydrophilic switch and hence influence cell behaviour (adhesion and detachment) in response to temperature.

- **Thermo-responsive polymers based on the LCST**

Poly (N-isopropylacrylamide) (PNIPAAm) is among the many intelligent polymers which exhibits a sharp phase transition in water across its LCST at 32°C. Below the LCST, PNIPAAm is soluble in water and forms an extended hydrophilic conformation and becomes hydrophobic above its LCST.

The LCST phenomenon is believed to be the result of interactions between the isopropyl amide groups on the polymer and molecules of water (75, 76) . Schild *et al.*, and Ilmain *et al.*, suggested that the LCST of PNIPAAm in aqueous solution is the result of the formation of hydrogen bonds between water molecules and the amide groups of PNIPAAm and their destabilization as the temperature increases (76) (Figure 1.5).

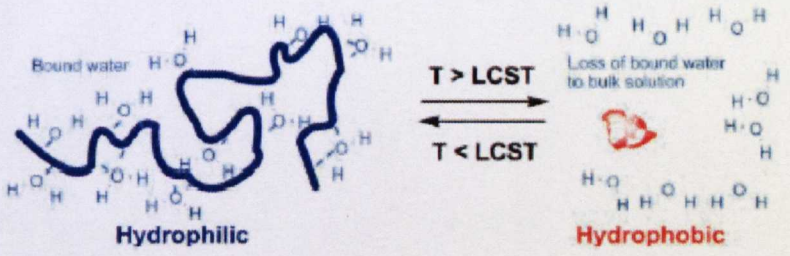

Figure 1.5. Schematic representation of the Lower Critical Solution Temperature (LCST) phenomenon in solution. Below the LCST, water interacts with polymer chains though hydrogen bonding (extended polymer forms); when the temperature is raised leads to loss of the bound water and the polymer chains adopt globule structures (77).

Synthetic polymer brushes are believed to be ideal building blocks for functional and stimulus-sensitive surfaces which have potential applications in biotechnology and the biomedical field particularly as surfaces for *in vitro* cell culture (78), scaffolds for tissue engineering (79) and to promote cell attachment (58, 80-82).

1.8 Applications of Thermo-responsive Grafted Surfaces for Bacterial and Mammalian Cell Adhesion

Synthetic polymers that undergo conformational changes in response to external stimuli are of special interest in biomedical fields including drug release systems, responsive polymer-biopolymer conjugates, controlled cell adhesion and tissue engineering. PNIPAAm in particular has been extensively investigated as a surface modifier because of the fact that the LCST of the PNIPAAm homopolymer lies close to body temperature. In addition, the LCST can be increased above and below 37°C by incorporation of co-monomers, making PNIPAAm-based materials particularly suitable for biomedical applications and cell culture. Another important fact that supports the use of PNIPAAm in biomedical applications is that the LCST is relatively insensitive to slight changes in pH, ionic concentration or chemical environment (76). Examples of bacterial and mammalian cell adhesion on PNIPAAm based responsive surfaces are described in the following sections.

1.8.1 Bacterial Cell Adhesion

The use of PNIPAAm and its co-polymers as bio-fouling release agents for prokaryotic cell adhesion has been reported. In these studies, PNIPAAm-coated glass slides were incubated in artificial sea water containing the marine bacterium *Halomonas marina*. Upon rinsing of the biofouled samples below the LCST, the dissolution of the coating released over 90% of the attached fouling material which was considered to be significant compared to glass controls (83).

In another study, end-grafted PNIPAAm homo- and co-polymers as potential passivators for the prevention of attachment of the foodborne pathogen *Listeria monocytogenes* was investigated. It was demonstrated that adsorption of this organism decreased above the polymer LCST, illustrating that these micro-organisms have a lower ability to colonise on hydrophobic surfaces (84).

1.8.2 Mammalian Cell Adhesion

Thermo-responsive polymers have been used in mammalian cell culture to avoid the deleterious effects of trypsin upon cell membrane receptors, in order for cells to grow and detach without damage to surface receptors. This in turn maintains their substrate adhesivity, growth, and secretion activities nearly identical to those prior to passaging.

Okano and colleagues reported an experiment where PNIPAAm was covalently attached to tissue culture polystyrene (TCPS) dishes to prepare a thermo-

responsive culture surface. Under culture conditions at 37°C, the substrate surface was relatively hydrophobic and bovine hepatocytes adhered, spread, and proliferated in the same way as to TCPS (58, 80). However, below 32°C (the LCST of the polymer), the dish surface became hydrophilic leading to the formation of a hydration layer between the dish surface and the cultured cells leading to cell detachment from the PNIPAAm grafted surface (Figure 1.6).

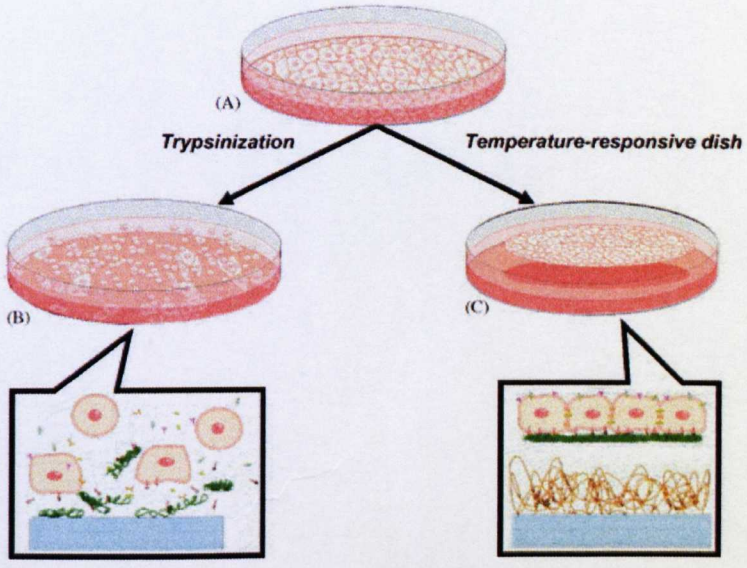

Figure 1.6. Cell sheet release from temperature-responsive culture surfaces. (A) Confluent monolayers of cells connect to each other via cell-to-cell junction proteins and to the surface via integrins. (B) Cells are released separately when treated by a protease (e.g. trypsin) due to disruption of these cell-to-cell connections. (C) When PNIPAAm-grafted surfaces are used; the cells are released as a contiguous cell sheet when the temperature is lowered below 32°C (85).

Bovine hepatocytes, which are highly sensitive to trypsinization, have been successively sub-cultured on a thermo-responsive polymer grafted surface at 37°C using PNIPAAm. The cultured cells were easily detached, without contamination and enzymatic treatment, by decreasing the temperature below 32° C (58).

While rat hepatocytes normally cannot be sub-cultured because of their intrinsic sensitivity to proteolytic enzymes, bovine aortic endothelial (BAE) cells were found to be stable and could be sub-cultured in this way (80). However, cells can be non-invasively harvested as intact sheets along with their deposited extracellular matrix (ECM) using this method so that critical cell surface proteins such as ion channels, growth factor receptors and cell-to-cell junction proteins remain intact.

In a further study, it was demonstrated, using immuno-staining techniques, that fibronectin (composed of fibrillar aggregates) was deposited by BAE cells and accumulated on PNIPAAm surfaces during culture. Furthermore, the deposited fibronectin matrix deposited by these cells was also recovered from temperature-responsive surfaces by low-temperature treatment, while trypsin treatment destroyed the matrix, enabling BAE cell sheets to re-attach easily to other surfaces (81).

In addition, these thermo-responsive polymers have been used to create a co-culture of two different cell types. This was achieved by overlaying human aortic endothelial cell (HAECs) sheets directly onto a monolayer of rat

hepatocytes. The maintenance of the differentiated cell shape of the hepatocyte and sustained albumin expression over 41 days of culture was demonstrated. It was proposed that this co-culture system could therefore be used for liver tissue engineering as it prolongs the expression of differentiated functions of hepatocyte (82).

1.8.3 Cell Sheet Engineering Approaches

As mentioned above, cell sheet engineering methods have been developed whereby cultured cells are harvested as intact sheets along with their deposited ECM from a temperature-responsive surface (58). It has been proposed that these cell sheets can be used for tissue engineering applications as they can be directly transplanted to tissue beds or even layered to create thee-dimensional (3-D) tissue-like structures (85). Therefore, various tissues and organs can be reconstructed using cell sheet engineering by thee different methods. First, single cell sheets can be directly transplanted to host tissues as in the cases of skin, corneal epithelium, bladder urothelium, and periodontal ligament (Figure 1.7A) (85, 86). Second, homotypic layering of cell sheets can be used to re-create 3-D structures e.g. cardiac muscles (Figure 1.7B). Finally, by stratifying different cell sheets, more complex laminar structures such as liver lobules and kidney glomeruli can be generated (Figure 1.7C) (85, 86). It has been suggested that using these cell sheet engineering approaches, several advantages over conventional regenerative therapies of cell injection and tissue reconstruction with biodegradable scaffolds can be achieved (85, 86).

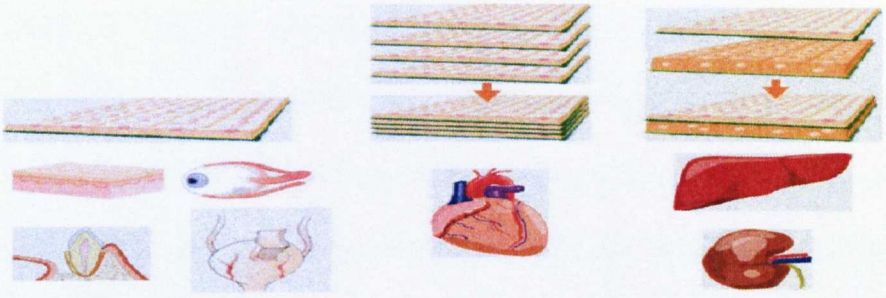

Figure 1.7. Possible uses of cell sheet engineering. Single sheet engineering was proposed for the culture of skin and corneal epithelium (A); moreover, 3D structures could be produced using a cell sheet approach e.g. for cardiac cells. More complex tissues including liver lobules and kidney glomeruli are proposed by stratifying different cell sheets (85).

1.8.3.i. Corneal Cell Sheet Engineering (Single Sheet Engineering)

Complete loss of corneal epithelial stem cells can result from severe trauma leading to corneal opacification and a loss of visual acuity. Recovery of corneal transparency and improved visual acuity has been demonstrated in patients receiving autologous corneal epithelial grafts using cultured corneal epithelial stem cells harvested using a dispase treatment (87). Many approaches have been tried to avoid dispase treatment and the damage caused to the cell membrane receptors of cell sheets including the use of carrier substrates such as amniotic membrane (88) and fibrin gel (89). However, the use of biological carrier substrates raises the issue of the risk of infection as they need to be surgically placed onto the host corneal stroma along with the cultured epithelial cells. In order to overcome the above problems, cell sheet tissue engineering has been

used to produce transplantable corneal epithelial sheets that are not proteolytically treated and avoid the use of biological carrier substrates. The recovered cell sheets from the thermo-responsive dishes were positioned directly on the host corneal stroma and adhered rapidly without the need of sutures (90). In addition, functional human corneal endothelial cell sheets harvested from temperature-responsive culture surfaces were shown to possess, ex vivo, morphologically and functionally similar characteristics to the native corneal endothelium. These sheets can be used clinically in patients with ocular endothelial decompensation (91).

1.8.3.ii. Myocardial Tissue Engineering (Multiple Cell Sheets)

Cell sheet engineering can also be used to reconstruct 3-D myocardial tissues by layering multiple individual cardiomyocyte sheets recovered from thermo-responsive culture dishes (85). These sheets showed spontaneous pulsation *in vitro* and adhered to each other due to the presence of deposited ECM. These cell-dense structures contained ECM and more closely resembled native tissue, compared to constructs created using biodegradable scaffolds. The formation of gap junctions upon the layering of the cell sheets also allowed for electrical communication, leading to functional and synchonized pulsations of the 3-D myocardial tissue grafts that could be macroscopically observed (92).

1.9 Protein Based Biomaterial Surfaces for Stem Cell Culture

Protein based biomaterials including scaffolds that are made of collagen have been used in stem cell culture. Human mesenchymal stem cells were cultured in collagen matrices which promoted their differentiation to the osteogenic pathway (93). Bone like tissue was engineered *in vitro* using porous silk scaffolds covalently bound to an RGD sequence where MSCs derived from human bone marrow showed increased mineralisation compared to collagen scaffolds (94).

Collagen based biomaterials proved to be suitable scaffolds for the culture of ESCs as it was also reported in another study that these scaffolds promoted the differentiation of ESCs to endothelial and cardiomyocytes after incorporation of fibronectin and laminin respectively (95).

Fibrin based scaffolds are also suitable to promote vasculature formation from ESCs; this study illustrated the proliferation of murine ESCs using both fibrin and PEGylated fibrin scaffolds compared to 2D suspension culture (96).

Protein based biomaterials are attractive to use for stem cell culture due to their natural origin and hence promotion of cell adhesion and bio-compatibility. Nevertheless, using purified proteins is an important step to avoid activating immune response if the scaffolds are to be delivered to the site of the diseased tissue. Synthetic biomaterials on the contrary, provides reproducibility due to their defined chemical structure and the ability to control mechanical properties.

1.10 Synthetic biomaterials for embryonic stem cell culture

Despite many studies into cell culture on polymeric surfaces including endothelial cells, hepatocytes, cardiacmyocytes and human mesenchymal stem cells, there has been limited literature relating to ESCs and their culture to maintain their capacity as therapeutic agents in clinical applications.

One study involved the culture of mESCs on photo-immobilized polymers to determine the ability of these polymer-based substrates to support the *in vitro* propagation of mESCs. These synthetic surfaces included the use of poly (acrylic acid, polyallylamine, gelatin and poly (2-methacryloyl-oxyethyl phosphorylcholine-co-methacrylic acid)) (PMAc50) that were coupled with azidophenyl groups (97). mESCs attached to the gelatin and polyallylamine surfaces whereas they formed embryoid bodies on the photo-immobilised poly (acrylic acid) and PMAc50 (97).

The culture of murine ES cells on scaffolds has been reported for the maintenance of these cells using different aliphatic poly (α-hydroxy esters) i.e. poly (D, L-lactide), PLLA, poly (glycolide) and PLGA which were alkali treated and supported their growth and proliferation of murine ESCs (98).

However, most of the reported literature describes the use of biomaterial substrates for the formation of embryoid bodies (EBs) or stem cell differentiation rather than expansion of undifferentiated ESCs (99-101).

As mentioned previously, the culture of hESCs is often dependent upon the inclusion of mouse fibroblast feeder layers (33). This has since been improved upon by using defined feeder free systems (34, 102). Alternatively, feeder free hESCs are often cultured on protein based substrates including materigel (34), laminin (103) or vitronectin (104). Since hESCs are anchorage dependent, proteins such as laminin and matrigel are used to promote their adhesion via integrins-matrix interactions. On the other hand, these proteins often exist in different isofroms or as higher fragmented proteins affecting the reproducibility of the culture substrates following the protein coating (105). Moreover, ECM proteins can loose biological function upon dehydration and usually have a short half life.

In addition, other studies have described the maintenance of two hESCs lines (SA167 and A5034.1) on feeder and matrix free culture systems when these cells were cultured in human fibroblast conditioned media for up to 43 passages on plastic surfaces without any modification. These hESCs maintained their morphology and pluripotency (expression of Oct-4, SSEA-3, SSEA-4 and SSEA-1) similar to cells cultured on Matrigel (106).

Synthetic culture substrates have also been proven to support the growth and maintenance of hESCs, this study used polystyrene modified substrates using plasma etching for hESCs culture. hESCs proliferated during serial passages on plasma etched TCPS and expressed stem cell markers, subsequent differentiation *in vitro* to all thee germ layers in addition to maintenance of a stable karyotype (107).

A very recent study investigated CRGDC-modified surfaces for hESCs adherence. A bi-functional linker was used to react the thiol on the peptide to

amine functionalised tissue culture plates. These synthetic substrates supported the adhesion of hESCs as the number of hESCs after 96 h of culture on these culture substrates was similar to cells cultured on matrigel (control). Moreover, these surfaces maintained the stem cell nature of hESCs in addition to the maintenance of the normal karyotype after 10 passages (108).

Stem cell culture on responsive surfaces has been shown using human mesenchymal stem cells and their applicability in tissue engineered cell-matrix systems was evaluated using various formulations of the thermo-responsive hydroxybutyl chitosan (HBC) polymer gel (LCST of 21-26°C) (109).

A more recent study demonstrated that thermo-responsive surfaces could be used for the attachment and detachment of mESCs. This study used PNIPAAM-PHB-PNIPAAM triblock copolymer co-coated with gelatin which showed adherence of these cells and detachment below the LCST of the polymer (at 4°C for 20 mins). This substrate maintained their pluripotency as these cells remained undifferentiated (110).

Using synthetic smart biomaterials for stem cell culture is proposed in this project. Temperature as an alternative to trypsinisation for cell detachment from the culture substrates is proposed and this is further described below in the aims and objectives of this research project.

1.11 Aims and Objectives

ESCs are stem cells derived from the inner cell mass of a blastocyst. Because of their capability to self-renew and to give rise to specialized cell types, embryonic stem cell based therapies have been proposed as having potential applications for regenerative medicine and tissue replacement after injury or disease including, for example, Parkinson's and Alzheimer's disease, spinal cord injury, stroke, burns, heart disease, diabetes, osteoarthitis and rheumatoid arthitis (111, 112).

However, realizing the clinical and industrial potential of such applications of hESCs is limited by the development of culture systems that are compatible with good manufacturing practice (GMP), physically and chemically stable, reproducible and of a well defined chemical composition. Such a cell culture surface could remove the need to enzymatically passage cells destined for cell therapies.

Evidence from the literature suggests that this would reduce the damage incurred to cells during passaging providing a better starting quality of cell for clinical applications.

Copolymers of 2-(2-methoxyethoxy) ethyl methacrylate (MEO_2MA) (113) and oligo(ethylene glycol) methacrylate (OEGMA) have been considered for use as switchable surface for mammalian cell culture (114, 115). These copolymers are promising for biomedical applications as they are composed of FDA-approved oligo (ethylene glycol) segments (116). The LCST of poly

(MEO_2MA-co-OEGMA) copolymers can be adjusted by altering the co-monomer compositions to obtain thermo-sensitive properties close to body temperature (117-120). Plasma polymers have the advantage that they may be used to alter the surface chemistry of most solid surfaces to incorporate functional groups suitable for subsequent chemical reactions (121, 122).

The aim of this research project is to fabricate environment-responsive surfaces (to temperature) using poly (MEO_2MA-co-OEGMA) copolymers for mammalian cell culture, including embryonic stem cells, to eliminate the need to detach cells from the culture surface using enzymes.

Figure 1.8 summarises the overall experimental approach of this research project where mESCs are cultured on thermo-responsive surfaces composed of poly (MEO_2MA-co-OEGMA). Polymer brushes at temperatures below the LCST are shown as chain-extended, forming a 'cell-resistant' surface, whereas collapse of the brushes above the LCST results in a surface more favourable for cell attachment and subsequent proliferation.

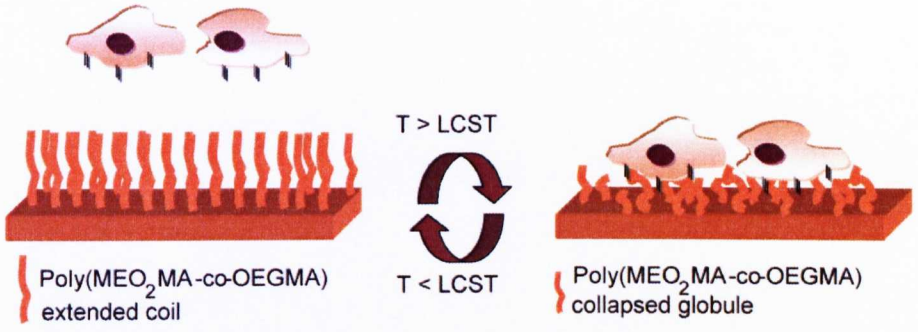

Figure 1.8. Schematic description of mouse ES cell attachment to poly (MEO_2MA-co-OEGMA) surfaces. Above the LCST when the polymer brushes are in their collapsed globular structures, mESCs are proposed to adhere to these surfaces. As the temperature is lowered to below LCST of thermo-responsive polymer substrates mESCs are supposed to be detached from these substrates when the responsive brushes adopted the hydrated extended coil conformation.

The key objectives to reach these aims are:

- Graft poly (MEO_2MA-co-OEGMA) from a glass substrate surface and examine the thermo-responsive behaviour (Chapter 2).
- Investigate mammalian cell adhesion and detachment using 3T3 fibroblasts (Chapter 3) and mouse embryonic stem cells (Chapter 4).
- Optimising embryonic stem cell adhesion to the thermo-responsive poly (MEO_2MA-co-OEGMA) surfaces (Chapter 5).

CHAPTER 2

Generation of Variable Adhesion Surfaces

Polymer surface engineering has attracted many scientists to investigate different chemistries particularly those that are applied to control bioadhesive processes such as cell attachment in response to an external stimuli e.g. temperature and pH. PNIPAAm is a well known thermo-responsive polymer that was extensively studied to control cell adhesion and detachment on this polymer grafted surfaces (76).

In this chapter, a brief overview of the techniques reported in the literature to produce polymer films is described most importantly polymer brushes. Synthesis of polymer brushes is also explained with given examples from reported studies leading to the main aim and objectives of this chapter including the generation thermo-responsive surfaces (brushes with switchable behaviour) using the homopolymers OEGMA and MEO_2MA.

2.1 Introduction to polymer brushes

2.1.1 Surface coating techniques

Deposition of thin organic coatings can be described in terms of the interaction between the molecules (constituents of the coating) and a substrate. The deposited molecules can interact with the substrate of interest by physical forces (123, 124) or chemical bonding.

A number of coating techniques are based on physical deposition of coatings including spray coating, spin coating (125-127) and dip coating (127); these processes are usually achieved by applying a solution resulting in evaporation of the solvent leaving a thin film of the material on the substrate. It is possible to produce layers with controllable and well defined thickness with good homogeneity if appropriate conditions are applied (Figure 2.1).

More sophisticated techniques allow better control of the internal structure of the deposited layers e.g. the Langmuir-Blodgett technique (128). This technique involves the deposition of organic material from the surface of a liquid onto a solid by immersing the solid substrate in the liquid; where the thickness and the molecular arrangement of the Langmuir-Blodgett films are controlled at the molecular level.

The organic molecules adsorbed to the surfaces using these processes are often attached to the surface by weak physical forces which mean that the deposited films may debond and hence there is a poor control of the coating density due to desorption during solvent exposure, displacement by molecules which have stronger interaction with the surface, de-wetting and delamination.

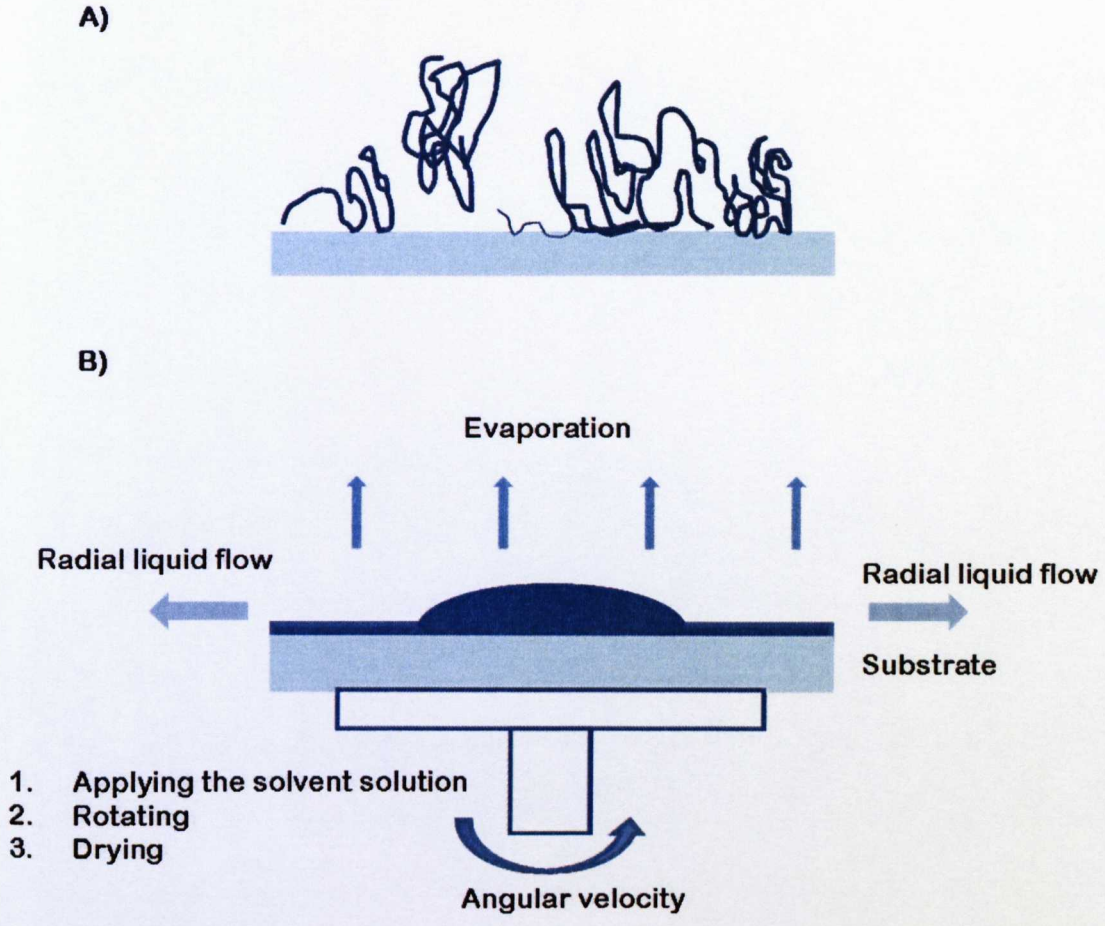

Figure 2.1. Schematic illustration of different processes used for the deposition of organic molecules and/or polymers on surfaces: **A)** Adsorption of the molecules to the surface from a solution and **B)** Spin-coating.

To overcome the above coating problems, polymer brushes are used which are defined as an assembly of tailor-made long macromolecular chains that are grafted with sufficiently high density by one polymer chain-end onto a surface or an interface and are stretched away from the surface where the distance between grafts is much less than the unperturbed dimensions of the tethered polymer (129, 130).

Polymer chains can be tethered to a solid substrate by physisorption or chemical bonding. This can also be performed with an interface between two liquids- in that

one part of the polymer chain prefers one part of the medium and the rest prefers the rest of the medium when adsorption is taking place- or between a liquid and air.

Polymer brushes are considered to be a central model for many practical polymer systems such as micelles, block copolymers at fluid-fluid interfaces (e.g. microemulsions and vesicles), grafted polymers on solid substrates, adsorbed diblock copolymers and end-grafted polymers (Figure 2.2).

Repulsive force between polymer brushes results from the high osmotic pressure inside the brushes and hence polymer brushes could be used in many applications including new adhesive materials (131, 132) especially for surgical implants (133, 134), protein-resistant biosurfaces (135), polymer surfactants (130, 136), lubricants (136) and surfaces for bacterial-resistant adhesion (137-139) . These synthetic materials have been found to be useful for many biomaterial applications e.g. scaffolds for tissue engineering (140-143) and supports for *in vitro* cell culture and biotechnological screening (144-147).

Stimuli-responsive polymer brushes are of particular importance to tissue engineering and cell culture in that polymer chains are tethered to a solid substrate surface and change their conformations in response to different stimuli (148). Polymeric materials that change their properties in response to biochemical stimuli can be highly specific to changes in the biochemical environment or by an enzymatic action (149); for example, it was found that drug carrying nanoparticles are susceptible to oxygen species present at the site of inflammation or tumour site leading to their degradation (150, 151).

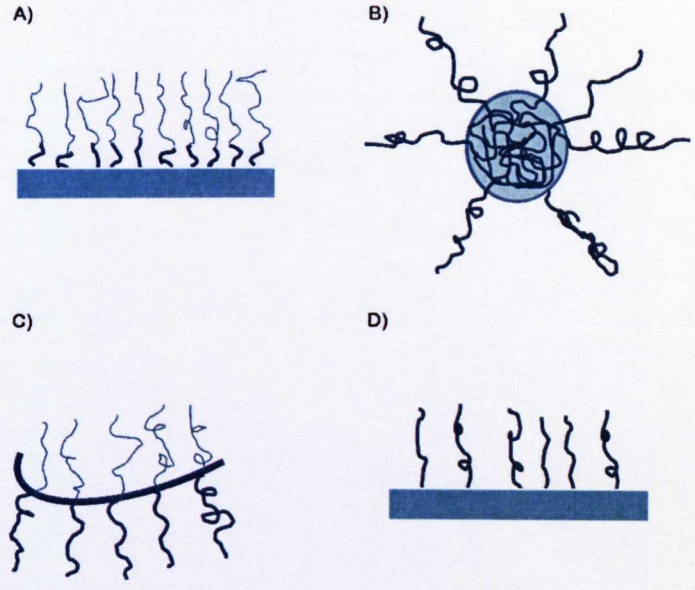

Figure 2.2. Polymer systems comprising polymers brushes. **A)** Adsorbed diblock copolymers. **B)** Polymeric micelle. **C)** Graft copolymer at fluid-fluid interfaces. **D)** End-grafted polymers.

Synthetic materials that are responsive to external stimuli e.g. pH, light and temperature are potential smart biomaterials (152-155). Triblock copolymer micelles have been generated from poly {(ethylene oxide)-block-glycerol monomethacrylate-block-2-(diethylamino) ethylmethacrylate} (PEO-GMA-DEAMA) and poly (ethylene oxide)-block-2- hydroxyethyl methacrylate-block-2-(diethylamino) ethyl methacrylate (PEO-HEMA-DEAMA) materials. They were synthesised via atom transfer radical polymerisation of GMA or HEMA and DEAMA using PEO- based macroinitiator. Full solubility was exhibited in aqueous solution at low pH but deprotonation of the DEA layers above pH 8 led to micellisation and the formation of the tri-layer micelles (156).

Light-responsive polymers are potentially useful to use for biological systems with a variety of mechanisms by which polymers can be switched, including isomerisation, elimination, photosensitization, and local heating. For example,

photoresponsive properties of PNIPAAm hydrogel partly modified with spirobenzopyran which was synthesized by radical copolymerization of NIPAAm, a vinyl monomer having a spirobenzopyran residue and cross-linker. This hydrogel was introduced to a surface of a porous membrane to examine its application to the mass transfer control; and it was found that the permeability of the membrane for 1 mM HCl was increased two times when the blue light irradiation was applied (157). In addition, photo-responsive cell culture surfaces were developed using poly (ethylene glycol) (PEG) functionalised with nitro-spirobenzopyran residues; which they enhanced cell adhesion that can be achieved locally by UV light irradiation (350-400nm)(73).

2.1.2 Theory of polymer brushes

The main idea of the polymer chains are forced to stretch away from the grafting sites of the surface where the polymer brushes were described with the following equation $F= F_{int} + F_{el}$; where F is the free energy of the system, F_{int} is the interaction energy per chain and F_{el} is high elastic free energy (158, 159). Alexander was one of the first scientists to describe the theory of polymer chains densely tethered to a substrate surface using numerical and analytical self-consistent field (SCF) calculations and by computer simulations (160).

The Alexander model considers a flat, non-adsorbing surface to which mono-disperse polymer chains are tethered; with an average distance of the anchor points **d** much smaller than the radius of gyration of the same unperturbed chains not in contact with the surface. This model describes the hydrodynamic properties of polymer brushes e.g. hydrodynamic thickness, permeability of a

brush and the force per area required to compress a brush. However, it does not attempt to examine the details of the conformations of polymer chains or the density profile of chain units at a distance from the grafting surface (158, 159). More sophisticated models have been developed to describe the segment density of the brushes, how the polymer chains are mixed or segregated in a mixed polymer brush of different chain length or different chemical composition, for surface-attached polymers in different regimes (mushoom, pancake, block and parabola)(124).

2.1.3 Synthesis of polymer brushes

A. Physisorption

Physisorption is a reversible process in which materials (i.e. small molecules or polymers) are non-covalently adsorbed to surfaces, tipically via van der Waals interactions. The characteristic dimensions of the structure depend on the selectivity of the surface, the interaction of the polymer to the substrate surface, solvent (161, 162) and the architecture of the polymer.

A non-covalent grafting (physisorption) is often not desirable as described in section 2.1.2. Polymer brushes in which the macromolecular chains are covalently bound to surfaces can be prepared by reacting anchor groups at the end or in a side chain of the polymer with appropriate sites at the surface or interface (chemical bonding), following a so-called 'grafting to' approach. Alternatively, polymer brushes can be obtained following a 'grafting from' strategy in which polymer

chains are grown from a surface functionalised with appropriate polymerisation initiators.

B. 'Grafting to' approach

The 'grafting to' approach involves reaction of reactive units present in the polymer chains with appropriate sites at the substrate (Figure 2.3) (163). End-functionalized polymer chains can be synthesized by anionic, cationic, living free radical and ring opening metathesis polymerisations (163-165).

Films generated by this approach are intrinsically limited in terms of brush density due to kinetic and thermo-dynamic restrictions. The steric hindrance provided by the grafted chains prevents the diffusion of further end-functionalised chains polymer to react with sites at the surface or they react at an extremely slow rate as the immobilization reaction proceeds (Figure 2.3). Thermodynamically, this reaction is unfavourable at high grafting densities as the polymer chain (attached to the surface) changes its conformation from coil to 'stretched like' resulting in entropy loss and hence inhibition of further attachment of polymer to the surface.

The synthesis of poly (styrene sulfonate) brushes was reported where polystyrene chains terminated by a reactive trichlorosilane groups were covalently grafted to silicon wafers using the 'grafting to' approach; and then the polystyrene brush was converted by sulfonation reaction with acetyl sulfonate (166).

Other groups also reported the attachment of 3-glycidoxypropyl trimeothoxysilane (GPS) to silicon wafers, to which then the carboxyl-terminated poly (2-vinylpyridine) (PVP) was grafted to the surface (167). Additionally, the graft of various thiol end-functionalised polymers to the surface was achieved using

reversible addition fragmentation chain transfer (RAFT) then attaching them to gold substrates via the sulphur linkage (168).

C. 'Grafting from' approach

'Grafting from' approach allows to overcome several shortcomings related to the 'grafting to' technique.

Polymer chains are either generated or self-assembled at the surface of the substrate functionalized with initiation sites and much higher graft densities can be obtained following the 'grafting from' approach (Figure 2.3). The properties of the brushes depend on the substrate (gold, silicon, nanoparticles), initiator deposition technique, polymer synthesis route (free radical, ring-opening metathesis or controlled radical polymerisation).

High graft densities were reported from a monocholorosilyl functionalised azo-initiator that was covalently attached onto a solid surface and the brushes were grown using free radical polymerisation (169, 170).

Controlled polymerisation techniques that can be used to produce uniform polymer brushes from silica and gold surfaces include ring-opening polymerisation (ROP) (171-173).

More controlled polymer brushes are produced when using controlled radical polymerisation (CRP) including Reversible Addition Fragmentation Chain Transfer (RAFT)(174, 175), nitroxide-mediated polymerisation (NMP)(176), and atom transfer radical polymerisation (ATRP) (177).

ATRP has been used to prepare well-defined copolymers of precise molar mass, composition and architecture when covalently attached to a flat or curved surface

compared to free radical polymerisation from surfaces. Surface-confined polymerisation with ATRP is beneficial as there is no polymerisation in solution, a quick rinse with solvent or water is sufficient to obtain clean surfaces free from adsorbed polymer. ATRP has been performed from flat silicon wafers (178) and gold substrates (179), nanopatterned networks (180), and highly functional linear polymers (181).

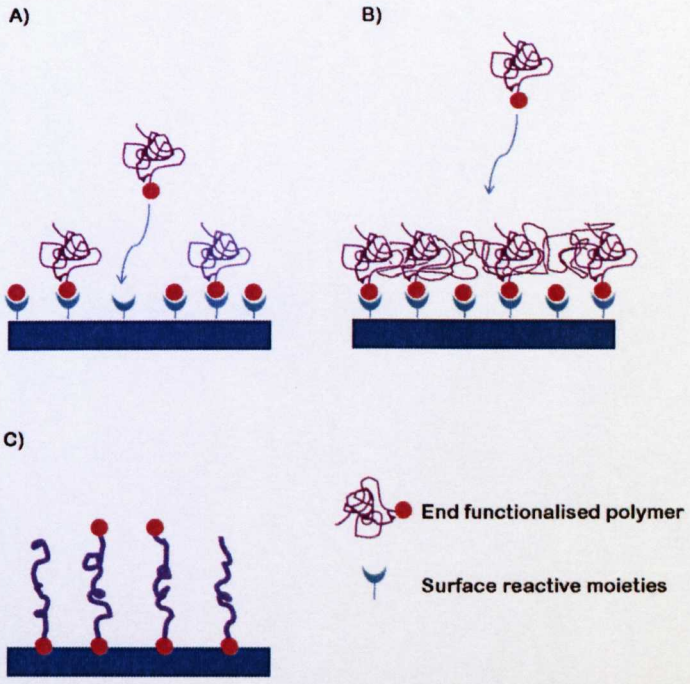

Figure 2.3. Schematic illustration of the 'grafting to' and 'grafting from' approach. **A.** Attachment of polymer end functionalised chains to the reactive moities at the surface; at low grafting densities, the chains reach the surface sites easily. **B.** As the grafting density of the attached polymer increases, a steric hindrance is created by the already attached polymer chains, so that the additional chains must diffuse through an existing polymer layer to reach the surface and this happens at an extremely slow rate. **C.** More controlled polymer brush densities using 'grafting from' approach.

2.1.4 Polymer brushes synthesis by Atom Transfer Radical Polymerisation

Atom transfer radical polymerisation (ATRP) has been extensively employed for the synthesis of polymer brushes from flat surfaces (182, 183); due to the easy experimental setup, use of readily accessible and inexpensive catalysts (usually copper complexes with pyridine based ligands, or aliphatic amines or imines). Mechanistically, ATRP is a radical process (184, 185), based on transition metal inner sphere electron transfer, where the added initiator **R-X** (**X** is halogen), attached to a surface (flat surface, particle or porous material), reacts reversibly with the transition metal catalyst ($\mathbf{M_t^n/L}$), where $\mathbf{M_t^n}$ is the transition metal in the lower oxidation state ***n*** complexed with an appropriate ligand ***L*** (aliphatic amines or imines, or pyridine based ligands); generating an oxidized transition metal halide complex ($\mathbf{X\text{-}\ M_t^{n+1}/L}$) and propagating radicals (**R***). The active radicals form at a rate ($\mathbf{K_{act}}$) and reversibly deactivate ($\mathbf{K_{deact}}$), but can also irreversibly terminate at a rate of $\mathbf{K_t}$. (186) (Scheme 2.1)

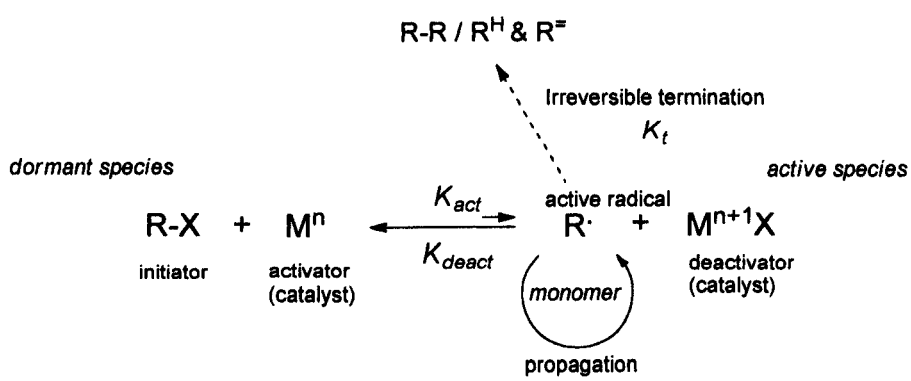

Scheme 2.1. Mechanism of metal complex-mediated Atom Transfer Radical Polymerisation (ATRP). $\mathbf{M_t^n}$: transition metal; **L:** complexing ligand; **R:** Polymer chain; **X:** Br or Cl.

2.2 Aims and objectives

The main aim of this thesis work was to generate thermo-responsive surfaces based on the MEO_2MA and OEGMA monomers as described in Figure 2.4 that shows schematic representation of the synthesis of poly (MEO_2MA-co-OEGMA) from the surface using ATRP.

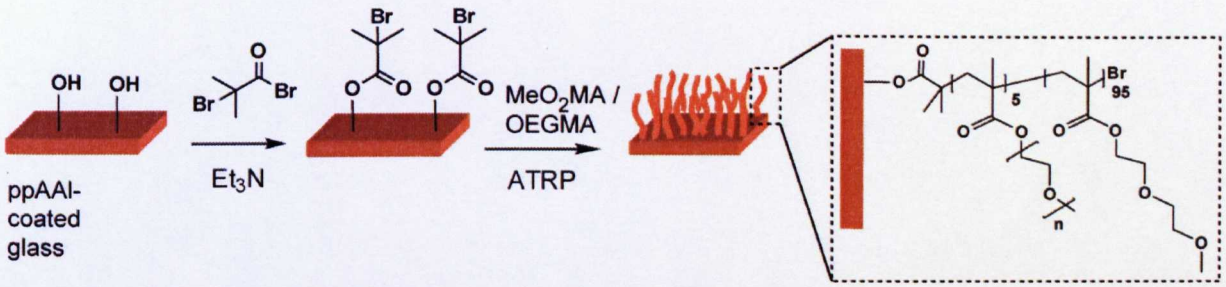

Figure 2.4. Schematic representation of initiator attachment to the plasma polymerised poly (allyl-alcohol) (ppAAl) and polymerisation of 2-(2'-methoxyethoxy) ethyl methycrylate-*co*-oligo(ethyleneglycol) methacrylate using a 'grafting from' ATRP approach.

The aim of this chapter was achieved though the following objectives:

- To prepare plasma polymerised poly (allyl-alcohol) (ppAAl) films using different plasma powers.
- To polymerise poly (MEO_2MA-co-OEGMA) from the initiation sites at the surface using ATRP.
- To analyse ppAAl and poly (MEO_2MA-co-OEGMA) substrates using X-ray photoelectron spectroscopy and Time of Flight Secondary Ion Mass Spectrometry.

- Thermo-responsive behaviour of the synthesised copolymer brushes was studied using water contact angle and atomic force microscopy.

2.3 Materials and Methods

2.3.1 Glass preparation

Glass coverslips (washed, cleaned and polished, VWR international) for coating with plasma polymers were first ultra-sonicated for 15 minute in ultrapure water, then washed and sonicated in acetone for another 15 minute and dried before use.

2.3.2 Plasma Treatment

The plasma reactor used in the experiments is shown in Figure 2.5. The plasma reactor consisted of a cylindrical borosilicated glass T-piece sealed with stainless steel end plates using Viton O-rings. A radiofrequency generator (13.56 MHz) was capacitively coupled to the glass deposition chamber via two external copper bands. The flow of ally alcohol vapour and oxygen into the glass chamber was adjusted using manual needle valves. The pressure in the chamber was maintained at below 20 millitorr (usually 10-15) before starting the deposition using a valve at the pumping line. A liquid nitrogen cold trap and alumina trap were used to prevent contamination of the rotary pump with condensable plasma products and the plasma reactor by pump oil (Fomblin). The allyl alcohol monomer (Figure 2.6) (sigma, UK) was degassed using a freeze thaw cycle for each power plasma experiment. The plasma treatment was performed at a power of 5 up to 100 W and

the reflected power reduced by tuning a manual matching on the radiofrequency generator.

The cleaned slides were placed in polystyrene 6-well plates as a support and introduced into the glass chamber. The cleaned glass substrates were oxygen plasma etched first for 5 minute under working pressure = 300 mTorr and at a power of 20 W and then treated immediately with plasma sustained in allyl alcohol vapour at a power of 5 up to 100 W under a working pressure of 300-370 mTorr (Table 2.1 with plasma polymerisation details), generating a plasma polymerised allyl alcohol (ppAAl) layer. The coated substrates were removed from the chamber and stored sealed at room temperature. Substrates coated with ppAAl were used for further studies following a minimum and maximum storage period of 48 h. The plasma chamber was cleaned with oxygen after each deposition (after each power) at a power of 20W and ~ 300 millitorr working pressure and the liquid nitrogen was topped up after each deposition.

Table 2.1. Details of the plasma polymerisation experiment (Power, thickness, time, incident, reflected, base pressure and working pressure).

Power (W)	Rate (A°/S)	Thickness (KA°)	Time (minute)	Incident	Reflected	Base pressure (millitorr)	Working pressure (millitorr)
5	2.5	1.498	10	5	0.3-0.5	13	320
10	2.8	1.501	9	10	0.8	14	315
15	3.0	1.478	9	15	0.5	14	330
20	3.8	1.470	10	20	0.1	15	330
50	4.5	1.490	5	50	0.3	14	343
75	4.2	1.475	7	75	4.5	14	350
100	3.5	1.454	7	100	8	13	360

A.

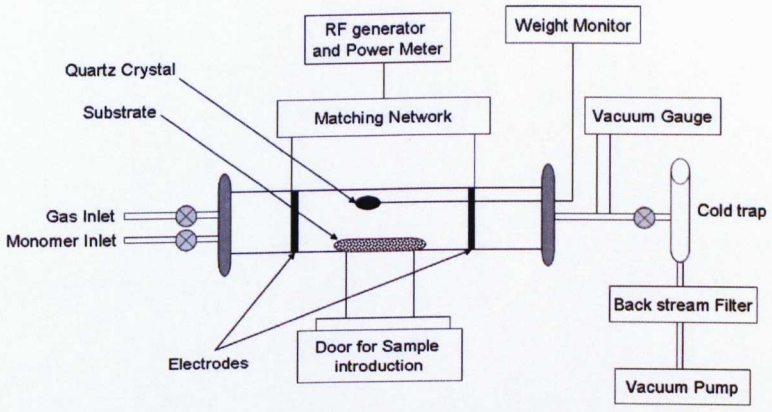

B.

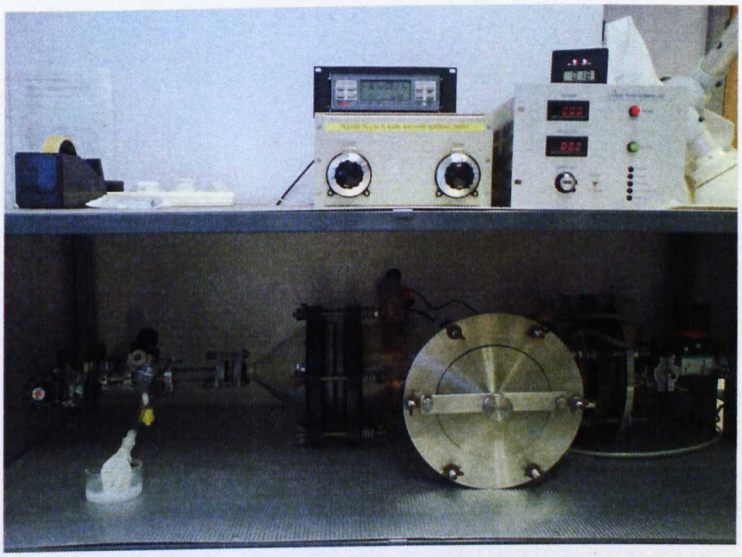

C.

Figure 2.5. A. Schematic diagram of plasma reactor used for these experiments. **B.** A photograph of the plasma reactor used in these experiments. **C.** A photograph of the plasma reactor during poly allyl alcohol deposition at power of 100 W.

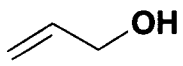

Figure 2.6. Chemical structure of allyl alcohol.

2.3.3 Surface initiated ATRP of Poly (MEO_2MA-co-OEGMA)

Glass substrates coated with ppAAl were placed in a Schlenk tube and treated with anhydrous THF (5 mL), triethylamine (0.5 mL) and 2-bromoisobutyryl bromide (1 mL) for 1 h at room temperature. The water contact angle was measured immediately after washing the surfaces with THF. The initiator-derivatised substrates were sealed into Schlenk tubes (using a septum and parafilm) and a solution of MEO_2MA (1.5 mL; 8.1 mmol) and OEGMA (0.5 mL; 0.9 mmol) was added to the tube. Degassed ethanol (~5 mL) was used to prepare a solution of CuBr (14 mg; 0.09mmol) and 2, 2'-bipyridine (28 mg; 0.18 mmol) which was then added to the Schlenk tube. The glass slides were immersed in the polymerisation solution under argon for the first 30 minute and then at room temperature overnight stirring using a plate stirrer at 50 rpm for the polymerisation mixture to mix. The glass substrates were washed subsequently with THF and cold H_2O to remove any unreacted monomers and solution grown polymer. Poly (OEGMA) grafted substrates were prepared using ATRP for AFM studies using 2 mL of OEGMA, 5 mL of degassed ethanol and a solution of CuBr (14 mg) and 2,2'-bipyridine (28mg).

2.3.4 Surface characterisation

2.3.4.1 Water contact angle (WCA) measurements

Static WCA measurments of the copolymer brushes was determined from sessile WCA measurements taken using distilled water using a CAM 200 sessile drop video capture apparatus from KSV Instruments LTD. The temperature of the substrate was maintained above and below the LCST by placing the substrate in an oven at 37°C or 20°C on a thermostatic block.

The water drop was gently placed onto the sample surface using a syringe and 20 images were taken at 1s intervals. The drop profile was fitted using the Young/Laplace equation and a linear regression was used to estimate the initial WCA at the point the drop formed on the surface. Readings were taken at five different positions on the glass substrate and the average and standard deviation are reported.

2.3.4.2 X-ray photoelectron spectroscopy (XPS)

Sample surfaces were analysed using the Kratos Axis Ultra with a mono-chomated Al K_α X-ray source (1486.6eV) operated at 15 mA emission current and 10 kV anode potential. The spectrometer was operated in fixed analyser transmission mode, with a pass energy of 80 eV for wide scans and a pass energy of 20 eV for high resolution scans. All samples were analysed at thee positions using an analysis area of approximately 300x700 μm defined by the slot aperture. Survey scans were acquired for 10 minute each and high resolution scans for up to

10 minute depending on the signal to noise observed. The survey scans had a step size of 0.5 eV and the high resolution, 0.1 eV. Samples were inserted into an airlock and the chamber was evacuated for approximately 30 minute before transfer of the samples into the main ultra high vacuum chamber. Electrons emitted from the top surface were taken though an electrostatic/magnetic lens system (hybrid lens) and a hemispherical analyser with electron detection and counting achieved with a delay line detector (DLD). The pressure in the analysis chamber was maintained at 3 $x10^{-9}$ Torr or less thoughout. The high resolution scans were charge corrected to the aliphatic component of the C1s core level (285.0 eV) for chemical state assignment and the areas quantified to compare the amounts of each element present, using CasaXPS software version 2.3.12 with empirically modified sensitivity factors provided by the manufacturer.

2.3.4.3 Atomic Force Microscopy (AFM)

AFM was used to characterise the topography of surfaces and to measure the adhesion force between Si_3N_4 AFM tip and polymer under water at variable temperatures to determine the surface change between hydrophilic and hydrophobic polymer states.

Glass surfaces grafted with poly (MEO_2MA-co-OEGMA) were rinsed with cold water, dried under a stream of nitrogen and mounted on a disc prior to AFM investigations. AFM studies were performed using multimode microscope and scanner (Veeco, Santa Barbara, USA) was used (Appendix 4).

Topography and adhesion measurements were conducted using V-shaped-silicon nitride cantilevers with a standard tip profile (4 cantilevers spring constant 0.06-

0.58 N/m tip height: 2.5 μm-3.5 μm from Veeco). Topographic imaging was performed in air and in water using a closed wet cell, modified to allow variable temperature adjustment. Contact mode imaging utilized an applied load and scan rate limited to ca. 1nN and 3 Hz, respectively, to minimize compression and lateral damage to polymer grafts and underlying surfaces.

Surface roughness measurements, expressed in terms of the roughness average, Ra, were obtained by topographically imaging polymer surfaces over a scan area of 5*5 μm.

Scanning probe atomic force microscopy was conducted in ultrapure water and at controlled temperatures using a MultiMode atomic force microscope (Digital instrument, Veeco) with a heating accessory (Appendix 4). The copolymer grafted glass slides were cut into 1x1 cm glass slides and mounted on top of the heater for imaging in ultrapure water (18 MΩ resistivity) at variable temperatures from 37°C to 20°C and adhesion force measurements taken at every 2°C; using the same sample, measurements were also taken in the reverse order (i.e. from 20°C to 37°C). The sample was equilibrated for 10 minutes at each temperature prior to measuring the adhesion force. Thee samples were examined that were prepared at different days and thee readings were taken at each temperature point and the average and standard deviation are reported. Poly (OEGMA) substrates were used as the control to study the adhesion forces at 37°C to 20°C.

2.3.4.4 Time of Flight Secondary Ion Mass Spectrometry (ToF-SIMS)

Time of Flight-Secondary Ion Mass Spectrometry data acquisition was carried out using SIMS IV time of flight instrument (ION-TOF GmbH, Munster, Germany)

equipped with a Bi^{+3} metal ion gun and a single stage reflectron analyzer. The instrument was operated at primary ion energy of 15 kV, a pulsed target current of 1.3 pA and a post acceleration of 10 kV. All doses were kept below the static limit, with a maximum dose of 10^{12} ions per cm^2 for both polarities combined. Raw data files were analysed using IonSpec TOF-SIMS software (ION-TOF GmbH). Mass calibration of the positive and negative spectra were calibrated to the H^+ and CH_3^+ peaks and H^-, O^- and OH^- peaks, respectively before further analysis. Peak lists were created after peak evaluation of each spectrum. The Tof-SIMS spectra of each treatment was normalised using the total counts of that surface for an area of 500 μm^2 that was analysed at a resolution of 256×256 pixels. Topographical images of characteristic positive and negative ion peaks of the samples were composed using Ion Image Software (ION-TOF GmbH). These offer pictorial representation of the ion species found on the surfaces of the thee different samples.

2.4 Results and Discussion

2.4.1 Plasma deposition of poly allyl alcohol (ppAAl) using different powers

Uncoated cleaned glass was analysed using XPS. It was established that the glass slide contained elements such as Si, Ca, B and Na indicating a silica glass with soda, lime and borate (Figure 2.7 and Table 2.2). Allyl alcohol was used in these experiments to provide hydroxyl groups for surface initiated polymerisation as it was shown that the amount of hydroxyl retained in the plasma polymerised allyl alcohol (ppAAl) was consistently higher compared to propargyl alcohol (another monomer commonly used in plasma polymerisation to produce hydroxylated polymers) at all plasma power levels (187). The surfaces were analysed by XPS after ppAAl deposition at different powers and after the treatment with 2-bromoisobutyryl bromide for each substrate. Spectra were corrected for sample charging by setting the C1s signal to 285 eV. A film of ppAAl was sufficiently thick to hide the substrate signal (Si2p and Si2s) in the subsequent XPS analysis was obtained after ~ 10 min of ppAAl deposition. Plasma polymers of ally alcohol were produced under a range of powers from 5 W to 100 W. Figure 2.8 to Figure 2.14 shows the wide scans of ppAAl deposited at different powers overlaid with the wide scans of ppAAl-2-bromo-isobutyrate surfaces. Only carbon and oxygen were amongst the dominant elements detected in the spectrum of ppAAl, and the 1s levels of carbon and oxygen occur at 285 and 530 eV, respectively. This indicated that the glass substrate (Si) was covered with a thickness greater than the

analysis depth of XPS which is 10 nm.Table 2.2 shows that elements of glass were present on the surface after the deposition of ally alcohol at 5, 10, and 15 W (including Na1s and NaKLL); which was hidden when the power of deposition was increased to 20 W and above indicating thicker films formed in the fixed deposition time.

Table 2.2. Elemental composition determined using XPS for ppAAl deposited at different powers. The binding energies (**eV**) for the present elements on the surface are as follows: **C1s**: 285.1, **O1s**:530, **Si2p**: 102, **NaKLL**: 497, **MgKLL**: 307, **Ca2p**: 352, **Zn2p**: 1016, **K2p**: 287, **B1s**: 189.

Name	Glass	5W	10W	15W	20W	50W	75W	100W
C1s	19.8±0.2	78.8±0.9	80.2±0.1	83.4±3.1	85.7±0.2	89.9±0.6	90.7±0.1	90.8±1.3
O1s	52.4±0.6	20.7±0.7	19.2± 0.3	16.3±3.0	14.1±0.0	10.1±0.6	9.3 ±0.1	9.1±1.3
Si2p	17.6 ±0.3	-	-	-	-	-	-	-
NaKLL	5.8 ±0.1	0.5±0.2	0.53±0.28	-	-	-	-	-
MgKLL	-	-	-	-	-	-	-	-
Ca2p	-	-	-	-	-	-	-	-
Zn2p	1.6±0.02	-	-	-	-	-	-	-
K2p	0.2±0.01	-	-	-	-	-	-	-
B1s	2.5±0.3	-	-	-	-	-	-	-

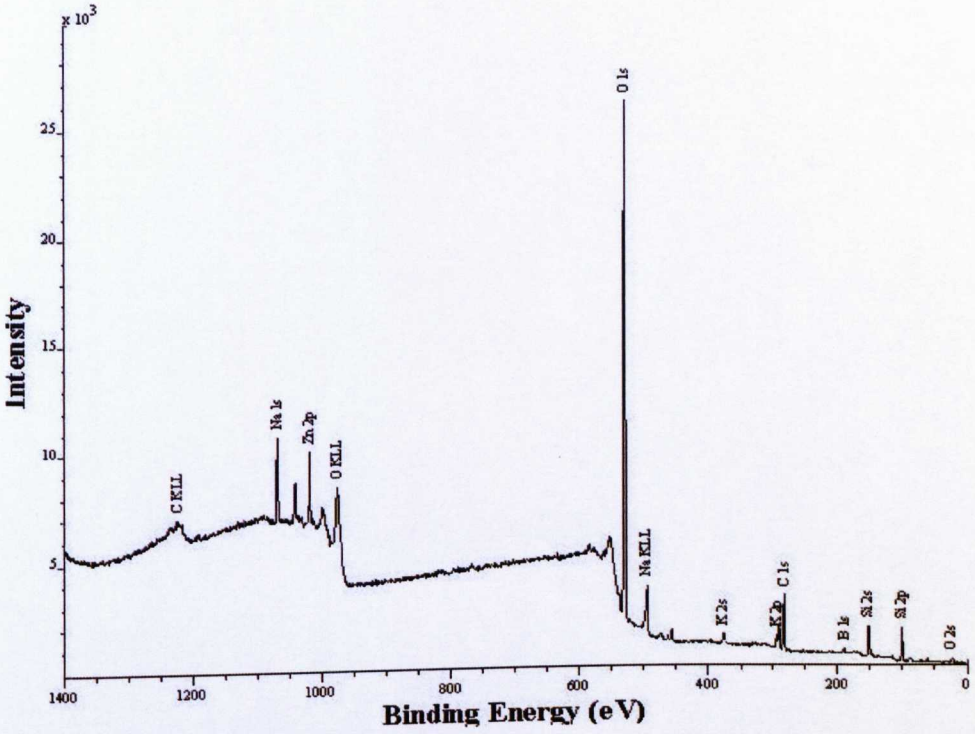

Figure 2.7. XPS survey scan of a cleaned glass substrate.

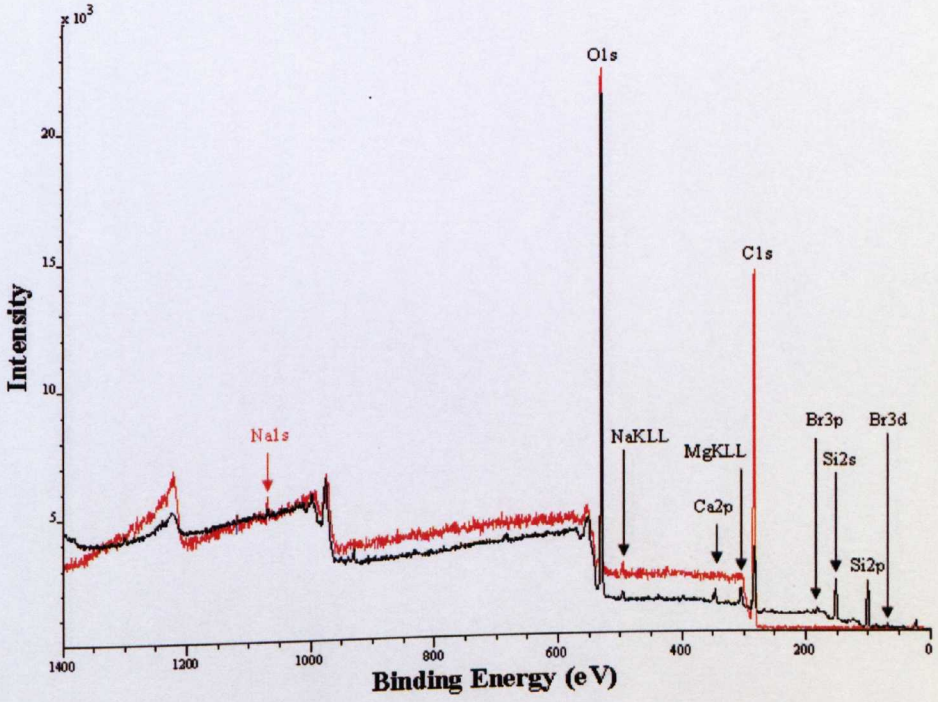

Figure 2.8. XPS wide scan spectra of ppAAl deposited at power = 5W (in red) and after treatment with 2 bromoisobutyryl bromide (in black).

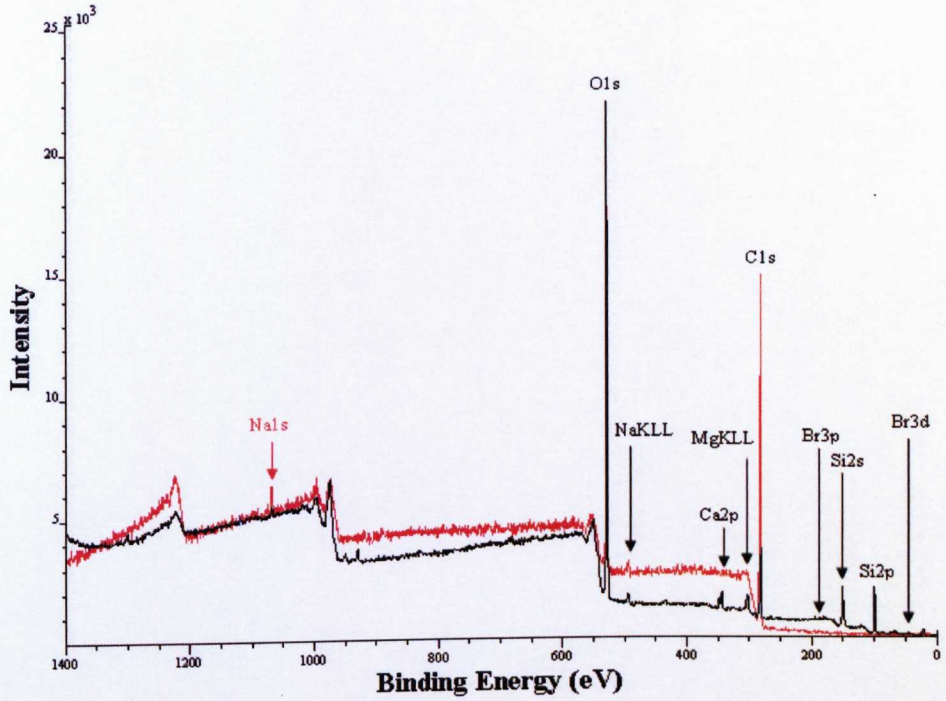

Figure 2.9. XPS wide scan spectra of ppAAl deposited at power = 10W (in red) and after treatment with 2 bromoisobutyryl bromide (in black).

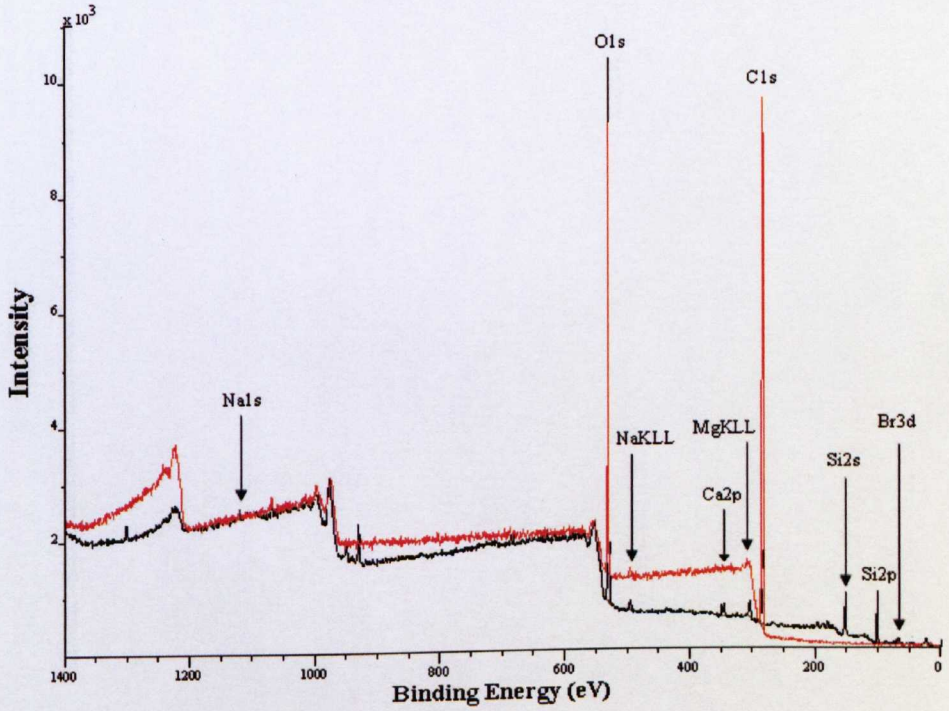

Figure 2.10. XPS wide scan spectra of ppAAl deposited at power = 15W (in red) and after treatment with 2 bromoisobutyryl bromide (in black).

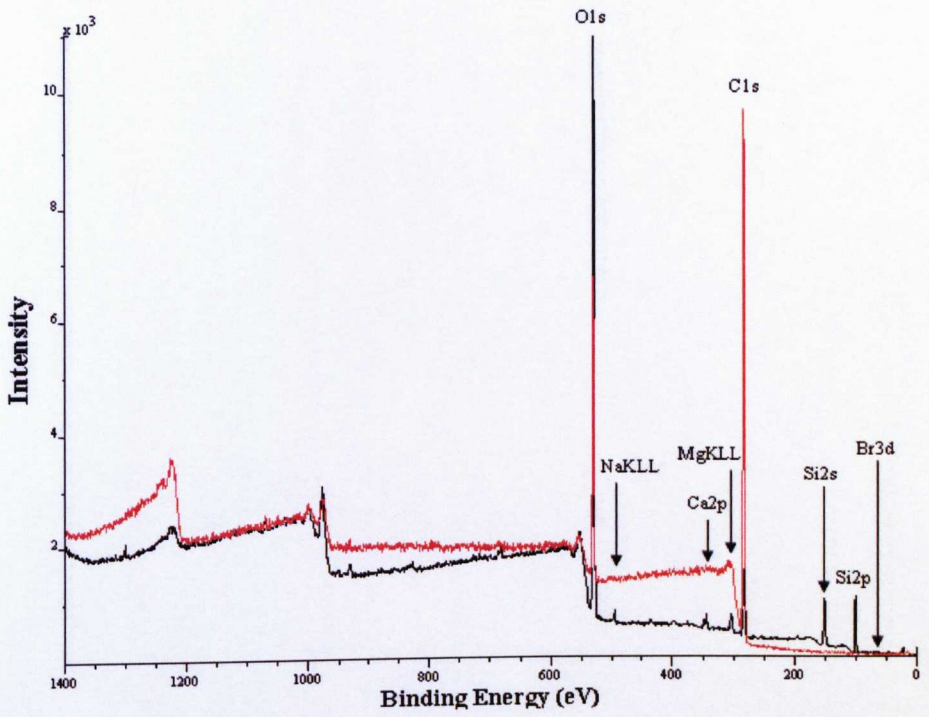

Figure 2.11. XPS wide scan spectra of ppAAl deposited at power = 20W (in red) and after treatment with 2 bromoisobutyryl bromide (in black).

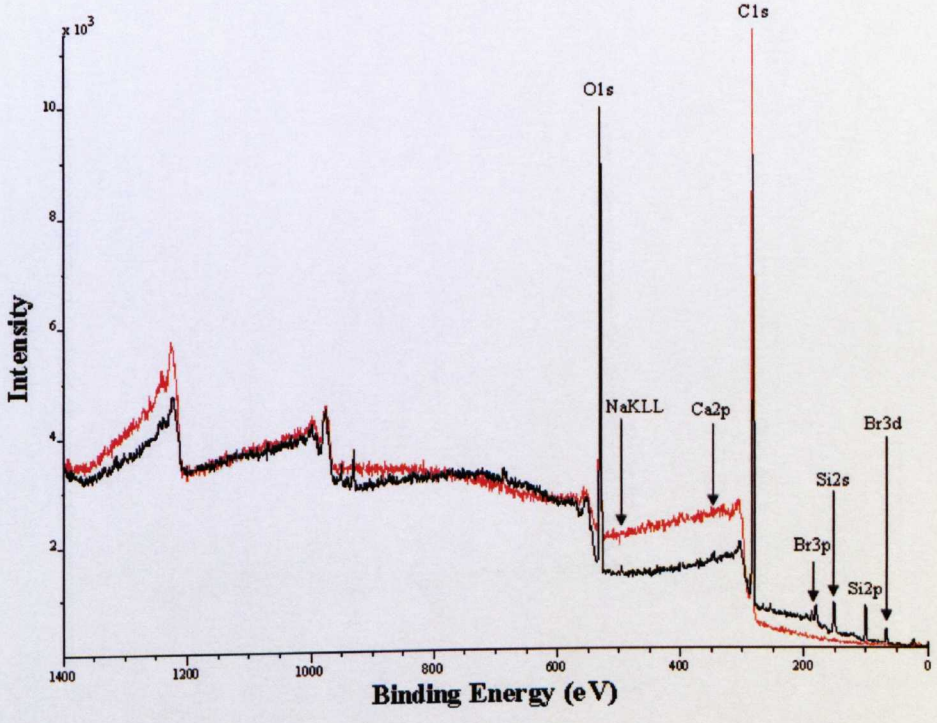

Figure 2.12. XPS wide scan spectra of ppAAl deposited at power = 50W (in red) and after treatment with 2 bromoisobutyryl bromide (in black).

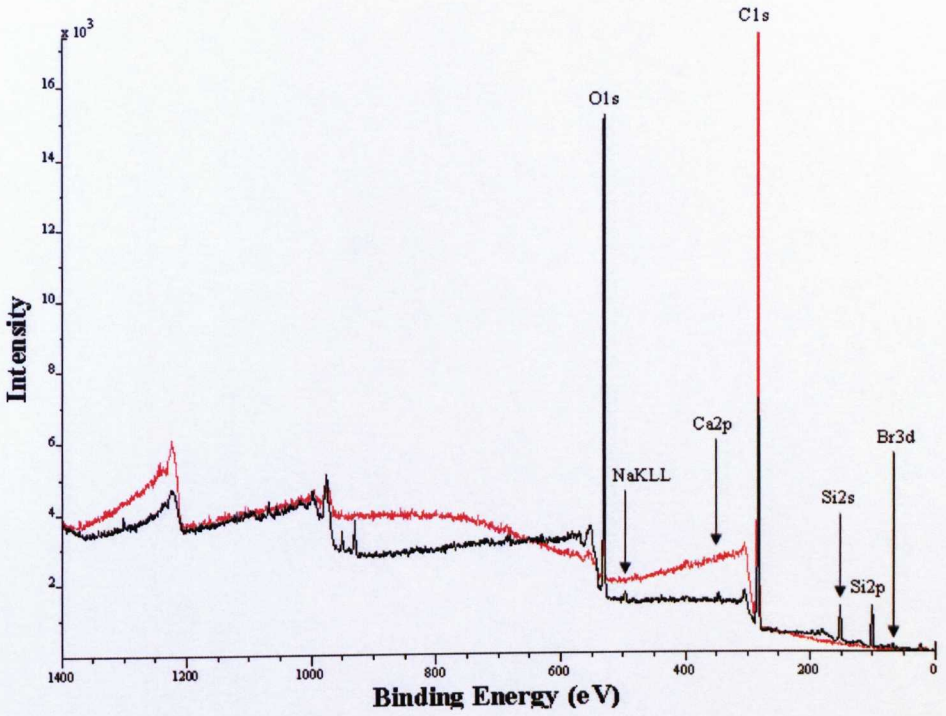

Figure 2.13. XPS wide scan spectra of ppAAl deposited at power = 75W (in red) and after treatment with 2 bromoisobutyryl bromide (in black).

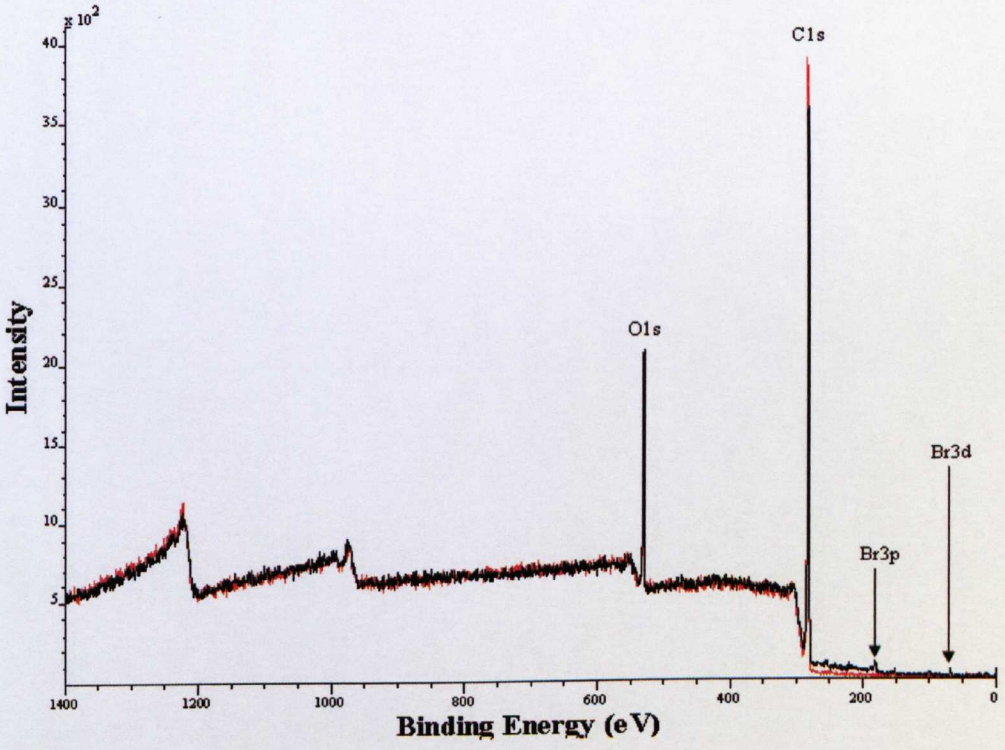

Figure 2.14. XPS wide scan spectra of ppAAl deposited at power = 100W (in red) and after treatment with 2 bromoisobutyryl bromide (in black).

Figure 2.15 shows the effect of plasma deposition power upon the elemental composition of ppAAl determined by XPS. These data illustrate that increasing power reduces the oxygen concentration of the deposit from 20.7 ± 0.7 at 5 W to 9 ± 1.3 at 100 W (Table 2.2 and Figure 2.15) i.e. this shows a deficiency of oxygen as the power increases while the concentration of carbon increases from 78 ± 1.3 at 5 W to 90 ± 1.3 at 100 W. This may be explained by increased fragmentation of the allyl alcohol monomer as the power increases, leading to an increase in cross-linking of the deposit as C-C/C-H accompanied by loss of oxygen to the deposit (188, 189).

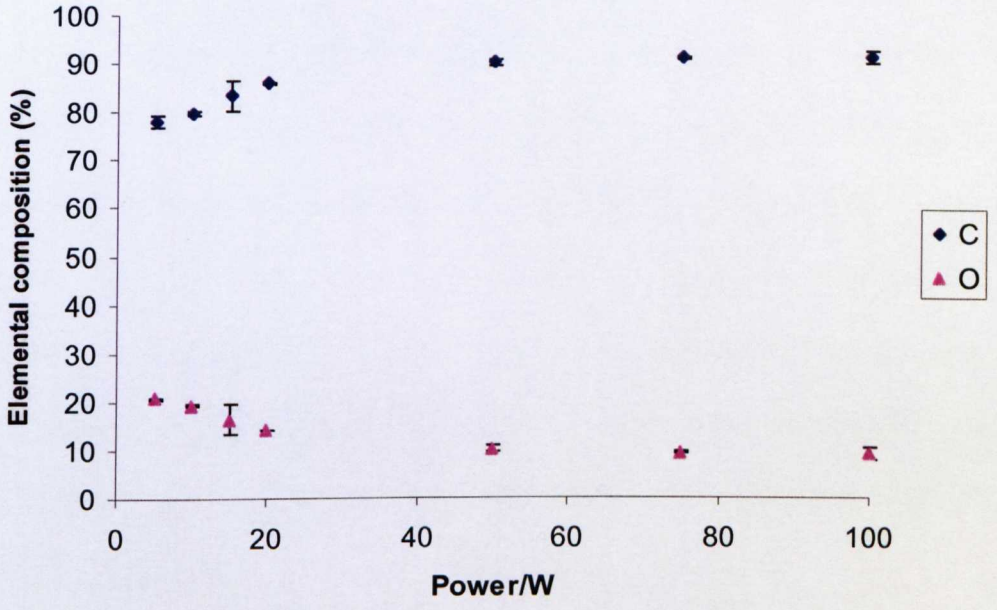

Figure 2.15. The elemental composition determined by XPS analysis of ppAAl versus plasma input power. This shows that as the plasma power increases, oxygen concentration decreases and carbon elemental composition increases.

Analysis of the C1s core level allows the functional composition of the surface to be investigated after the deposition of ally alcohol at different powers.

The following functionalities were fitted: alcohol/ether (C-OH/R) at a shift (from the C-C peak) of + 1.5 eV; carbonyl (O-C-O/C=O) at +3.0 eV; carboxylic acid/ester (COOH/R) at 4.0 eV (Figure 2.16) (190).

The retention of hydroxyl functionalities in ppAAl was first shown by Short *et al.* who suggested that by using C1s core level fits, hydroxyl groups content could be estimated under the assumption that the amount of alcohol was directly related to the COH/R peak. This required that the amount of ester is minimal, which is a reasonable consideration given the disparity between the intense COH/R and weak COOH/R signals for all ppAAl. This is estimated by dividing the proportion of carbons in hydroxyl functional groups in the plasma polymer by those in the monomer (33.3%) we may therefore estimate the retention of hydroxyl groups in the ppAAl deposit relative to the monomer (190-192). The carbon in hydroxyl groups was found to be 27.6, 22.3, 14.1 and 12.2 % for ppAAl deposited at 5, 20, 50 and 100 W respectively from high resolution C1s analysis. Then the retention (%) of hydroxyl functionality in the ppAAl deposited was calculated relative to the monomer and it was found to be 82%, 66.9%, 42% and 36% at 5, 20, 50 and 100 W respectively.

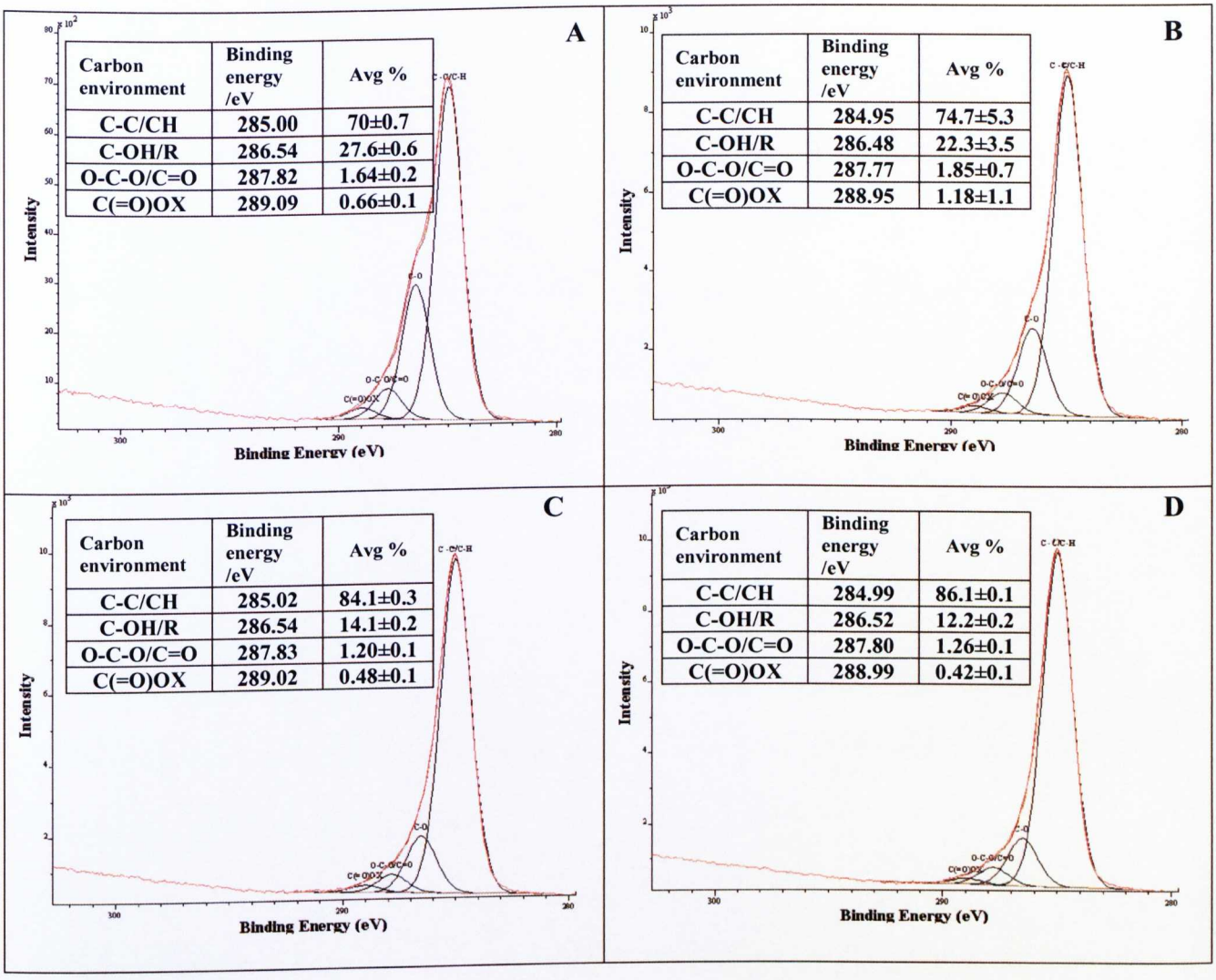

Figure 2.16. C1s core level high resolution spectra recorded for ppAAl (**A.**5 W, **B.**20 W, **C.**50 W, **D.**100 W) representing the following main peaks; **C-C/C-H** (polymer backbone), **C-OH/R** (alcohol/ether), **O-C-O/C=O** and **C (=O) OX**.

At low power, the plasmas can be described as energy deficient, a regime characterised by high retention of monomer functionality in the plasma polymer deposit, and exhibiting a low deposition rate which explains the highest hydroxyl group retention (82%) (188).

At high power, the plasmas can be described as monomer deficient with the deposits featuring a loss of functional group relative to the monomer, compared to the deposits at lower power, exhibiting higher deposition rates, which leads to more fragmentation of the allyl alcohol monomer (188). This indeed was observed during the plasma polymerisation process (section 2.3.2) as shown in Table 2.1 where the deposition rate was increased from 2.5 A°/S at 5 W compared to 2.8 A°/S, 4.5 A°/S and 3.5 A°/S for 20, 50 and 100 W respectively.

2.4.2 XPS analysis of ppAAl-2-bromo-isobutyrate surfaces

Substrates coated with ppAAl at different powers (5 to 100 W) were treated with 2-bromoisobutyryl bromide in the presence of anhydrous triethylamine and anhydrous tetrahydrofuran as described in section 2.3.3.

Table 2.3 includes the elemental compositions of ppAAl-2-bromo-isobutyrate treated surfaces. The elemental composition of Si2p decreased from 15.4 % to 1.5 % as the power was increased from 5 to 100 W indicating that the treatment (to produce initiation sites using 2-bromoisobutyryl bromide) affected the ppAAl deposited films at lower powers.

This could be due to the deposition rate influencing the thickness of the ppAAl layer deposited at the highest power i.e. 100 W and hence less Si2p elemental composition 1.5% after the treatment with 2-bromoisobutyryl bromide. In addition, the percentage of Br3d at lower power or higher did not change significantly as indicated in Table 2.3 (0.7 ± 0.2 or 0.6 ± 0.3 at 5 W and 100 W respectively).

Therefore, on that basis, surfaces with ppAAl deposited at 100 W were used for further treatments (surface-initiated polymerisation).

Table 2.3. Elemental composition determined by XPS for ppAAl-2-bromo-isobutyrate surfaces. The binding energy for **Br3d** is 66.7 eV.

Name	Glass	5 W	10 W	15 W	20 W	50 W	75 W	100 W
C1s	18.2±0.5	36.8±1.9	27.5±3.5	27.7±1.3	28.0±8	68.2±1.4	51.7±0.7	85.7±4.3
O1s	52.5±0.3	45±1.2	48.6±2.7	49.9±1.0	44.4±3.9	23.2±3.2	35.7±2.9	12.8±1.0
Si2p	18.2±0.2	15.4±2.3	18.3±0.5	17.4±0.8	17.5±3.2	5.2±0.9	9.5±1.2	1.5±0.9
NaKLL	5.8±0.8	0.9±0.3	0.8±0.3	0.7±0.01	2.8±0.3	0.4±0.02	0.5±0.05	-
MgKLL	-	-	2.6±0.3	2.8±0.04	3.9±1.8	1.2±0.4	1.5±0.3	-
Ca2p	-	0.8±0.7	1.0±0.4	1.1±0.2	2.2±0.03	0.3±0.03	0.4±0.02	-
Zn2p	1.6±0.01	-	-	-	-	-	-	-
K2p	0.1±0.03	-	-	-	-	-	-	-
B1s	3.4±0.5	-	-	-	-	-	-	-
Br3d	-	0.7±0.2	0.6±0.07	0.6±0.1	0.5±0.06	0.7±0.2	0.5±0.2	0.6±0.3

The thickness of the ppAAl after the second treatment with 2-bromoisobutyryl bromide was calculated using equation 2.1, Si2p was selected to be the main component of the glass substrate and C1s core level from the top layer of the substrate of the ppAAl (193, 194).

$$dc = - Lc\,(Ec)\cos\theta.\ln\{1-Ic/Ic_{\infty}\}$$

Equation 2.1. dc: thickness, **Lc(Ec)**: the effective attenuation length at the energy of the C1s photoelectrons of energy **Ec** in the top layer (core level) (=3.6nm)(195), **θ**: take off angle, **Ic**: the intensity of the C1s core level, $\mathbf{Ic_{\infty}}$: The intensity of carbon determined from the intercept with the y-axis of a plot of C1s (from overlayer of the polymer) against Si2p (from glass).

Table 2.4 shows the details of the calculated thickness of the ppAAl using equation 2.1 the thickness dc (nm) was increased from 1.9 to 11 nm for substrates treated at 5 and 100 W respectively.

Table 2.4. Details of the calculated thickness using equation 1 plotted against Br3d elemental composition (%).

P/W (W)	C1s intensity	dc (nm)	Br 3d
5	4000	1.9374	0.7 ± 0.2
10	3800	1.811	0.6 ± 0.07
15	1420	0.57	0.6 ± 0.1
20	1460	0.59	0.5 ± 0.06
50	3100	1.402	0.7 ± 0.2
75	1340	0.54	0.5 ± 0.2
100	9200	11.345	0.6 ± 0.1

From Table 2.4 and Figure 2.17 the thickness (dc) of the top layer (ppAAl-2-bromo-isobutyrate) surfaces increased from 1.9 nm for surfaces previously plasma polymerised at a power of 5 W to 11 nm at 100 W. This indicates that the following treatment to the ppAAl, i.e. 2-bromoisobutyryl bromide in the presence of THF and triethylamine, do not alter the physicochemical properties of the ppAAl coated substrates at 100 W due to the cross linked layer produced by the highest power.

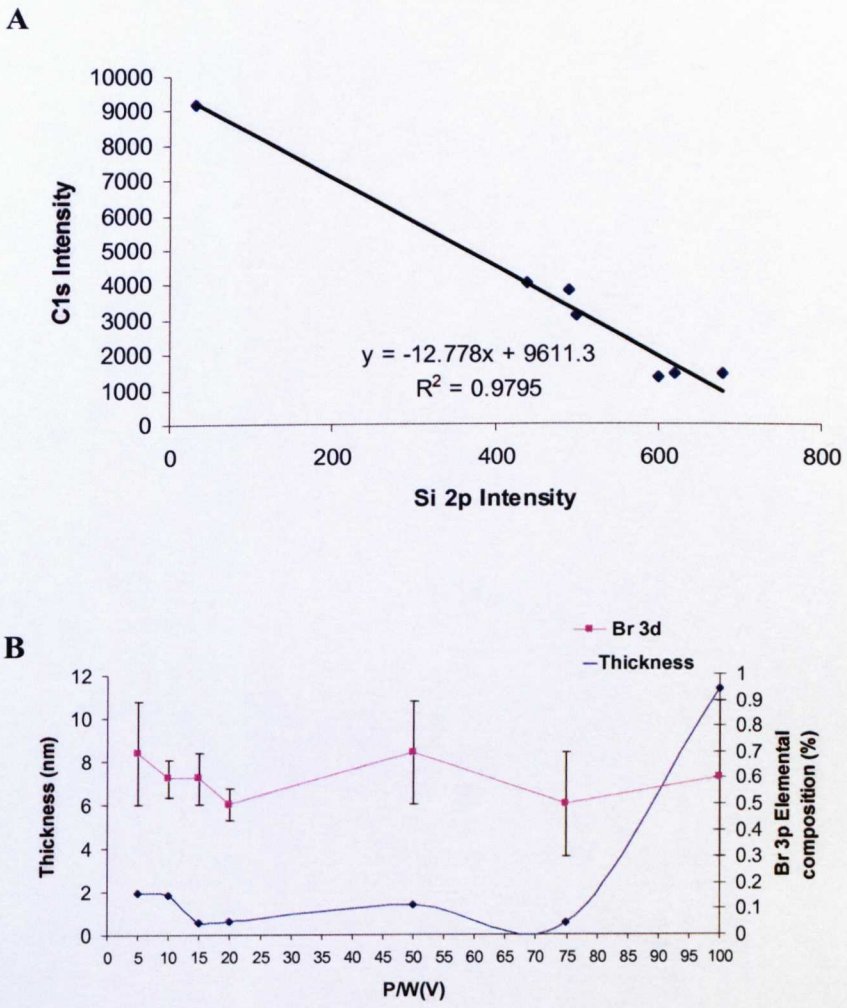

Figure 2.17. A. The relationship of the C1s and Si2p intensities. **B.** The carbon overlayer calculated thickness (dc in nm) derived from equation 2.1 against the concentration of the Br 3d.

2.4.3 Poly (MEO_2MA-co-OEGMA) polymerisation and XPS analysis

From the above results, we concluded that surfaces coated with ppAAl at a power of 100 W is the one that is resistant to the treatment with the initiator (2-bromoisobutyryl bromide) in the presence of THF and triethylamine anhydrous. Therefore, they were selected for further polymerisation at room temperature with

MEO_2MA and OEGMA in ethanol using CuBr and Bipy for overnight. Plasma polymerisation of allyl alcohol and subsequent synthesis of immobilised ATRP initiators were repeated and the copolymer was ATRP polymerised from freshly prepared surfaces.

Table 2.5. Elemental compositions for ppAAl surfaces, ppAAl-2-bromo-isobutyrate surfaces and Poly (MEO_2MA-co-OEGMA) graft surfaces.

Assignments	Quantification (Atomic %)		
	ppAAl	ppAAl-2-bromo-isobutyrate	Poly (MEO_2MA-co-OEGMA)
C1s	85.2 ± 0.1	85.05 ± 1.5	74.8 ± 1.2
O1s	14.8 ± 0.3	12.3 ± 1.11	18.44 ± 0.8
Si2p	-	1.2 ± 0.3	-
NaKLL	-	0.5 ± 0.05	0.7 ± 0.01
Ca2p	-	-	1.6 ± 0.2
Zn2p	-	-	0.24 ±0.3
Br3d	-	0.7 ± 0.08	0.21 ± 0.03
MgKLL	-	-	4.01 ± 0.04

XPS analysis showed that poly (MEO_2MA-co-OEGMA) was grafted from the surface as the elemental composition of the bromine (originally contained in the ppAAl-2-bromo-isobutyrate substrates) decreased from 0.7 % to 0.21 % illustrating that polymer brushes are grafted from the surface using ATRP. The elemental percentage for carbon and oxygen were 74.8 % and 18.44 % respectively compared to 85% and 12 % elemental composition detected on ppAAl-2-bromo-isobutyrate surfaces indicating that the composition of the surface is different after grafting MEO_2MA and OEGMA from the previous treatment.

Table 2.6. XPS C1s core level curve fit results for polymer graft surfaces

Assignments	Peak energy/eV	Quantification (%)	Notes
C -C/C-H	285.021	77.4 ± 0.7	Polymethacrylate backbone
O-C(=O)-C-CH_3- secondary shift	285.721	2.9 ± 0.09	Ester repeating unit
C-O	286.659	13.4 ± 0.46	
O-C-O/C=O	287.835	3.4 ± 0.1	
C(=O)OX	289.221	2.87 ± 0.08	

Table 2.5 and Figure 2.18A indicates the elemental composition after ATRP grafting of poly (MEO_2MA-co-OEGMA); no silica signal was detected which shows that the polymer layer is greater than 10 nm (XPS depth analysis). The presence of sodium from the glass could be due to the mobility of this species allowing it to contaminate the upper surface.

Table 2.6 and Figure 2.18B shows the C1s core level after the grafting which is characterised by the O-C(=O)-C-CH_3- at 285.7 eV indicative of end group of poly (OEGMA). A similar C1s high resolution was previously reported by Lutz *et al*(196).

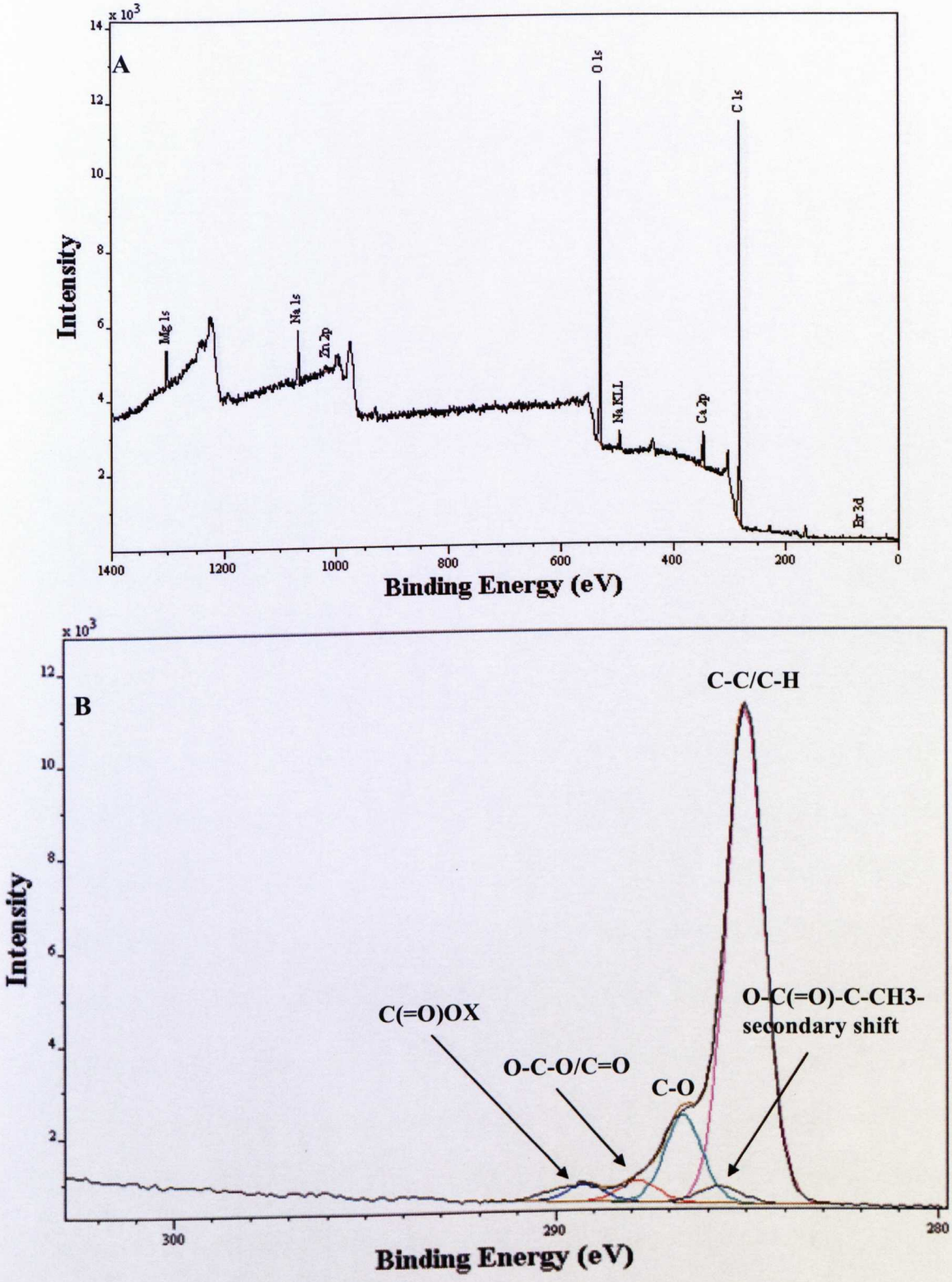

Figure 2.18. A. XPS wide scan of poly (MEO_2MA-co-OEGMA). **B.** C1s core level spectra recorded after growth from the surface of poly (MEO_2MA-co-OEGMA) brushes via ATRP. Component peaks from the poly (methacrylate) backbone include C-C/C-H and C (=O) OX and the end group of poly (OEGMA).

2.4.4 ToF-SIMS characterisation

In Figure 2.19 (A-D), the positive ToF-SIMS spectra of glass, ppAAl, ppAAl-2-bromo-isobutyrate surfaces and after ATRP polymerisation of (MEO_2MA-co-OEGMA) surfaces are displayed.

The positive spectrum of the glass contained mainly glass elements as indicated from the XPS data (Table 2.2) including Na^+ at 23 m/z, Mg^+ at 24 m/z and Si^+ at 28 m/z (Table 2.7, and Figure 2.19A). These signals disappeared when the glass was treated with ppAAl deposition (Figure 2.19B).

In the low mass range (m/z 0-40) of the positive spectrum of ppAAl, the majority of the peaks are assigned to the general hydrocarbon ions including $C_2H_2^+$ (at m/z 26), $C_2H_3^+$ (at m/z 27), CH_3O^+ (at m/z 29), $C_3H_2^+$ (at m/z 38) and $C_3H_3^+$ (at m/z 39). In the high mass range (m/z 40-150) the peaks are assigned to the oxygen containing ions e.g. peaks at m/z 43.02, 45.03, 55.02, 57.03, 67.02 are of greater intensity which corresponds to $C_2H_3O^+$,$C_2H_5O^+$, $C_3H_3O^+$, $C_3H_5O^+$ and $C_4H_3O^+$ respectively. A more detailed list of the characteristic ions and their masses are indicated in Table 2.7. This agrees with the literature as these ions were seen previously in the gas-phase plasma mass spectrometry (MS) of the ppAAl (190, 192). Other ions that were seen in the spectrum including C_5H_9 at 69 m/z, C_6H_9 at 81 m/z and C_7H_7 at 91 m/z (Table 2.7); these peaks thought to be the result of the monomer fragmentation during plasma polymerisation at a high power of 100 W (Figure 2.19.B). Similar Positive spectrum was reported by Oran *et al.* as other secondary ions e.g. C_5H_9 were present after plasma polymerisation of allyl alcohol at a lower power (20 W) (197).

After the treatment of the ppAAl with 2-bromoisobutyryl bromide in the presence of THF and triethylamine; the following signals were of great intensity in the positive spectra, C_2H_5 at 29 m/z, C_2H_3O at 43 m/z, C_2H_5O at 45 m/z, C_3H_7O at 59 m/z, C_5H_9O at 69 m/z and the m/z 132 is dominant in the high mass region m/z 100-200 corresponding to $C_{11}H_2^+$ (Table 2.7 and Figure 2.19C). However, ToF-SIMS analysis did not reveal any bromine containing adducts.

Poly (MEO_2MA-co-OEGMA) obtained by ATRP polymerisation from ppAAl-2-bromo-isobutyrate surfaces was also analysed. Signals of high intensity at m/z 26, 32, 45, 48, 68, 83 and 119 which correspond to $C_2H_2^+$, CH_4O^+,$CaOH^+$, $C_5H_8^+$, $C_6H_{11}^+$, and $C_9H_{11}^+$ respectively (Figure 2.19D and Table 2.7).

Peaks at m/z 45, 67, 71 and 100 corresponding to the high contaning oxygen species $C_2H_5O^+$, $C_4H_3O^+$, $C_4H_7O^+$and $C_6H_{11}O^+$ were thought to be indicative of the methoxy containing groups in the copolymer brushes.

The elements from the glass including Na^+ and Si^+ signals were no longer detected when the surface was treated with ppAAl.

Additionally, ppAAl-2-bromo-isobutyrate surfaces did not display any of the glass signals confirming the XPS data that showed the surfaces treated with 100 W is not affected by triethylamine and THF when reacting the hydroxyl groups with 2-bromoisobutyryl bromide. However, Na^+ was detected after the ATRP polymerisation which again confirms the XPS data (Table 2.5 and Figure 2.18.A). This could result from the mobility of these species leading to the contamination of the surface during analysis.

A

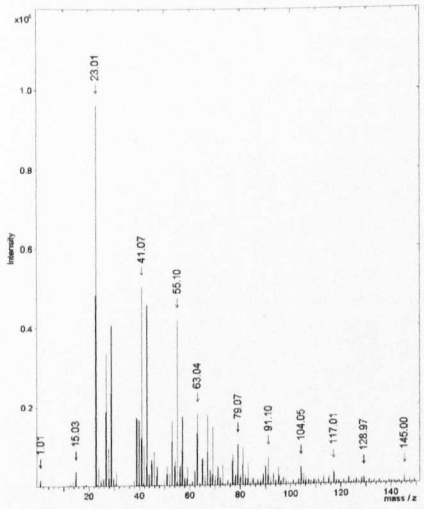

B

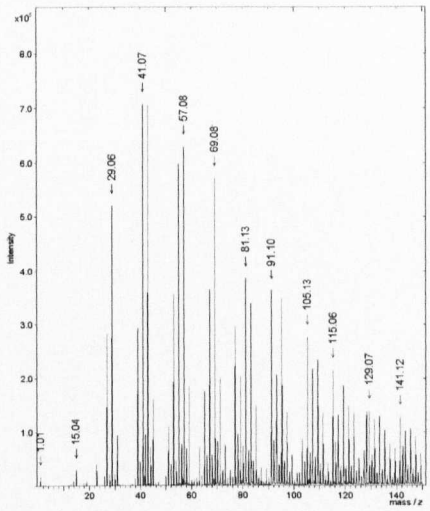

C

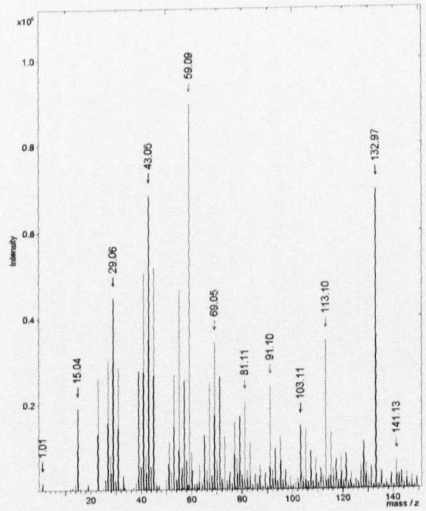

D

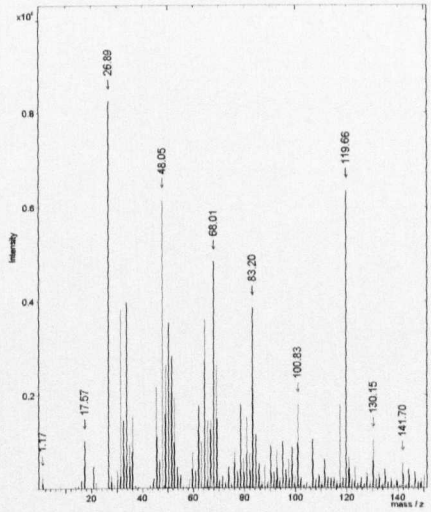

Figure 2.19. Positive ion ToF-SIMS spectra of **A.** cleaned glass (control), **B.** ppAAl, **C.** ppAAl-2-bromo-isobutyrate surfaces and **D.** Poly (MEO_2MA-co-OEGMA) grafted surfaces.

Figure 2.20 (A-D) represents the ToF-SIMS negative spectra for glass, ppAAl, bromoisobutyrate surfaces and after ATRP of MEO_2MA and OEGMA from the initiation sites to identify characteristic peaks.

Peaks with high intensity at low mass range in the ppAAl, ppAAl-2-bromo-isobutyrate surfaces, and after the ATRP of MEO_2MA and OEGMA (Figure 2.20B) e.g. m/z 13.00, 25.00 and 41.00 are assigned to CH^-, C_2H^- and C_2HO^-.

Table 2.7 represents the entire peak list for the negative spectra. ToF-SIMS analysis of bromoisobutyryte bromide surfaces and after the ATRP polymerisation revealed an additional peak of a high intensity appearing at m/z 79 corresponding to Br^-; this complements the XPS results shown in Table 2.5.

Although there has been reports describing PEG treated surfaces using ToF-SIMS (198, 199), there is limited literature with regard to poly (MEO_2MA-co-OEGMA) surfaces.

From the ToF-SIMS data, it was concluded that oxygen containing groups were present including C_4H_7O, C_2H_3O, C_3H_7O and C_3H_3O; these thought to be corresponding to the methoxy contained in the grafted polymer brushes as shown in the topographical ToF-SIMS images.

Table 2.7. Characteristic positive and negative peaks of cleaned glass, ppAAl, bromoisobutyryte and poly (MEO_2MA-co-OEGMA) surfaces.

Positive ions				Negative ions		
	Ion	**Mass**			**Ion**	**Mass**
1.	Na^+	22.99	46.$C_{10}H_{11}^+$ 131.08	1.	C^-	12.00
2.	Mg^{2+}	23.98	47.$C_{11}H_9^+$ 141.07	2.	CH^-	13.00
3.	$C_2H_2^+$	26.01		3.	CH_2^-	14.01
4.	$C_2H_3^+$	27.02		4.	O^-	16.00
5.	Si2+	27.98		5.	OH^-	17.00
6.	CH_3OH^+	29.05		6.	C_2H^-	25.00
7.	CH_4O^+	32.45		7.	CHO^-	29.00
7.	$C_3H_2^+$	38.01		8.	CH_3O^-	31.02
8.	K	38.96		9.	C_3^-	36.00
9.	$C_3H_3^+$	39.02		10.	C_3H^-	37.00
10.	Ca^{2+}	39.96		11.	C_2O^-	39.99
11.	$C_3H_4^+$	40.02		12.	C_2HO^-	41.00
12.	$C_3H_5^+$	41.04		13.	CHO_2^-	45.00
13.	$C_3H_6^+$	42.04		14.	C_4^-	48.00
14.	$C_2H_3O^+$	43.02		15.	C_4H^-	49.00
15.	$C_2H_5O^+$	45.03		16.	SiH_5O^-	49.01
16.	$C_4H_3^+$	51.02		17.	C_3O^-	51.99
17.	$C_4H_4^+$	52.03		18.	C_3HO^-	53.00
18.	$C_4H_5^+$	53.03		19.	$C_3H_6O^-$	58.04
19.	$C_4H_6^+$	54.04		20.	$C_2H_3O_2^-$	59.01
20.	$C_3H_3O^+$	55.02		21.	SiO_2^-	59.96
21.	$C_4H_7^+$	55.05		22.	C_5^-	60.00
22.	$C_4H_8^+$	56.06		23.	C_5H^-	61.00
23.	$C_3H_5O^+$	57.03		24.	$C_5H_3^-$	63.02
24.	$C_4H_9^+$	57.54		25.	C_4HO^-	65.00
25.	$C_3H_7O^+$	59.05		26.	$C_3H_3O_2^-$	71.01
26.	$C_5H_5^+$	65.04		27.	$C_3H_5O_2^-$	73.05
27.	$C_4H_3O^+$	67.02		28.	$SiHO_3^-$	76.96
28.	$C_5H_8^+$	68.01		29.	Br^-	79.96
29.	$C_5H_9^+$	69.07		30.	$C_5H_8O^-$	83.20
30.	$C_4H_7O^+$	71.05		31.	C_6HO^-	89.00
31.	$C_6H_5^+$	77.04		32.	$C_5HO_2^-$	92.99
32.	$C_6H_9^+$	81.07		33.	C_8H^-	97.00
33.	$C_6H_{11}^+$	83.09		34.	$C_8H_4^-$	100.03
34.	$C_7H_7^+$	91.05		35.	$C_8H_5^-$	101.04
35.	$C_6H_{11}O^+$	99.10		36.	$C_8H_7^-$	103.06
36.	$C_8H_9^+$	105.07		37.	C_9^-	107.99
37.	$C_8H_{10}^+$	106.07		38.	$C_9H_5^-$	113.04
38.	$C_7H_9O^+$	109.07		39.	$C_{10}H^-$	121.01
39.	$C_9H_7^+$	115.06		40.	$C_{11}H_3^-$	135.02
40.	$C_9H_8^+$	116.06		41.	$C_{11}H_6^-$	137.00
41.	$C_9H_9^+$	117.07				
42.	$C_9H_{11}^+$	119.66				
43.	$C_{10}H_8^+$	128.06				
44.	$C_{10}H_9^+$	129.07				
45.	$C_{10}H_{10}^+$	130.15				

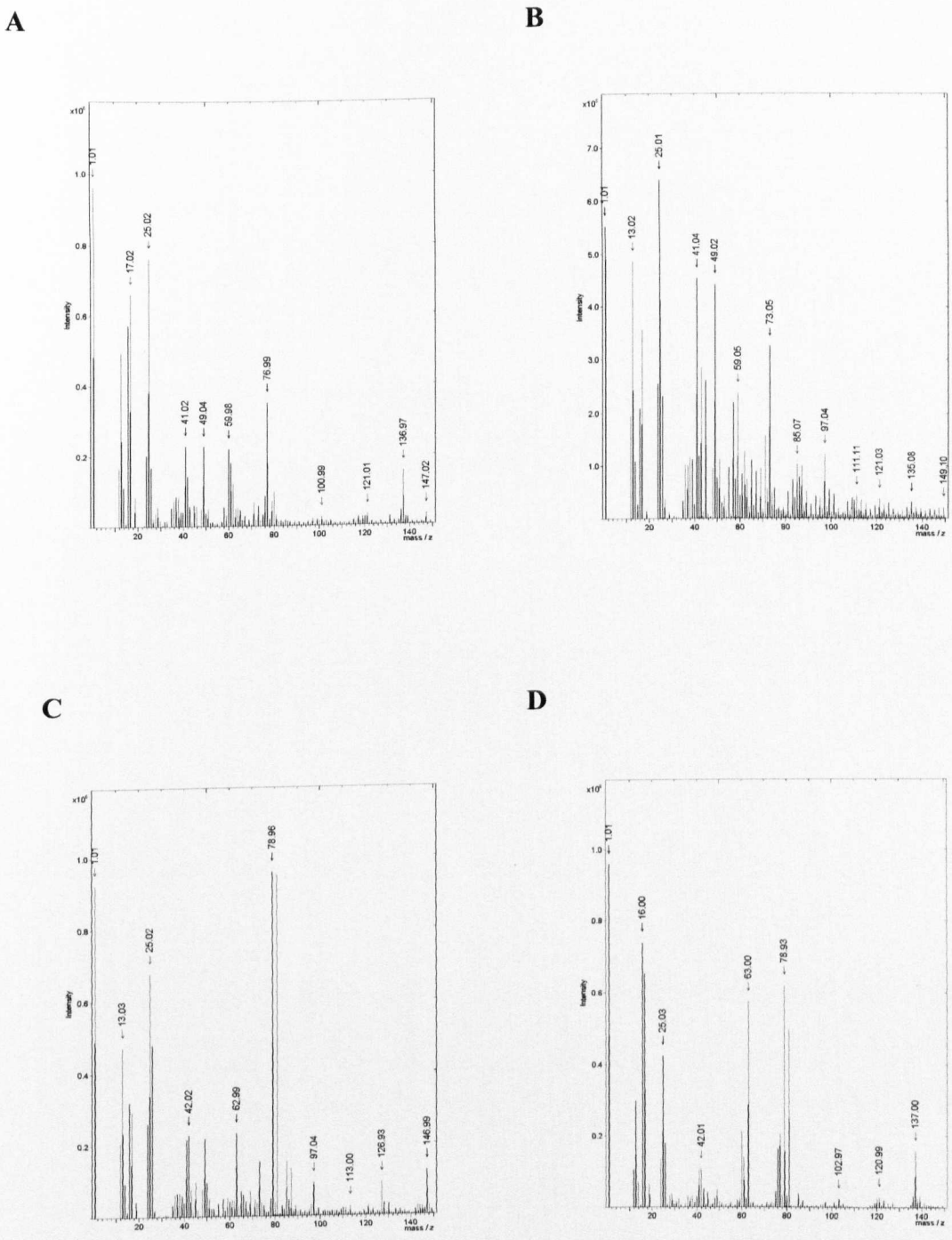

Figure 2.20. Negative ion ToF-SIMS spectra of **A.** Cleaned glass (control), **B.** ppAAl coated glass, **C.** ppAAl-2-bromo-isobutyrate surfaces and **D.** Poly (MEO_2MA-co-OEGMA) grafted surfaces.

ToF-SIMS imagining was used to investigate the effect of surface modification treatments as the specific ions could be used to create chemical maps of their distributions on the surface.

Glass elements including Na^+, K^+, Ca^{2+} and Si^{2+} were the main ions present in the positive topographical images counting for 938661, 137987, 168730 and 93908 ions of the total ion which is 11751420 (Figure 2.21). In the negative images with total ions of 12653082, silica ions e.g. $SiHO_3^-$ (347444 ions) and SiO_2^- (223873) were of great intensity as indicated in Figure 2.21. Although, the glass substrates were cleaned using ultrapure water, acetone and plasma oxygen etching, there were features present in the topographical images of the glass analysed. This could be due to contamination during the preparation for the ToF-SIMS analysis.

The intensity of the total ion available for analysis in the positive spectrum of the glass is much less compared to the positive spectrum of ppAAl (10^7 ions for cleaned glass, 3.7×10^7 ions for ppAAl treated glass, 2.4×10^7 ions for 2-bromoisobutyryl bromide-modified surfaces and 2×10^7) indicating the successful deposition of ppAAl onto the glass substrates.

Figure 2.22 represents positive and negative topographical images of plasma coated allyl alcohol. The most dominant ions were of the hydrocarbon e.g. $C_3H_5^+$ (658983 ions) and $C_4H_7^+$ (585508 ions), $C_2H_3O^+$ (742149 ions) was the oxygen containing ion of great intensity and well distributed on the surface after plasma polymerisation with allyl alcohol as it is shown in Figure 2.22. Na^+ (44253) and K^+ (22804) were present in the positive topographical images but to a lesser extent compared to cleaned glass (Figure 2.21 and Figure 2.22).

The silica containing ions ($SiHO_3^-$ and SiO_2^-) displayed on cleaned glass disappeared when the surface was plasma polymerised with allyl alcohol and instead ions like C_2H^- and C_2HO^- with 792922 and 434474 counts respectively were of great intensity.

Regarding surfaces that were treated with 2-bromoisobutyryl bromide, Br^- was the highest intensity peak as indicated in Figure 2.20C, which was of great intensity (869082 ions of a total ion of 15927014) (Figure 2.23); they were decreased to 587180 ions when poly (MEO_2MA-co-OEGMA) was grown from the surface by ATPR (Figure 2.24); this adds to the XPS data shown in Table 2.5 and Figure 2.18 that there is still Br^- after polymerisation, this could be explained by thickness of the layer which is expected to be more than 10 nm (exceeding the depth analysis of ToF-SIMS which is 2 nm). Additionally, the intrinsically low initiation efficiency (typically < 10%) which is always observed in ATRP "grafting from" reactions could result in a reduced amount of Br^- ions detected after the polymerisation.

Positive ion images after polymerisation revealed that $C_3H_5^+$ was the most intense ion with 600294 counts; oxygen containing ions e.g. $C_3H_7O^+$ and $C_4H_7O^+$ with 249482 and 203000 ions were present (thought to be indicative of methoxy containing chains of the copolymer brushes) which was not observed in the images for ppAAl and cleaned glass images as indicated in Figure 2.21 and 2.22.

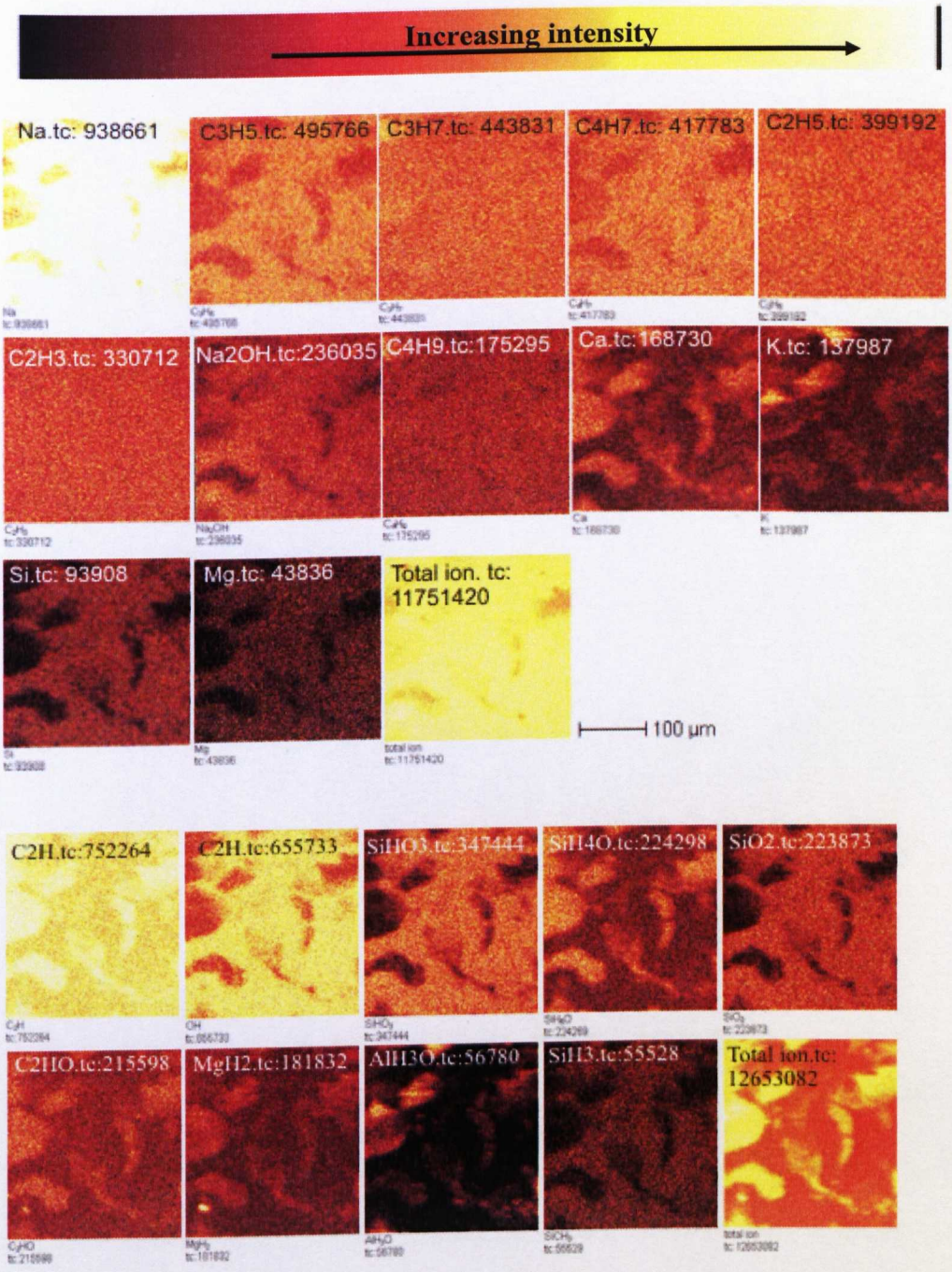

Figure 2.21. Topographical images for positive (top) and negative (bottom) ions of the cleaned glass. Field of view: 500×500 μm^2. Micron Bar =100µm. The scale on the top indicates that the brighter the image looks the more abundant the given secondary ion is at the surface.

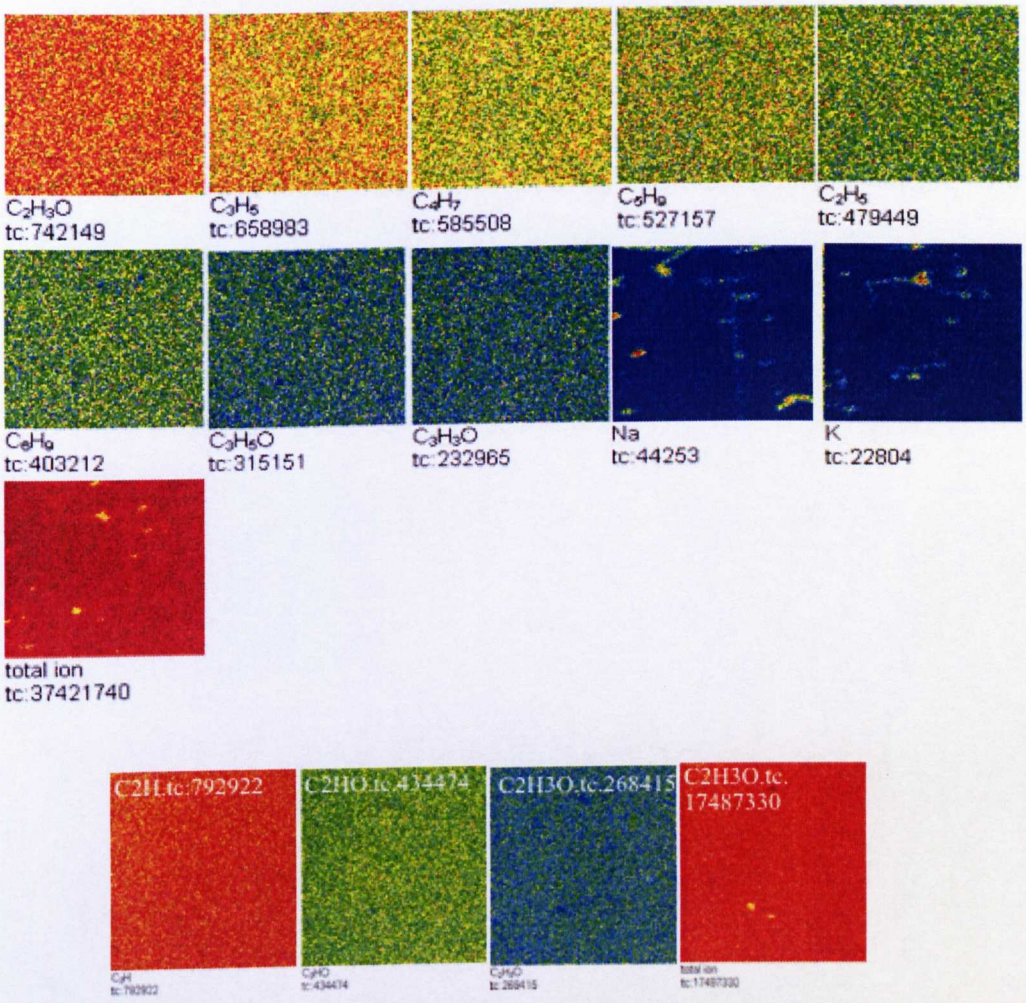

Figure 2.22. Topographical images for positive (top) and negative (bottom) ions of the ppAAl substrates. Field of view: 500×500 μm^2. Positive spectrum shows that the glass is covered with plasma coated allyl alcohol as the main component C_2H_3O. K and Na counts were considerably low compared to unmodified glass substrate (see also Figure 2.21). The main negative ion was observed to be C_2H. Micron Bar =100μm.

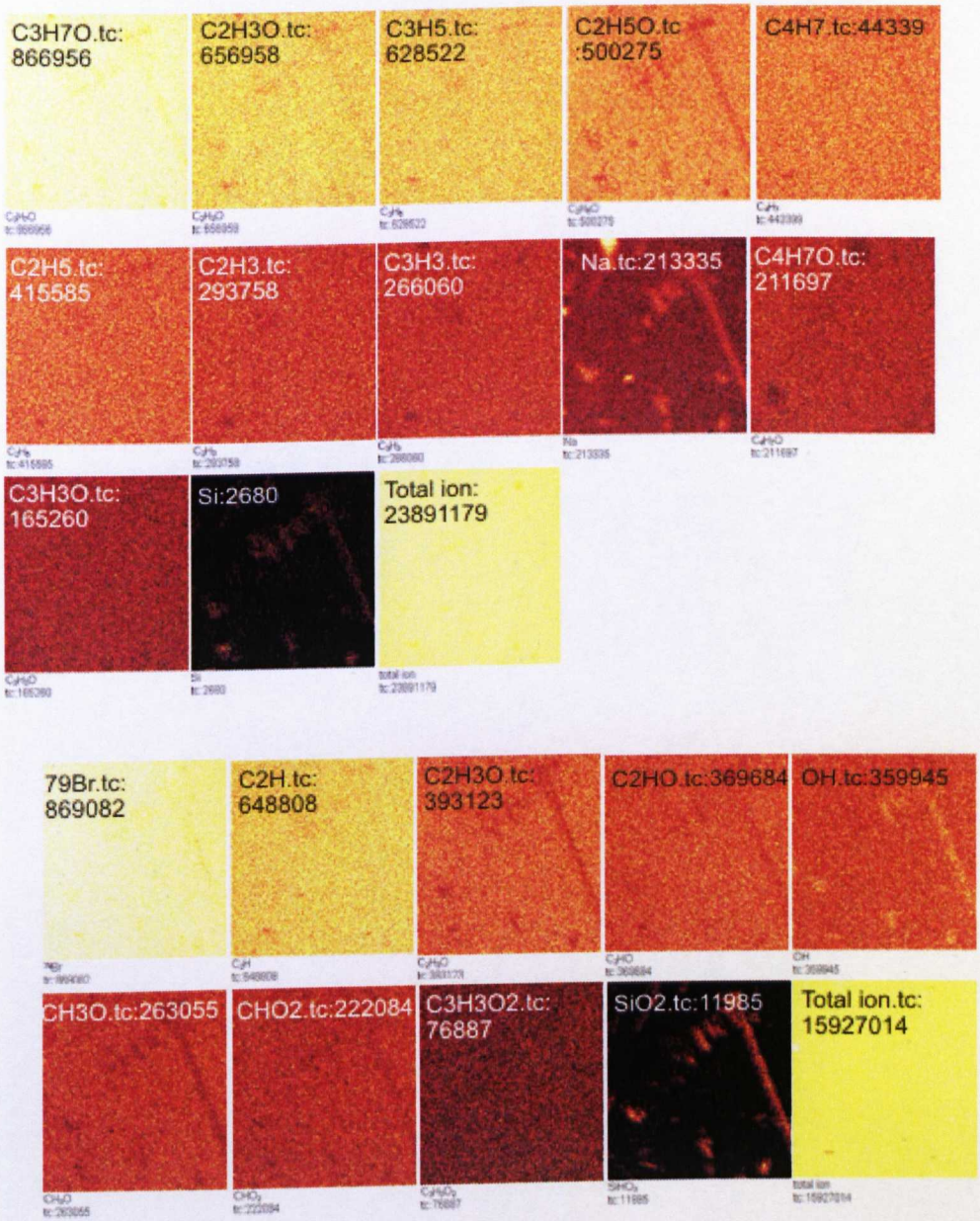

Figure 2.23. Topographical images for positive (top) and negative (bottom) ions of the. PAAl-*g*-2-bromoisobutyrate. Field of view: 500×500 μm^2. Micron Bar =100μm. The scale on the top indicates that the brighter the image looks the more abundant the given secondary ion is at the surface.

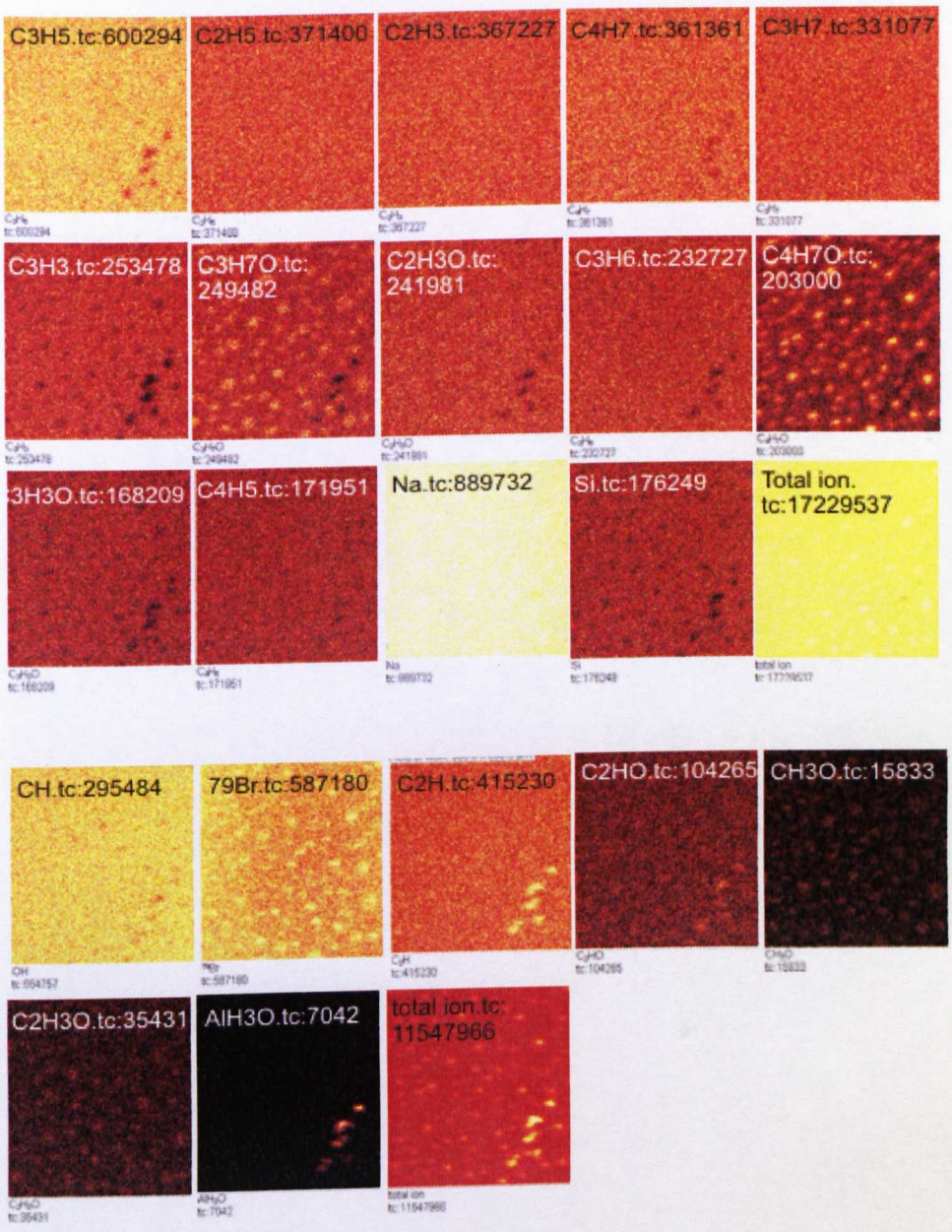

Figure 2.24. Topographical images for positive (top) and negative (bottom) ions of the poly (MEO_2MA-co-OEGMA). Field of view: 500×500 μm^2. Micron Bar =100μm. The scale on the top indicates that the brighter the image looks the more abundant the given secondary ion is at the surface.

2.4.5 Water contact angle and atomic force microscopy analysis

The physico-chemical properties of the polymer brushes i.e. the wettability of surfaces (the phase transition temperature) was analysed using WCA and AFM.

WCA was determined from advancing contact angles for ultra pure water; a sequence of drop images at same temperature was recorded with the contact angle software.

Advancing water contact angles were recorded for all surfaces i.e. ppAAl surfaces deposited at different plasma powers, isobutyryl bromide-modified surfaces and after the synthesis of grafted poly (MEO_2MA-co-OEGMA) below, and above the phase transition of the surface.

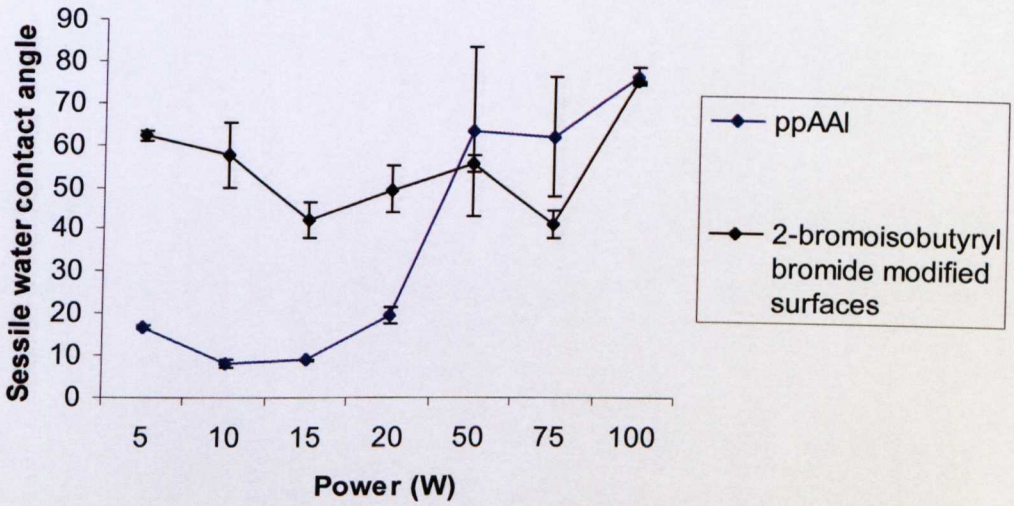

Figure 2.25. Sessile water contact angle of ppAAl deposited at different powers (W).

Figure 2.25 shows the sessile water contact angle of ppAAl surfaces deposited at different plasma powers. Surfaces deposited at low power for 5, 10, 15, 20W showed hydrophilic surfaces of water contact angle at 16°±0.6, 8.2°± 0.8, 8.9°±0.1 and 19.6°±1.8 respectively (Figure 2.25). However, the contact angle increased for surfaces at a power from 50 to 100 W as the power increases, the more cross-linked the ppAAl layers is and hence the contact angle increased from 1.6°± 1.8 at 20V to 76.3° ± 2.3 at 100 W. When all these surfaces were treated with 2-bromoisobutyryl bromide in the presence of THF and triethylamine anhydrous, the contact angle dramatically increased indicating that more hydrophobic surfaces had been formed with WCA increasing from 16° for ppAAl at 5W to 62°± 1.3 at 100 W, as shown in Figure 2.25.

Confirmation of poly (MEO_2MA-co-OEGMA) growth and temperature-dependent wettability changes of the resultant polymer brushes were also investigated using water contact angle (Table 2.8).

Table 2.8. Water contact angle, θ_w of polymer surfaces. Data shown for each surface is the mean of 5 independent measurements for thee surfaces and the standard deviation from the mean.

Surface	θ_w at 20 °C	θ_w at 37 °C
PAAl-*g*-2-bromoisobutyrate	71° ± 9.9	74° ± 2.5
PAAl-*g*-P(MEO_2MA-co-OEGMA)	50° ± 5.0	64 ± 0.7

As apparent from Table 2.8 and Figure 2.26, the grafting of the amphiphilic co-polymer reduced the contact angle from 71 to 50 ° C (at 20°C). At this temperature the polymer chains at the surface were expected to be strongly hydrated. At 37°C, a 14° decrease in the water contact angle ($\theta \approx 64$°C) was

apparent and indicative of the collapse of the polymer brushes above their phase transition temperature; these values are in good agreement with literature data for similar polymer brushes (120, 196).

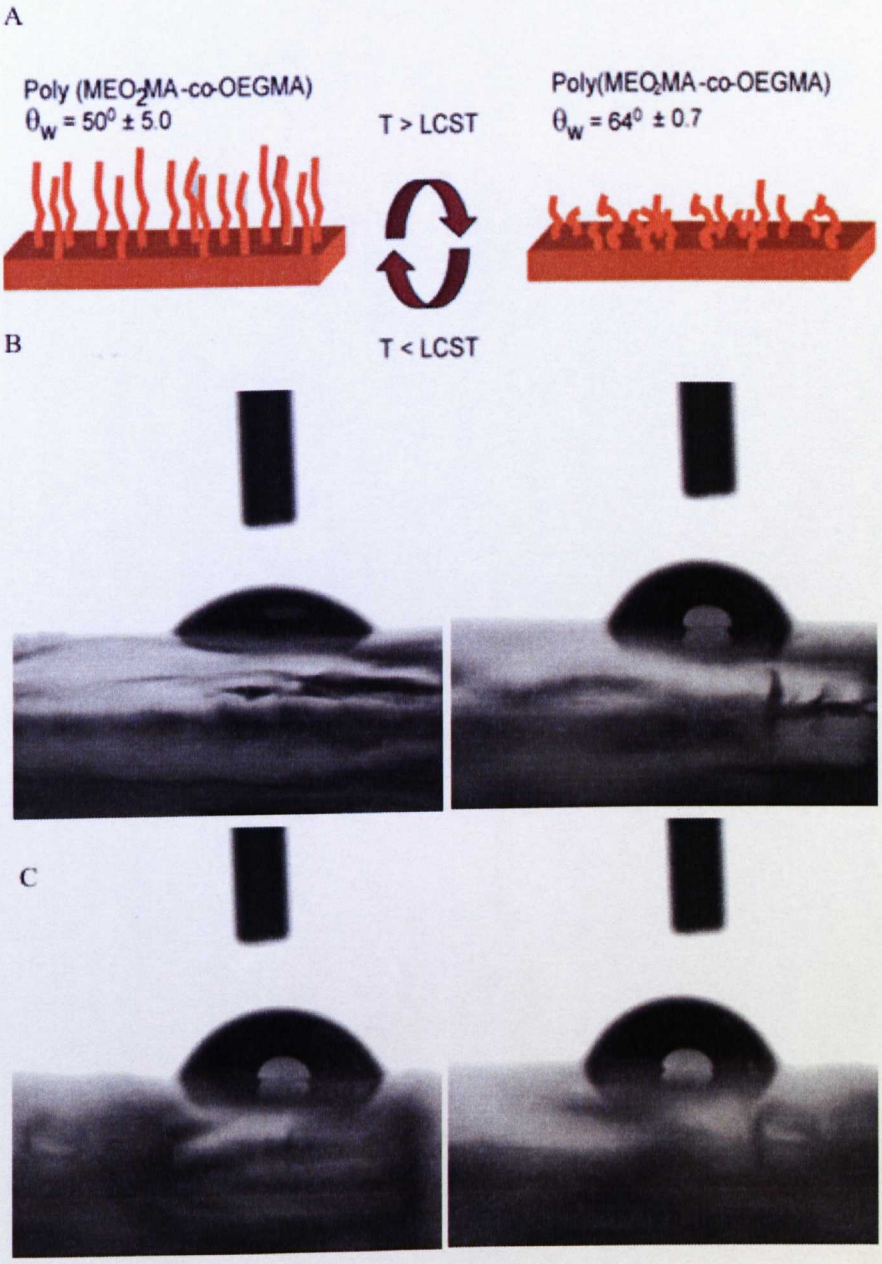

Figure 2.26. A. Water contact angles for poly (MEO_2MA-co-OEGMA) grafted surfaces above and below the LCST indicated with schematic of reversible brush conformations. **B** and **C** representative drop images of poly (MEO_2MA-co-OEGMA) and PAAl-*g*-2-bromoisobutyrate surface above LCST and poly (MEO_2MA-co-OEGMA) below LCST.

Atomic force microscopy in air for ppAAL deposited at P=100 W showed that the polymer layer is smooth with a surface roughness of 0.86 ± 0.1 nm; round features were present on these surfaces which thought to be formed when ppAAl was deposited at a power of 100 W. 2-bromoisobutyryl bromide-modified surfaces were homogenous as well (surface roughness of 0.66 ± 0.3) (Figure 2.27).

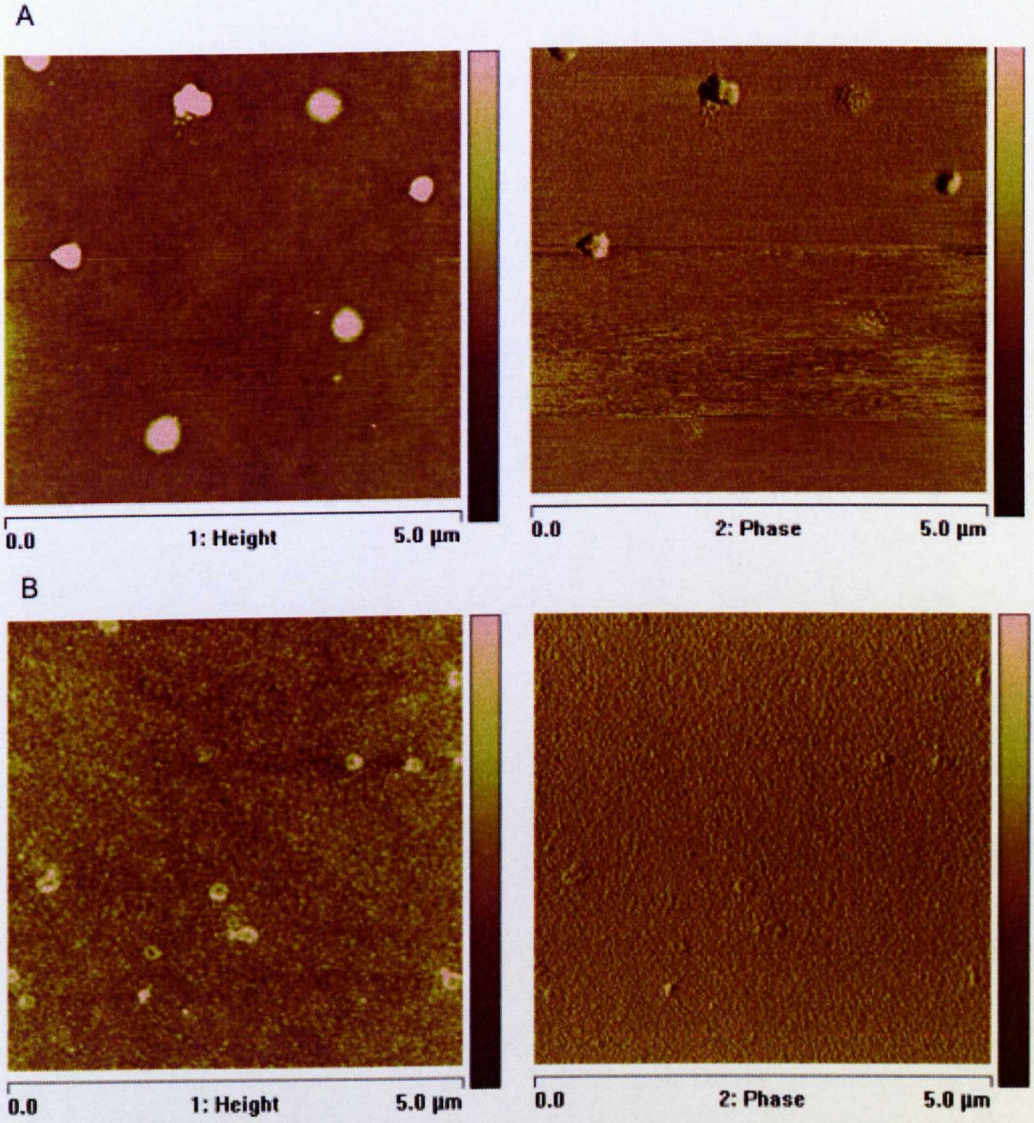

Figure 2.27. AFM topography images of ppAAl imaged in air (A: height and phase images) and PAAl-*g*-2-bromoisobutyrate imaged in air (B: height and phase images).

Changes in surface topography were apparent in AFM when the surface was imaged in air above and below the LCST (Figure 2.28). Surface roughness, for an area of 5 x 5 μm was estimated to be ~ 8 ± 1.8 nm below the LCST and ~ 3 ± 0.7 nm when the temperature was increased to 37°C. The roughness of the surface increased below the LCST, possibly due to the hydrated chains of the thermo-responsive layer, which is then decreased below the LCST indicating the globule structures formed by ther copolymer brushes.

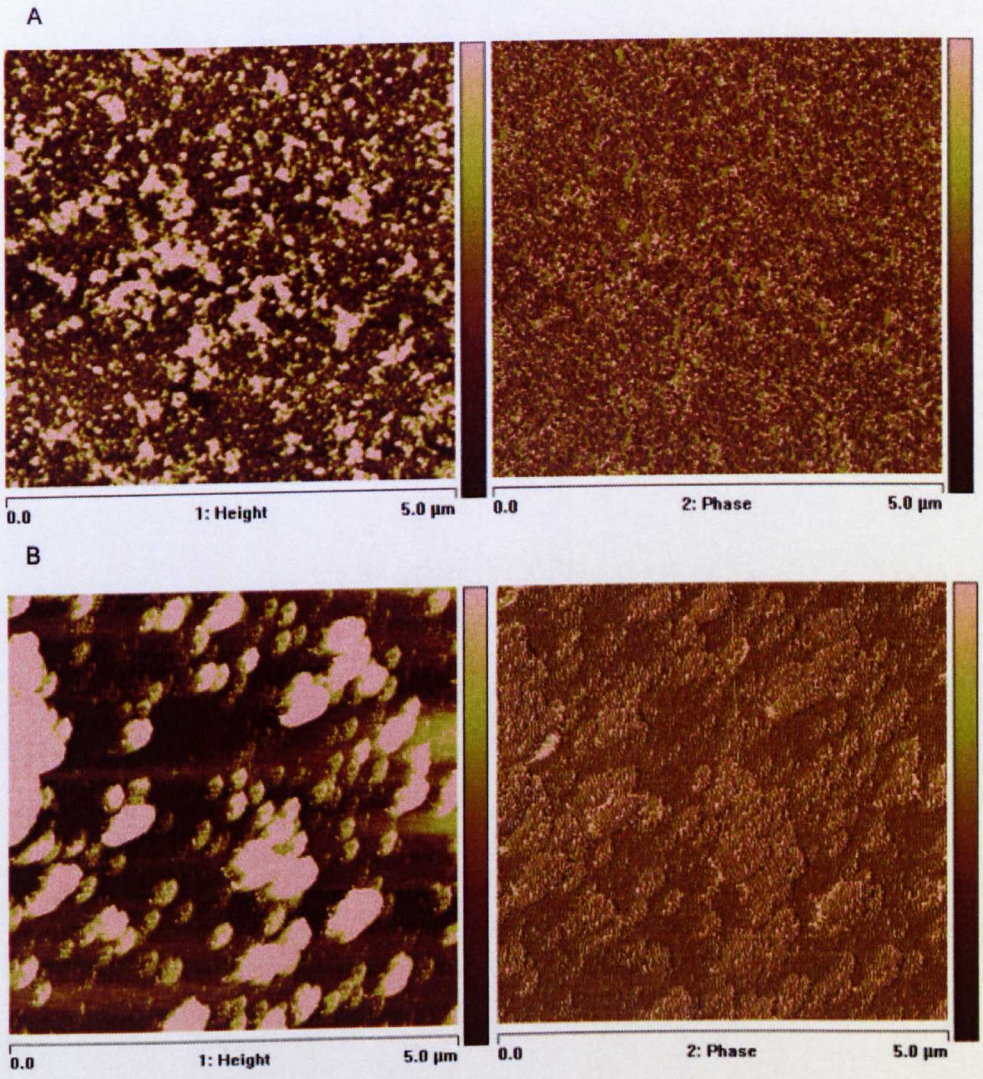

Figure 2.28. Representative AFM images of poly (MEO_2MA-co-OEGMA) grafted surface at (20°C) **(A)** and above (37°C) **(B)** the LCST in air (scan size: 5*5 μm^2 , z-range: 10 nm).

The phase transitions of the copolymer brushes (5-95% of OEGMA to MEO_2MA) were further explored using variable temperature AFM to evaluate topography and measure adhesion forces between the AFM tip and the polymer brushes. No large overall topography changes were apparent in AFM micrograph of surfaces imaged in water (Figure 2.29). However, adhesion pull off forces from AFM force distance curves indicated significant changes in surface properties across the temperature range (Figure 2.30A). A gradual decrease in the adhesion between the AFM tip and the copolymer brush surface was observed as the temperature was decreased from 37°C to 28°C (Figure 2.30.A and 2.30.B-1 and 2). This effect was reversible as illustrated by the increase in adhesion force when the surfaces were heated back to 37°C again (Figure 2.30A). The shape of the force-temperature curve implied a non-linear change in polymer brush hydration state at ~ 28°C, close to the expected solution state LCST of the polymer at 32°C in solution (200). This behaviour was in accord with prior AFM adhesion data for thermo-responsive polymer brush surfaces (201), with the increase in tip adhesion above the solution LCST arising from the increased tip interaction with the hydrophobic surface.

Stefanie *et al.* studied recently the the thermo-responsive behaviour of poly (MEO_2MA-co-OEGMA) where two kinds of regimes were identified above and below the LCST of the copolymer brushes. Repeatable heating/cooling cycles showed that the thermo-responsive properties of the surface provide reproducible adhesion force values (202).

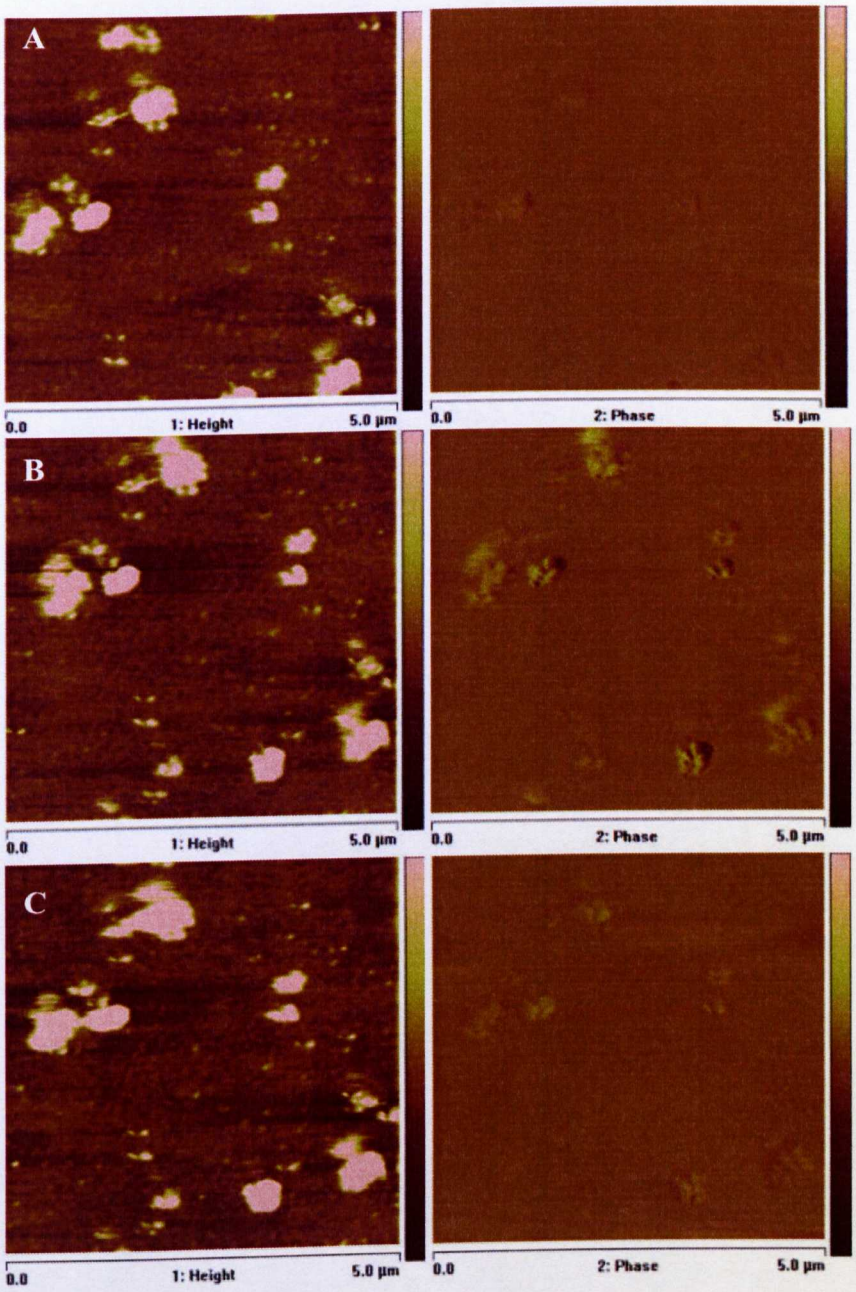

Figure 2.29. Representative AFM images of poly (MEO_2MA-co-OEGMA) graf‘ed surface at 37°C **(A)**, at 20°C**(B)**, and back at 37°C **(C).** (scan size: 5*5 μm^2 , z-range: 10nm). These images were taken at approximately the same area.

A

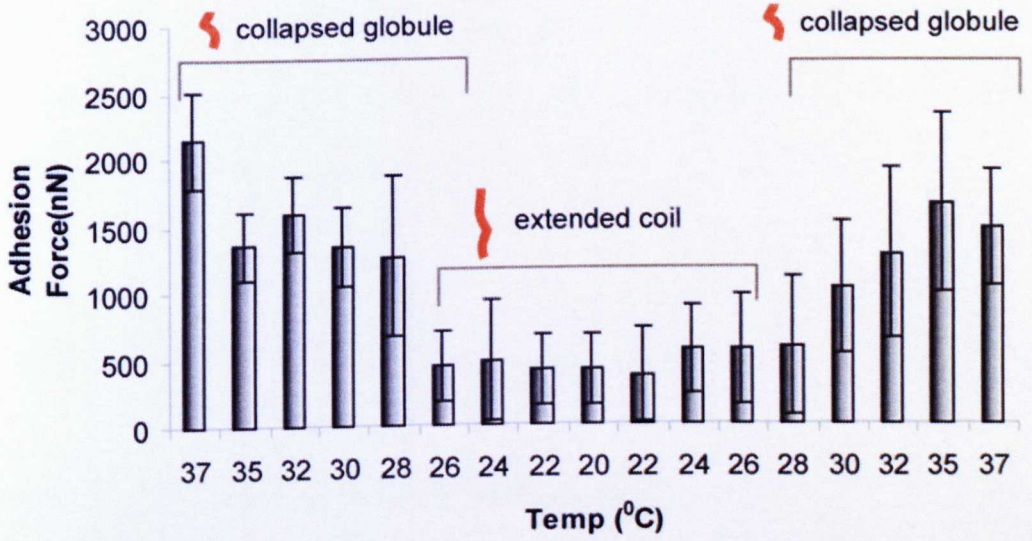

B

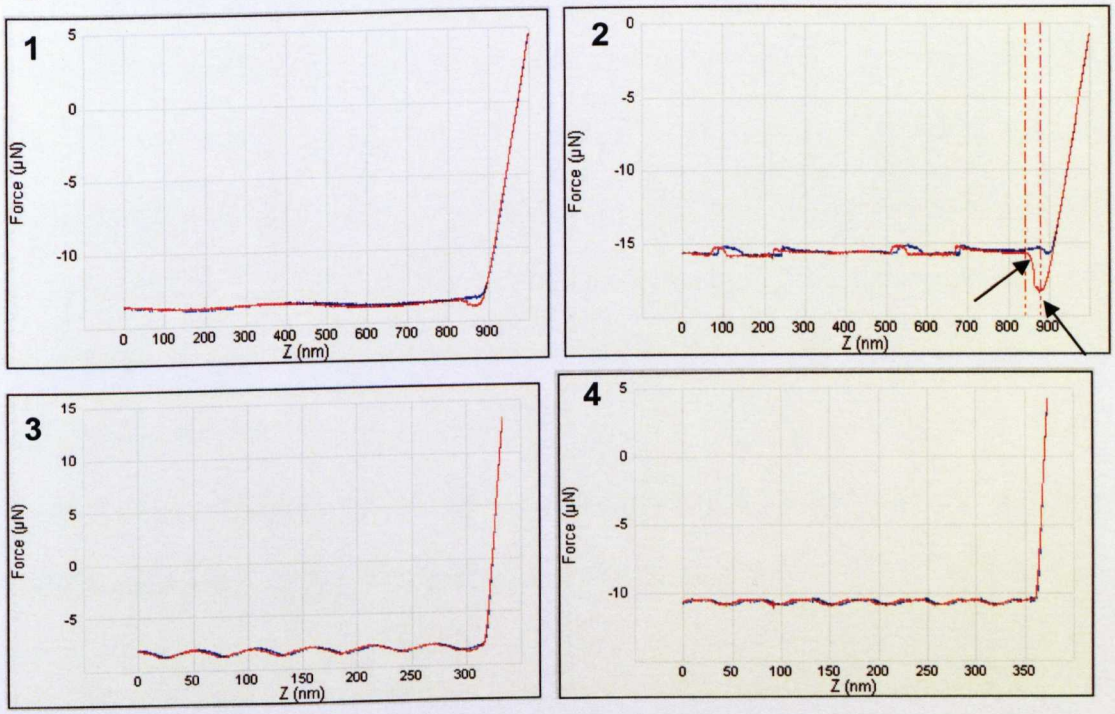

Figure 2.30. **A**. AFM force distance graph showing the interaction between the AFM tip and the copolymer brush surface across the temperature range (from 37°C to 20°C). **B**. Representative force distance curves obtained for ozone cleaned Si_3N_4 AFM tip at poly (MEO_2MA-co-OEGMA) surfaces. At 20°C **(1)** low adhesion between tip and surface indicated by small pull-off trace (arrowed) in contrast to the higher pull-off force observed at 37°C **(2)**. Poly (OEGMA) control surfaces showed no adhesion between the AFM tip and the polymer layer as it has LCST of 90°C, below **(3)** and above the LCST **(4)**.

The combination of contact angle changes and variations in adhesion force with temperature were indicative of a surface that could reversibly be switched from a hydrophilic to a hydrophobic state.

2.5 Conclusion

Synthesis of poly (MEO_2MA-co-OEGMA) from a surface by ATRP was achieved from the initation sites formed by reaction of 2-bromoisoburyl bromide with immobilised hydroxyl groups (generated from ppAAl). This was demonstrated from the XPS and ToF-SIMS analysis of the surface. The thermo-responsive behaviour indicated that the grafted poly (MEO_2MA-co-OEGMA) was hydrophobic at 37°C (above the LCST) and hydrophilic at 20°C (below the LCST). AFM adhesion force experiment revealed that the change of conformation of these copolymer brushes occur at around 28°C.

These surfaces therefore will be used to explore the cell adhesion of 3T3 fibroblasts and their passage on them which is presented in Chapter 3.

CHAPTER 3

Evaluation of variable bio-adhesion surfaces using mouse 3T3 fibroblasts as a model mammalian cell type.

3.1 Introduction

Proteolytic treatment (with trypsin) digests the proteins responsible for cell adhesion to the substrate by hydrolyzing membrane associated protein molecules, most importantly integrins. This can affect cell adhesion to further substrates and also cell quality after passaging. As a consequence, there is a pressing need to develop non-proteolytic cell culture treatments.

Okano and colleagues have reported an experiment where PNIPAAm was covalently attached to tissue culture polystyrene (TCPS) dishes to prepare a thermo-responsive culture surface (58). Bovine hepatocytes and bovine aortic endothelial cells (BAE) adhered, spread, and proliferated to the same extent as TCPS on the PNIPAAm surfaces at 37°C (80, 81). However, below 32°C (the LCST of the thermo-responsive polymer), the dish surface became hydrophilic leading to the formation of a hydration layer between the dish surface and the cultured cells which resulted in cell detachment from the PNIPAAm grafted surface (58, 80, 81).

In these experiments, cells were harvested as intact cell sheets along with their deposited extracellular matrix (ECM) and critical cell surface proteins such as ion channels, growth factor receptors and cell-to-cell junction proteins remained intact (81).

Following on from the Okano study, further cell sheet engineering methods have been proposed whereby cultured cells are harvested as intact sheets along with their deposited ECM from a temperature-responsive surface (82, 85, 86). These cell layers can be used for tissue engineering applications as they can be directly transplanted to tissue beds or even layered to create thee-dimensional (3-D) tissue-like structures. For example, transplantable corneal epithelial sheets were recovered from thermo-responsive substrates without proteolytic treatment and avoiding the use of biological carrier substrates. These recovered sheets were positioned directly on host corneal stroma and adhered rapidly without the need for sutures (90).

Therefore, it has been proven that stimuli responsive surfaces can be used for cell sheet engineering. However, it has not been shown that these surfaces can be used for passaging of individual cell populations. This forms the basis of the main aim of this chapter which was to illustrate the suitability of these surfaces for enzyme free cell passaging using mouse 3T3 fibroblasts as a model mammalian cell type and using the poly (MEO_2MA-co-OEGMA) fabricated in Chapter 2.

3.2 Aims and objectives

The aim of this chapter was to use thermo-responsive surfaces to passage 3T3 fibroblasts from poly (MEO_2MA-co-OEGMA) using temperature as the

detachment factor (i.e. not enzymes). Cells cultured on TCPS and detached with trypsin/EDTA were used as the control. Cells were cultured on both surfaces up to passage 10 and growth curves and cytoskeleton staining was carried out. These aims were achieved though the following objectives:

1. To examine thermo-responsive batch-to-batch variability, thee batches of poly (MEO_2MA-co-OEGMA) thermo-responsive surfaces were grafted on different days.

2. To confirm the thermo-responsive nature of these surfaces, WCA measurements were taken on one surface from each batch.

3. To analyse poly (MEO_2MA-co-OEGMA) surfaces after UV sterilisation using XPS to see whether the composition of the copolymer layer had changed using this sterilisation method.

4. 3T3 fibroblast were then cultured on these surfaces, and passaged with temperature for the thermo-responsive surfaces and trypsin on TCPS surfaces for a total of 10 passages as shown in Figure 3.1.

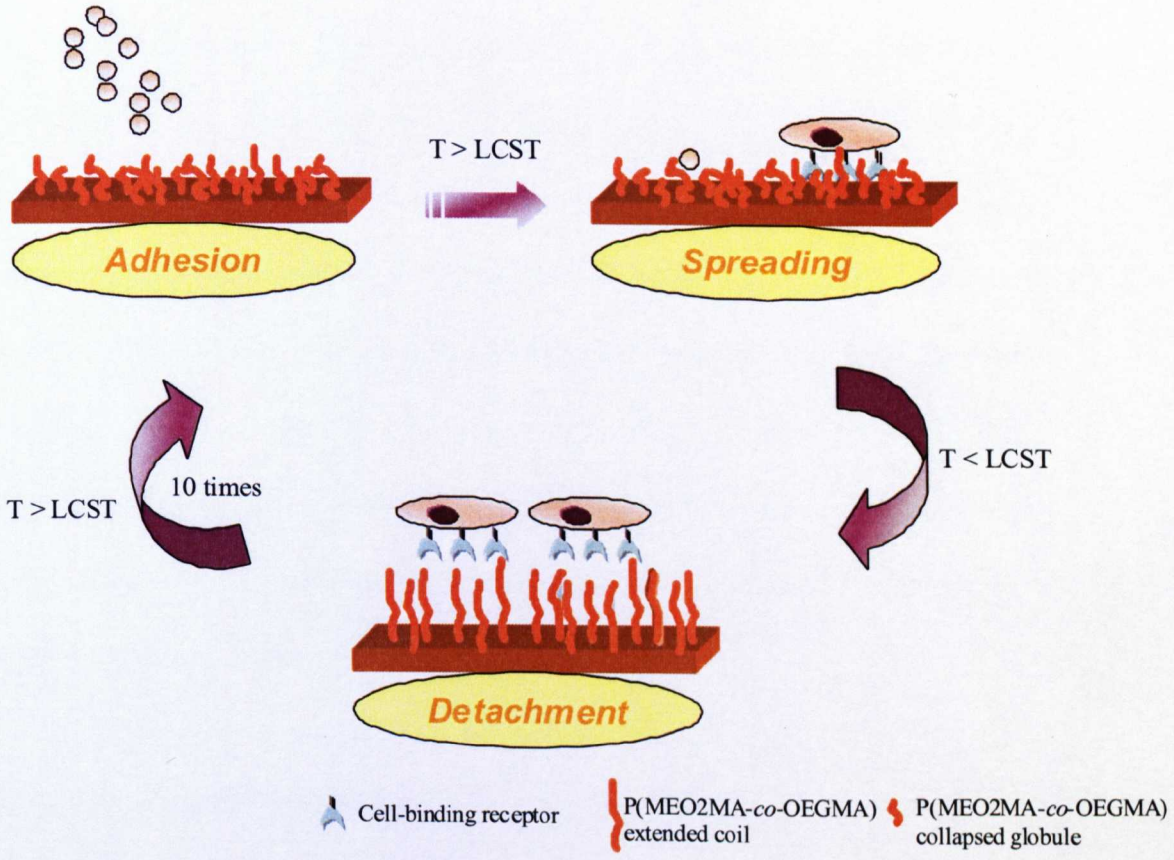

Figure 3.1. Schematic illustration of the passaging experiment using the poly (MEO_2MA-co-OEGMA) thermo-responsive surfaces. At 37°C (above the LCST), cells adhere and spread, and they detach when the temperature is lowered to 20°C (below the LCST).

3.3 Materials and Methods

3.3.1 Surface preparation and sterilisation

Surfaces were freshly prepared as described in Chapter 2 (section 2.3). Briefly, glass substrates were cleaned and then plasma coated with poly allyl alcohol at a power of 100 W. These surfaces were then treated with 2-bromosiobutyryl

bromide in the presence of THF and triethylamine anhydrous. Poly (MEO_2MA-co-OEGMA) was then grafted from the surface using ATRP in ethanol. The surfaces were UV sterilised at a wavelength of 280 nm for 20 min in a class II microbiological safety cabinet; XPS was performed as described in Chapter 2 (section 2.3.4.2) at that point to confirm that the sterilisation method did not affect the surface chemistry of the substrates. The prepared poly (MEO_2MA-co-OEGMA) surfaces were used fresh for cell culture purposes; these surfaces were then transferred to 6 well plates and sterilised using UV. WCA was conducted as described in Chapter 2 (section 2.3.4.1).

3.3.2 3T3 fibroblast culture

3.3.2.1 3T3 maintenance

Mouse 3T3 NIH fibroblasts were obtained from the European Collection of Cell Cultures (ECACC2). All cell culture media and supplements were supplied by Invitrogen, UK. The cells were cultured in complete 3T3 cell culture medium which comprised of Dulbecco's Modified Eagle Media (DMEM) supplemented with 10% Foetal calf serum (FCS), antibiotic/antimyocotics (penicillin-**100 units/mL,** streptomycin- **100 µg/mL**, amphotericin B-**0.25 µg/ml**) and L-glutamine (2 mM)(Appendix1).

3T3 fibroblasts were cultured on tissue culture polystyrene dishes (in T75 Nunc Flasks) in a humified atmosphere with 5% CO_2 at 37°C until they reached 80% confluency. Cells were passaged, either for use in experiments or for further expansion, by first washing with warm PBS (pH 7.4), followed by incubation with

5 mL 0.25% trypsin combined with 0.02% EDTA in PBS for approximately 5 minutes at 37°C. Culture medium containing 10% FCS was subsequently added to deactivate the trypsin and the cell suspension was centrifuged at 1000 rpm using a Sigma Laboratory centrifuges 3K15 (Scientific Laboratory Supplies, UK) for 3 minutes. The supernatant was then aspirated and the cells were re-suspended in 10 mL of complete 3T3 fibroblast media. In order to obtain a single cell suspension, the cells were passed gently though a needle few times (BD Blunt Fill Needle 19G). The cell passage number used in this study were between 10-30.

3.3.2.2 3T3 mouse fibroblast culture attachment and detachment

3T3 fibroblasts were maintained and passaged on TCPS as described in section 3.3.2.1. For the experiments described in this chapter, the starting passage number of cells was 15; cells were grown to 80% confluency and removed from the TCPS culture surface using trypsin. Cells were pelleted by centrifugation, washed, and resuspended in 3T3 complete medium (Appendix 1). They were then plated onto poly (MEO_2MA-co-OEGMA) grafted surfaces and TCPS at a density of 10^4 cells/ml in total of 2 mL and cultured at 37°C in complete media under a humified atmosphere of 5% CO_2 in air. The medium was changed the day after seeding the cells and the glass slides transferred to fresh culture dishes after washing them with warm PBS to remove unattached cells. Detachment studies were carried out following 72 or 96 h of culture where the temperature was lowered from 37°C to 20°C for 2 h under 5% CO_2 in air. This experiment was performed on 9 samples (3 batches prepared on different days).

3.3.3 Cell viability using trypan blue exclusion method

The viability of the cells was assessed using Trypan blue exclusion method. Cell suspension (50 µl) was placed in an Eppendorf and mixed with 0.4% (v/v) trypan blue solution and was allowed to stand for 15 min. The whole mixture was then placed in a Neubauer haemocytometer chamber under a light microscope (10 × objective) (Appendix 2). Cells that took up the dye (blue) were counted as non-viable and the ones did not take the dye (clear) were counted viable cells. The viability of cells was calculated as follows: total viable cells (unstained)/ total cells (stained and unstained) × 100.

3.3.4 Passaging experiment

Cells were cultured on freshly prepared poly (MEO_2MA-co-OEGMA) surfaces for every passage and TCPS was used as the control where cells were detached using trypsin/EDTA. Cells detached from poly (MEO_2MA-co-OEGMA) were gently pipetted for 5-10 mins, and then they were passed though a G19 needle to ensure a single cell suspension was obtained (203). This experiment was conducted with 9 samples for each passage (3 batches prepared on different days).

3.3.5 Growth curve (cell proliferation)

Cells were detached from the TCPS or thermo-responsive surfaces using trypsin/EDTA and temperature respectively as described above. Cells were counted after each passage using Trypan Blue exclusion method as described

above (section 3.3.3). Population doublings (PDs) at each passage was calculated using the formula $\{\log_{10}$ (total cell counts/cells seeded)$/\log_{10}2\}$ where the initial cell number seeded was 1×10^4 cells/mL. Proliferation rates were calculated as the cumulative population doublings (CPD) as a function of time.

3.3.6 Phase contrast microscopy

An inverted Leica microscope (Leica model DMIRB/RED) was used to visualise the cells and the images were captured using a Leica DC200 digital imager (Leica, UK). A Nikon Eclipse TS100 microscope (Nikon, UK) was also used in some experiments.

The images were captured using Q capture software; they were analysed using Leica Qwin analysis software V2.8 where the area covered by cells was estimated as a percentage of area represented by the whole image; average and standard deviation were calculated. Five images were taken for each sample as shown below.

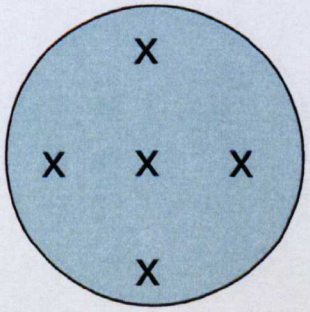

TCPS

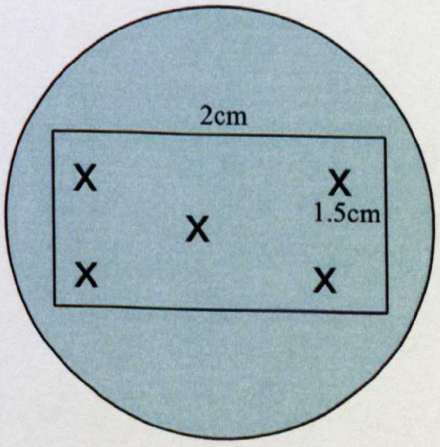

Test samples

3.3.7 Phalloidin staining and Confocal Microscopy

Cells grown on either TCPS (control) or on poly (MEO_2MA-co-OEGMA) substrates were fixed with 4% (w/v) paraformaldehyde (PFA) for 30 mins at room temperature in a laminar flow cabinet (externally vented class I MSC); then they were permealised with 0.1% (v/v) Triton-X 100 in PBS for 1h at room temperature after washing with PBS for 5 mins. They were washed again with PBS 4 to 5 times, and incubated with 1 μg/ml TRITC-Phalloidin in PBS for 1h. Samples were mounted using Vectashield containing DAPI (Invitrogen) and stored at 4°C wrapped in foil until images were taken using a confocal microscope.

Confocal microscopy (The University of Nottingham, Queen's Medical Centre) was carried out using a Leica TCS SP2 confocal laser scanning microscope (Leica, UK) and associated software. The stained cell monolayers were scanned using a glycerol immersion lens with an objective magnification selected after positioning the sample and adjusting the parameter on the Leica programme. The viewer window was used to arrange, manipulate and produce images with the right intensity, and finally both multi-channel and single images were named accordingly and saved as snapshots.

3.3.8 Statistical analysis

All the results are presented as mean ± standard deviation (SD) and N is the number of multiple wells where $n > 4$. Statistical analyses were performed using the unpaired Student's t-test: differences between data sets were considered to be statistically significant when $P < 0.05$.

3.4 Results and Discussion

In Chapter 2, poly (MEO_2MA-co-OEGMA) was grafted from a glass surface after reacting 2-bromoisobutyryl bromide to the hydroxyl groups on the poly allyl alcohol surface layer. WCA and AFM were used as techniques to study poly (MEO_2MA-co-OEGMA) thermo-responsive properties. Changes in thermo-responsiveness, from hydrophobic to hydrophilic, was proposed to study cell adhesion in this chapter using 3T3 fibroblasts as a model mammalian cell type. First, poly (MEO_2MA-co-OEGMA) grafted surfaces were analysed after sterilisation using UV. Secondly, 3T3 fibroblasts response to these surfaces was studied including adherence and detachment. Finally, 3T3 fibroblast proliferation assay was studied for several times by passaging them using poly (MEO_2MA-co-OEGMA) surfaces for up to 10 passages.

3.4.1 Surface Analysis after Sterilisation of the Surface with UV

Sterilisation is a critical step for most biomedical applications including cell culture. Therefore, before using poly (MEO_2MA-co-OEGMA) grafted surfaces for cell culture, they were sterilised using UV for 20 min; XPS was used as a technique to investigate whether the surface chemistry was affected following this sterilisation method (204, 205).

Table 3.1. Elemental composition determined using XPS for poly (MEO_2MA-co-OEGMA) grafted surfaces before and after UV sterilisation.

Elemental composition (%)	Poly (MEO_2MA-co-OEGMA)	Poly (MEO_2MA-co-OEGMA) after UV sterilisation
C1s	69.1 ± 2.0	71.05 ± 5.76
O1s	21.5 ± 0.7	23.65 ± 0.19
Si2p	-	-
Br3d	0.21 ± 0.3	0.18 ± 0.02
NaKLL	1.9 ± 0.27	0.88 ± 0.60
Mg1s	2.5 ± 0.5	3.03 ± 1.09
Ca2p	1.45 ± 0.6	1.04 ± 0.08

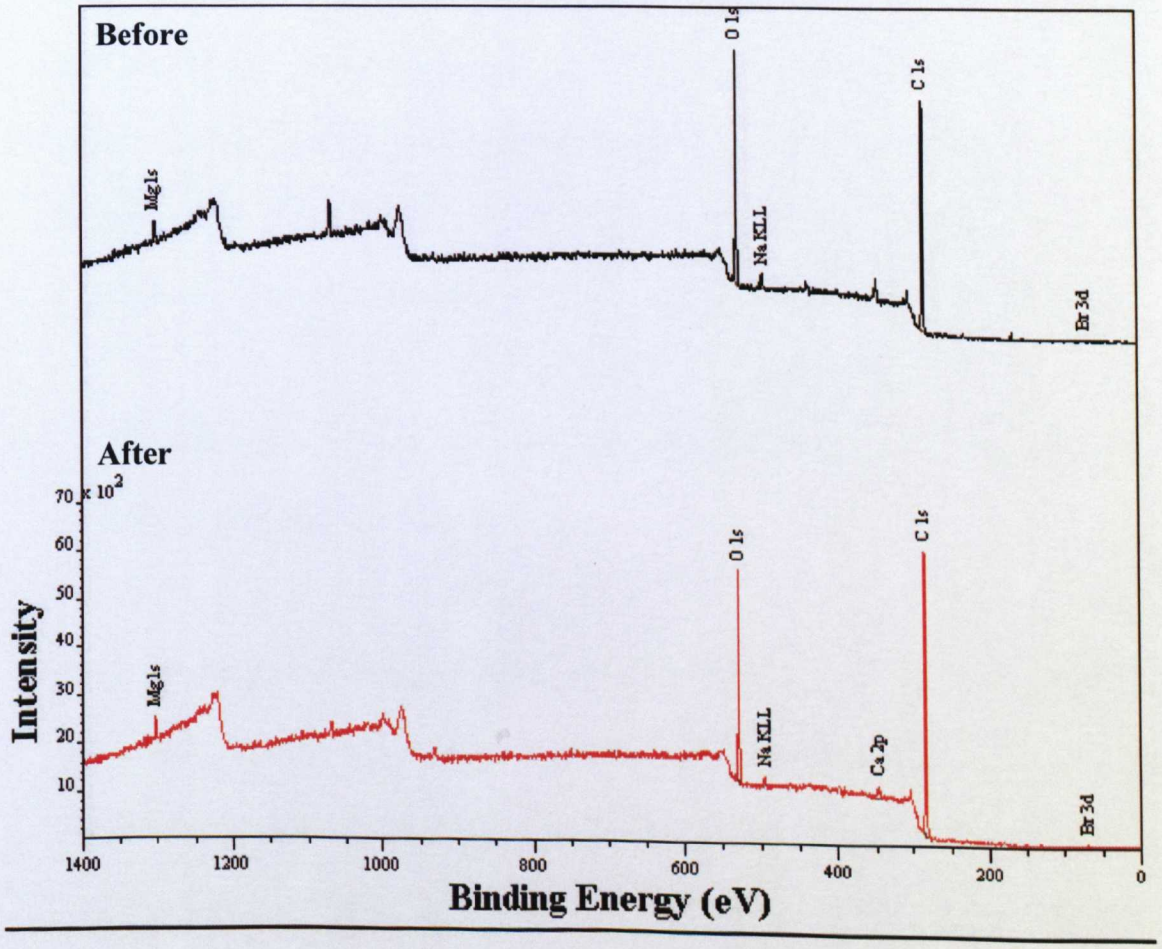

Figure 3.2. XPS wide scan of poly (MEO_2MA-co-OEGMA) before (black) and after (red) sterilisation with UV.

Table 3.1 shows the elemental composition determined from XPS analysis of the same surface before and after UV sterilisation. Examination of the post-sterilisation of the poly (MEO_2MA-co-OEGMA) did not reveal a significant difference in the elemental composition compared to pre-sterilisation of the surface as shown in Table 3.1. The key elements C1s (69 and 71 % before and after sterilisation respectively) and O1s (21 and 23%) were present.

The main glass element, Si2p, signal was not detected using XPS in both spectra; however, other glass elements were detected including Ca2p, NaKLL and Mg1s with small percentage which might be due to contamination of the surface before XPS analysis (Table 3.1 and Figure 3.2). This agrees with the reported literature that UV could be used to sterilise surfaces without causing degradation to the polymer layer or surface distortion (205). At the same time, UV irradiation can induce bacterial cell photochemical lesions or mutations in the DNA (204, 206).

3.4.2 3T3 Fibroblasts Adhesion and Detachment on the poly (MEO_2MA-co-OEGMA) Grafted Surfaces

After sterilisation of the poly (MEO_2MA-co-OEGMA) surfaces, 3T3 fibroblasts were seeded on these samples (and control TCPS) and adhesion observed over a culture period of 96 h (4 days). Figure 3.3 shows that 3T3 fibroblasts attached when cultured on these surfaces at 37°C (above the LCST of the responsive copolymer) exhibiting a similar morphology as those cultured on TCPS. The temperature was lowered to 20°C i.e. below the LCST of the copolymer brushes where no detachment of cells was observed on TCPS (control) in addition to maintaining their morphology on TCPS. However, cells changed morphology

from spread to round which indicated their detachment from the poly (MEO_2MA-co-OEGMA) surface as shown in Figure 3.3. Complete detachment was achieved by gentle agitation of the substrate to release the cells.

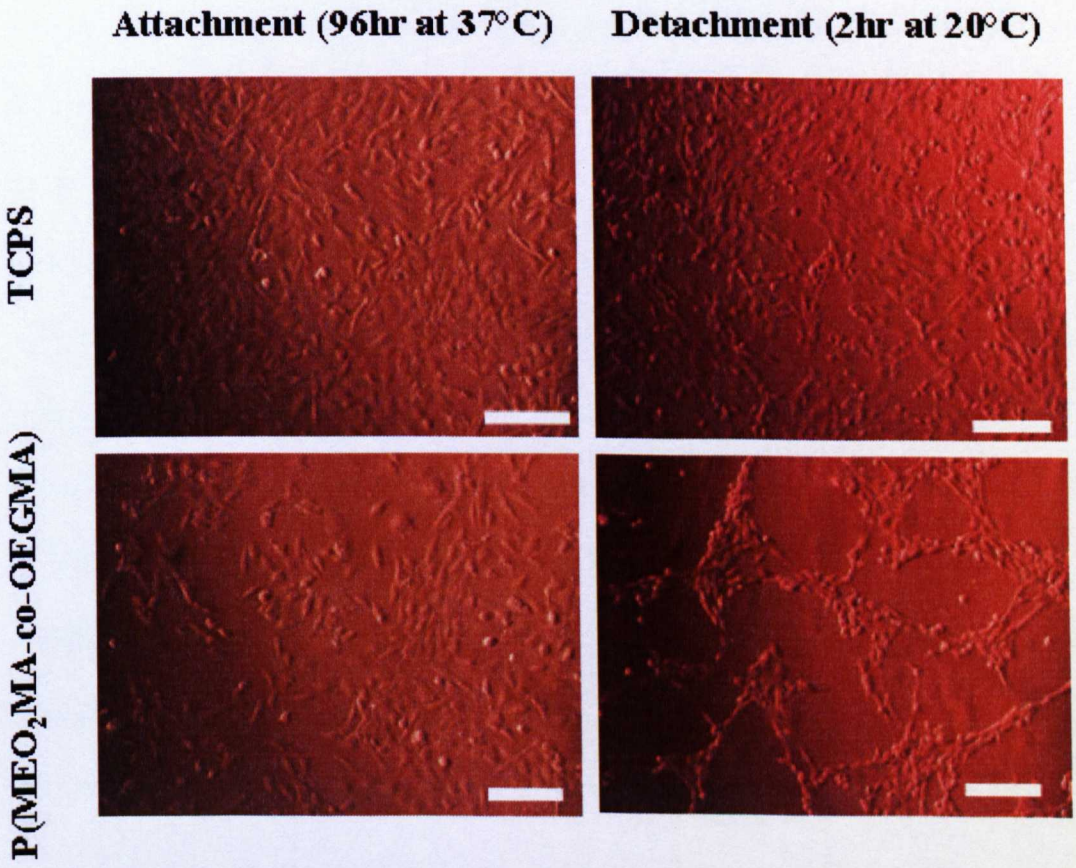

Figure 3.3. Representative images of mouse 3T3 fibroblast cell adhesion and subsequent detachment when cultured poly (MEO_2MA-co-OEGMA) surfaces. 3T3 fibroblasts exhibited a similar morphology on the thermo-responsive polymer surface as when compared to control TCPS. The temperature was lowered to 20°C and beginnings of cell detachment was observed on the polymer surface only (cells remained adhered in control TCPS samples). Scale bars: **100µm** and N=9 (3 batches and total of 9 samples).

In a recent report it was shown that when cultured on poly(MEO_2MA-co-OEGMA) functionalised surfaces at 37°C, 3T3 fibroblasts spread and proliferated possibly due to the brushes being in their globular hydrophobic structure. Upon cooling at 20°C a detachment of 3T3, likely due to the hydrated state of the brushes forming a then hydrophilic structure was observed, indicating that these thermo-responsive materials could be utilised for mammalian cell culture (196). In addition, 3T3 fibroblasts were reported to adhere to the thermo-responsive substrates based on PNIPAAm and *N-tert*-butyl-acrylamide copolymers as clumps of cells (207). However, it was shown in the same study that 3T3 fibroblasts adopted the spindle shape when these copolymer substrates pre-coated with laminin, collagen and poly (L-lysine) leading to more flattened cell shape (207). While 3T3 fibroblasts adhered and spread on poly (MEO_2MA-co-OEGMA) surfaces only (196), it was observed previously that TCPS treated with PNIPAAm homopolymer only, had led to neither adhesion nor proliferation of fibroblasts which was improved by incubation with collagen (208).

Quantitative analysis was performed using Leica Q-win software to estimate the area covered by cells after 96 h of culture at 37°C and 2 h of detachment at 20°C. The analysis was carried out on 9 samples (3 batches prepared on thee different days) (Figure 3.4).

Despite 3T3 fibroblast growth and proliferation on poly (MEO_2MA-co-OEGMA) grafted surfaces as shown in Figure 3.3, the area covered by 3T3 fibroblasts on the thermo-responsive surfaces was significantly different ($p=0.001$) to cells cultured on TCPS following 96 h of culture at 37°C. As shown in section 3.6.2, 3T3 fibroblasts were cultured on the thermo-responsive surface (3 cm^2) places in 6 well plates, which lead to a percentage loss of the original seeded cell population

on the surfaces to the 6 well plates. The thermo-responsive surfaces were transferred to a new 6 plates with only the cells adhered to the surface after washing them with warm PBS to remove unattached cells.

The temperature was subsequently lowered to 20°C for 1 h when the polymer brushes are in their hydrated conformation, 3T3 fibroblasts changed morphology from spread to round cells as shown in Figure 3.3. The percentage area covered by cells was lowered compared to both thermo-responsive surfaces at 37°C and cells cultured on TCPS indicating that they were detaching from the thermo-responsive surfaces and not from the TCPS surfaces ($p=0.0002$ after 2 h at 20°C) (Figure 3.4). Complete detachment of cells was observed with gentle agitation; the detached cells suspension was obtained with pipetting and passing them though G19 needle.

Okano *et al* has described the mechanism of cell detachment from thermo-responsive substrates (81, 209, 210). In this study, it is also thought to be controlled first by surface hydration of the temperature-responsive poly (MEO_2MA-co-OEGMA) as the temperature is decreased from 37°C to 20°C. This surface hydration and expansion of polymer chains causes cell morphology changes from spread to rounded cells.

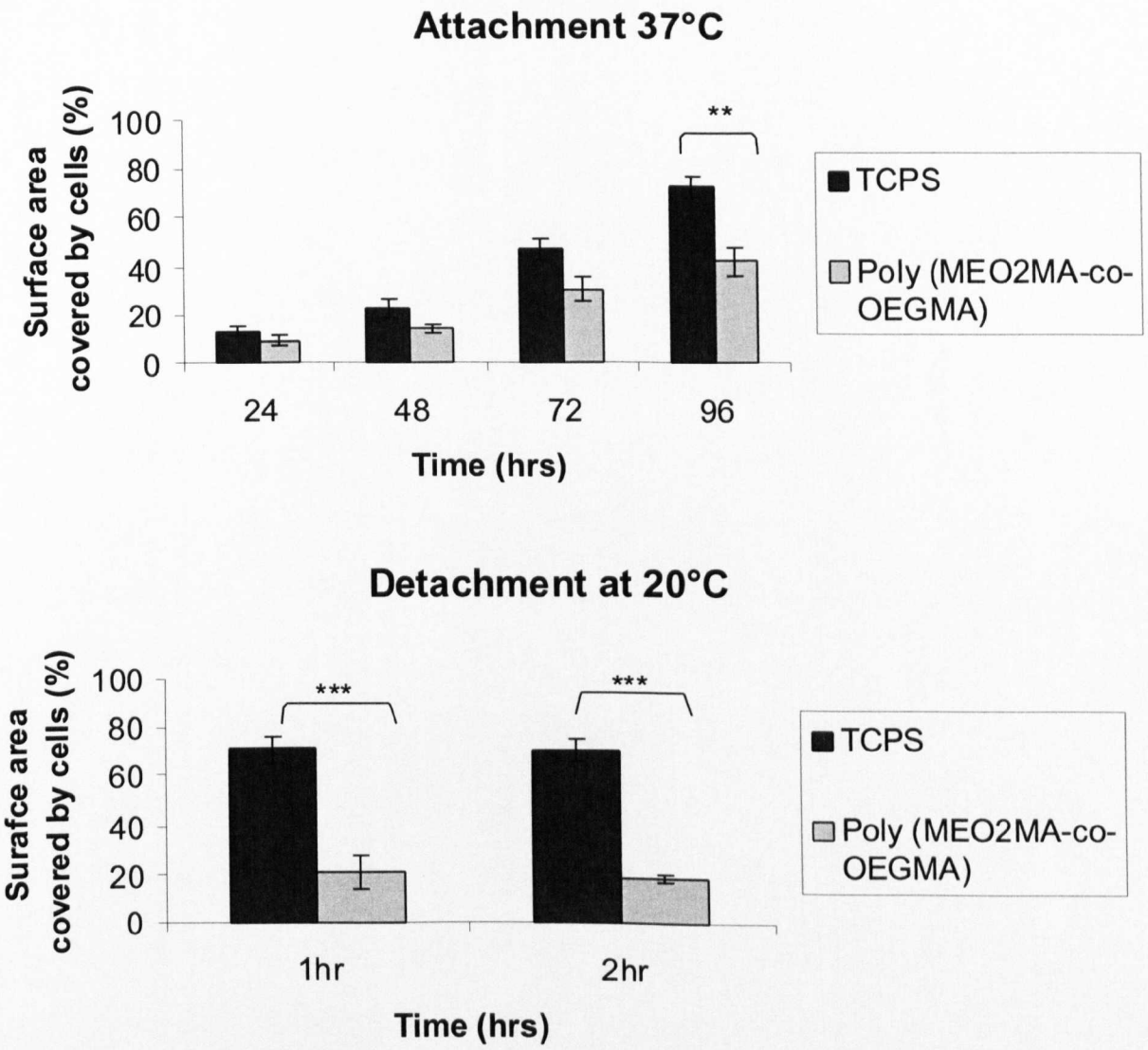

Figure 4.4. Surface area covered by cells, expressed as a percentage of the total surface area, following attachment (24, 48, 72, 96 h at 37°C) and detachment (1 and 2 h at 20°C). Error bars representing standard deviation of 9 samples (from 3 different surfaces batches for the thermo-responsive polymer only; N=9 for TCPS controls).

3.4.3 WCA of the same surface though temperature cycles

Thermo-responsive properties of the grafted poly (MEO_2MA-co-OEGMA) on the surface were studied using WCA at different temperatures above and below the

expected LCST i.e. 37°C and 20°C. As the main aim of this chapter is the culture of 3T3 fibroblasts as a model mammalian cell type on the poly (MEO_2MA-co-OEGMA) surfaces and taking advantage of the temperature change of the copolymer brushes, these surfaces were proposed to be used for culture and passage using temperature as the attachment/detachment factor.

To explore the potential to use the same surface for repeated cell culture and passaging, an individual surface was examined to determine whether the thermo-responsive behaviour is consistent though temperature cycles. Poly (MEO_2MA-co-OEGMA) brushes were synthesised as indicated in Chapter 2 (section 2.2.2); WCA therefore was measured though thee cycles above and below the LCST of the same surface. Figure 2.5 represents the WCA measurements on the same surface; the surface was hydrophobic at 37°C i.e. copolymer brushes are in their collapsed conformation, 63°, 63.8° and 64.9° on cycle 1, cycle 2 and cycle 3 respectively. When the temperature was lowered to 20°C i.e. copolymer brushes are in their hydrated state, the WCA was decreased to 48°, 55.4° and 49.5° on cycle 1, cycle 2 and cycle 3 respectively. This effect was also observed when the thermo-responsive behaviour was studied at the microscopic level (Figure 2.30). In addition, WCA was determined after culturing the cells on the thermo-responsive surfaces. WCA measurements were 67.01° ± 4.3 at 37°C and 51° ± 3.9 at 20°C and hence the thermo-responsive behaviour of the poly (MEO_2MA-co-OEGMA) surfaces after using them for cell culture was maintained.

Therefore, it was concluded that cells could be passaged and sub-cultured using the same substrate grafted with the thermo-responsive copolymer brushes. However, to ensure quality of the surfaces for future experiments fresh substrates were made for the subsequent passaging experiment where WCA of the poly

(MEO_2MA-co-OEGMA) grafted surfaces was measured before sterilising for their further use in the passaging experiment. Table 3.2 represents the WCA of a sample from batch 1 (from 3 batches used) which was used for passage 1, 5 and 10 respectively. Treated surfaces with 2-bromoisobutyryl bromide were included as the control. Control surfaces showed no thermo-responsiveness change at 37°C and 20°C as indicated in Table 3.2.

Table 3.2. WCA of one surface of each batch to test the thermo-responsiveness of the surface before cell culture; **A** is ppAAl-2-bromo-isobutyrate surfaces (which was used as a control) and **B** is poly (MEO_2MA-co-OEGMA) surfaces.

Passage number surfaces/Batches		**Batch 1**		**Batch 1**		**Batch 1**	
		A	**B**	**A**	**B**	**A**	**B**
P1	> LCST	69.8±4.6	62.9±2.6	70.4±1.7	61.1±1.8	72.3±3.1	64.6±2.1
	< LCST	70.3±0.7	45.6±1.7	73.5±5.5	47.4±1.1	73.1±5.6	43.4±1.3
P5	> LCST	73.5±2.9	64.2±2.2	71.6±2.1	63.1±1.9	72.6±3.8	66.1±4.9
	< LCST	70.5±5.1	46.1±0.9	71.8±2.9	45.9±1.1	73.0±2.6	45.5±1.7
P10	> LCST	73.6±2.5	66.1±4.7	73.2±3.8	65.9±4.6	73.7±1.9	65.8±4.4
	< LCST	74.8±5.4	50.3±1.1	74.8±4.8	49.6±0.7	71.6±7.2	49.1±0.6

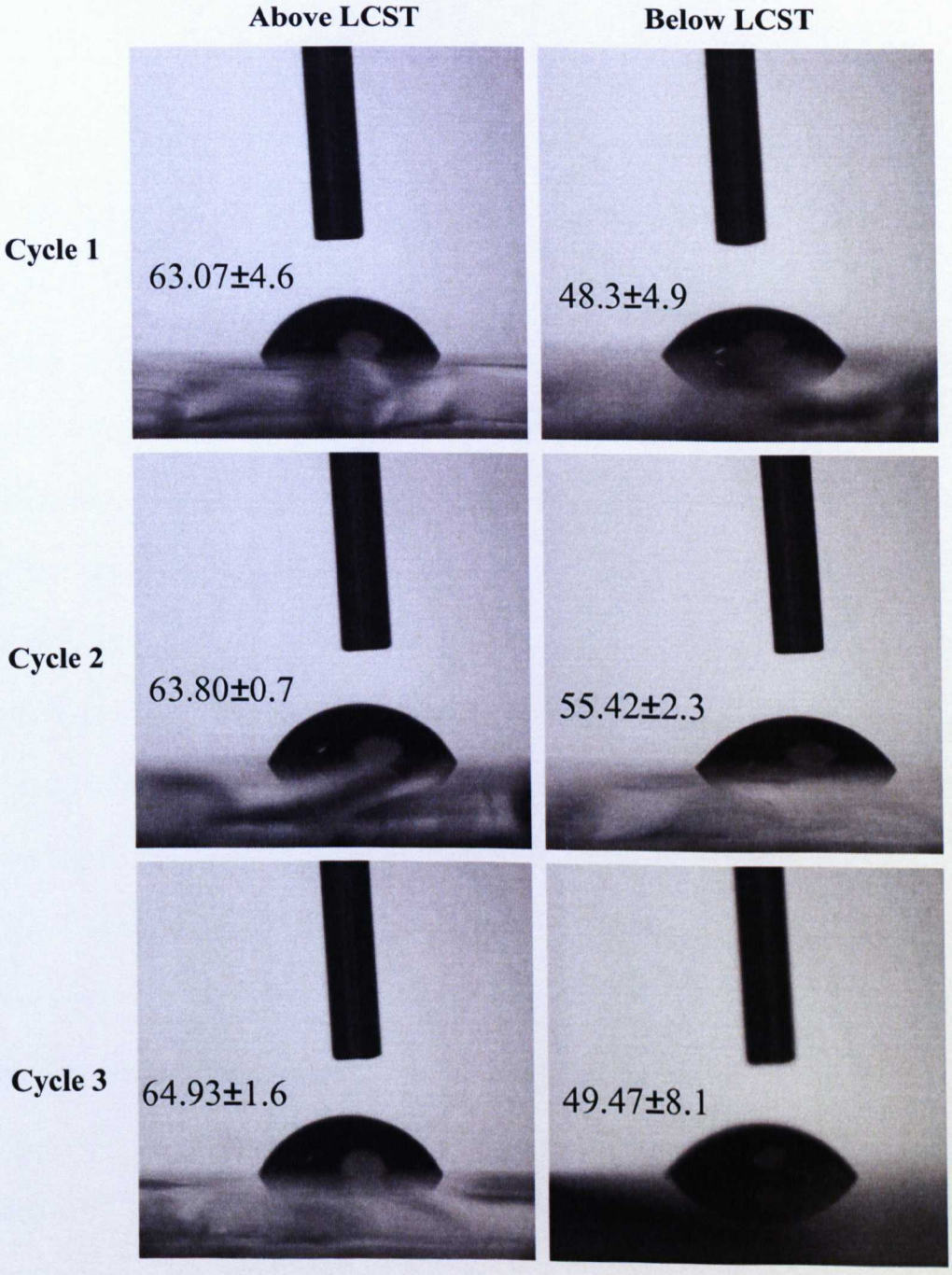

Figure 3.5. WCA measurements of poly (MEO_2MA-co-OEGMA) surface after thee temperature cycles. At cycle 1, 2 and 3 the surface was hydrophobic at 37°C and hydrophilic at 20°C.

3.4.4 Growth curve for mouse 3T3 fibroblasts

As shown in section 3.4.2, 3T3 fibroblasts adhered and spread on poly (MEO_2MA-co-OEGMA) grafted surfaces indicating that these surfaces are bio-adherent at 37°C. However, when the temperature of the culture medium was decreased from 37°C to 20°C, cell's morphology was changed from spread to round and hence detachment was observed compared to TCPS control substrates. Passaging of 3T3 fibroblasts using trypsin/EDTA dissociated the adhered cells on TCPS leading to individual cell suspension. However, cultures passaged using temperature as the detachment factor produced clumps of cells which were dissociated using gentle pipetting and passing the cell suspension though a G19 needles to ensure a single cell suspension was obtained.

Population doublings (PDs) were calculated at each passage using the formula $\{\log_{10}$ (total cell counts/cells seeded)$/\log_{10}$ (2)$\}$ and proliferation rates were calculated by hours in culture (on TCPS or poly (MEO_2MA-co-OEGMA))/cumulative population doublings (CPDs) over 10 passages.

Analysis of these proliferation rates indicated that the average population doubling interval for 3T3 fibroblasts on TCPS was 14.48 ± 0.16 h and on poly (MEO_2MA-co-OEGMA) was 20.37 ± 4.8 h. This indicated that poly (MEO_2MA-co-OEGMA) substrates are bio-adherent materials which supported the growth and proliferation of 3T3 fibroblasts (Figure 3.6).

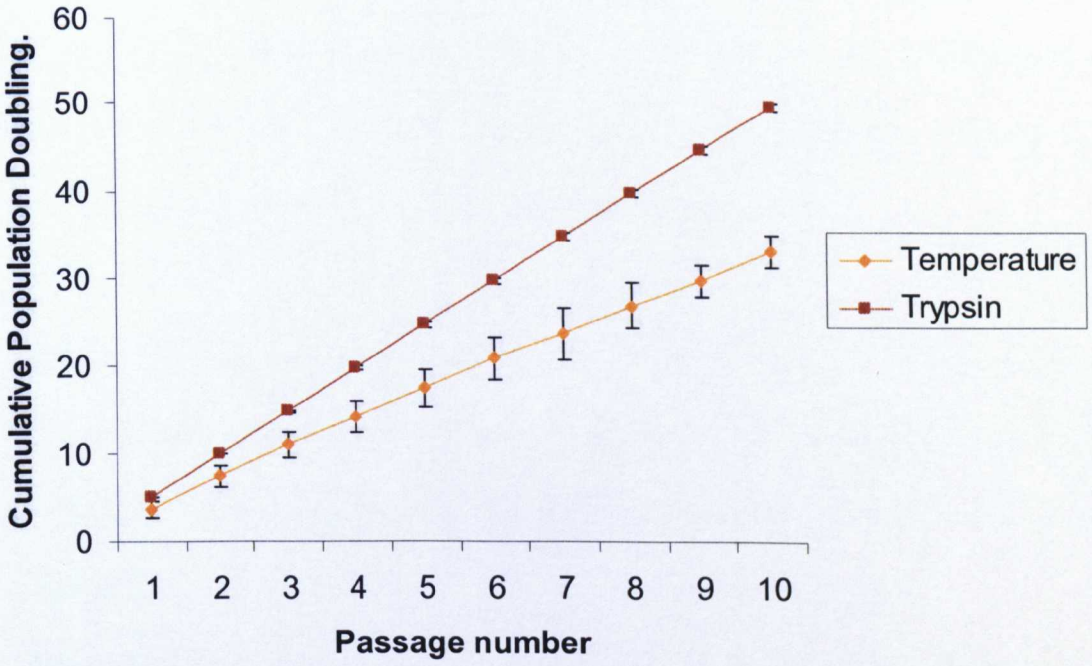

Figure 3.6. Growth curve for mouse 3T3 fibroblasts which they were serially passaged, over 10 passages, using trypsin and temperature from TCPS or poly (MEO_2MA-co-OEGMA) respectively.

3.4.5 Cell morphology

Morphology of the cells was studied to further examine the status of cells during their culture time on TCPS and poly (MEO_2MA-co-OEGMA) thermo-responsive surfaces. Therefore, cell morphology was observed though the 10 passages on poly (MEO_2MA-co-OEGMA) compared to cells grown on TCPS. It was found that cell morphology on the thermo-responsive surface was similar to cells grown on TCPS at passage 1. However, the morphology changed when these cells were passaged from 2 up to 10 (Figure 3.7) as they tended to show a more rounded shape compared to the characteristic spindle fibroblast shape as seen when cultured on TCPS.

Khor *et al* observed a similar behaviour when culturing keratinocytes on poly (ε-caprolactone) films and described these clumps of cells as cellular differentiation zones (211). Similarly, mouse fibroblasts adhered on these films as cellular groups which disappeared when the cells reached confluency (212).

Herein, cells cultured on poly (MEO_2MA-co-OEGMA) substrates tended to form dense cellular patches (as shown in Figure 3.7) which were described as nuclei of growth; however, these dense cellular groups disappeared when the cells reached confluency.

The presence of these cellular zones was thought to be due to the passaging process. The cell suspension of the detached cell sheets from the thermo-responsive surfaces was obtained by gentle pipetting and passing though a G19 needle. However, it is possible that some of the detached cell clumps did not break completely into a single cell suspension as happens when cells are detached from TCPS using trypsin/EDTA.

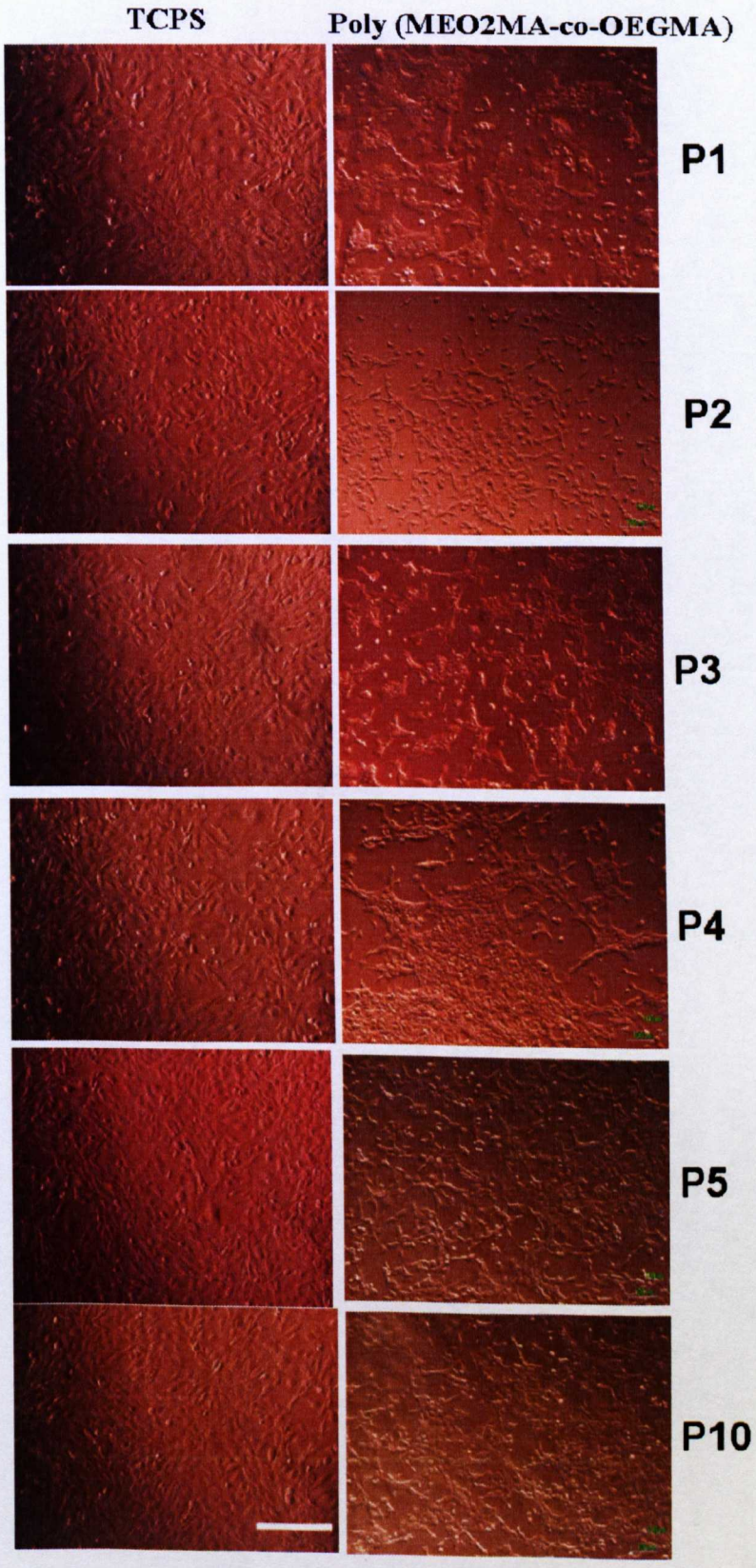

Figure 3.7. Representative images illustrating the cellular morphology of 3T3 fibroblasts on TCPS (left column) and on poly (MEO_2MA-co-OEGMA) following serial passaging over 10 passages. Scale bar = **100µm.**

3.4.6 Phalloidin staining

Upon seeding, cells spread on the culture substrates (TCPS or poly (MEO_2MA-co-OEGMA)); this involves major intracellular events including cytoskeletal re-arrangements i.e. the formation of actin fibers and focal adhesion complex that further interacts with the surface (213). Herein, Actin was stained using phalloidin to investigate the spreading of these cells on poly (MEO_2MA-co-OEGMA) in comparison to TCPS after passage 10. In addition, Phalloidin staining was also carried out to study the effect of temperature passaging on the cytoskeleton compared to cells cultured on and detached from TCPS with trypsin/EDTA.

3T3 fibroblasts were well spread after passage 10 on TCPS (Figure 3.8) as these cells developed actin fibres to form stress fibres. However, 3T3 fibroblasts cultured on poly (MEO_2MA-co-OEGMA) surfaces up to passage 10, showed populations of more rounded cells with actin around the nucleus despite their spreading. This was previously discussed and described as groups of cellular densities in section 3.4.5.

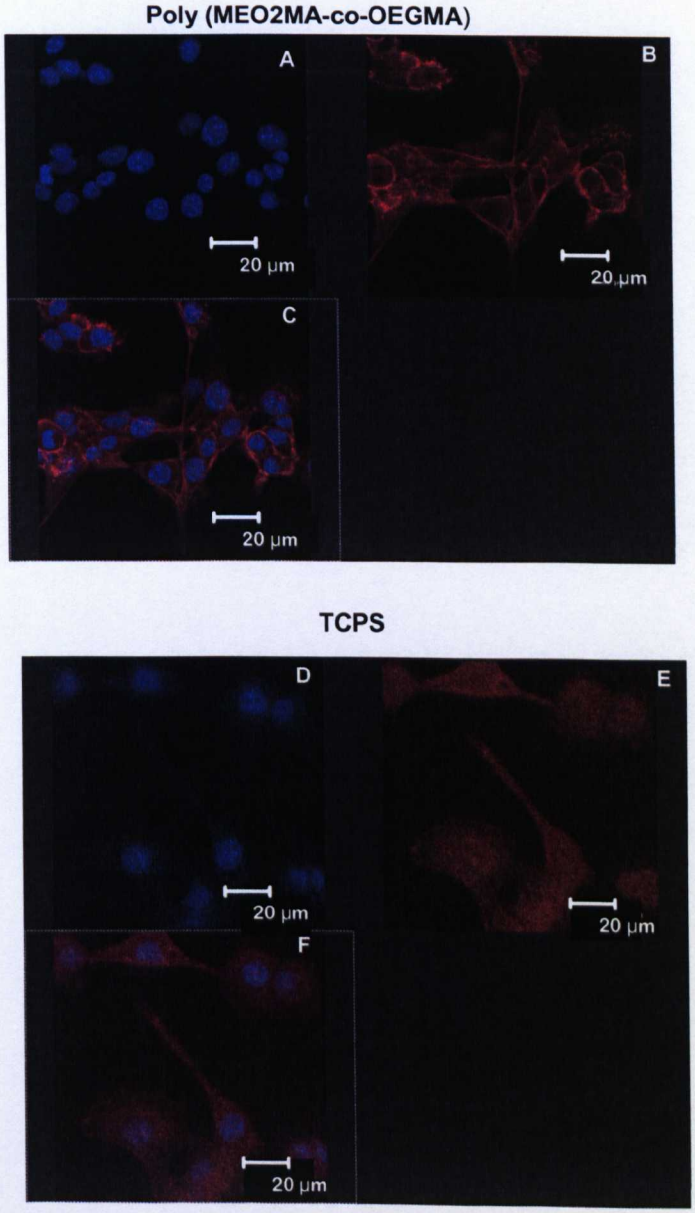

Figure 4.8. Representative fluorescent images of Phalloidin stained actin of 3T3 fibroblasts after passage 10 following culture on TCPS (right) and poly (MEO_2MA-co-OEGMA). Actin filaments are shown in red (**B** and **E**) and the nuclei of cells are in blue (**A** and **D**).Overlapping of the actin staining (red) and the nuclei (blue) are shown in C and F for both test samples. Scale bars = **20 µm**.

3.5 Conclusion

Thermo-responsive substrates as smart materials for cell culture have been extensively studied using the well known thermo-responsive polymer PNIPAAm; where cells adhered, spread and proliferated on substrates grafted with this polymer. However, the presence of multiple secondary amide functions can easily interact with other proteins for example though hydrogen bonding (214, 215). This had led to the need to develop switchable surfaces that exhibits similar thermo-responsive properties to PNIPAAm and biocompatible properties as PEG. PEG-based materials are usually used as bio-repellent for numerous applications including blood compatible materials. However, the random copolymerisation of MEO_2MA and OEGMA can produce copolymers of different LCSTs that can be adjusted according to monomer composition. Therefore, poly (MEO_2MA-co-OEGMA) polymer brushes were synthesised as described in Chapter 2 for mammalian cell culture.

These thermo-responsive surfaces supported the growth and proliferation of 3T3 fibroblasts similar to that seen for cells cultured on TCPS. However, the morphology of these cells showed the formation of groups of cellular densities on poly (MEO_2MA-co-OEGMA) compared to cell monolayers seen on the TCPS. These cell clusters were thought to be a consequence of the passaging process using temperature which generated cell clusters rather than cell suspensions as seen with cells cultured on TCPS using trypsin/EDTA.

Since these substrates supported the growth and proliferation of 3T3 fibroblasts as a model mammalian cell type, they were proposed for the investigation of the response of mouse embryonic stem cells as a model stem cell type. This will be described in the following chapter (Chapter 4).

CHAPTER 4

Culture and passage of mouse embryonic stem cells from thermo-reversible poly (MEO_2MA-co-OEGMA) surfaces

4.1 Introduction

Currently, the use of embryonic stem cells (ESCs) for therapeutic purposes i.e. tissue engineering and cell based treatment therapies is the focus for many research programmes (61, 216-220). However, their ultimate application within a clinical setting is not only dependent on the ability to control their differentiation, but also to develop practical culture systems for the safe expansion of cell populations and maintaining them in their undifferentiated state, such that pluripotent cells can be produced in high numbers, in a reliable and consistent manner and without safety implications for the patient.

Efficient *in vitro* expansion of ESCs is required to prevent uncontrolled differentiation of these cells and as they need to be sub-cultivated or passaged every 2-3 or 5-7 days for mouse or human ES cells respectively. Spread ESC colonies are usually enzymatically dissociated from the culture surface and from each other, usually with trypsin/EDTA, to obtain individual cells which can then be re-plated onto fibroblast feeder layers or gelatin treated substrates for further

expansion (221). It has been reported that excessive use of trypsin to detach hESCs from culture substrates can result in a decreased number of viable cells over time and therefore affecting their utility for clinical applications (222). Besides the risk of contamination by adventitious infectious agents, hESCs can incorporate and express immunogenic molecules when exposed to animal products in culture (e.g. trypsin derived from egg white) (223).

Synthetic 'smart' biomaterials, in which the bio-adhesive properties of the surface can be changed by altering environmental factors such as temperature, have been previously described (224). Such chemically defined surfaces have been used in differentiated mammalian cell culture to avoid the deleterious effects of trypsin upon cells (225-235). The Okano group in particular have pioneered the use of switchable surfaces employing the well-known thermo-responsive polymer PNIPAAm as the molecular switch for cell adhesion (ON) and detachment (OFF) (225, 236). Despite the promising results shown using PNIPAAm, this polymer can induce cellular cytotoxicity when it is switched from an extended hydrophilic coil conformation to a chain-collapsed globule (hydrophobic) across its LCST, which occurs at 32°C (237). Moreover, the amide functional groups in the chemical structure of PNIPAAm can easily interact with other amide groups present in the surrounding molecules including proteins (214, 238).

Copolymers of 2-(2-methoxyethoxy) ethylmethacrylate (MEO_2MA) and oligo (ethylene glycol) methacrylate (OEGMA) are promising for biomedical applications as they are composed of FDA-approved oligo (ethylene glycol) segments (116). The LCST of poly (MEO_2MA-co-OEGMA) copolymers can be adjusted by altering the co-monomer compositions to obtain thermo-responsive properties close to body temperature as with PNIPAAm i.e. 32°C (117-120).

Therefore they have been proposed for use in cell culture systems. A recent report has shown the attachment, proliferation and detachment of 3T3 mouse fibroblasts on these substrates, controlled by temperature cycling around the LCST of the copolymer grafts (239).

However, while there is now extensive literature on the use of synthetic polymer surfaces for differentiated mammalian cell culture (85, 86, 240) there is only one recent report describing the use of thermo-responsive polymer grafts for ESC culture using PNIPAAm (110).

Thermo-responsive poly (MEO_2MA-co-OEGMA) surfaces were grown via ATRP from plasma-polymer treated glass substrates as described in Chapter 2.

These substrates were used to culture 3T3 fibroblasts as a model mammalian cell type, on which, they spread and proliferated (Chapter 3). Thereafter, the application of these surfaces for controllable attachment/detachment of mouse embryonic stem cells (mESCs) as a potential method to manipulate ESCs in culture without the use of enzymes or surface coatings (i.e. gelatin) is described in this chapter.

4.2 Aims and Objectives

The aim of this chapter was to use poly (MEO_2MA-co-OEGMA) thermo-responsive surfaces for mESCs expansion and passaging using the temperature as the detachment factor and compare it with trypsinization treatment of these cells grown on gelatin (control). This aim was achieved though the following objectives:

1. To observe mESCs response i.e. adhesion on poly (MEO_2MA-co-OEGMA) only.
2. To promote mESCs adhesion by incubating the surface with different reagents.
3. Thereafter, detachment of the cultured mESCs was carried out from the thermo-responsive poly (MEO_2MA-co-OEGMA)/fibronectin substrates.
4. The use of these substrates to passage mESCs, in the presence of LIF as the differentiation inhibitor, using temperature as the detachment factor.
5. To check the undifferentiated state of the mESCs after passage 10 in comparison with trypsin/EDTA detached cells from gelatin coated surfaces.

4.3 Materials and Methods

4.3.1 Poly (MEO_2MA-co-OEGMA) synthesis

As described in Chapter 2 (section 2.3), glass substrates were cleaned and plasma coated with allyl alcohol at a power of 100 W; thereafter, surfaces were treated with 2-bromoisobutyryl bromide in the presence of THF and triethylamine anhydrous. Poly (MEO_2MA-co-OEGMA) brushes were grafted from the initiation sites using ATRP in ethanol. The substrates were used for cell culture within 48 h.

4.3.2 mESCs culture on poly (MEO_2MA-co-OEGMA)

Feeder free mouse embryonic stem cells were supplied by Dr Chistina Tuffarelli (Developmental Genetics and Gene Control - The University of Nottingham). Feeder free mouse embryonic stem cells (E14Tg2A) were cultured for two days

(to 80% confluence) on flasks pre-coated with 0.1% (*w/v*) gelatin in PBS at 37°C, 5% CO_2 in air. Complete mESCs culture medium contained DMEM supplemented with L-glutamine (2 mM), antibiotic/antimyocotic (penicillin at 100 units/mL, streptomycin at 100 µ/mL, amphotericin B at 0.25 µg/mL), 15% (*v/v*) FBS (ES-cell qualified), 0.5 mL of 2-Mercaptoethanol. LIF was then added to 100 mL of the prepared mESCs media in a concentration of 1000 units per mL of (Appendix1). Prior to the initial passage, the cells were washed with warm PBS (pH 7.4) and incubated with 1 mL trypsin/EDTA solution for 3 minute at 37°C. Culture medium containing 15 % (*v/v*) FBS was subsequently added to inactivate the trypsin and the cells pelleted by centrifugation at 1000 rpm using a Sigma Laboratory centrifuges 3K15 (Scientific Laboratory Supplies, UK) for 3 minutes. The cells were re-suspended in complete mESCs culture medium and 10^6 were seeded on freshly pre-coated gelatin T25 flasks for further expansion or use directly in experiments with the thermo-responsive polymer surface. The cell passage number used in this work were between 2-10.

The thermo-responsive surfaces were transferred to sterile 6 well non-tissue culture treated plates and sterilised under UV for 20 min prior to cell culture on these substrates. mESCs adhesion response was first investigated with untreated poly (MEO_2MA-co-OEGMA) substrates only. Following these experiments, the incubation of the thermo-responsive surfaces with 100% (*v/v*) FCS, 2% (*w/v*) gelatin and 200 µg/mL fibronectin respectively (i.e. not as a mixture) for 18 h at 37°C was investigated as a means to aid mESCs attachment. In this experiment, two batches of substrates made on different days, composed of 3 samples in each batch, were tested for the poly (MEO_2MA-co-OEGMA) alone sample and for each surface treatment. A single cell suspension where 10,000 cells/mL (in a total

of 2mL; 20,000 cells/mL) were seeded on these surfaces and cultured for 96 h at 37°C, 5% CO_2 in air. mESCs (20,000 cells/mL) cultured on gelatin coated plates for 96 h as above were used as a control.

4.3.3 Incubation Conditions of Poly (MEO_2MA-co-OEGMA) with Fibronectin and Subsequent mESC Adhesion

The incubation of poly (MEO_2MA-co-OEGMA) with fibronectin according to the conformation of the copolymer brushes i.e. hydrophilic (at 20°C) and hydrophobic (at 37°C) was studied to investigate the most appropriate conditions for fibronectin adsorption to the thermo-responsive surfaces and subsequent effect on mESCs adhesion.

Poly (MEO_2MA-co-OEGMA) thermo-responsive surfaces were incubated with 200 μg/mL fibronectin at (1) 37°C for 18 h, at (2) 20°C for 18 h, and (3) at 20°C for 18 h and then at 37°C for 3 h as shown in Figure 4.1. mESCs were cultured on 6 samples (2 batches) for each fibronectin pre-conditioning method, with a cell density of 10,000 cells/mL in a total of 2 mL (20,000 cells/mL). Thermo-responsive samples were washed with warm PBS 24 h after cell seeding to remove the unattached cells and transferred to new culture plates where the culture media was changed and allowed to incubate at 37°C for a further 96 h of culture. Gelatin coated TCPS was used as a control where 20,000 cells/mL were seeded and cultured for 96 h under the same conditions.

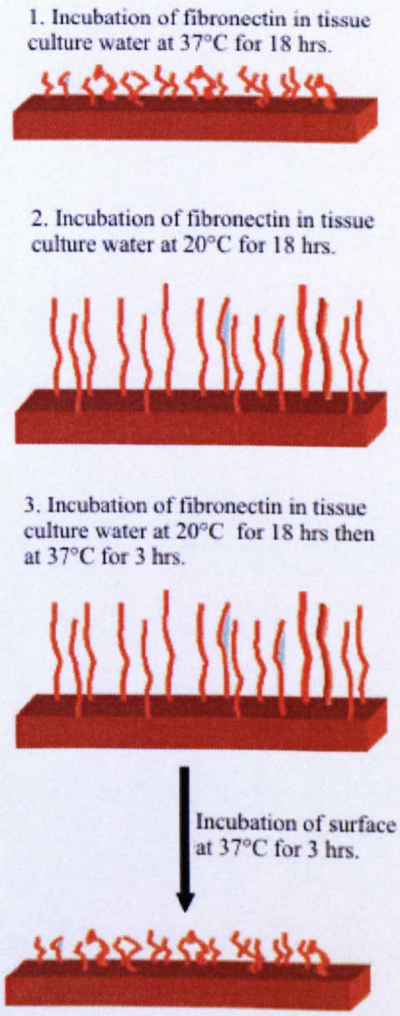

Figure 4.1. Schematic diagram of the different incubation conditions for fibronectin adsorption on poly (MEO_2MA-co-OEGMA) surfaces when the bushes are in the hydrophobic globule brush state (1), in the hydrophilic extended brush state (2), and incubation of fibronectin when the polymer brushes are in their hydrophilic conformation followed by subsequent collapse in the hydrophobic conformation (3).

4.3.4 Incubation of poly (MEO_2MA-co-OEGMA) with different concentrations of fibronectin

Poly (MEO_2MA-co-OEGMA) surfaces, following sterilisation under UV for 20 minutes, were incubated at 37°C for 18 h with different concentrations of

fibronectin, 100, 50, 25, 10 and 5 μg/mL in tissue culture water. mESCs were then seeded on (2 individual batches; 6 samples in total) for each concentration of fibronectin at a density of 10,000 cells/mL in a total of 2mL (20,000 cells/mL). Thermo-responsive samples were then washed with warm PBS after 24 h of culture to remove the unattached cells and transferred to new culture plates and then incubated at 37°C, 5% CO_2 in air for a further 72 h.

4.3.5 Detachment of mESCs from the poly (MEO_2MA-co-OEGMA) at different temperatures

Detachment assay was conducted following 72 h of mESCs culture by lowering the temperature of the culture medium to 4°C, 10°C and 20°C for 2 h. Detached cells were then centrifuged and re-suspended in a fresh complete mESCs culture media. Trypan blue exclusion was conducted to assess the viability of the detached cells as described in Chapter 3 (section 3.3.3).

4.3.6 FITC-fibronectin staining of the poly (MEO_2MA-co-OEGMA) to confirm the adsorption of fibronectin to the surface

Poly (MEO_2MA-co-OEGMA)/fibronectin surfaces were incubated for 18 h at either 37°C (hydrophobic state; condition 1) or 20°C (hydrophilic state, condition 2) with 5 μg/ml of fibronectin in dH_2O and washed with warm PBS prior to immuno-staining. This was conducted with primary fibronectin antibody (rabbit anti-human fibronectin polyclonal antibody) at a dilution of 1:200 in 0.1% BSA solution overnight at 37°C. Sample surfaces were washed with PBS and then

incubated with a secondary antibody (Alexa fluor® 488 anti-rabbit IgG produced in goat (Invitrogen) at 1:200 dilution in 0.1% BSA for 4 h at room temperature. Surfaces were rinsed with PBS and mounted with Vectashield without DAPI stain (Invitrogen). A similar protocol was used to immuno-stain fibronectin on poly (MEO_2MA-co-OEGMA)/fibronectin following incubation with cells and their subsequent detachment at 10°C. Images of immuno-stained fibronectin adsorbed onto the thermo-responsive surfaces at 37°C, 20°C and after detachment of cells at 10°C were acquired using a Leica DM IRB fluorescence microscope (with a QICAM camera and Qcapture imaging software). Image analysis was performed using Corel Photopaint software and average fluorescence intensities of at least 5 representative positions on the surface were recorded for thee thermo-responsive/fibronectin surfaces.

4.3.7 Surface analysis of Fibronectin coated poly (MEO_2MA-co-OEGMA) surfaces

To investigate the chemistry of poly (MEO_2MA-co-OEGMA) surfaces following incubation with fibronectin at 37°C for 18 h, XPS and WCA were used as described in Chapter 2 (section 2.3.4.1 and 2.3.4.2 respectively).

4.3.8 Passaging experiment of mESCs using poly (MEO_2MA-co-OEGMA) surfaces, treated with 5 µg/ml of fibronectin

Fresh surfaces were prepared for each passaging experiment (2 individual batches with 6 samples in total were prepared as described in Chapter 2). Poly (MEO_2MA-

co-OEGMA) surfaces were incubated with 5 μg/mL of fibronectin in dH_2O overnight at 37°C and then mESCs were seeded on the surfaces at a density of 20,000 cells in 2 mL. A single cell suspension after detachment assays (gained by either lowering the temperature from 37°C to 10°C or by using trypsin) was obtained by pipetting the cells gently for 5-10 mins and then passing them though a 19G needle. The detached cells were pelleted by centrifugation and then re-suspended in fresh culture media. They were then counted after each passage using Trypan Blue exclusion method to determine viability and re-seeded to a freshly prepared poly (MEO_2MA-co-OEGMA) surface (with 5 μg/mL fibronectin adsorbed) and incubated at 37°C, 5% CO_2 in air for 72 h. Population doublings (PDs) at each passage were calculated using the formula $\{\log_{10}$ (total cell counts/cells seeded)$/\log_{10}$ (2)$\}$ where the initial cell number seeded was 20,000 cells/ 2 mL. Proliferation rates were calculated and expressed as a function of hours in culture/ cumulative population doublings (CPD).

4.3.9 Viabilty assay using trypan blue and Alamar blue assay

Typan blue is conducted on the tested samples and controls as described in section 3.3.3. Alamar blue was used to monitor cell viability on the various test surfaces used. Cell culture media was aspirated and the culture surface washed with warm and sterile PBS. With respect to the thermo-responsive polymer surfaces, the substrates were transferred to fresh culture wells where 1 mL of Alamar blue prepared solution (Appendix 3) was added and incubated at 37°C, 5% CO_2 for 90 min. Thereafter, 100 μL were transferred to 96 microlitre well plates and wrapped

with foil paper until ready for fluorescence measurements using MFX 300 plate reader at Ex (560 nm/Em 590 nm).

4.3.10 Cell Imaging and Images Analysis

A Leica inverted light microscope (Leica model DMIRB) was used to image the cells by phase-contrast after 72 or 96 h from the initial seeding time and images were captured using a QICAM camera (using the computer program DC viewer: version 3.2.0.0) for both control and polymer-grafted surfaces. Qwin Leica software associated with the microscope was used to estimate the average surface area covered by cells for 5 representative images per surface; mean and standard deviation were calculated as described in Chapter 3 (section 3.3.6).

4.3.11 Immuno-staining for Oct3/4, Brachyury, Nestin and GATA-4

mESCs cultured on either the thermo-responsive surfaces/fibronectin surfaces or on gelatin coated substrates (control), were fixed with 4% (*w/v*) paraformaldehyde (PFA) for 30 min at room temperature and then washed with PBS for 5 min. Cells were permeabilised with 0.1% (*v/v*) Triton X-100 in PBS for 1 h at 4°C followed by incubation in PBS containing 4% (*v/v*) goat serum (blocking solution) for 1 h at room temperature. Thereafter, they were incubated at 4°C overnight with primary antibody (mouse monoclonal antibodies) diluted in 1% (*v/v*) BSA in PBS (OCT-4, 1:200; GATA4, 1:200; Nestin, 1:200; Brachyury, 1:200). Cells were then washed thee times for 30 minutes in PBS supplemented with 0.05% (*v/v*) Tween 20. This solution was removed and replaced with Alexa fluor® 488 anti-mouse IgG

produced in goat (Invitrogen; 1:200) diluted in 1% (*v/v*) BSA for 2 h at 4°C. Unbound secondary antibody was removed with thee washes with PBS supplemented with 0.05% (*v/v*) Tween 20 in 30 minutes. The sample was then mounted using Vectashield mounting solution containing DAPI (Invitrogen) and then stored at 4°C in the dark until images could be taken as described in section 2.9.1. Primary and secondary antibodies staining conducted in parallel with the tested samples and the positive control (gelatin) (data not shown).

4.3.12 RNA extraction and reverse transcription-polymerase chain reaction (RT-PCR)

Total RNA was extracted from mESCs cultured on both thermo-responsive surfaces/fibronectin (3 samples) and control (3 samples) surfaces using the RNeasy Mini Kit (Qiagen) following manufacturer's instructions. In brief, each sample was treated with RNease-free DNase to avoid DNA contamination and RNA was subsequently quantified using a Nanodrop (ND-1000 spectrophotometer using the associated software ND-1000 3.3).

5.3.11.i. Reverse transcription (RT)

A total of 1 μg of total RNA for each sample was reversed transcribed to cDNA with an oligo-dT. First, RT1 (13μL) was prepared as shown in Table 5.1 and incubated at 65°C for 10 min to denature the RNA which was subsequently incubated on ice for 1 min. RT2 (7μl) was added and mixed with each RT1 reactiona. A RT cycle at 55°C for 120 mins was used, followed by 85°C for 5

minutes to inactivate the transcriptor reverse transcriptase enzyme. The cDNA product was stored at -20°C until further use.

Table 4.1. Reverse transcription mixture volumes used for both cells collected from gelatin coated surfaces and the thermo-responsive/fibronectin substrates.

	Reverse Transcription 1 (RT1)		
Reagent	Stock concentration	Volume	Final conc
Template	1 µg	1 µL	1 µg/L total
Oligo dT	500 ng/µl	1 µl	25 ng/µl
H_2O	-	up to 13 µl	-
	Total	13 µl	

	Reverse Transcription 2 (RT2)		
Reagent	Stock concentration	Volume	Final conc
RT buffer	5X	4 µl	1X
RNase inhibitor	40 u/µl	0.5 µl	20u
dNTP mix	10mM each	2 µl	1mM each
RTase	20 u/µl	0.5 µl	10u
	Total	7 µl	

5.3.11.ii. Polymerase chain reaction (PCR)

Polymerase chain reaction (PCR) was conducted using the prepared cDNA (as described above) and the appropriate primer sequences (Provided by the Tissue Engineering Group, The University of Nottingham). The sizes of final PCR products, annealing temperatures and cycle numbers are described in Table 4.3. Table 4.2 shows the mixture volumes for the PCR reaction; cDNA template was added to PCR 1 and PCR 2 pre-prepared mixtures. Thereafter, the whole mixture was cycled using ThermoHybaid P×2 thermal cycler under the following conditions: at 94°C for 5 minutes for one cycle (initial de-naturation); 30 cycles at 94°C for 30 seconds (de-naturing); then a cycle at 55-

60°C (depending on the melting temperature of the primers as indicated in Table 5.3) for 30 seconds (annealing) and 72°C for 1 minute (extension) and a final step at 72°C for 10 minutes (final extension). The final product then was stored at -20°C until further use.

Table 4.2. Polymerase chain reaction mixture volumes for both the control (cells from gelatin coated surfaces) and sample (cells collected from the thermo-responsive surfaces).

	PCR 1		
Reagent	Stock concentration	Volume/reaction	Final conc
dNTP mix	10mM each	1 µl	0.2 mM each
Forward primer	5 µM	5 µl	0.5 µM
Reverse primer	5 µM	5 µl	0.5 µM
H_2O	-	up to 25 µl	-
	Total	25 µl	

	PCR 2		
Reagent	Stock concentration	Volume/reaction	Final conc
PCR buffer	10X	5 µl	1X
Taq polymerase		0.25 µl	
H_2O	-	19.75 µl	-
	Total	25 µl	

Table 4.3. Cycling temperatures for primers used for PCR reaction i.e. GAPDH, Oct3/4, Nestin, Brachyury and GATA4.

Gene	Primer-probe sequence 5'-3'	Product size bp	Annealing temp. (°C)	Cycle no
GAPDH	F: TGAGGCCGGTGCTGAGTATGTCG R: CCACAGTCTTCTGGGTGGCAGTG	302	60°C	30
Oct-4	F: AGCACGAGTGGAAAGCAACT R: AGATGGTGGTCTGGCTGAAC	248	60°C	30

GATA4	F: CTGGAAGACACCCCAATCTC R: GTAGTGTCCCGTCCCATCTC	130	55°C	30
Brachyury	F: GCTGTTGGGTAGGGAGTCAA R: CCCCGTTCACATATTTCCAG	380	60°C	30
Nestin	F: AGGCGCTGGAACAGAGATT R: TTCCAGGATCTGAGCGATCT	150	55°C	30

5.3.11.iii. Gel electrophoresis and imaging

Products were analysed on a 2% (*w/v*) agarose gel using Tris-borate-EDTA (TBE) buffer; 4-5 µl of ethidium bromide was added to the prepared agarose solution prior to casting. PCR samples were mixed with 10 µl of loading buffer and loaded into individual wells of the gel immersed in TBE. An electrical current was applied across the gel and PCR products allowed to run for 20-30 mins; these then were imaged using a gel imager using UV.

The images of the gels after electrophoresis were captured in BMP format and analysed using Corel photopaint × 4 where the image analysis option was used to quantify the grey intensity of the bands ranging from 0 (black) to 255 (white).

All PCR reactions were carried out using a positive control (mESCs cultured on 0.1% *w/v* gelatin coated flasks) and GAPDH was used as the housekeeping gene.

4.3.13 Statistical analysis

Data were expressed as mean ± standard deviation (SDV). Statistical analyses (using Microsoft Excel® 2003) were performed using the unpaired Student's t-test: differences between data sets were considered to be statistically significant when $P < 0.05$.

4.4 Results and Discussion

Initial studies involved the culture of mESCs (E14Tg2A line) on poly (MEO_2MA-co-OEGMA) surfaces above the LCST at 37°C for 96 h. It was observed that this thermo-responsive surface did not support cell adhesion as visualised by the formation of embryoid bodies (Figure 4.2) compared to the characteristic cell monolayers seen when cultured on the gelatin surface control (Figure 4.2). Indeed, surfaces based on poly (ethylene glycol) (PEG) as self-assembled layers have shown reduced protein adsorption and hence low mammalian cellular attachment (241).

This lack of cell adhesion is due to the steric repulsion of proteins caused by the PEG layer in addition to the lack of ionic interaction between the cells and the PEG chains (242-244). Non-linear PEG analogues composed of methoxy-terminated oligo (ethylene glycol) also showed high resistance to protein adsorption and hence low cell attachment (241, 245-250). Therefore, the incubation of poly (MEO_2MA-co-OEGMA) thermo-responsive surfaces with different proteins including 100% FCS (*v/v*), 2% gelatin (*w/v*) and 200 μg/mL of fibronectin in a total of 2 mL was conducted and subsequent cell attachment was investigated. Low attachment was observed on surfaces treated with a complex mixture of proteins such as FCS and gelatin due to inherent resistance of the surface to protein adsorption (245) which in turn could be due to the adsorption of water in the dis-ordered copolymer brushes (251) (Figure 4.2).

Fibronectin is a high molecular weight extracellular glycoprotein that aids the adhesion of mammalian cells to surfaces by the interaction with integrins on cell membranes (252). Integrins are a family of surface adhesion receptors which are

composed of α and β subunits (253-255); fibronectin specifically binds to $\alpha_5\beta_1$, $\alpha V\beta_1$ on embryonic stem cells (256). Therefore, poly (MEO_2MA-co-OEGMA) surfaces were incubated with 200 μg/ml of this glycoprotein and the mESCs adhered, spread and proliferated as shown in Figure 4.2 in a similar fashion as on the gelatin (control) (Figure 4.2).

Several studies have been carried out to investigate fibronectin adsorption to hydrophobic and hydrophilic surfaces as it can adsorb to both types of surfaces. It was found that it adsorbed to each type of surface in different conformations which could in turn affect cell attachment (257, 258). Therefore, incubation of fibronectin on poly (MEO_2MA-co-OEGMA) surfaces when the polymer chains are in the globular (hydrophobic, 37°C) or in the extended chain conformations (hydrophilic, 20°C) was investigated. In addition, the adsorption of fibronectin to the surface at 20°C (hydrophilic extended chain conformation) followed by incubation of the surface at 37°C was carried out as it was thought that incorporation of the fibronectin would occur when the brushes collapsed (hydrophobic conformation). This is explained in Figure 4.1, which shows schematic description of the different fibronectin incubation conditions on the poly (MEO_2MA-co-OEGMA) thermo-responsive surface.

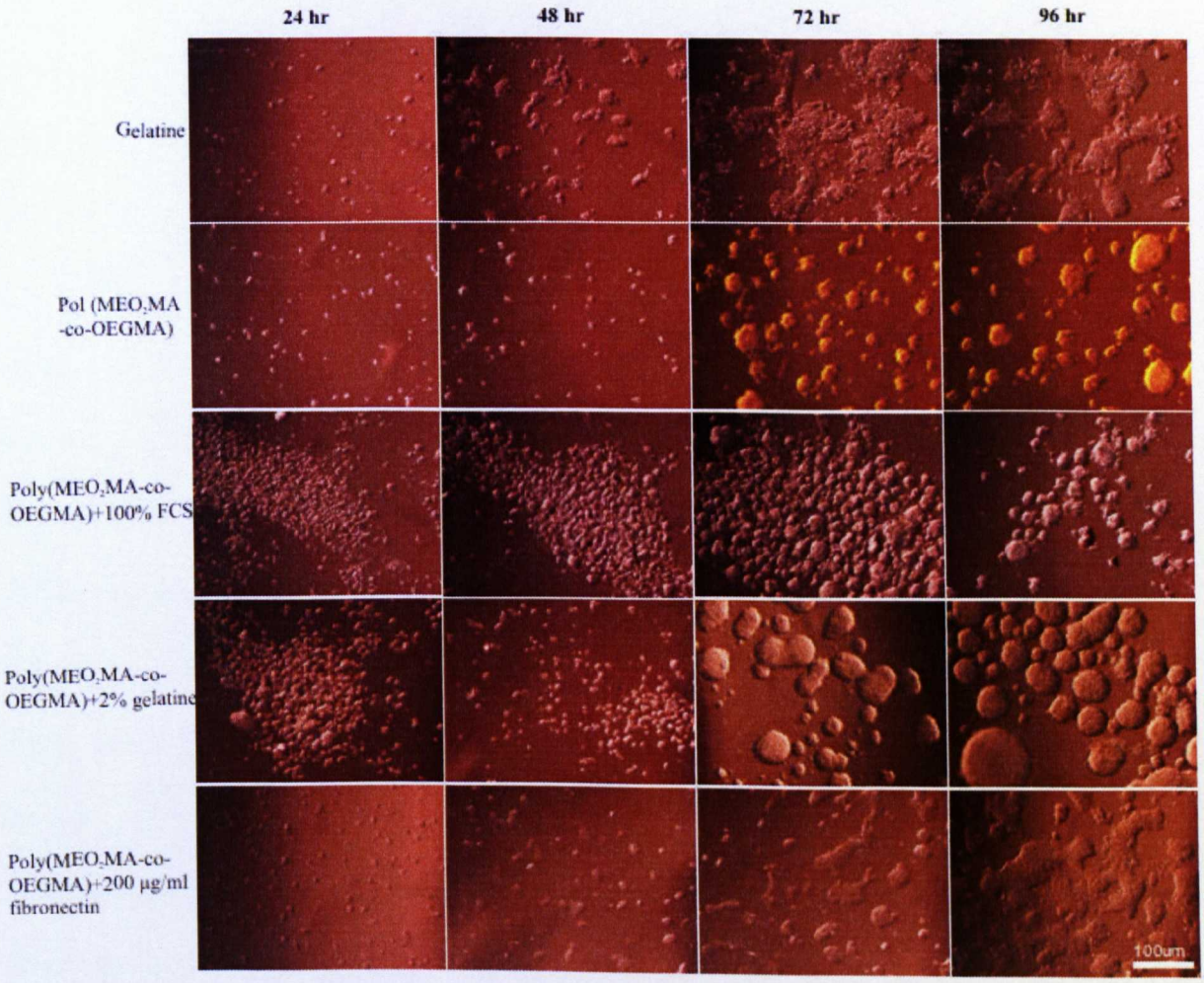

Figure 4.2. Representative images for mESC adhesion response studies on untreated poly (MEO_2MA-co-OEGMA) surfaces and after different pre-conditioning treatments to the surface following culture for 96 h at 37°C. Scale bar = **100 µm**

Figure 4.3 indicates ESC response to the poly (MEO_2MA-co-OEGMA) surfaces when the fibronectin (200 μg /mL, 400μg/mL) was adsorbed to the surface under different conditions described above. Cells adhered, spread and proliferated on poly (MEO_2MA-co-OEGMA) surfaces which were preincubated with fibronectin at 37°C for 18 h (hydrophobic conformation of the copolymer brushes; globular) (Figure 4.3). Although, cells attached to the thermoresponsive surfaces when fibronectin adsorption was carried out at 20°C i.e hydrophilic extended conformation of the copolymer brushes, it appeared that some of the them did not adhere to some parts of the surface forming embryoid bodies as shown in Figure 5.3 (black arrows). In the third incubation condition where poly (MEO_2MA-co-OEGMA) surfaces were incubated with fibronectin at 20°C (hydrophilic state of the brushes) for 18 h followed by subsequent collapse of the brushes at 37°C for 3 h (hydrophobic state of the brushes), cells adhered in a manner comparable to the gelatin (control) (Figure 4.3).

However, lowering the temperature to below the LCST of the poly (MEO_2MA-co-OEGMA) (20°C) some mESCs detached as colonies from the surface but most of them remained adhered to the surface in all conditions.

Figure 4.4 represents the above data in graphical format following image analysis and expressing the data as percentage surface area covered by cells. Data is presented for all methods of fibronectin after 24, 48, 72 and 96 h of culture. There was no significant difference between the attachment of mESCs to surfaces previously incubated with 200 μg/mL fibronectin at 37°C for 18 h and gelatin (control) after 96 h of culture ($p=0.16$) where the percentage of surface area covered with cells was estimated to be 50 ± 2.5% and 47 ± 5.5% for gelatin coated TCPS and poly (MEO_2MA-co-OEGMA)/fibronectin surfaces respectively.

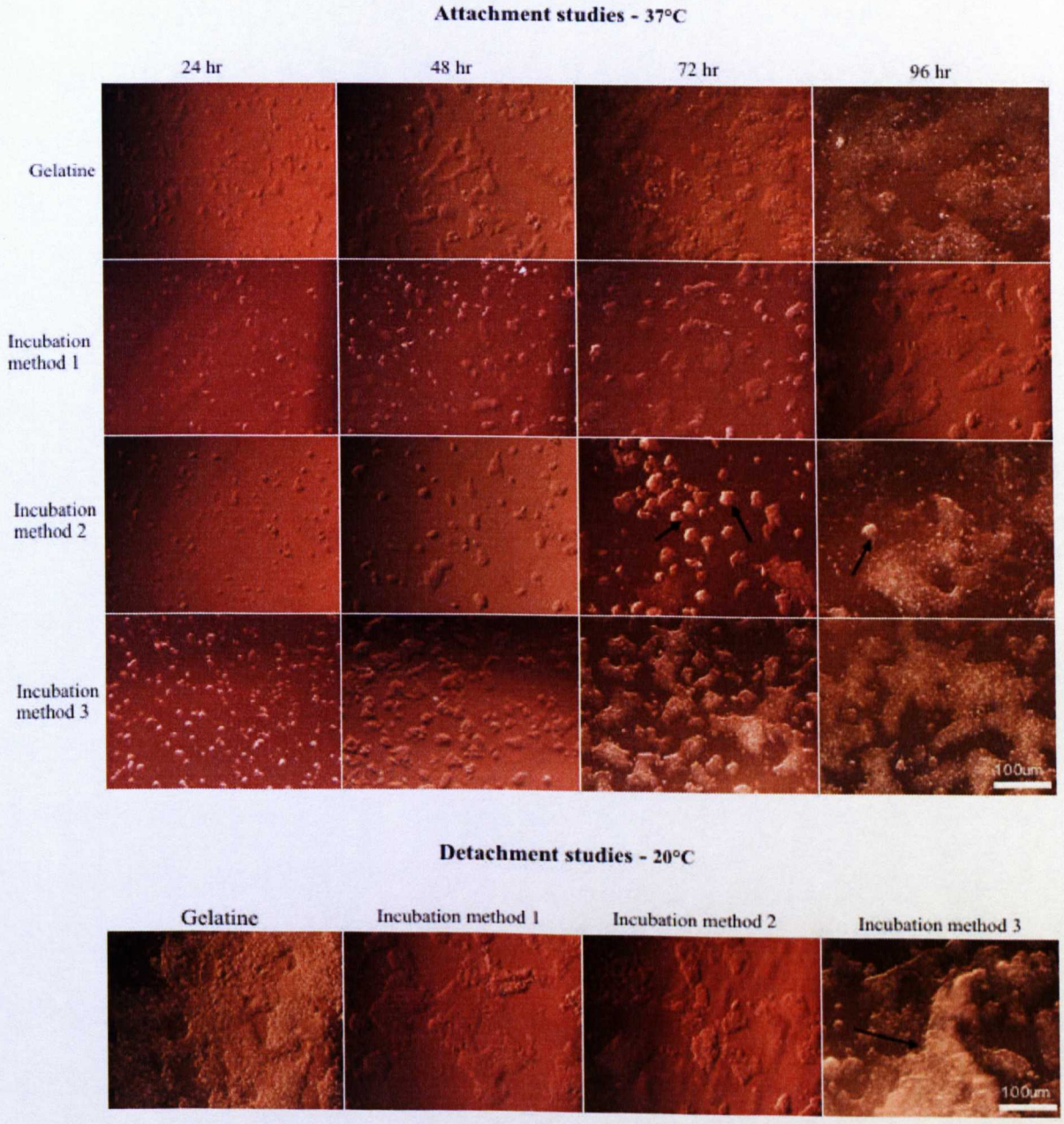

Figure 4.3. Representative images of mESC attachment (37°C; 96 h) and detachment (20°C; 2 h) respectively on poly (MEO_2MA-co-OEGMA)/fibronectin (200 μg/mL) surfaces. Fibronectin pre-treatment was carried out at either (1) 37°C (hydrophobic conformation) for 18 h, (2) 20°C (hydrophilic conformation) for 18 h or (3) 20°C for 18 h followed by 3 h incubation at 37°C . Detachment studies for all fibronectin adsorption methods were also investigated. Arrows show detached mESC islands from the thermo-responsive surfaces.

mESC cells cultured on poly (MEO_2MA-co-OEGMA) surfaces incubated with 200 μg/mL fibronectin using method 2 and method 3 of fibronectin adsorption showed that there was a significant difference between the percentage coverage of cells on these surfaces compared with gelatin (control) as the p values were estimated to be p=0.003 and p=0.04 respectively. The incubation of the thermo-responsive surfaces with fibronectin using all the different incubation conditions promoted mESCs adhesion and spreading. However, cells cultured on the poly (MEO_2MA-co-OEGMA) surface incubated with 200 μg/mL fibronectin at 37°C for 18 h showed no significant difference when compared with mESCs cultured on gelatin (control). In addition, cell morphology was comparable between the two surfaces. Therefore, from the data in Figures 4.3 and 4.4, it was concluded that adsorption of fibronectin to the thermo-responsive surfaces at 37°C for 18 h was the optimal of the thee methods tested and so this method was adopted for all further studies using fibronectin.

Anchorage dependent cells require an adhesion promoter in order to adhere to synthetic substrates (259). Fibronectin promoted the adhesion of fibroblasts to material surfaces including glass and plastic (260). Moreover, ESC adhesion is also promoted when grown on fibronectin coated culture substrates though binding with to $\alpha_5\beta_1$, $\alpha V\beta_1$ on embryonic stem cells (256). Adsorption of fibronectin to hydrophilic and hydrophobic substrates was previously studied and it was reported that both substrates were biologically active leading adhesion of cells on both surfaces. However, at low concentrations of fibronectin, cells adhered only to the hydrophilic surfaces (coated with fibronectin) while low levels of albumin promoted adhesion to the hydrophobic substrates (coated with fibronectin) (257). Herein, the hydrophilic nature of poly (MEO_2MA-co-

OEGMA) (method 2) seems to affect adsorption of fibronectin in which this latter biological activity was reduced and hence the formation of embryoid bodies after mESC seeding.

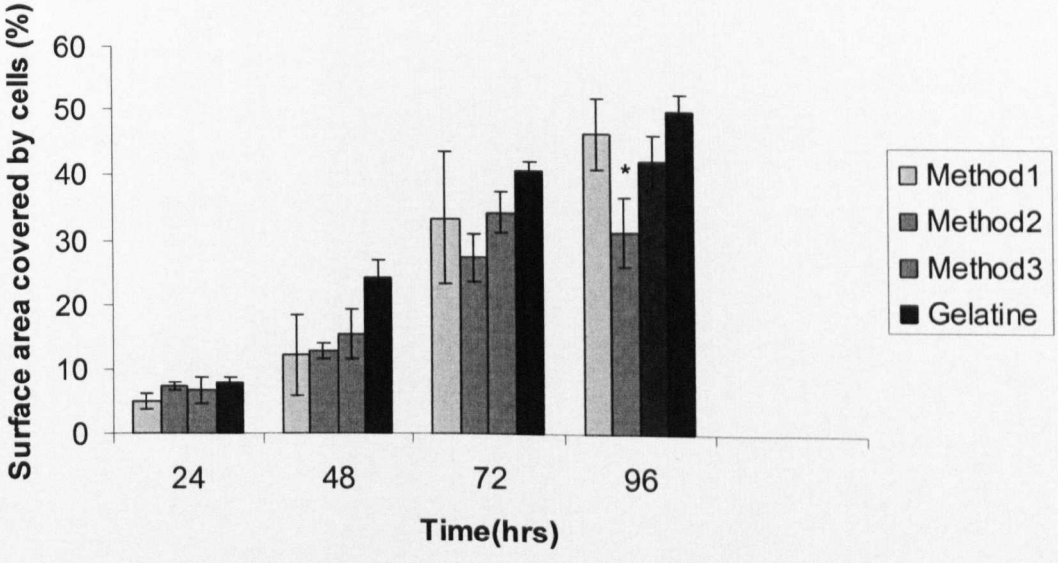

Figure 4.4. Surface area, expressed as a percentage of the total surface area, covered by cells at several time intervals over a total culture time of 96 h at 37°C on poly (MEO_2MA-co-OEGMA) surfaces previously incubated with fibronectin using method 1 (p value = 0.16), method 2 (p=0.003), and method 3 (0.04). Error bars represent standard deviation of 6 samples studied.

The lowest concentration of fibronectin needed for mESC adhesion was determined next. The fibronectin concentration was lowered from 200 μg/mL to 100 μg/mL, 50 μg/mL, 25 μg/mL, 10 μg/mL and 5 μg/mL. mESCs were cultured on all thermo-responsive surfaces preincubated with fibronectin at 37°C for 18 h; the cells showed adherence and spreading to all surfaces including the lowest pre-incubation concentration of 5μg/mL fibronectin as shown in Figure 5.5. The manufacture's recommended concentration of fibronectin required to achieve cell adhesion to a surface was (5μg/cm^2 (Sigma-Aldrich)) (261) which was observed in this work for mESCs adherence as shown in Figure 4.5.

Quantitative data was generated using image analysis of representative images of each surface and the data expressed as the percentage of the surface area covered by cells was analysed after 24, 48, and 72 h of culture as shown in Figure 4.6.
The surface area covered by cells was 42%, 37% and 39% for gelatin (control), surface/ 5 μg/mL fibronectin and surface/ 100 μg/mL fibronectin respectively.
There was no significant difference in the data between gelatin (control) coated TCPS and all surfaces preincubated with fibronectin at various concentrations at 37°C (p values were: 0.3, 0.1, 0.7, 0.9 and 0.7 for 5, 10, 25, 50 and 100 μg/mL incubated thermo-responsive surfaces respectively).
This indicates that incubating the thermo-responsive poly (MEO_2MA-co-OEGMA) surfaces with fibronectin supported adhesion, spreading and proliferation of mESCs in a similar manner to gelatin coated plates.

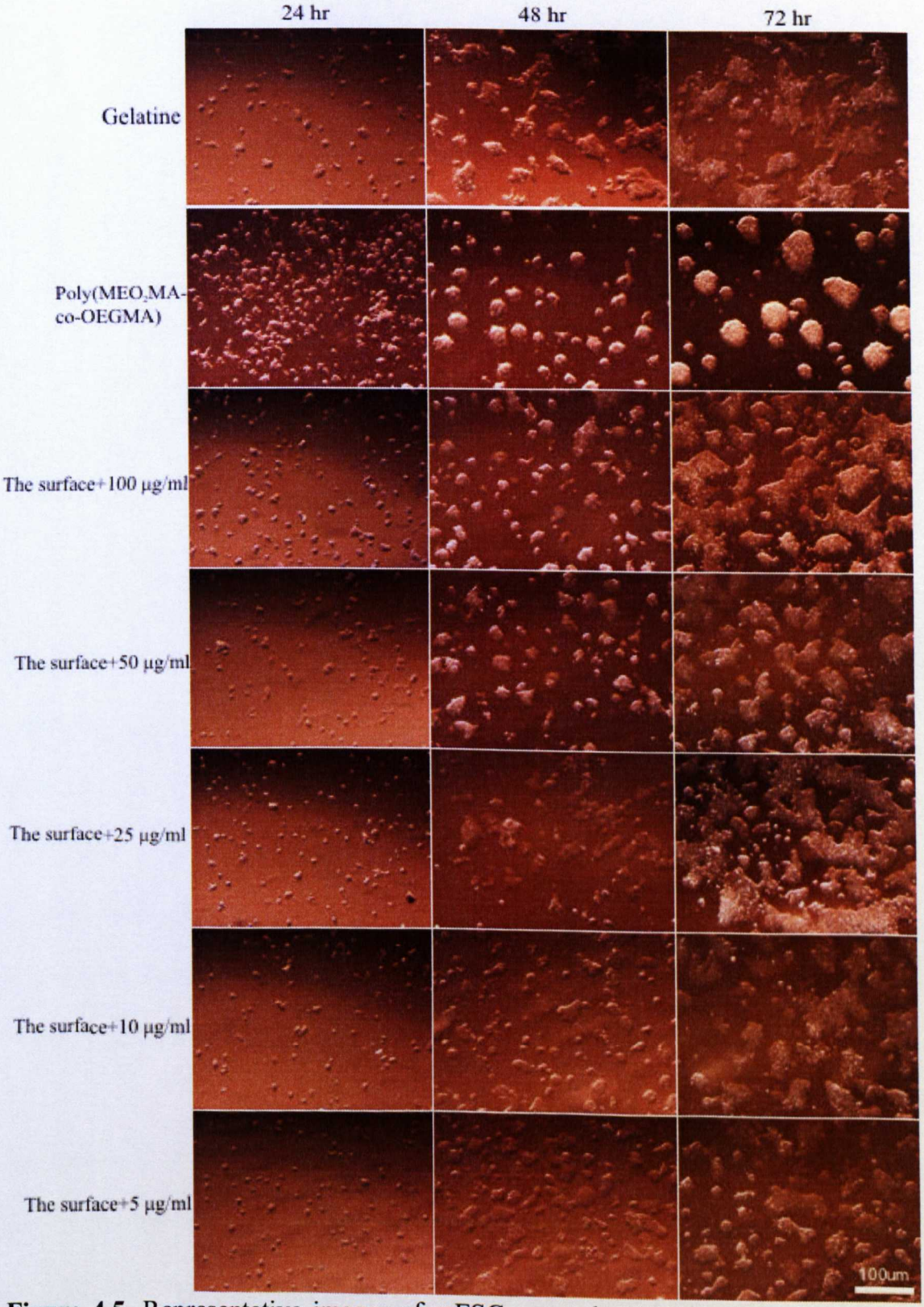

Figure 4.5. Representative images of mESCs on poly (MEO_2MA-co-OEGMA) (labelled as 'The surface' on the figure) surfaces previously incubated with different concentrations of fibronectin. Images are shown over a 72 h culture period. Scale bar for all images is **100 μm**.

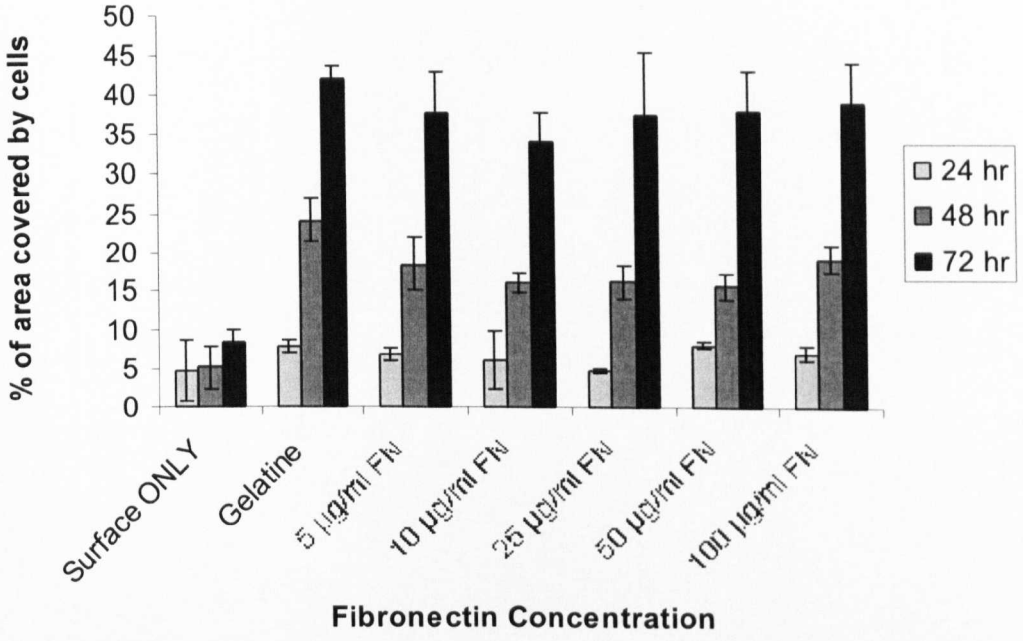

Figure 4.6. Percentage surface area covered by cells on poly (MEO_2MA-co-OEGMA) surfaces preincubated with various concentrations of fibroenctin (at 37°C for 18 h) compared with gelatin coated TCPS (control). Error bars representing standard deviation; N=6 samples. Note that the data presented for the surface only represents embryoid bodies un-attached to poly (MEO_2MA-co-OEGMA) surfaces. *p* values were: 0.3, 0.1, 0.7, 0.9 and 0.7 for 5, 10, 25, 50 and 100 µg/mL incubated thermo-responsive surfaces respectively.

Detachment of the cells from the surface was carried out at 20°C for 2 h to investigate whether the concentration of fibronectin would affect the detachment of these cells. Incomplete cell detachment was observed on all surfaces incubated with different concentrations of fibronectin as shown in Figure 4.7. Because fibronectin is a high molecular weight glycoprotein, it was thought that the poly (MEO_2MA-co-OEGMA) surfaces may be less responsive due to the adsorbed

fibronectin layer therefore affecting the detachment of mESCs from these surfaces at 20°C. This hypothesis was confirmed previously on PNIPAAm-co-acrylic acid thermo-responsive copolymers grafted on a polystyrene matrix where albumin did not affect mouse fibroblast STO cells cell detachment and incomplete recovery of these cells was observed from the thermo-responsive surfaces incubated with fibronectin (262).

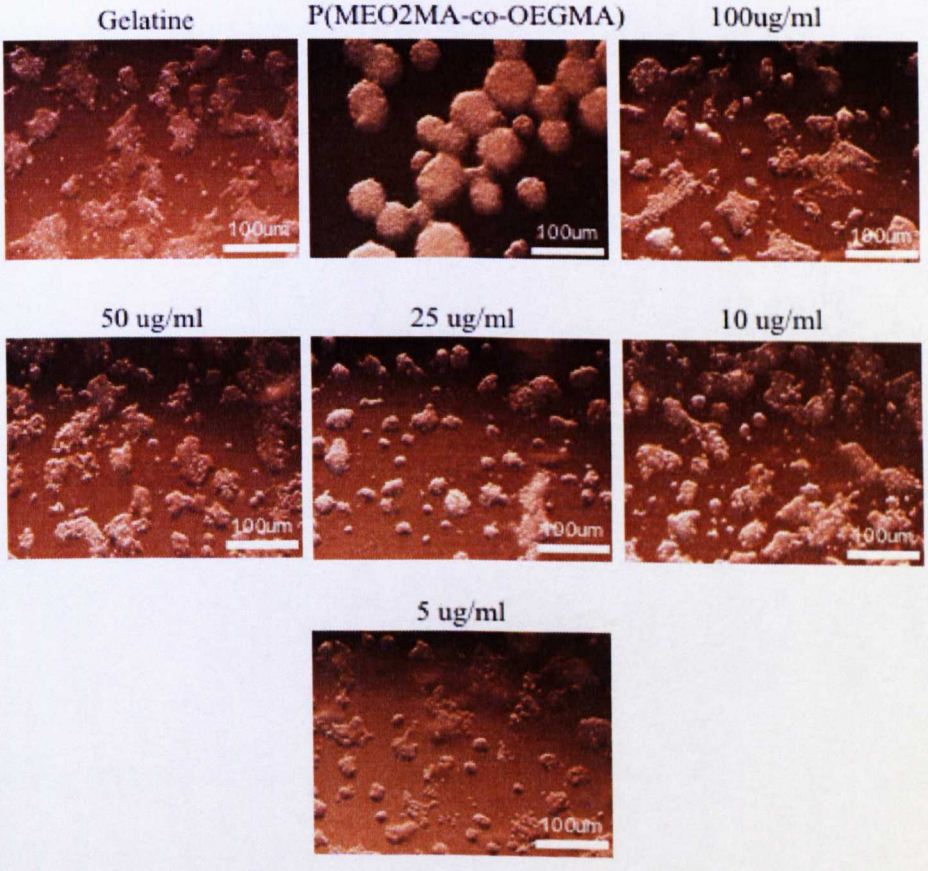

Figure 4.7. Representative images for detachment assay after 2 h at 20°C of mESCs from poly (MEO_2MA-co-OEGMA) preincubated with different concentrations of fibronectin previously adsorbed at 37°C for 18 h.

In conclusion, future mESCs studies in this work on the poly (MEO_2MA-co-OEGMA) thermo-responsive surfaces were conducted with prior adsorption of fibronectin at a concentration of 5 μg/mL at 37°C for 18 h.

The adherence and subsequent detachment of mESCs to the poly (MEO_2MA-co-OEGMA)/fibronectin surfaces was repeated to confirm and further probe cell adhesion and proliferation on the surfaces. Figure 4.8 shows representative images of the attachment assay of mESCs on the poly (MEO_2MA-co-OEGMA)/fibronectin surfaces where cells adhered, spread and proliferated on all samples in a similar manner to the gelatin control (N=9).

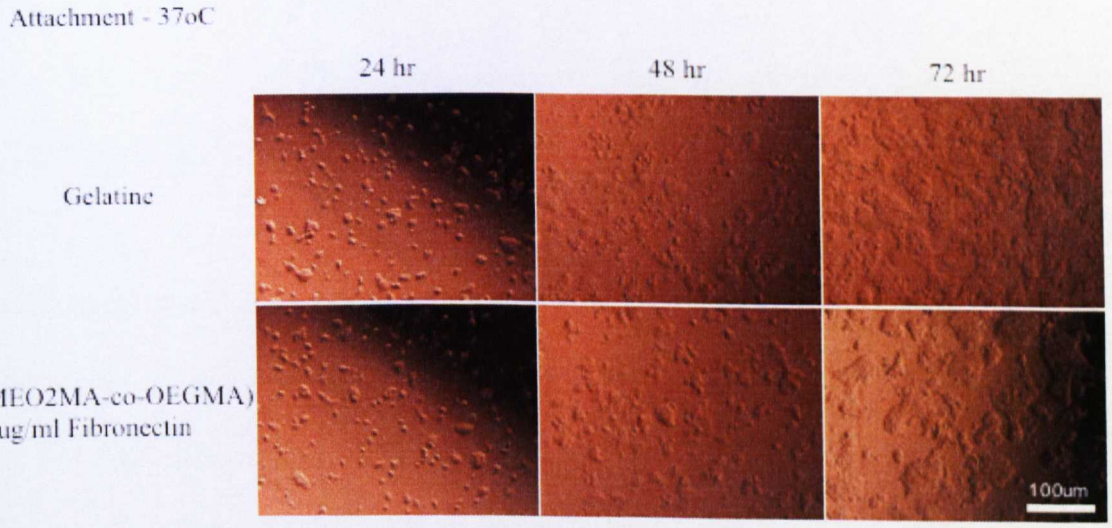

Figure 4.8. Representative images of mESCs cultured on poly (MEO_2MA-co-OEGMA) treated with 5 μg/ml fibronectin and gelatin coated TCPS as the control.

Cell spreading was quantitatively estimated by measuring the surface area covered by cells over a 72 h period. The percentage surface area covered by cells was 39% and 32% for gelatin coated TCPS and poly (MEO_2MA-co-OEGMA)/fibronectin; and there was no significant difference between the two substrates as the p value was estimated to be 0.07 (Figure 4.9).

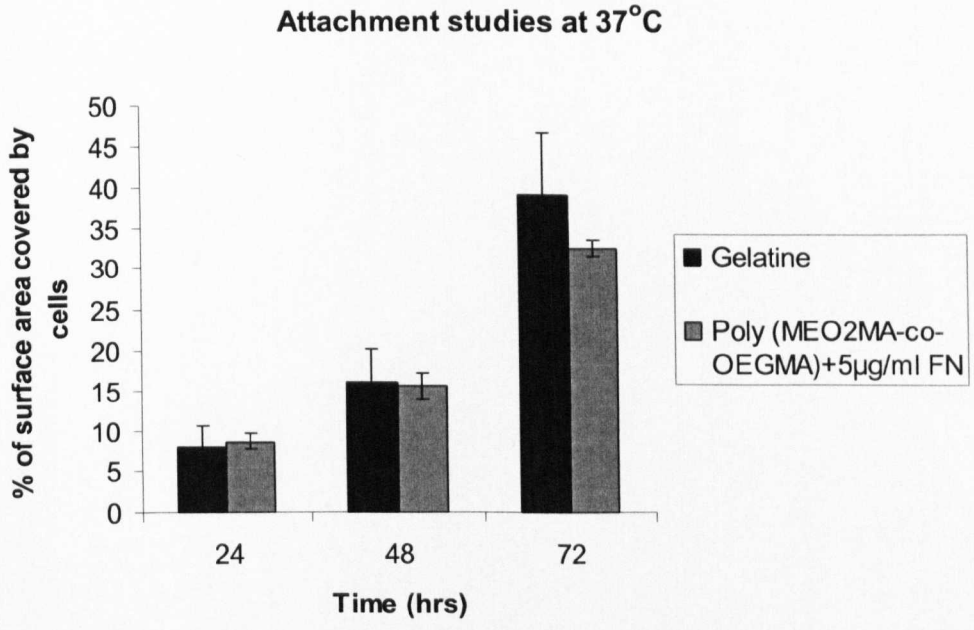

Figure 4.9. mESCs attachment to gelatin and poly (MEO_2MA-co-OEGMA) brushes preincubated with 5 µg/ml of fibronectin (FN) after 72 h at 37°C for 9 samples from 3 different batches. P value= 0.07.

Alamar blue was performed on mESCs to investigate the viability and proliferation of these cells on the poly (MEO_2MA-co-OEGMA)/fibronectin surfaces. Cell number grown on poly (MEO_2MA-co-OEGMA)/fibronectin was determined from the calibration curve previously obtained by growing mESCs on TCPS coated with gelatin. Figure 4.10.A shows the fluorescence intensity of mESCs grown on gelatin (control) and poly (MEO_2MA-co-OEGMA)/fibronectin. The number of cells cultured on gelatin coated TCPS increased from 42,000 cells/mL after 72 h of culture compared to 26,000 cells/mL after 24 h of culture on gelatin (Figure 4.10B). mESCs cultured on poly (MEO_2MA-co-OEGMA)/fibronectin proliferated from the initial seeded density (20,000 cells/mL to 35,000 cells/mL). The cell number determined from the thermo-responsive surfaces/fibronectin surfaces was lower compared to cells cultured on gelatin

coated TCPS. The calculated p value (0.0003) indicated that there is a significant difference between cells cultured on gelatin and poly (MEO_2MA-co-OEGMA)/fibronectin surfaces.

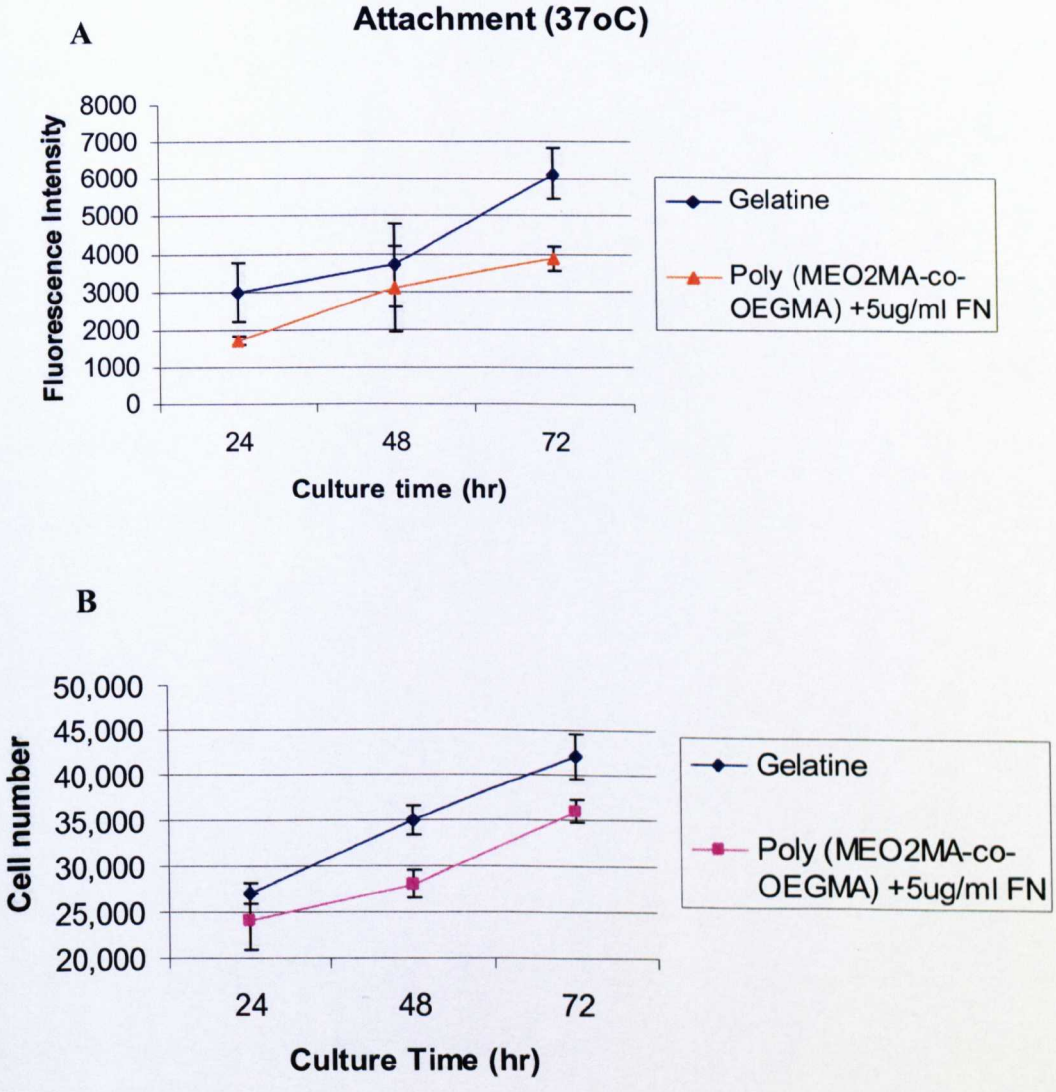

Figure 4.10. A. Alamar blue fluorescence intensity at 560nm during the cell culture time up to 72h. **B.** Cell number estimated from the calibration curve at the time point (24, 48 and 72 h) for cells cultured on gelatin coated TCPS and poly (MEO_2MA-co-OEGMA)/fibronectin. P=0.0003

The above data confirms (Figure 4.8, 4.9 and 4.10) initial data that the thermo-responsive surfaces incubated with 5 μg/ml of fibronectin supported the adhesion and spreading of mESCs in a similar manner to gelatin coated TCPS.

As observed from Figure 4.7, mESCs did not completely detach from the thermo-responsive surface when the temperature was lowered to 20°C which was probably due to the strong interaction between cells and fibronectin (262). A further detachment assay of these cells at different temperatures (4°C, 10°C and 20°C) was therefore conducted to investigate the most appropriate temperature for complete detachment of mESCs from the thermo-responsive/fibronectin surface. In this experiment, the percentage surface area covered by cells was determined using image capture and subsequent analysis was performed. Viability following detachment at each temperature was also investigated using Tryptan Blue Exclusion.

Complete detachment was noticed when the temperature of the culture medium was lowered to 4°C for 2 h and 80% recovery of cells was observed on surfaces when the temperature was decreased to 10°C compared to gelatin (control) (Figure 4.11). Figure 4.12 presents the percentage surface area covered by cells for the different temperatures; there was a significant difference between the number of cells detached from the thermo-responsive/fibronectin surface compared with those cells cultured on gelatin (control) $p=0.0027$ for 4°C and $p=0.003$ for 10°C, but there was no significant difference between the number of cells detached from the surface at 20°C and the cells grown on gelatin (control) ($p=0.06$).

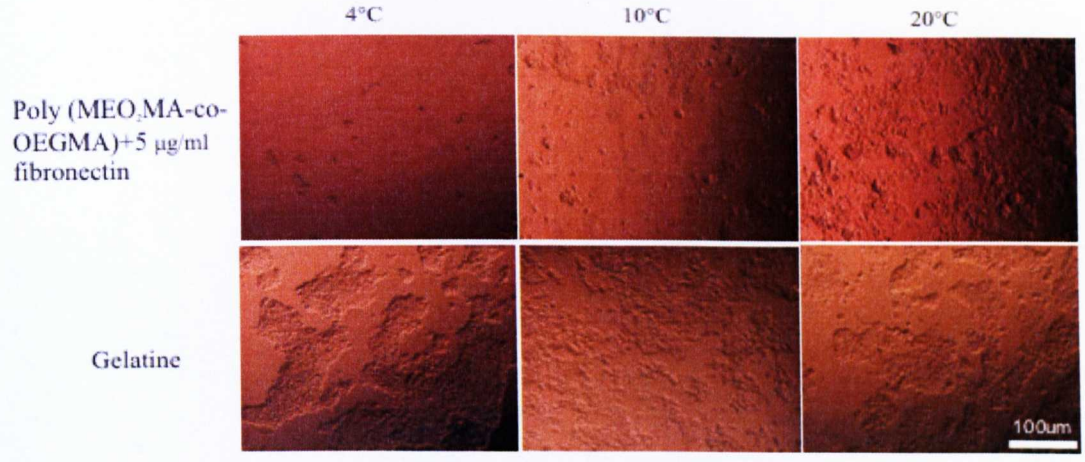

Figure 4.11. Representative images of mESC detachment at different temperatures 4°C, 10°C and 20°C. Scale bars = **100 µm** for all images.

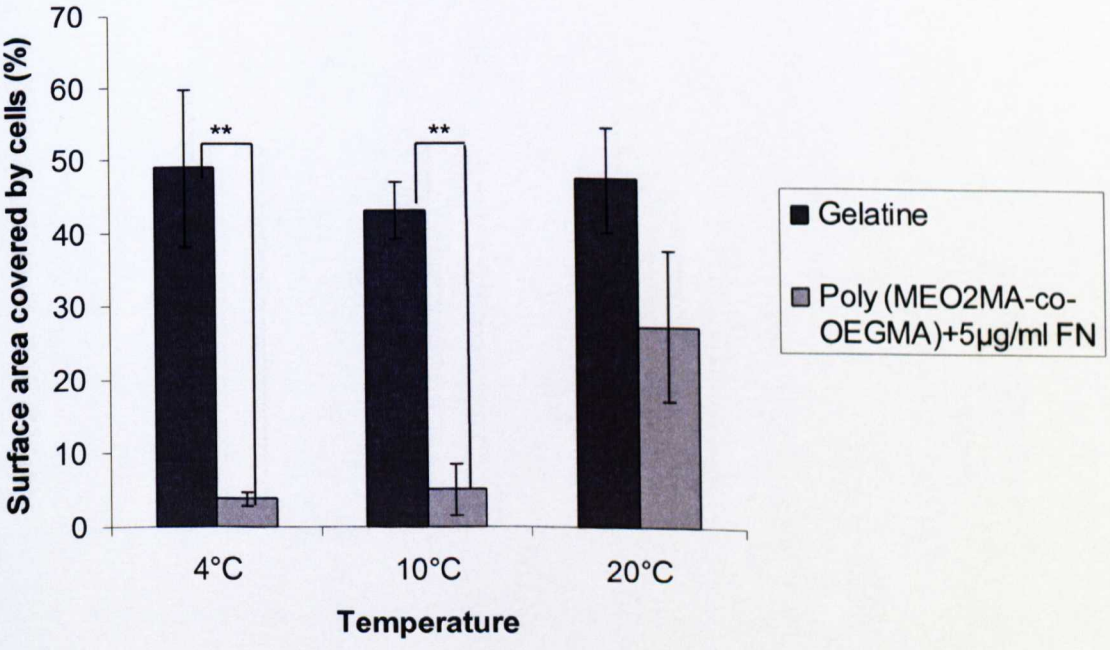

Figure 4.12. Percentage surface area covered by cells following detachment at different temperatures 4°C, 10°C and 20°C (2h). N= 6 and p values were 0.0027, 0.003 and 0.06 for cells detached from poly (MEO_2MA-co-OEGMA)/fibronectin at 4°C, 10°C and 20°C respectively.

mESCs detached from the thermo-responsive/fibronectin surfaces at 10°C and 20°C for 2 h showed a higher viability (82% and 86% respectively) compared to mESCs detached from the thermo-responsive/fibronectin surfaces at 4°C (40%).

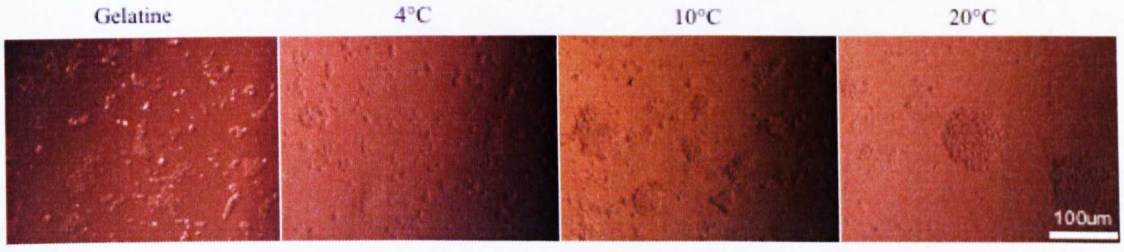

Figure 4.13. Representative images for the re-attachment studies after 24 h using detached cells from poly (MEO_2MA-co-OEGMA)/fibronectin at different temperatures (4°C, 10°C and 20°C).

The ultimate aim of this chapter was to passage mESCs using the thermo-responsive poly (MEO_2MA-co-OEGMA)/fibronectin surfaces. Therefore, re-attachment studies were performed to study if detached cells from different temperatures would adhere to fresh thermo-responsive surfaces preincubated with fibronectin. Indeed, the detached mESCs recovered from all surfaces incubated at the different temperatures re-attached to a fresh thermo-responsive/fibronectin surface after 24 h of culture as shown in Figure 4.13. mESCs are usually seeded as single cell suspensions following trypsinization and spread as colonies on gelatin coated TCPS. Cells detached from the thermo-responsive/fibronectin surfaces as colonies were re-attached to fresh substrates as single cell suspension via pipetting and passing though G19 needle following detachment. However, a population of the detached mESCs were not disaggregated to individual cells hence they remained as colonies. These colonies adhered to fresh thermo-responsive substrates as colonies as can be seen in Figure 4.13.

From Figure 4.4 and Figure 4.12, it can be concluded that fibronectin adsorbs to the poly (MEO_2MA-co-OEGMA) surfaces at 37°C when the copolymer brushes are globule structures and yet allows detachment of mESCs from these surfaces at 10°C (and 4°C) for 2 h when the copolymer brushes are in their hydrated state.

Fibronectin adsorption and subsequent release from the poly (MEO_2MA-co-OEGMA) was immuno-stained to examine how the fibronectin is distributed on the surface of the thermo-responsive surfaces. Figure 4.14 shows that fibronectin is uniformly distributed across the surface when preincubated on poly (MEO_2MA-co-OEGMA) surfaces at 37°C for 18 h but is lost following cell detachement at 10°C. Figure 4.15 quantifies the average fluorescence intensity for the surface incubated with fibronectin at 37°C and 20°C for 18 h and after detachment of the cells at 10°C. The intensity of fibronectin incubated at 37°C when the poly (MEO_2MA-co-OEGMA) brushes were in their globule structures was higher than the intensity for surfaces incubated at 20°C (Figure 4.15) when the thermo-responsive surface was in its hydrophilic state. This explains the results presented in Figure 4.3 where a population of mESC formed embryoid bodies were formed on the thermo-responsive surface previously incubated with fibronectin using method 2 (at 20°C). After detachment of the cells from the surface, fibronectin adsorbed to poly (MEO_2MA-co-OEGMA) surfaces is lost once the cells are detached from the thermo-responsive surface at 10°C and hence a low fluorescence intensity was observed when the temperature was lowered to 10°C (Figures 4.14 and 4.15).

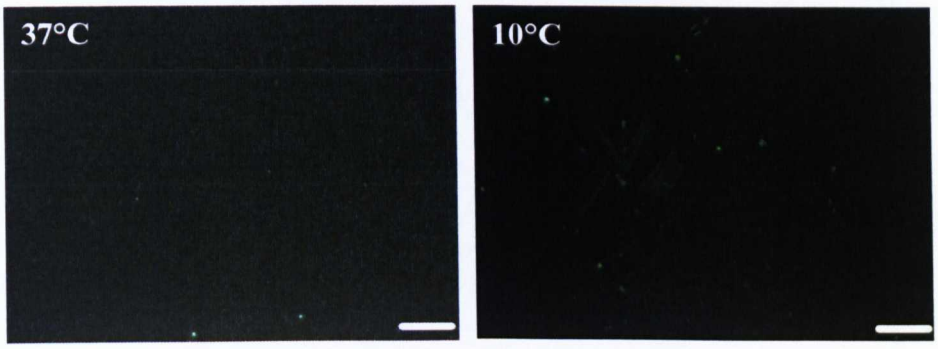

Figure 4.14. Representative fluorescence microscopy images of surfaces immuno-stained with fluorescent antibodies to fibronectin after incubation of fibronectin with a poly (MEO_2MA-co-OEGMA) thermo-responsive surface at 37°C for 18 h and after detachment of cells at 10°C for 2 h. Scale bars = **100µm**

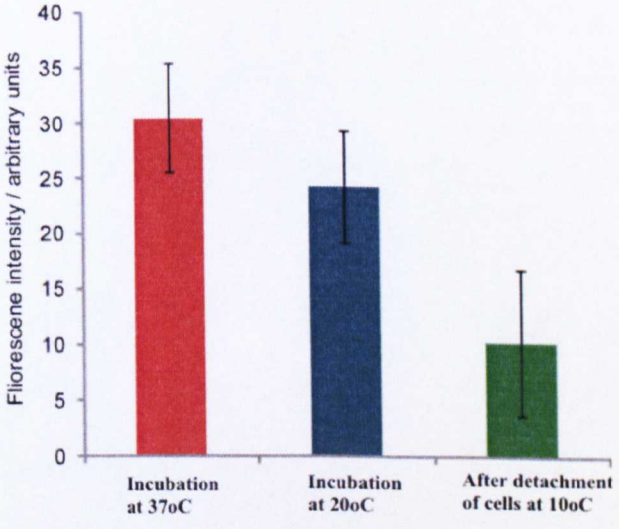

Figure 4.15. Average fluorescence intensities of Poly (MEO_2MA-co-OEGMA) surfaces following incubation with fibronectin at 37°C for 18 h, washing with warm PBS and immuno-staining with a FITC-anti fibronectin antibody. Error bars represent standard deviation for thee samples.

Analysis of the surface following fibronectin adsorption was also conducted by WCA and XPS to further investigate the thermo-responsive behaviour and the chemistry of the thermo-responsive/fibronectin surfaces respectively.

Table 4.4. WCA data measured for the thermo-responsive poly (MEO_2MA-co-OEGMA) before and after the incubation of fibronectin at 37°C.

Surface	**ppAAl-2-bromo-isobutyrate**		**Poly (MEO_2MA-co-OEGMA)**	
	-5 μg/ml fibronectin	+5 μg/ml fibronectin	-5 μg/ml fibronectin	+5 μg/ml fibronectin
37°C	66.6 ± 6.5	63.8 ± 10.7	63.2 ± 3.9	66.5 ± 16.9
10°C	65.96 ± 4.54	67.85 ± 9.02	47.4 ± 10.7	57.4 ± 1.7

From the data in Table 4.4 the thermo-responsiveness of the surface was maintained after the incubation of the surface with 5 μg/ml of fibronectin as the WCA decreased from 66.5° to 57.4°; however, the surface seems to be more thermo-responsive without the fibronectin layer as the WCA decreased by an average of 20° (which is confirmed in Table 4.10) (compared to 10° difference after the surface was treated with fibronectin).

XPS was used to analyse the poly (MEO_2MA-co-OEGMA) surface after preincubation with 5 μg/ml fibronectin. An additional nitrogen peak was presented on the spectrum of the poly (MEO_2MA-co-OEGMA)/fibronectin surface (Table 4.5 and Figure 4.16) which was not detected on poly (MEO_2MA-co-OEGMA) surfaces only as shown in Figure 2.15. This indicated successful deposition of the fibronectin glycoprotein on the surface at 37°C when the copolymer brushes were in their globule structures.

Table 4.5. XPS elemental analysis of poly (MEO_2MA-co-OEGMA) thermo-responsive surfaces incubated with 5 μg/ml fibronectin at 37°C.

Element	Elemental composition (%)
Si2p	2.2 ± 0.6
C1s	68.4 ± 1.3
N1s	9.0 ± 0.3
O1s	19.2 ± 1.0
Na1s	1.0 ± 0.08
Br3d	0.16 ± 0.01

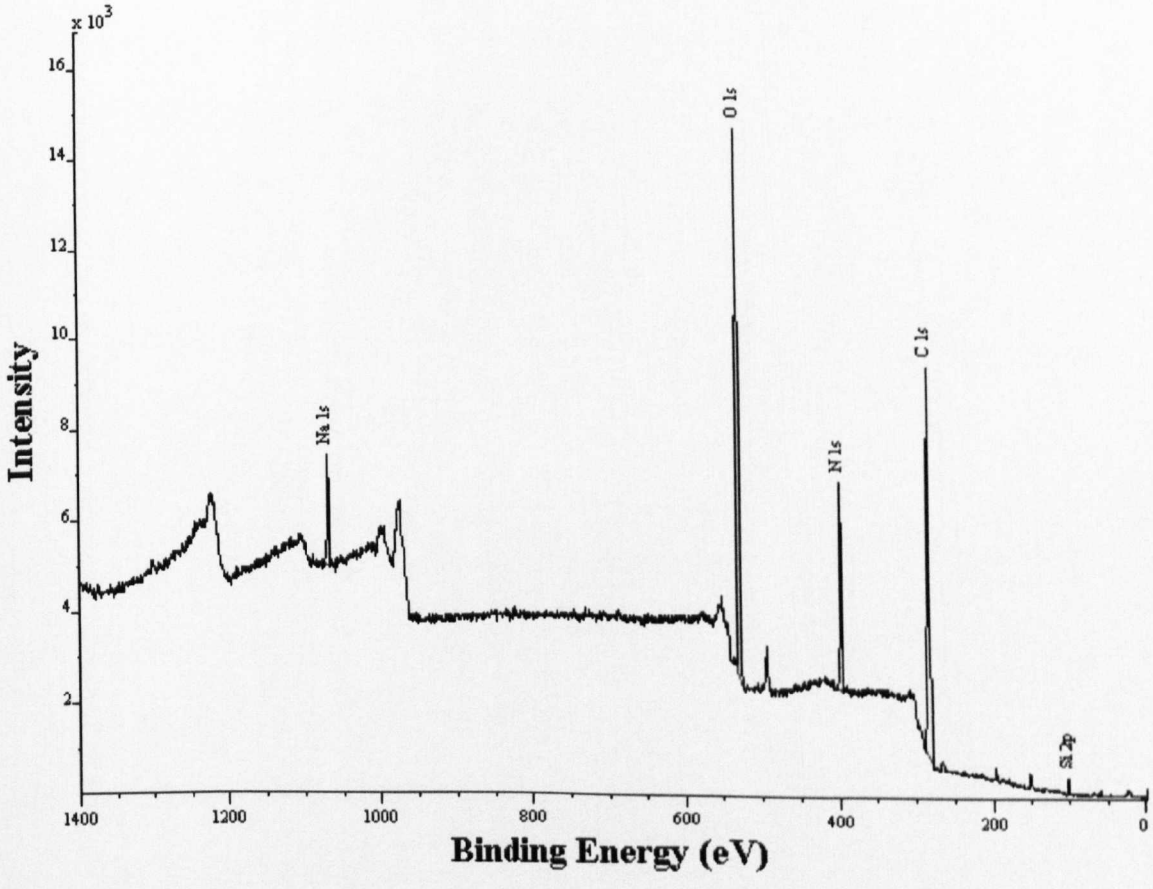

Figure 4.16. Wide scan of a representative poly (MEO_2MA-co-OEGMA) thermo-responsive surface preincubated with 5 μg/ml fibronectin.

mESCs cultured on gelatin were passaged by the incubation of these cells with 1 mL trypsin/EDTA for 3-5 min at 37°C with gentle agitation to release the cells as a single cell suspension. They were detached from the poly (MEO_2MA-co-OEGMA)/fibronectin surfaces by lowering the temperature from 37°C to 10°C. On the thermo-responsive surfaces, mESCs detached as colonies and a single cell suspension was obtained by pipetting the cells and then passing the cell suspension though a G19 needle to ensure that they re-attached to a fresh surface as a single suspension (as would be achieved if using trypsin to passage the cells). Growth curve was obtained to study the proliferation rates of mESCs on both gelatin-coated TCPS detached with trypsin/EDTA and the thermo-responsive surfaces by temperature. The population doublings were estimated using the formula $\{\log_{10}(\text{total cell counts/cells seeded})/\log_{10}(2)\}$ after cells detachment. Thereafter, proliferation rates were calculated by hours in culture (either on gelatin-coated wells or poly (MEO_2MA-co-OEGMA))/cumulative population doublings (CPDs) over 10 passages.

Analysis of these proliferation rates indicated that the average interval for mESCs detached from TCPS using trypsin/EDTA was 15.26 ± 0.93 h and for mESCs detached from poly (MEO_2MA-co-OEGMA) was 21.03 ± 3.1 h. This indicated that poly (MEO_2MA-co-OEGMA)/fibronectin could support the growth of mESCs but that the growth rate was slower (Figure 4.17).

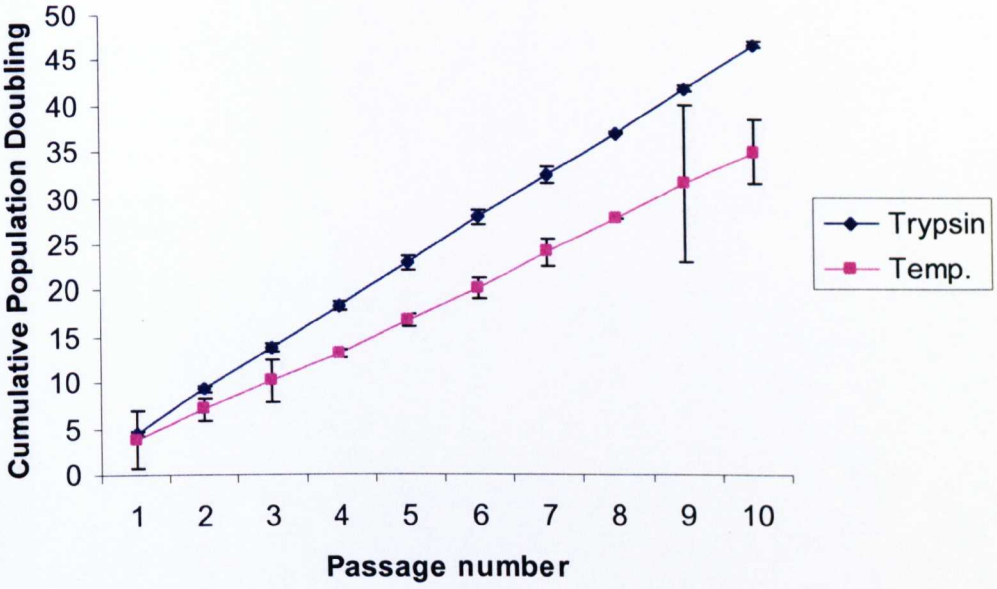

Figure 4.17. Growth curve of mESCs which they were serially trypsin and temperature passaged from TCPS or poly (MEO_2MA-co-OEGMA) respectively. N=6 in total of 6 samples

mESCs were also imaged to study any change in morphology over the 10 passages on poly (MEO_2MA-co-OEGMA)/fibronectin surfaces compared to cells grown on gelatin coated TCPS. It is observed that the morphology changed when these cells were passaged on the thermo-responsive surfaces (Figure 4.18) in that they adopted a more fibroblastic shape as shown in passage 5 onwards.

Despite attemps to distrupt the colonies obtained from the thermo-responsive/fibronectin surfaces by pipetting and passing the cell suspension though a needle of G19, this was not always effective. It is possible that the colonised state of the detached mESCs when replated could initiate the differentiation of the cells as several reports described that cell aggregates are essential prior to cell differentiation (100, 263). Other study groups showed that mESC detached from the thermo-responsive surfaces as colonies and to obtain

cell suspension for cell counting, the detached cells were resuspended in 0.25% of trypsin for 3 min (110).

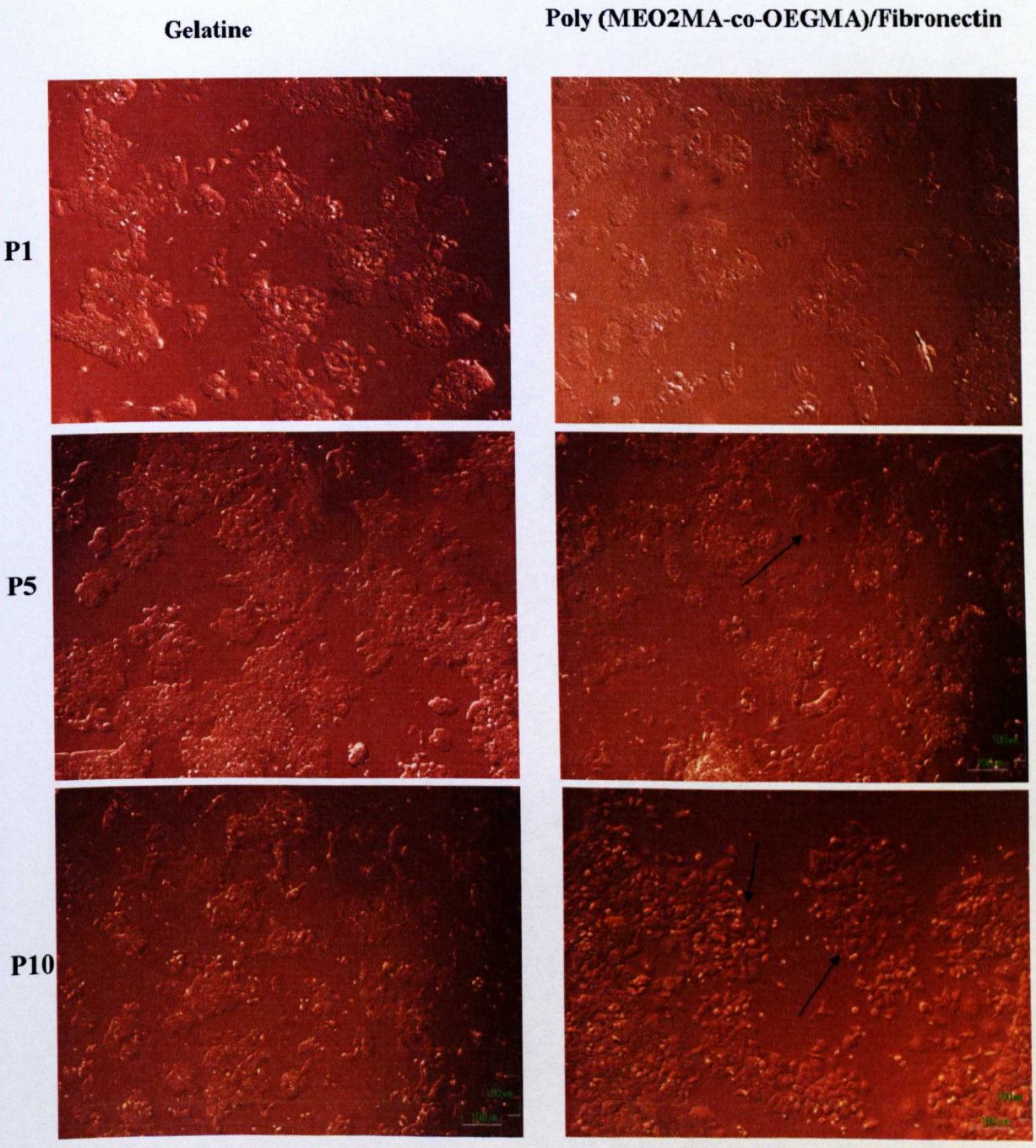

Figure 4.18. Representative images illustrating morphology of mESCs on gelatin coated TCPS and on poly (MEO_2MA-co-OEGMA)/fibronectin surfaces over 10 passages. Black arrows show the fibroblast shape of mESC at passage 5 and 10 compared to the colonies grown on gelatin coated TCPS. Scale bars = **100 µm**

As shown in Figure 4.18, the morphology of cells grown on poly (MEO_2MA-co-OEGMA)/fibronectin surfaces changed at passage 5 compared to cells cultured on gelatin-coated TCPS which is attributed to cell differentiation.

mESCs maintenance in the undifferentiated state is achieved by incubating the cells with Leukemia Interleukin Factor (LIF) which belongs to the IL-6 cytokine family (38-40). The biological mechanism of LIF required to prevent ES cell differentiation is thought to be via heterodimerization of two members of the class I cytokine receptors gp130 protein and the low-affinity LIF receptor (LIF-R) (41, 42); this results in activation of the Signal Transdcucers and Activator of Transcription 3 protein (STAT3) signalling pathway though Janus Kinases (JAK) which then induces transcription of self-renewal genes (43-46) including Oct3/4 and Nanog. Oct3/4 is widely regarded as a marker for self-renewal of pluripotent ES cells (47-49); Oct3/4 is a POU domain-containing transcription factor that is down-regulated if ESCs are differentiated (50) while Nanog sustains their pluripotency even in the absence of LIF (48). The minimum concentration of LIF reported to maintain the undifferentiated state of mESCs was reported to be 500pM (39, 51).

Reverse transcriptase polymerise chain reaction (RT-PCR) was conducted to confirm mESC pluripotency and/or differentiation thoughout the different passages 1, 5 and 10 on poly (MEO_2MA-co-OEGMA)/fibronectin surfaces compared with gelatin coated TCPS (control; Figure 4.19).

The Oct3/4 bands of the cells collected from gelatin and poly (MEO_2MA-co-OEGMA)/fibronectin were present after passage 1, 5 and 10. Therefore, mESCs maintained their pluripotency evidenced by the continued expression of Oct3/4 as seen in the control (mESCs grown on gelatin coated TCPS). However, the

intensity of the Oct3/4 decreased for cells collected from the thermo-responsive surfaces which indicate their possible differentiation as shown in Table 4.6.

Table 4.6. Quantitative measurements of the intensity for Oct3/4 bands for cells collected from gelatin coated TCPS and poly (MEO_2MA-co-OEGMA)/fibronectin surfaces.

Passage number/ Surface	Gelatin	Poly(MEO_2MA-co-OEGMA)/fibronectin
P 1	83.61	77.1
P 5	85.03	50.85
P10	82.96	47.95

The expression of differentiation markers including brachyury (mesoderm), nestin (ectoderm) and GATA4 (endoderm) were also tested at each stage i.e. after passage 1, 5 and 10 for cells cultured on gelatin coated TCPS and thermo-responsive/fibronectin surfaces. Cells collected from poly (MEO_2MA-co-OEGMA) surfaces after passage 1 did not show any differentiation as indicated in Figure 4.19. This was previously reported as differentiation was not observed on gelatin (97) and on thermo-responsive surfaces after the first culture cycle (110). However, at passage 10 on the thermo-responsive surfaces evidence of mESC differentiation was observed by the presence of PCR products for nestin and GATA-4 with an intensity of 28 and 25 respectively. These were absent from cells cultured on gelatin coated TCPS.

Fibronectin was used to aid mESCs adherence to the thermo-responsive surfaces though the interaction of RGD and cell surface integrins. It has been previously

reported that mESCs underwent differentiation on surfaces pre-conditioned with fibronectin and laminin. The mechanism of differentiation is not fully understood, but inhibition of the mESCs self-renewal was observed via the stimulation of ECM-integrin interactions (256). Although the amount of LIF in the media reported to keep the cells in their undifferentiated state is 500pM and that this was higher in this work, this was not sufficient to override the effect of the presence of fibronectin on the culture surface.

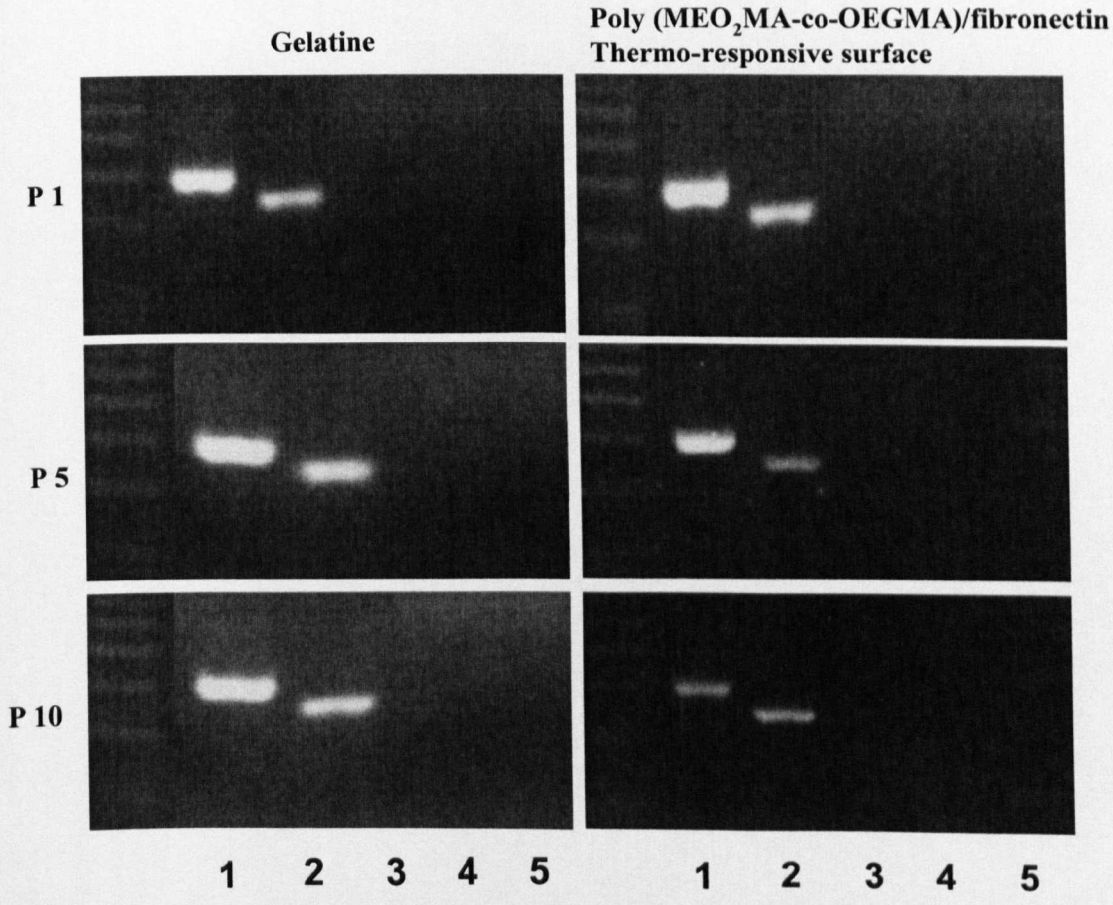

Figure 4.19. RT-PCR images data for mESCs cultured on gelatin (control) and on poly (MEO2MA-co-OEGMA)/fibronectin thermo-responsive surfaces. **1:** GAPDH. **2:** OCT-4. **3:** Brachyury (mesoderm). **4:** Nestin (ectoderm). **5:** GATA-4 (endoderm).

Oct3/4 immuno-staining was also performed for mESCs after their culture on poly (MEO_2MA-co-OEGMA)/fibronectin at the different passages; additionally, GATA-4, Brachyury and Nestin were stained for evidence of differentiation for endoderm, mesoderm and ectoderm lineages respectively.

Oct3/4 expression was maintained thoughout culture on poly (MEO_2MA-co-OEGMA)/fibronectin thermo-responsive surfaces as shown in Figure 4.20 indicating that the cells are still pluripotent on these surfaces confirming the data presented in Figure 4.19 and in comparison to gelatin (control; Figure 4.21). However, the data presented in Figure 4.19, revealed that mESCs underwent differentiation which was also demonstrated after immuno-staining of these cells at passage 5 and 10 as shown in Figure 4.21 where a positive staining was observed for brachyury after passage 5.

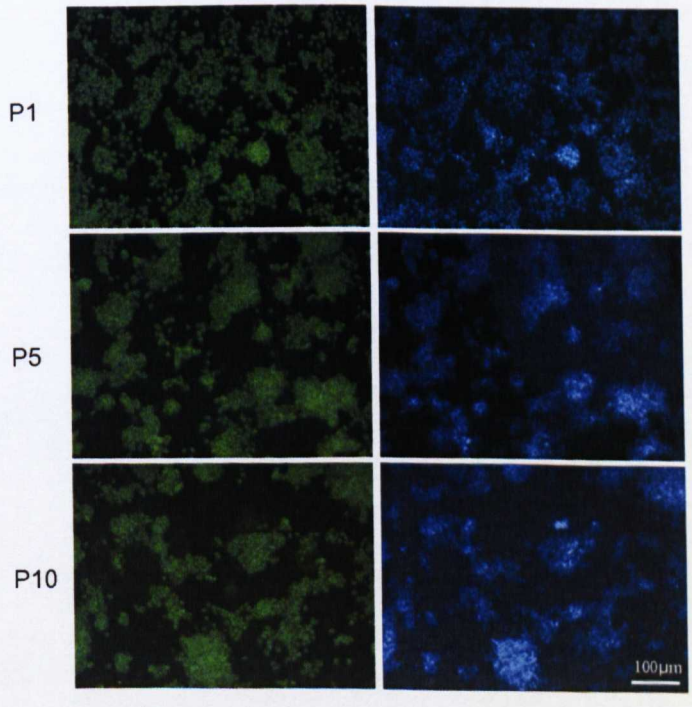

Figure 4.20. Representative images of Oct-3/4 immuno-staining (LH;green) of mESCs at passage 1, 5 and 10. Blue staining (RH) is DAPI staining to identify cell nuclei. Scale bars = 100 µm for all images.

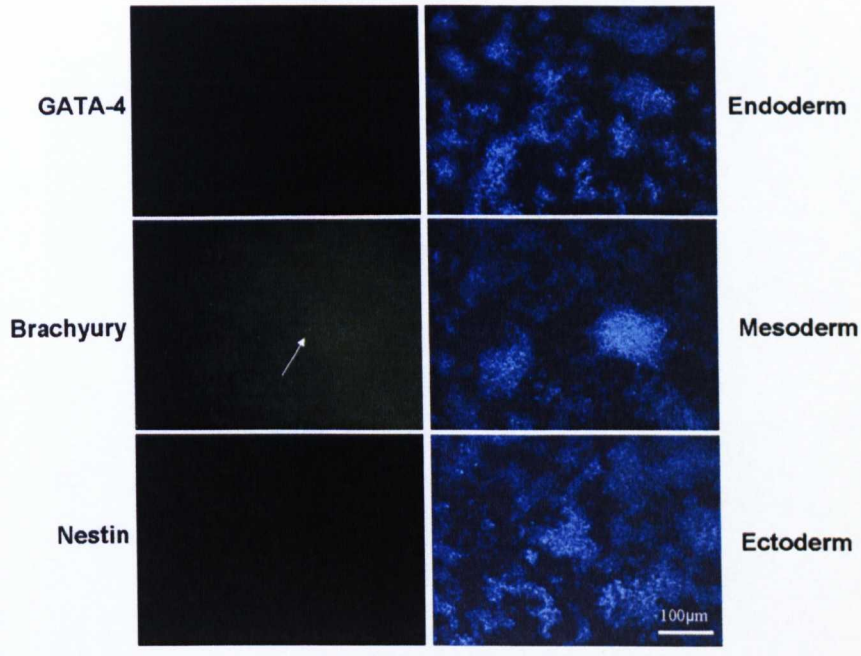

Figure 4.21. Representative images of immuno-staining for the thee differentiation markers (green) at passage 5. Blue staining (RH) is DAPI staining to identify cell nuclei. Scale bars = 100 μm

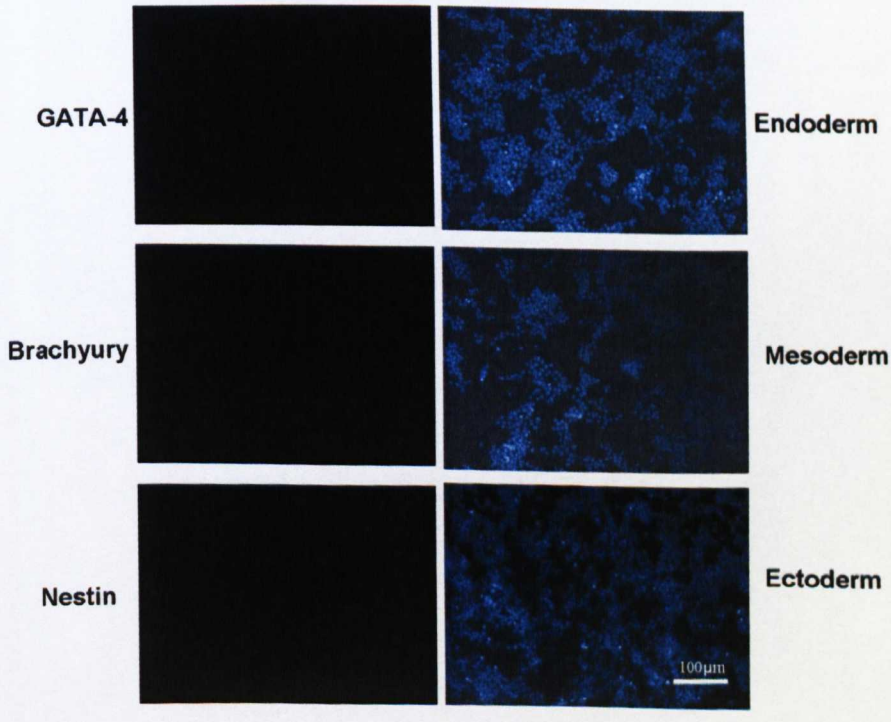

Figure 4.22. Representative images for Immuno-stained (LH; green) GATA4, Brachyury and Nestin for cells collected after passage 10. Blue staining (RH) is DAPI staining to identify cell nuclei. Scale bars = 100 μm.

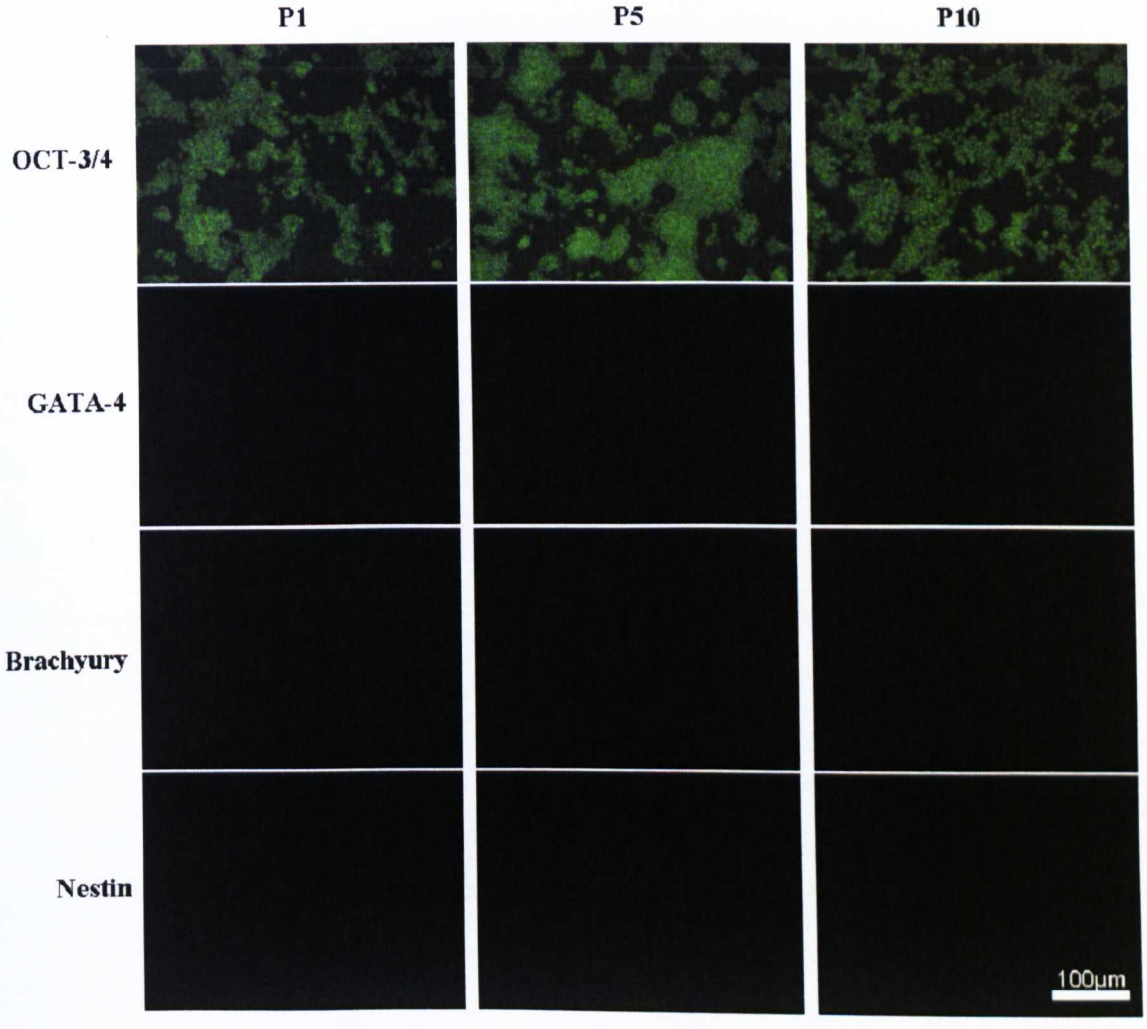

Figure 4.23. Representative images for Immuno-stained (LH; green) OCT-3/4, GATA4, Brachyury and Nestin for cells collected after passage 1, 5 and 10 for gelatin (control). Scale bars = 100 µm.

4.5 Conclusion

ESCs are known for their differentiation to all germ layers and hence they can produce all the cells in the body. These cells have been proposed for tissue regeneration and cell based therapies to treat various diseases. The maintenance of ESCs is an important step for further use in clinical applications or scientific research; this usually involves the culture of ESCs on fibroblasts layers derived from animals or humans and their detachment with enzymes, potentially affecting the quality of the cells.

To avoid the current culture methods of ESCs, thermo-responsive surfaces have been proposed for differentiated mammalian cells such that these surfaces change conformation according to temperature.

Poly (MEO_2MA-co-OEGMA) thermo-responsive surfaces were synthesised using ATRP as shown in Chapter 2 and used in this chapter to examine the response of mESCs as a model stem cell type. mESCs were cultured on poly (MEO_2MA-co-OEGMA) thermo-responsive surfaces leading to the formation of embryoid bodies due to the low adhesion of these cells to the hydrophobic conformation of the thermo-responsive surfaces at 37°C (above the LCST). Pre-conditioning of the thermo-responsive surfaces with 100% FCS, or gelatin still resulted in low attachment of cells. Fibronectin was found to aid mESCs attachment and spreading across the thermo-responsive surfaces.

Experiments were conducted to determine the appropriate conditions for fibronectin preconditioning with respect to copolymer brushe conformation at above and below the LCST. Of the methods studied, it was concluded that the most appropriate method for fibronectin adsorption was incubation at 37°C for 18

h when the copolymer brushes are in their globule state. The optimal temperature for cell detachment was also investigated and it was found that mESCs completely detached from the surface at 10°C and viability was maintained at similar levels to detachment at 20°C. From the growth curve, it was concluded that these surfaces could support the growth of mESCs over 10 passages, but light microscopy images indicated that cell morphology changed at passage 5 though to 10 to a more of fibroblast shape compared to cells cultured on gelatin-coated TCPS. RT-PCR data showed Oct3/4 PCR bands after passage 1, 5 and 10 for both cells collected from gelatin coated TCPS or poly (MEO_2MA-co-OEGMA)/fibronectin surfaces. However, the grey intensity of Oct3/4 decreased when comparing cells collected from poly (MEO_2MA-co-OEGMA)/fibronectin at passage 1, 5 and 10 to cells collected from gelatin coated TCPS, indicating that a population of cells were undergoing differentiation on these surfaces. This was attributed to the presence of fibronectin to aid mESC attachment to the thermo-responsive surfaces and the maintained colonised state of the detached mESC on replating.

Although, Oct3/4 staining was seen thoughout passages 1 to10, positive staining for the differentiation marker Brachyury was observed after passage 5 indicating their differentiation to mesodermal cell lineage.

As gelatin is used as a culture surface to expand mESCs whilst maintaining the undifferentiated state, the synthesis of a gelatin peptide sequence and its attachment to the thermo-responsive surfaces to replace the need to use fibronectin was proposed. This is discussed in the following chapter to first investigate whether this sequence would aid mESC attachment to a surface. The attachment of this peptide to the thermo-responsive surface is studied as well.

CHAPTER 5

The synthesis of 4-pentynoic acid- AGPRGEHyPG to promote embryonic stem cell adhesion to the thermo-responsive surfaces

5.1 Introduction

Within this thesis so far, poly (MEO_2MA-co-OEGMA) brushes have been considered for use as a switchable surface for mammalian cell culture (Chapter 4, 5 and (196)). The LCST of these copolymers can be adjusted by altering the co-monomer compositions to obtain similar thermo-responsive properties as the LCST of PNIPAAm (264). However, inadequate interaction between the thermo-responsive surface and mESCs was observed leading to low adhesion of cells to these surfaces and hence the formation of embryoid bodies (Chapter 4).

Approaches to improve these surfaces for embryonic stem cell culture were investigated including fibronectin adsorption to the thermo-responsive surfaces. The surfaces now supported the growth and proliferation of 3T3 fibroblasts over 10 passages. However, although these surfaces supported the growth and proliferation of mESCs, fibronectin adsorbed poly (MEO_2MA-co-OEGMA) thought to be involved in the induction of mESCs differentiation as shown in

Chapter 4. This observation is supported by reports that showed that ECM components and integrin signalling regulate ES cell self-renewal (256). Integrin signalling was activated in mESCs cultured on fibronectin and laminin; activation of ERK1/2 inhibits mES cell self-renewal (265).

Collagen and gelatin however do not activate mESC integrin signalling and hence supported the proliferation of undifferentiated mESCs (256). Research groups investigated further the interaction between collagen and mESCs that leads to their attachment. The discoidin domain receptor (DDR1) was proposed to mediate the adhesion of mESCs to collagen but the inhibition of this receptor did not change the attachment efficiency to type I collagen and the undifferentiated state of mESCs (266). Also, this receptor was not expressed in the interaction between gelatin and cells and therefore this receptor is not involved in the attachment of mESCs (266). Electrostatic interaction was proposed to play a significant role in maintaining mESCs attachment and undifferentiated state when the cells are cultured on gelatin (267).

Using whole proteins such as fibronectin, gelatin or collagen to promote cell adhesion can be disadvantageous in cell culture because only a part of the protein is required for cell adhesion, due to their stochastic orientation on the surface (268). Therefore, material modification by immobilization of cell recognition motifs is an alternative approach to improve the use of biomaterials for controlled interaction between cells and synthetic substrates.

Cell-recognition motifs (small immobilized peptides) are more popular than whole proteins for surface modification for cell culture as they exhibit higher stability towards sterilisation conditions (269), heat treatment and pH-variations (269), storage (270) and conformational shifting as well as easier characterisation and

cost effectiveness (271). In addition, ECM proteins contain many cell recognition motifs while peptides have only a single motif and therefore, they can selectively address one particular type of cell adhesion receptor as it is the case with (Arginine-Glycine-Aspartic acid) RGD in fibronectin/ Laminin. Peptides have attracted significant attention because of their diverse biological functionalization e.g. RGD containing motif is known to be vital for integrin-receptor mediated cell attachment which influences cell migration, growth and differentiation (272). Functionalization of polymers using RGD peptide has been reported previously in the literature where RGD was synthesised and chemically attached to PLLA copolymers which improved cell adhesion compared to the original untreated copolymer films (273). Hepatocyte adhesion when cultured on the polymeric substrates was limited which lead to the grafting of adhesion peptides e.g. RGD to polycaprolactone (PCL) and poly (L-lactic acid) PLLA; this indeed significantly enhanced the hepatocyte adhesion on PEG-PLLA-RGD surfaces compared to PLLA surfaces(274). In another study, spatially controlled adhesion and spreading of BAE cells was reported on patterned surfaces composed of RGD functionalised PLA-PEG-biotin surfaces indicating controlled adhesion of anchorage dependent mammalian cells (275).

Gelatin coated TCPS is usually used as a culture substrate to maintain many mESCs types in the undifferentiated phenotype. Because gelatin promoted mESCs cell growth and remained undifferentiated (256), an insight into the structure of gelatin and mechanism of cell attachment is discussed here. Gelatin is a protein that is produced by the de-naturation of collagen that is isolated from animal skin and bones. The gelatin molecule contains large sequences that do not include RGD-motifs which might not be exposed for cell attachment because it was

reported previously that for gelatin of about 350 amino acids contains at least one RGD motif (276, 277).

The formation of recombinant gelatin particles for cell adhesion have been previously reported where cell carrier particles with recombinant gelatin polypeptides including the RGD motif were synthesised. It was proposed that these particles could be used for *in vitro* cell culture and cell delivery to the body for example myocardiocytes to deliver at myocardial scar tissue (276).

In addition, RGD-enriched gelatin were prepared by recombinant technology and investigated for use as an anchorage-dependent cell culture support (277). The produced RGD-enriched gelatin contained four RGD motifs in a total sequence of 250 amino acids. Cell attachment for green monkey kidney cells, Chinese hamster ovary cells, normal rat kidney fibroblast and madin darby canine kidney cells, was observed on RGD-enriched gelatin which is thought to be due to the more even distribution of RGD motifs (277).

Gelatin contains the amino acid glycine at almost 1 in every 3 residues and arranged every third residue following proline and 4-hydroxyproline residues. A typical structure is as follows: -Ala-Gly-Pro-Arg-Gly-Glu-4Hyp-Gly- (AGPRGEHyPG) (278, 279).

Bio-conjugation of proteins and peptides to polymers has been reported previously using both living polymerisation and click chemistry which are well-established methods for the preparation of well defined end-functional polymers (280-282). An example was that reported where, preparation of oligo (ethylene glycol) methyl ether methacrylate grafting from a surface was prepared using ATRP and click chemistry was then used to functionalise these surfaces with different ligands to improve bio-specific interactions (283).

In this chapter therefore, investigation of a gelatin peptide sequence is studied to whether it promotes mESCs adhesion on the thermo-responsive poly (MEO_2MA-co-OEGMA) surfaces.

5.2 Aims and objectives

The ultimate aim of this chapter was to investigate gelatin peptide sequence to functionalise the thermo-responsive poly (MEO_2MA-co-OEGMA) surfaces to make it conductive to mESCs adhesion as described in Figure 5.1. This was promoted by using a combination of both ATRP and click chemistry, the bromine end functionalised of poly (MEO_2MA-co-OEGMA) in this study was proposed to be converted to azide functionalised copolymer chains after reaction with sodium azide. The alkyne in this case was 4-pentynoic acid and was attached at the end of the peptide used.

Thermo-responsive surfaces were then functionalised with the AGPRGEHyPG peptide and analysed using XPS and WCA as described in Figure 5.2. mESCs cell adhesion was studied on TCPS adsorbed solution of the peptide to see whether the chosen gelatin sequence would promote mESCs adhesion. Thereafter, attachment of this peptide to the thermo-responsive poly (MEO_2MA-co-OEGMA) was investigated for mESCs attachment.

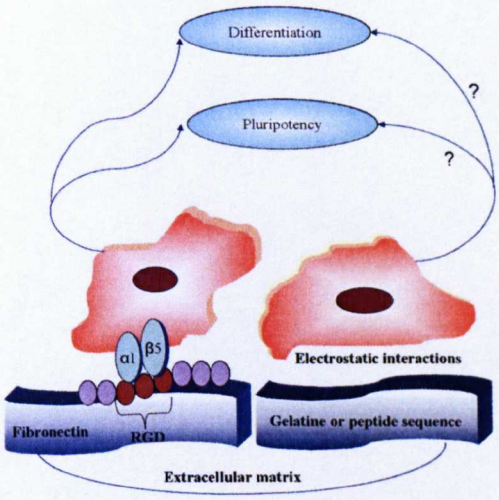

Figure 5.1. Schematic representation of mESCs cultured on fibronectin coated polymer brushes though the interaction with the RGD motif to aid their cell adhesion (Chapter 4). Electrostatic interactions are proposed for the cell adhesion of stem cells on gelatin or the proposed gelatin peptide sequence (267).

The following objectives to reach the main aim were as follows:

1. To synthesise AGPRGEHyPG peptide sequence.
2. Thereafter, mESCs were seeded on peptide adsorbed TCPS to investigate whether the gelatin peptide would promote mESCs adhesion.
3. To functionalise the poly (MEO_2MA-co-OEGMA) with the AGPRGEHyPG peptide.
4. mESCs were cultured on the immobilized peptide thermo-responsive surface to investigate mESC adhesion.

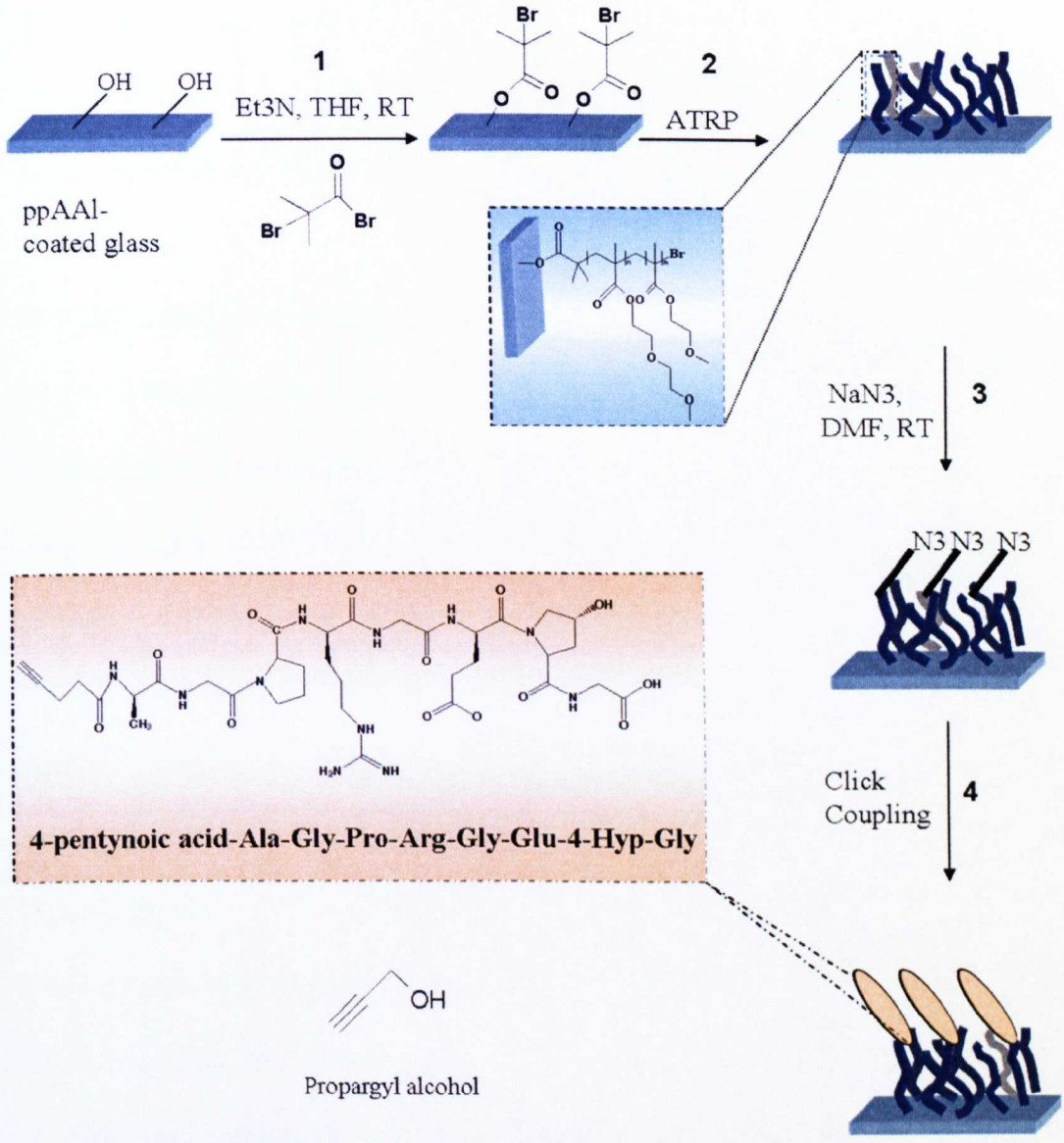

Figure 5.2. Schematic representation of the combined ATRP and click chemistry to attach the gelatin peptide to the thermo-responsive surface. Cleaned glass substrates were first plasma coated with allyl alcohol as described in Chapter 2, followed by the reaction of 2-bromoisobutyryl bromide with hydroxyl groups present. ATRP of poly (MEO_2MA-co-OEGMA) was achieved; bromine end groups of the polymer brushes were converted into azide groups after a reaction with NaN_3. Click coupling between the 4-pentynoic acid modified AGPRGEHyPG peptides and the azide groups on the polymer brushes was conducted; propargyl alcohol click chemistry was also performed as a control.

5.3 Materials and methods

5.3.1 Synthesis of Alkyne-modified AGPRGEHyPG and its purification

The alkyne-modified AGPRGEHyPG was synthesised by solid phase synthesis as follows: Fmoc-amino acids i.e. alanine, glycine, proline, 4-hydroxyproline, glutamine and arginine, preloaded Wang Fmoc-Glycine (100-200 mesh) resin and coupling agent HCTU were purchased from Novabiochem. Trifluoroacetic acid (TFA), N-Methylpyrrolidone (NMP), Dichloromethane (DCM), Dimethylformamdie (DMF) and Diisopropylethylamine (DIEA) were supplied by Applied Biosystems. Triisopropylsilane (TIPS), Piperidine and 4-pentynoic acid were supplied by Sigma Chemicals. Diethyl ether was supplied by Fisher Chemicals.

The synthesis was carried out on an automated peptide synthesis machine (Model 433A, Applied Biosystems) utilising 'FastMoc' chemistry (By Kevin Bailey). Briefly, solid support resin is weighed into reaction vessel. The quantity of resin used was 0.1mmol equivalents, weight required calculated from the manufacturers provided substitution ratio for each individual batch of resin. The reaction vessel was sealed using porous Teflon filters enabling reagents to enter and exit the sealed chamber whilst retaining the resin. 1 mmol of Fmoc amino acids and pentynoic acid were weighed into cartridges and sealed using rubber stoppers and aluminium crimp seals tops. This enables reagents to be delivered to the cartridges via a needle whilst retaining an air tight seal at the rubber stopper.

Briefly, the preloaded resin containing the C terminal glycine was treated with NMP washes to allow the resin to swell. The Fmoc deprotection of the c terminal

amino acid attached to the preloaded resin and the subsequent N terminus of the growing peptide chain was carried out using 3 additions of 99% piperidine with intermittent mixing of the resin. Excess reagent was washed from the resin using NMP prior to each additional stage of synthesis. Fmoc amino acids were solublised using 2 mL of NMP to which 2 mL of 0.45M HCTU in DMF were added. Solublised Fmoc amino acid was transferred to an activation vessel . 3 mL of 2M DIEA in NMP was added to initiate activation of the amino acid and the solution was transferred to the reaction vessel. Coupling was carried out in the reaction vessel for a total of 90 minutes per cycle with intermittent mixing of the resin using an integrated vortexing device to which the reaction vessel was attached. During coupling of the activated amino acid to the amino acid cartridge was washed out with NMP which was also used later in the cycle to wash the resin. Subsequent amino acid additions to the growing chain were achieved by repeated use of these outlined synthesis cycles with the exception of the final addition of 4-pentynoic acid in which the initial addition of piperidine was omitted since this was not an Fmoc protected monomer. All amino additions were carried out as single couplings with the exception of the 4-pentynoic acid which was double coupled. Final washing of the resin following addition of the final monomer was carried out first with NMP followed by DCM.

The resin was allowed to air dry for 2 h. The peptide was cleaved from the resin using 5 mL of a solution comprising 95% TFA, 2.5% water and 2.5% TIPS. Side protecting groups from relevant amino acids were simultaneously removed during this process. Cleavage and deprotection was carried out with mild stirring at room temperature for 1.5 h. The deprotection solution and resin were filtered though a pasteur pipette packed with a small volume of glass wool into 20 mL of ice cold

diethyl ether in a 30 mL glass centrifuge tube. Precipitation of the peptide was observed. The precipitate was pelleted by centrifugation at 2000 rpm for 5 min. The supernatant containing residual TFA and TIPS was discarded. The pellet was resuspended in 20 mL of fresh diethyl ether and centrifuged. The pelleted peptide was washed a total of 5 times using this method before air drying and crushing to a dry fine powder by spatula..

An aliquot of the peptide was dissolved in 0.1% trifluoroacetic acid in water at a concentration of approximately 0.2 mg per mL. Approximately 50 mcg of peptide in solution was loaded onto a Supelco Discovery Wide Pore C18 reverse phase column (dimensions 25cm X 2.1mm).

A reverse phase acetonitrile gradient was performed. Initial sample loading conditions were 0% acetonitrile in 0.1% trifluoroacetic acid. These conditions were maintained for 5 min following which acetonitrile was introduced in a linear gradient from 0% to 70% in 40 min. The flow rate during the chomatography was maintained at 0.3 mL per min.

Eluting components were identified using a UV-visible detector at 220 nm. Data collection was enabled by use of Clarity data collection and analysis software linked to the output from the detector. Eluting components were collected manually and the component representing the highest proportion of observed eluting material selected for additional analysis by mass spectrometry.

Mass spectrometry of the primary collected component was carried out using a MALDI instrument (Waters). Collected samples were introduced onto a stainless steel target plate previously treated with a matrix solution of alpha cyano 4-hydroxy cinnamic acid incorporating a peptide standard as an internal calibrant.

5.3.2 Azide-functionalised poly (MEO_2MA-co-OEGMA)

Poly (MEO_2MA-co-OEGMA) thermo-responsive surfaces were grafted from the surface synthesised as described in Chapter 2 (section 2.3.2). The nucleophilic substitution reaction of the terminal bromine group of poly (MEO_2MA-co-OEGMA) with sodium azide (NaN_3) was performed to introduce azide groups onto the thermo-responsive surfaces to be utilised by the click chemistry. The surfaces were immersed in DMF solution (5 mL) of NaN_3 (5 mg) for overnight at room temperature in a dry environment. The substrates were then washed extensively with DMF and deionized water and dried under a stream of nitrogen.

5.3.3 Click coupling of the peptide to azide-terminated poly (MEO_2MA-co-OEGMA)

Click chemistry was performed by placing the glass substrates with N_3-terminated poly (MEO_2MA-co-OEGMA) glass substrates in ethanol/ultrapure water solution (10 ml, 1:2 *v/v*), ascorbic acid (14mg), copper (I) bromide (14mg), Bipy (28mg) and 500 μg/ml of the alkyne modified peptide. The reaction mixture was stirred for overnight at room temperature using plate shaker at 100 rpm. After the reaction, the substrates were thoroughly washed with ethanol and then deionised water and dried under a stream of nitrogen. Propargyl alcohol was used as the control for the click coupling between azide groups on the polymer brushes and the propargyl alcohol as shown in Figure 5.2.

5.3.4 mESC culture on TCPS-gelatin peptide modified surfaces and on gelatin peptide modified thermo-responsive surfaces

mESCs were maintained as described in Chapter 4. The purified gelatin peptide was adsorbed to TCPS coated by incubating the surface with a 1 mg/ml solution (500 µl per well) in tissue culture water of the purified peptide was prepared overnight at room temperature under agitation. The well plates were washed after with warm PBS (pH 7.4) before seeding with mESCs (10,000 cells/ mL per well) in a complete mESCs culture media for 24 h and they were cultured at 37°C under humified environment with 5% CO_2 in air. mESCs cultured on gelatin coated TCPS was used as the control.

Poly (MEO_2MA-co-OEGMA)-g-4-pentynoicacid-AGPRGEHyPG thermo-responsive surfaces were first sterilised under UV for 20 min in a 6 well non-culture treated TCPS plate prior to adding 10,000 cells/ml in a total of 2 mL to each well including gelatin coated wells as the control. The cells were imaged using an inverted phase contrast microscope and a camera after washing them with PBS as described in Chapter 3.

5.4 Results and discussion

The bioconjugation of non-toxic, non-immunogenic polymers such as PEG-based polymers with peptides, enzymes or proteins is an important aspect of the modern biotechnology. Bioconjugation of PEG-based polymers with various proteins or peptides has been reported previously involving mostly RGD segment within fibronectin or laminin as it is recognised by many cell receptors of the integrin

family (284). Gelatin is often used for mESCs culture and maintenance of these cells in their undifferentiated state as reported before (256). Herein, a typical peptide representing gelatin was chosen to be studied for mESCs adherence. Thereafter, click coupling of this peptide to the thermo-responsive surfaces was also studied.

A combination of ATRP and click chemistry was used in this chapter to prepare peptide functionalised PEG-based polymer brushes. First, poly (MEO_2MA-co-OEGMA) was prepared using ATRP in the presence of catalyst system Cu Br/Bipy as described in Chapter 2, then the nucleaophilic substitution of the halogen (-Br) end groups of poly (MEO_2MA-co-OEGMA) into azides was achieved. 4-pentyonic acid-AGPRGEHyPG was chosen to be a typical gelatin sequence to be investigated in this work. It was prepared by solid phase synthesis using standard Fmoc protection chemistry, the terminal amino-functionality of the peptide was converted to an alkyne moiety though the coupling with 4-pentynoic acid.

5.4.1 Peptide synthesis analysis and purification

The coupling of the amino acids for 4-pentyonic acid-AGPRGEHyPG was performed using Fmoc protocols and analysed using HPLC and MALDI.

Figure 5.3 shows the MALDI-TOF results of the synthesised peptide which indicated the expected molecular weight of the 4-pentyonic acid-AGPRGEHyPG.

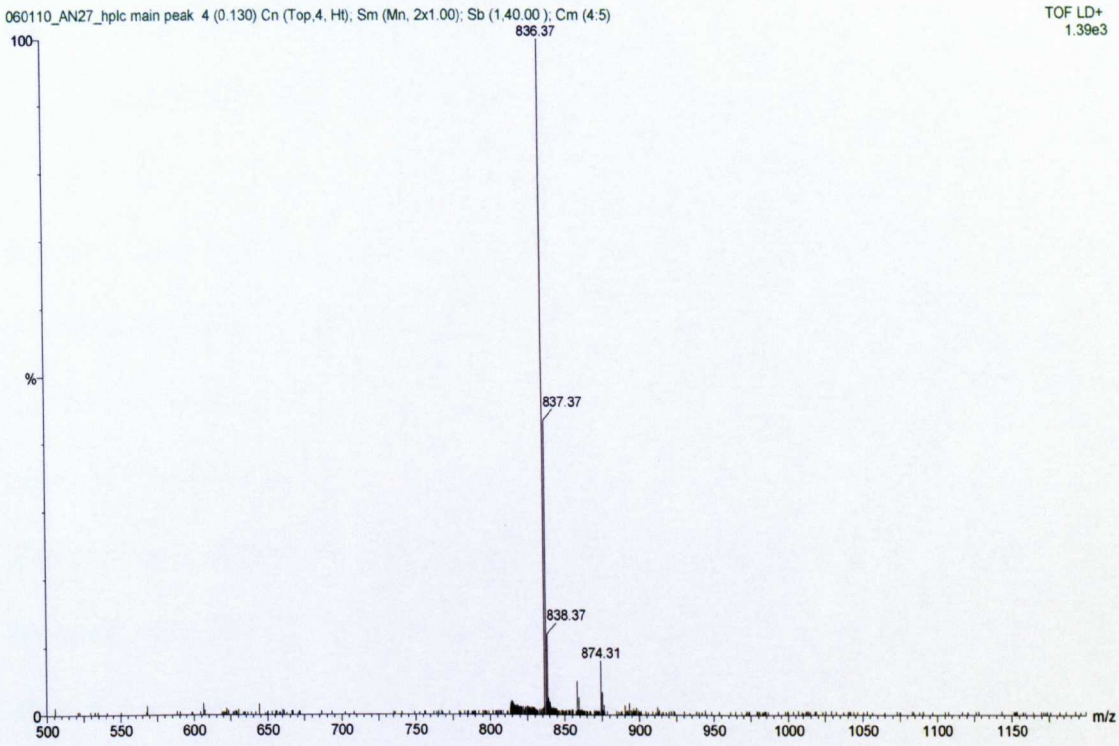

Figure 5.3. MALDI-TOF mass spectrum of the main peak of the purified component (AGPRGEHyPG) with a molecular weight of 836.5 m/z.

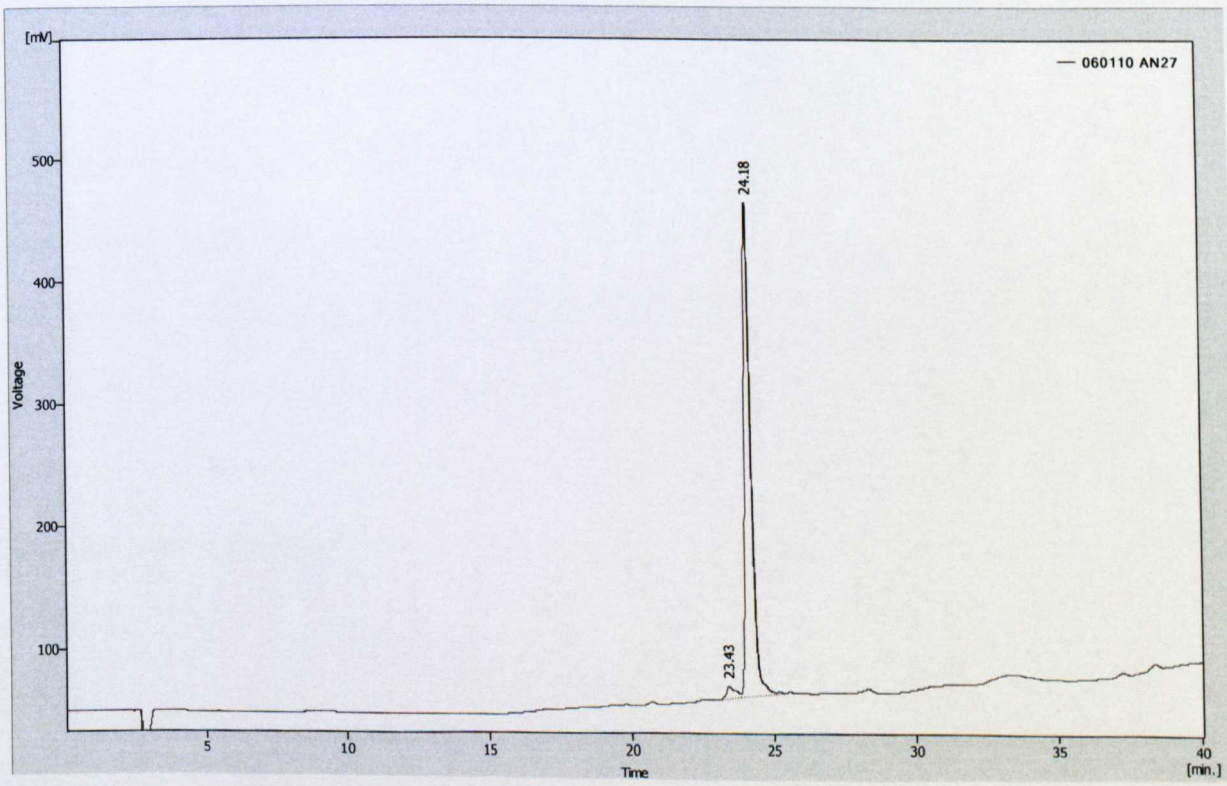

Figure 5.4. Reverse-phase HPLC analysis of 4-pentynoic acid modified AGPRGEHyPG following purification of the main component peak (90% pure).

5.4.2 Click chemistry of 4-pentynoic acid- AGPRGEHyPG to the thermo-responsive surfaces and subsequent analysis by XPS and WCA

N_3-terminated copolymer brushes and click coupling of 4-pentynoic acid-AGPRGEHyPG was performed as described in section 5.3.3. Surface analysis of the thermo-responsive surfaces and after the subsequent treatments was conducted using XPS and WCA.

The surface was analysed using XPS following reaction with 2-bromoisobutyryl bromide (1) (PAAl-*g*-2-bromoisobutyrate), ATRP of OEGMA and MEO_2MA from the initiation sites (2) (PAAl-*g*-Poly (MEO_2MA-co-OEGMA)). Thereafter, azide groups were introduced to the copolymer chains to produce N_3-teminated poly (MEO_2MA-co-OEGMA) (3), click chemistry between the azide groups and propargyl alcohol (4) and finally with 4-pentynoic acid- AGPRGEHyPG (5).

Br3d elemental composition was estimated to be 0.89% and 0.23% for PAAl-*g*-2-bromoisobutyrate and PAAl-*g*-poly (MEO_2MA-co-OEGMA) after ATRP respectively. However, following nucleophilic substitution of bromine, at the end of the thermo-responsive surfaces with the azide groups from NaN_3, XPS wide scan did not show any bromine peak indicating the successful substitution of bromine terminated copolymer brushes to N_3-terminated surfaces.

Table 5.1. Elemental composition of PAAl-g-2-bromoisobutyrate (1), PAAl-g-poly (MEO_2MA-co-OEGMA) ATRP (2), azide group introduction to the copolymer chains (NaN_3 reaction with halogen groups at the end of the polymer chains) (3), click chemistry of propargyl alcohol (4) and finally with 4-pentynoic acid- AGPRGEHyPG (5). The mean and standard deviation represents thee points on each surface.

Elements/ Composition (%)	1	2	3	4	5
Si2p	0.74 ± 0.34	0.58 ± 0.18	11.91 ± 0.63	6.18 ± 2.53	1.49±0.49
C1s	85.63 ±0.48	78.65 ± 0.38	35.03 ± 1.59	66.32±7.79	71.73±1.69
O1s	12.24 ±0.09	20.53 ± 0.49	46.74 ± 0.97	26.24±5.66	20.78±0.81
N1s	-	-	2.38 ± 0.36	0.97±0.38	5.99±0.74
NaKLL	-	-	3.04 ± 0.32	-	-
Br3d	0.89 ± 0.06	0.23 ± 0.04	-	-	-
Ca2p	-	-	0.88 ± 0.17	-	-

In addition, further XPS analysis of the surface at this point of modification identified the appearance of a new (N1s) peak on the XPS spectrum as shown in Table 5.1 and Figure 5.5. NaKLL was also present on the XPS spectrum although the surface was extensively washed with DMF, which could be from the contamination of the surface by these species. Some of the glass elements were detected including Si2p and Ca2p which signify that some the thermo-responsive poly (MEO_2MA-co-OEGMA) is affected.

The Si2p and N1s elemental composition was significantly decreased when the click coupling was performed using propargyl alcohol as shown in Table 5.1, which indicates successful click chemistry on these surfaces. Thereafter, 4-pentynoic acid- AGPRGEHyPG click coupling was achieved using the same

conditions as with the propargyl alcohol click experiment. N1s elemental composition was increased to 5.99% which indicates the attachment of the alkyne modified peptide to the azide converted bromine at the end of the polymer brushes.

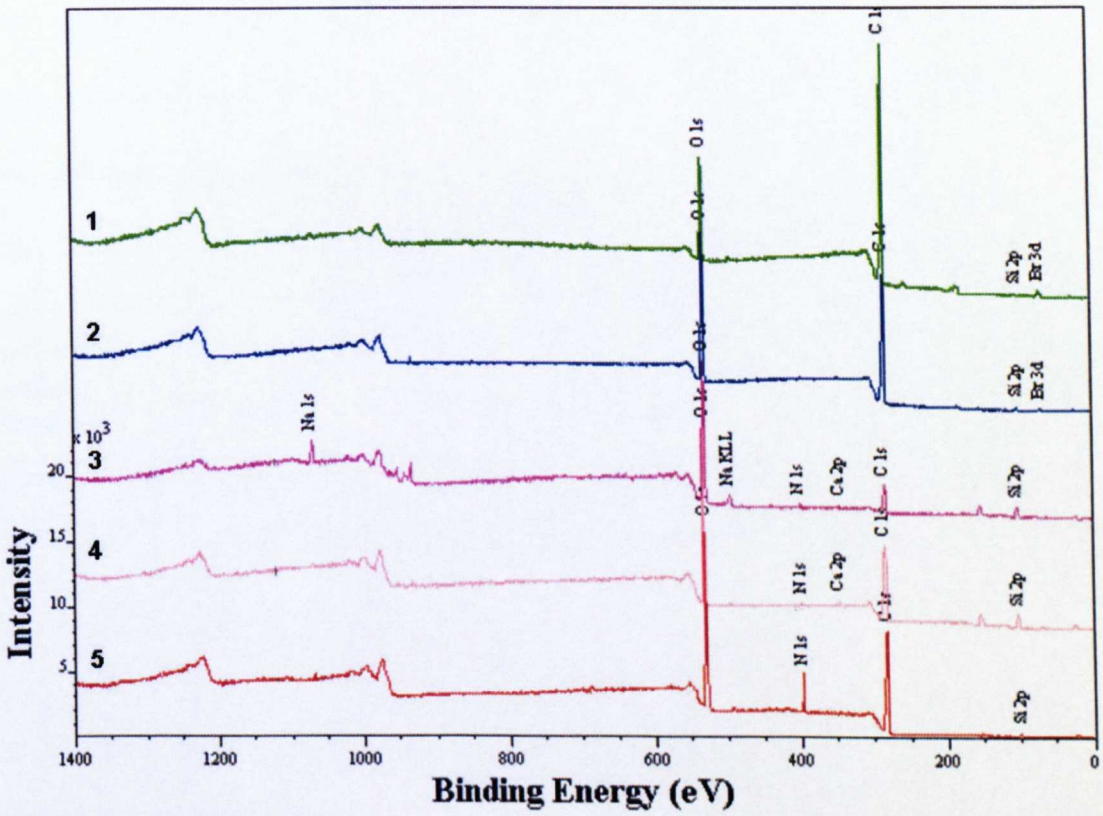

Figure 5.5. Wide XPS scans for different treatments to the surface. **1.** (green) PAAl-*g*-2-bromoisobutyrate. **2.** (blue) PAAl-*g*-poly (MEO_2MA-co-OEGMA)-Br. **3.** (purple) PAAl-*g*-poly (MEO_2MA-co-OEGMA)-N_3. **4.** (pink) Poly (MEO_2MA-co-OEGMA)-g-propargyl alcohol. **5.** (red) Poly (MEO_2MA-co-OEGMA)-g-4-pentynoic acid- AGPRGEHyPG.

The WCA was also measured to check the thermo-responsiveness of poly (MEO_2MA-co-OEGMA) brushes after attachment of the peptide. Table 5.2 shows the WCA for PAAl-*g*-2-bromoisobutyrate (control) and PAAl-*g*-poly (MEO_2MA-

co-OEGMA) ATRP and after the click coupling with 4-pentynoic acid-AGPRGEHyPG both above (37°C) and below (10°C) the LCST.

Table 5.2. WCA shown for PAAl-*g*-2-bromoisobutyrate (control) and PAAl-*g*-poly (MEO_2MA-co-OEGMA) ATRP and after the click coupling with 4-pentynoic acid- AGPRGEHyPG above and below the LCST. The mean and standard deviation represent the average WCA measurements of thee samples.

Temperature/ Surface treatment	PAAl-*g*-2-bromoisobutyrate	PAAl-*g*-poly (MEO_2MA-co-OEGMA)	Poly (MEO_2MA-co-OEGMA)-g-4-pentynoic acid-AGPRGEHyPG
37°C	**66.11±0.96**	**67.62±2.93**	**63.14±9.04**
10°C	**67.25±0.78**	**44.99±0.36**	**56.36±10.74**

Table 5.2 shows the WCA for the different surface treatment. The WCA of Poly (MEO_2MA-co-OEGMA)-g-4-pentynoic acid- AGPRGEHyPG at 37°C was hydrophobic (63.14 ± 9.04) as well as the poly (MEO_2MA-co-OEGMA) only. However, the WCA at 10°C was 56.4 which is 11° higher compared to the copolymer brushes only at 10°C indicating that the surface becomes more hydrophobic following attachment of the peptide. This phenomem was observed with fibronectin (Chapter 4) which was thought to be due to the high molecular weight

This could be due to the high molecular weight of the peptide attached to the polymer brushes which in turn could affect the conformation of the brushes below the LCST.

5.4.3 mESCs culture on peptide adsorbed to TCPS

mESCs are anchorage-dependent cells which showed low adhesion to the thermo-responsive poly (MEO_2MA-co-OEGMA) alone. Under standard culture conditions, these cells are often cultured on gelatin coated TCPS (97). Gelatin is a protein which is thought to aid the attachment of mESCs though the electrostatic interaction with the cells (256, 267).

Gelatin sequence was chosen to investigate and initial experiments were conducted to assess the adhesion of mESCs to peptide adsorbed to TCPS and this cell adhesion was compared to the whole molecule (gelatin).

A solution of peptide 1 mg/ml was prepared and filtered though 0.2 μm filter, and then 500μl of which was allowed adsorb to the surface of TCPS overnight at room temperature. The adsorption to this surface was confirmed from WCA measurements of AGPRGEHyPG coated TCPS which was 24.95±2.6 (compared to TCPS only, 64.29±2.34) when it was measured of these surfaces before and after the adsorption of the peptide to TCPS. XPS was also used to investigate the chemical composition of TCPS and after coating it the peptide synthesised (Table 5.3 and Figure 5.6).

Table 5.3. Elemental composition determined by XPS for TCPS and TCPS coated AGPRGEHyPG.

Name	TCPS	TCPS+ AGPRGEHyPG
C 1s	89.7 ± 0.2	87.4 ± 0.8
O 1s	8.7 ± 0.1	8.2 ± 0.3
N 1s	1.4 ± 0.1	4.3 ± 0.5
Ca 2p	0.2 ± 0.06	-

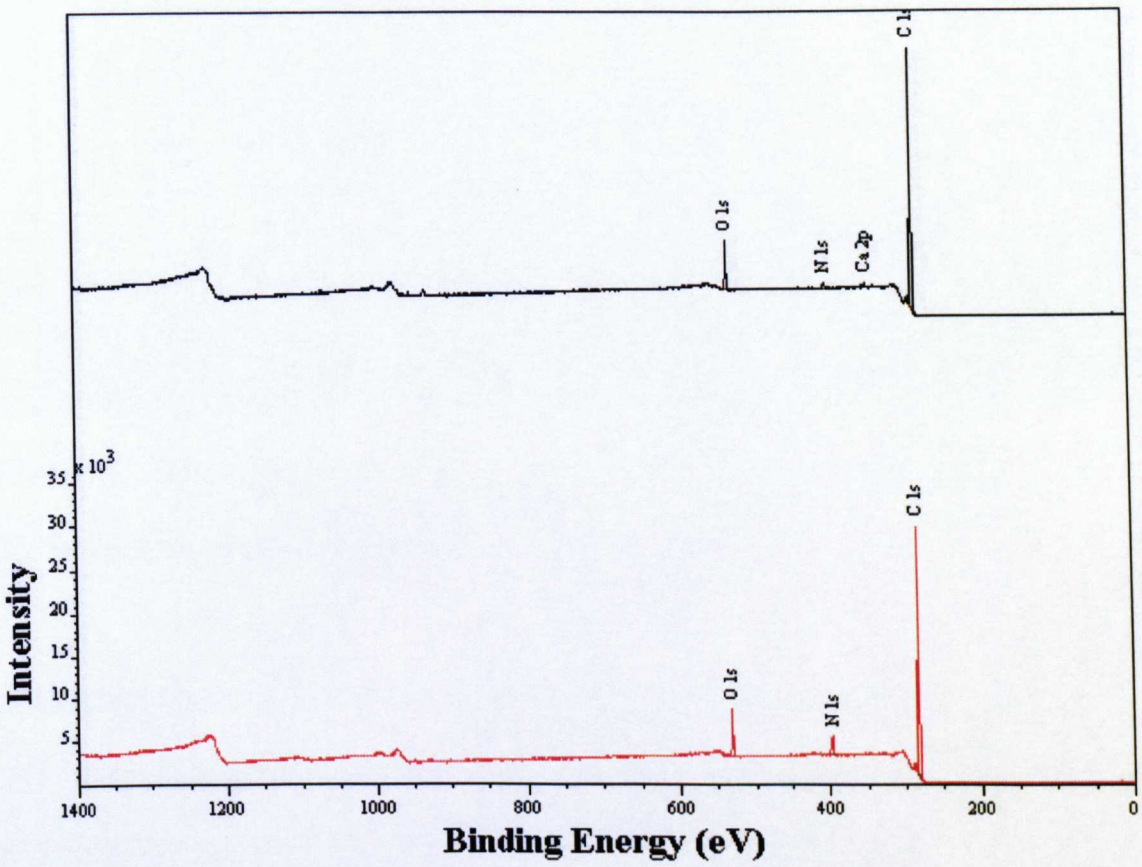

Figure 5.6. XPS wide scan spectra for TCPS (control; black) and TCPS coated with AGPRGEHyPG peptide sequence (red).

From Table 5.3 and Figure 5.6, XPS data showed that a characteristic nitrogen peak (N1s) was detected indicative of the successful deposition of the peptide on TCPS.

mESCs were then seeded on the peptide and gelatin coated TCPS (control) (N=4 i.e. 4 samples) and allowed to adhere for 24 h. mESCs adhered to the peptide coated TCPS in a similar fashion to the gelatin control as shown in Figure 5.7.

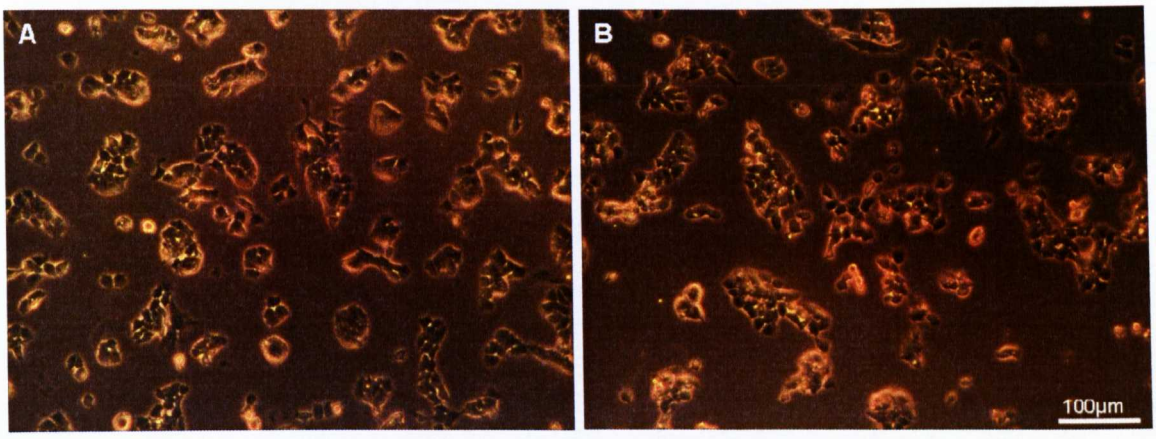

Figure 5.7. Representative images of mESC cells cultured on A: gelatin (control) and B: AGPRGEHyPG coated TCPS.

Click chemistry was performed on azide converted bromine groups on the poly (MEO_2MA-co-OEGMA) thermo-responsive surfaces with 4-pentynoic acid-AGPRGEHyPG and mESCs were cultured on these surfaces. Figure 5.8 shows adherence of mESCs on the peptide sequence attached thermo-responsive surfaces compared to mESC on poly (MEO_2MA-co-OEGMA) surfaces only where they did not adhere and spread as well as (Chapter 4, Figure 4.2).

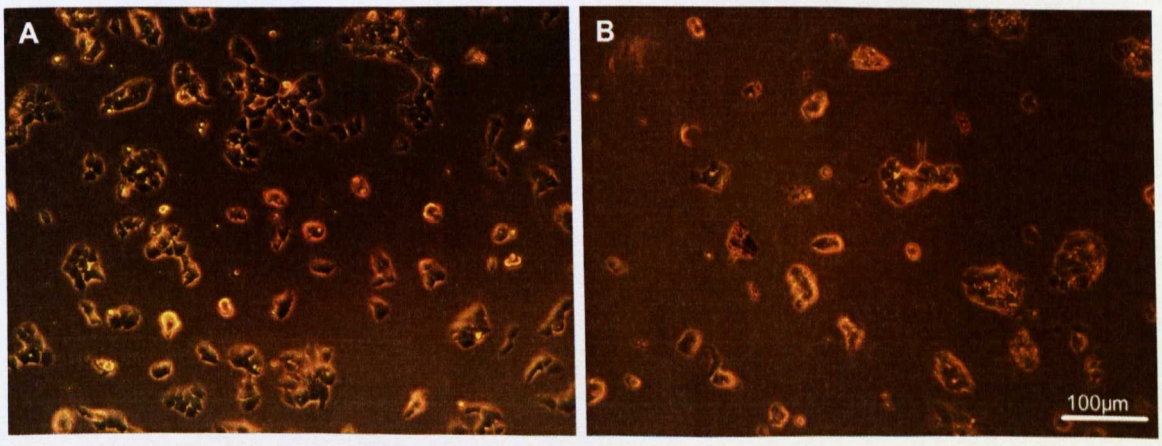

Figure 5.6. Representative phase contrast images showing mESCs adherence to gelatin (**A**). **B** shows the phase contrast images for Poly (MEO_2MA-co-OEGMA)-g-4-pentynoic acid- AGPRGEHyPG.

From the images taken of mESCs on the peptide modified surfaces, the surface area covered by cells was estimated using image J software and is presented in Figure 5.8. mESCs adhered to peptide and gelatin coated TCPS; there was no significant difference between the two surfaces (p=0.06) which shows that mESCs grew and spread on the peptide as well as the gelatin coated TCPS. Cells were observed over 24 h on these surfaces and they adhered, although, there was a significant difference between gelatin coated TCPS (control) and Poly (MEO_2MA-co-OEGMA)-g-4-pentynoic acid- AGPRGEHyPG cultured cells as shown in Figure 5.7 and 5.8 (p=0.008).

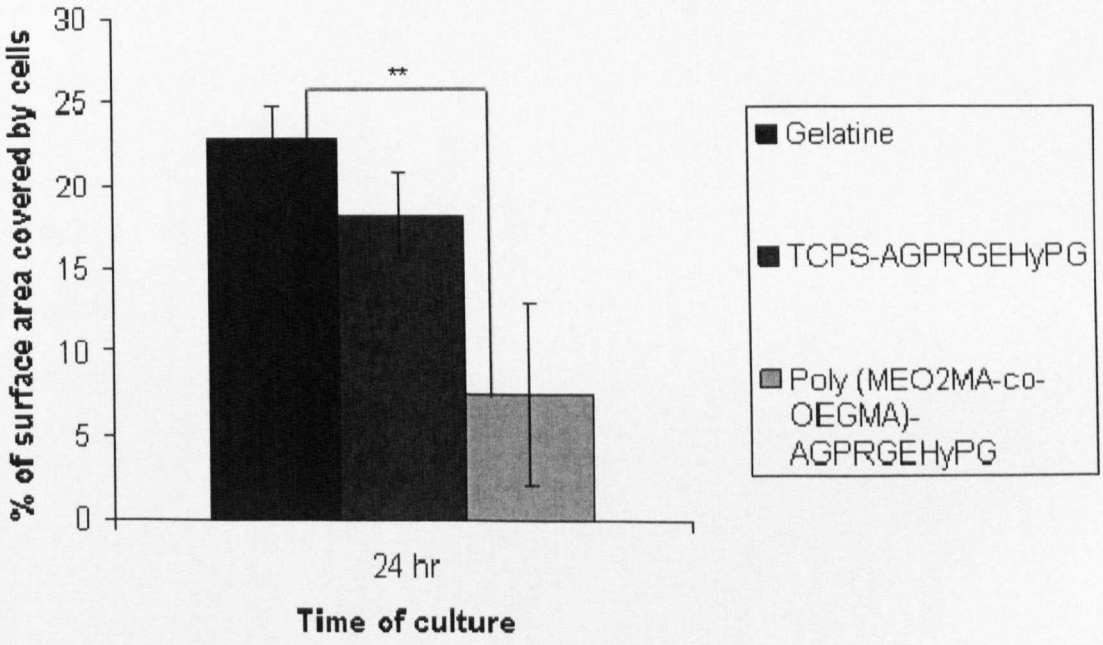

Figure 5.7. The surface area estimated for cells covering the surface of TCPS coated gelatin; TCPS coated AGPRGEHyPG and Poly (MEO_2MA-co-OEGMA)-g-4-pentynoic acid- AGPRGEHyPG surfaces. N=4 (total of 4 samples).

5.5 Conclusion

In Chapter 4, mESCs showed low adhesion on poly (MEO_2MA-co-OEGMA) thermo-responsive surfaces and although this was enhanced when fibronectin was adsorbed to the surface, this appeared to induce differentiation. mESC are usually cultured on gelatin coated TCPS for their maintenance. Then, the idea of choosing a novel peptide (a typical gelatin sequence) was synthesised, which to our knowledge is not previously reported in the literature.

TCPS coated with AGPRGEHyPG showed spreading and adherence of mESC after 24 h of culture as well as the gelatin (control) maintaining their colonised state. This is very interesting data which needs to be further investigated to determine the minimum concentration of the peptide that promotes the cell adhesion is required.

The peptide was attached to the poly (MEO_2MA-co-OEGMA) via click coupling after converting bromine at the end of the polymer chains to azide groups. Successful coupling of the peptide to the poly (MEO_2MA-co-OEGMA) was indicated by the characteristic N1s peak on the XPS data as it was increased with peptide-copolymer brushes compared to the previous treatments.

Poly (MEO_2MA-co-OEGMA)-g-4-pentynoic acid- AGPRGEHyPG surfaces supported the spreading and adherence of mESC after 24 hours. Therefore, preliminary results with this peptide look very promising for mES cells culture.

CHAPTER 6

General discussion, conclusions and future work

Embryonic stem cells (ESCs) are derived from the inner cell mass of a blastocyst. Because of their capability to self-renew and to give rise to specialized cell types, embryonic stem cell based therapies have been proposed as potential applications for regenerative medicine and tissue replacement after injury or disease including Parkinson's, Alzheimer's disease, spinal cord injury, stroke, burns, heart disease, diabetes, osteoarthitis and rheumatoid arthitis (16, 17).

Maintenance of ESCs is an important step prior to their further use in various applications; these cells are usually maintained in their undifferentiated state on feeder layers derived from animal or human tissues or on proteins such as gelatin or Matrigel. In addition, to prevent their differentiation, ESCs are usually sub-cultured every 3 and 7 days for mESCs and hESCs respectively using trypsin/EDTA. This maintenance process is disadvantageous as these current culture methods could dramatically affect the quality of the cells in that ESCs could become infected when using non-purified proteins and feeder layers derived from animal tissues (32-37). Moreover, trypsin is well known protease that can

damage essential cell membrane receptors during detachment of ESCs from the culture substrates (55).

Synthetic smart substrates have been extensively studied for culture and detachment of differentiated mammalian cells particularly polymeric surfaces that change conformation in response to an applied external stimulus (80). Despite many studies into cell culture on polymeric surfaces including endothelial cells, hepatocytes, cardiomyocytes and human mesenchymal stem cells, there are limited reports relating to the use of these materials for ESC culture.

The aim of this research project was to fabricate environment-responsive surfaces (to temperature) for mammalian cell culture, including mouse embryonic stem cells as a model stem cell type. Such a culture system could eliminate the need to detach cells from the culture surface using proteolytic enzymes as well as using proteins and feeder layers to aid their attachment and maintain their undifferentiated state.

Copolymers of 2-(2-methoxyethoxy) ethyl methacrylate (MEO_2MA) and oligo(ethylene glycol) methacrylate (OEGMA) copolymers have been proposed for use as switchable surface for mammalian cell culture (196, 264). The LCST of this copolymer could be adjusted by altering the co-monomer compositions to obtain similar thermo-responsive properties as the well know thermo-sensitive poly (N-isopropyl acrylamide). Chapater 3 detailed the synthesis and analysis of thermo-responsive copolymer brushes. Copolymers were grafted from the surface using ATRP after reacting an ATRP initiator (2-bromoisobutyryl bromide) with

the hydroxyl groups present following deposition of plasma polymerisation of allyl alcohol on to the glass surface. XPS and ToF-SIMS analysis showed that the elemental composition of these surfaces indicated successful grafting of poly (MEO_2MA-co-OEGMA). XPS results showed that the grafted thermo-responsive layer was above 10 nm (the XPS depth of analysis) as the main glass element Si2p was not detected on the poly (MEO_2MA-co-OEGMA) surfaces. Future work with regard to obtaining different thicknesses of the copolymer brushes is required to determine whether there is a correlation between these polymeric layers and mammalian cell adhesion.

These copolymer grafted brushes showed thermo-responsive behaviour when they were examined using the water contact angle analysis and atomic force microscopy as shown in Chapter 3. Water contact angle data showed that poly (MEO_2MA-co-OEGMA) properties changed from hydrophilic at 20°C to hydrophobic at 37°C. The LCST of poly (MEO_2MA-co-OEGMA) in solution is 32°C when choosing 95:5 MEO_2MA to OEGMA monomer composition. Further studies were performed at the microscopic level using atomic force microscopy to investigate the LCST of the poly (MEO_2MA-co-OEGMA) when grafted from the surface. It was found that the thermo-responsive copolymer brushes switch their status from hydrophobic at 37°C to hydrophilic 20°C at 28°C. Because poly (MEO_2MA-co-OEGMA) substrates showed successful grafting and the desired thermo-responsive behaviour, we proposed using these surfaces as a switchable culture system for mammalian cells.

Poly (MEO_2MA-co-OEGMA) thermo-responsive surfaces supported the adhesion, spreading, proliferation and detachment of mouse 3T3 fibroblasts up to passage 10 as described in Chapter 4. There was a difference between cell morphology of 3T3 fibroblasts when cultured on TCPS and on the thermo-responsive surfaces with regard to how the cell population as a whole grows. Many factors could affect the cell morphology including surface material and culture time on the polymeric substrates.

The ultimate aim of this work was to study the response of stem cells to thermo-responsive polymer surface. This was conducted using a feeder free mESC line as stem cell type model. mESCs did not adhere to the thermo-responsive polymer surfaces as fabricated and lead to the formation of embryoid bodies. This was thought to be caused by the hydrophobic nature of the copolymer brushes. Additionally, OEGMA-based polymers have previously shown resistance to protein adsorption and hence low cell adhesion. Poly (MEO_2MA-co-OEGMA) surfaces were therefore treated with different proteins including 100% and 2% gelatin and fibronectin. Cell adhesion to the thermo-responsive polymer following incubation with gelatin was not observed, resulting again in the formation of embryoid bodies. However, incubation of these surfaces with fibronectin dramatically improved cell adhesion where mESCs adhered, spread and proliferated as seen on gelatin coated TCPS (positive control).

Optimal conditions and concentrations for fibronectin adsorption to the thermo-responsive surfaces were studied and it was found that 5 μg/ml fibronectin and adsorption at 37°C for 18 h was sufficient to encourage mESC attachment.

Subsequent detachment of mESC is achieved by lowering the temperature of the culture medium to 10°C for 2 h.

In Chapter 5, mESCs were cultured on the poly (MEO_2MA-co-OEGMA) thermo-responsive surfaces for up to 10 passages using the temperature as the detachment factor and compared it with trypsinised cells cultured on gelatin coated TCPS.

Morphological changes of the cells was observed after passage 5 where mESCs adopted a fibroblastic cellular morphology compared to the colonies growth of cells on the control. This was attributed to the difficulties in obtaining a single cell suspension following detachment of the cells from the thermo-responsive surfaces in comparison with individual cells produced when using trypsin. This in turn meant that the cells were seeded on the next surface in clusters leading to different population kinetics believed to induce differentiation. This was confirmed when analysis of mESCs at passage 5 and 10 at the genetic level using RT-PCR was performed. Expression of Oct3/4 was maintained thoughout the 10 passages but decreased band intensity was observed compared to the control and passage 1. Immuno-staining results also showed positive staining for Oct3/4 at passage 1, 5 and 10 but brachyury staining after passage 5 in cells cultured on the thermo-responsive surfaces as shown was also present.

Maintaining of mESCs on gelatin is a standard culture procedure and with the inclusion of LIF in the culture media, no differentiation is observed over many passages. To overcome the issues in Chapter 5 with respect to fibronectin appearing to stimulate mESC differentiation, a novel peptide of a typical repeat

sequence of gelatin was studied as described in Chapter 6. This peptide was synthesised using solid-phase peptide synthesis and the expected molecular weight confirmed. It was subsequently attached to the thermo-responsive brushes using click chemistry and mESCs adhesion assessed.

Preliminary results showed adhesion of mESCs to this peptide which is very promising both adsorbed onto TCPS and following attachment to the copolymer brushes. Unfortunately due to time constraints, it was not possible to carry out a cell passaging experiment as described in Chapter 5. This would form the basis for future work. The mechanism of attachment of these cells to gelatin and this peptide sequence is an important aspect to understand and further work is required in this area also.

Future work following from this thesis would include optimisation of the thermo-responsive surface for mESCs culture. Firstly, the polymerisation has to be stopped at rather low monomer conversion in order to obtain a copolymer with a higher degree of terminal halogen functionality. This in turn would provide more azide groups and hence more alkyne modified peptide is attached to the copolymer brushes for improved cell attachment. This leads to higher concentration of monomers in the solution which could be washed extensively with water to remove the adsorbed monomers. Secondly, the use of poly (MEO_2MA-co-OEGMA)-**AGPRGEHyPG** needs to be studied for the long-term culture of mESCs and compared to the gelatin coated TCPS. Finally, surface analysis of the peptide modified copolymer brushes is also an essential step to ensure that the peptide is attached to the brushes and disturbed. Distribution of the

peptide across the surface is a challenging task in that ToF-SIMS could be a useful technique to determine certain amino acids i.e. glycine distribution. Moreover, immuno-staining imaging of fragments of the peptide could be a useful assay to detect the densities of the peptide across the surface.

Thermo-responsive hydrogels based on poly (MEO_2MA-co-OEGMA) could be useful to produce a thicker culture substrate. Additionally, incorporation of peptides into the hydrogel has been reported previously and therefore incorporation of this peptide to the thermo-responsive hydrogels could lead to mESCs facile attachment, growth and detachment.

The studies conducted within this thesis were in 2D culture. It is possible that a better culture condition could be achieved though the synthesis of 3D chemistries using beads to increase surface cell culture could be a potential aim for long term applications.

Attachment of cells to their surroundings is an essential event to determine cell morphologies and maintaining cell functions; this cell-substrate interactions can have a significant impact on biomaterial-based therapies. Understanding of stem cell structures and mechanisms related cell-substratum interaction is therefore necessary. For example topographical changes effects of the surfaces is an important aspect to design stem cell culture substrates. Using mESCs as a stem cell model to further study ligands that promote stem cell adhesion is also a key factor to maintaining these cells undifferenatiated.

A good understanding of the mechanisms of ESCs adhesion to the gelatin or other proteins used to promote cell adhesion will be instrumental in detecting future designs of biomaterials for ESCs expansion.

In conclusion, poly (MEO_2MA-co-OEGMA) surfaces were synthesised from the surface using ATRP. They were therefore used for mammalian cell culture including stem cell culture taking advantage of their thermo-responsive properties. Short term future work would involve the transfer of the thermo-responsive surfaces technology to use for human embryonic stem cell culture.

Appendix

1. Preparation of culture medium

- **3T3 fibroblast media**

Ingredient	*Volume*	*Final concentration*
Dulbecco's Modified Eagle	500 mL	N/a
L-glutamine (200 mM)	5 mL	2 mM
Antibiotic/Antimycotic (100× solution)	5 mL	100 U penicillin 100 µg streptomycin 0.25 µg amphotericin B
Foetal calf serum (heat inactivated)	50 mL	10 %

- Feeder free mouse embryonic stem cell media

Ingredient	*Volume*	*Final concentration*
Dulbecco's Modified Eagle	500 mL	N/a
L-glutamine (200 mM)	5 mL	2 mM
Antibiotic/Antimycotic (100× solution)	5 mL	100 U penicillin 100 µg streptomycin 0.25 µg amphotericin B
Foetal Bovine serum (ESC qualified)	50 mL	15 %
β-Mercaptoethanol	0.5 mL	

- All additives were aliquoted and stored at 4°C and passed though 0.2 µm filters before adding them to the medium.
- Medium were dated and given a 2 weeks expiry and stored at 4°C.

2. Counting cells with Tryptan blue

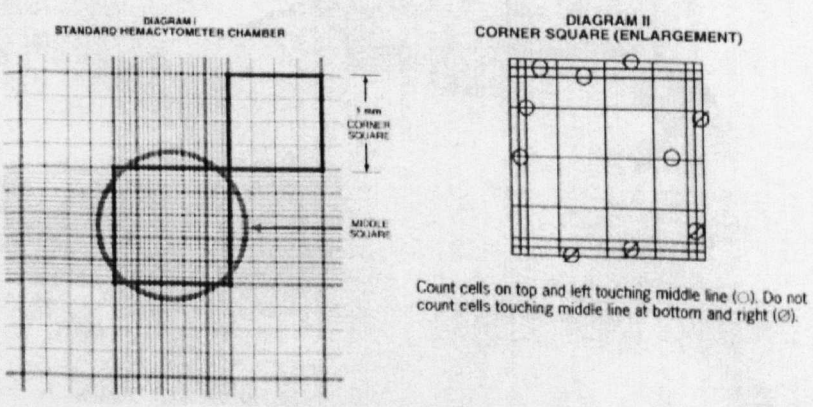

3. Alamar blue working solution

- 1 ml Alamar Blue stock solution,
- 9 ml HBSS without phenol red without serum

4. Atomic force microscopy

AFM set up for topography and adhesion measurements

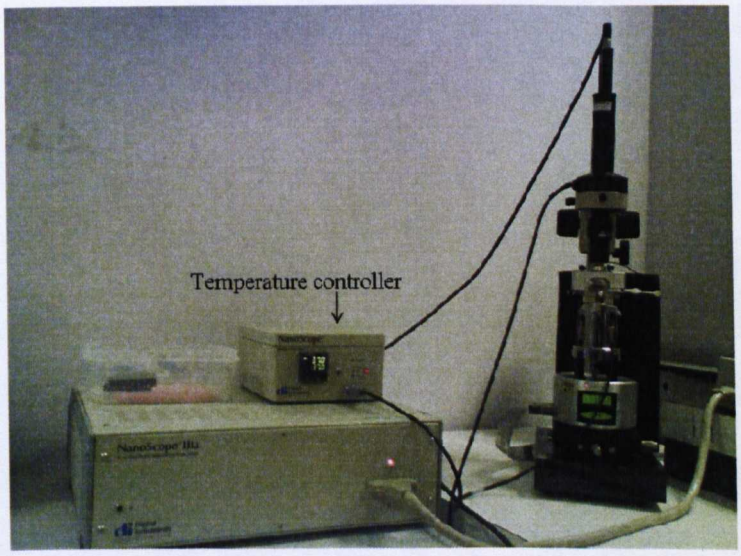

Heating accessories

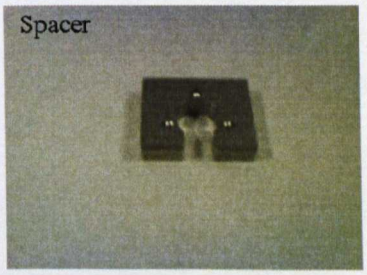

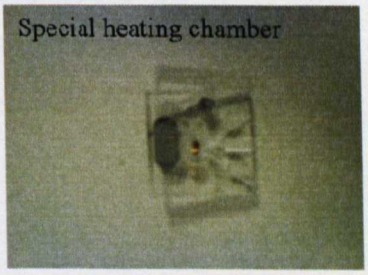

Reference

1. Nedime S, Keith WN. Therapeutic potential of adult stem cells. European journal of cancer (Oxford, England : 1990). 2006;42(9):1243-6.

2. Tanavde VM, Malehorn MT, Lumkul R, Gao Z, Wingard J, Garrett ES, et al. Human stem-progenitor cells from neonatal cord blood have greater hematopoietic expansion capacity than those from mobilized adult blood. Experimental Hematology. 2002;30(7):816-23.

3. Dimitriou H, Matsouka C, Perdikoyanni C, Stiakaki E, Bolonaki I, Lydaki E, et al. Phenotypic characteristics of cord blood hemopoietic cells. Leukemia Research. 1998;22(8):755-8.

4. Korbling M, Estrov Z. Adult Stem Cells for Tissue Repair -- A New Therapeutic Concept? N Engl J Med. 2003 August 7, 2003;349(6):570-82.

5. Rizouli V, Gribben JG. The role of stem cell transplantation in chronic lymphocytic leukemia. Seminars in Hematology. 2004;41(3):246-53.

6. Jabbour E, Keating MJ, Champlin RE, Khouri IF. Stem cell transplantation for chronic lymphocytic leukemia: should not more patients get a transplant? Bone Marrow Transplant. 2004;34(4):289-97.

7. Agnieszka B, Takumi T, Yusuke Y, Makoto T, Fumitaka T, Gary Q, et al. Adipose tissue-derived mesenchymal stem cells as a source of human hepatocytes. Hepatology. 2007;46(1):219-28.

8. Goss JA, Schock AP, Brunicardi FC, Goodpastor SE, Garber AJ, Soltes G, et al. Achievement of insulin independence in three consecutive type-1 diabetic patients via pancreatic islet transplantation using islets isolated at a remote islet isolation center. Transplantation. 2001;74(12):1761-6.

9. Freed CR, Greene PE, Breeze RE, Tsai W-Y, DuMouchel W, Kao R, et al. Transplantation of Embryonic Dopamine Neurons for Severe Parkinson's Disease. N Engl J Med. 2001 March 8, 2001;344(10):710-9.

10. Strauer BE, Brehm M, Zeus T, Kostering M, Hernandez A, Sorg RV, et al. Repair of Infarcted Myocardium by Autologous Intracoronary Mononuclear Bone Marrow Cell Transplantation in Humans. Circulation. 2002 October 8, 2002;106(15):1913-8.

11. van Laar JM, Tyndall A. Adult stem cells in the treatment of autoimmune diseases. Rheumatology. 2006 October 1, 2006;45(10):1187-93.

12. Jiang Y, Vaessen B, Lenvik T, Blackstad M, Reyes M, Verfaillie CM. Multipotent progenitor cells can be isolated from postnatal murine bone marrow, muscle, and brain. Experimental Hematology. 2002;30(8):896-904.

13. Alvarez-Dolado M, Pardal R, Garcia-Verdugo JM, Fike JR, Lee HO, Pfeffer K, et al. Fusion of bone-marrow-derived cells with Purkinje neurons, cardiomyocytes and hepatocytes. Nature. 2003;425(6961):968-73.

14. Terada N, Hamazaki T, Oka M, Hoki M, Mastalerz DM, Nakano Y, et al. Bone marrow cells adopt the phenotype of other cells by spontaneous cell fusion. Nature. 2002;416(6880):542-5.

15. Smith AG. EMBRYO-DERIVED STEM CELLS: Of Mice and Men. Annual Review of Cell and Developmental Biology. 2001;17(1):435-62.

16. Keller G. Embryonic stem cell differentiation: emergence of a new era in biology and medicine. Genes & Development. 2005 May 15, 2005;19(10):1129-55.

17. Murielle M, Surinder KB. Concise Review: Recent Advances on the Significance of Stem Cells in Tissue Regeneration and Cancer Therapies. Stem Cells. 2006;24(11):2319-45.

18. Narayan AD, Chase JL, Lewis RL, Tian X, Kaufman DS, Thomson JA, et al. Human embryonic stem cell-derived hematopoietic cells are capable of engrafting primary as well as secondary fetal sheep recipients. Blood. 2006 March 1, 2006;107(5):2180-3.

19. M.K. RLCC-PKPPYaC. Generation of Hepatocyte-Like Cells From Human Embryonic Stem Cells. Cell Transplantation. 2003;12:1-11.

20. C Mummery DW, CE van den Brink, SD Bird, PA Doevendans, T Opthof, A Brutel de la Riviere, L Tertoolen, M van der Heyden, and M Pera. Cardiomyocyte differentiation of mouse and human embryonic stem cells. J Anat. 2002;200(3):233–42.

21. Reubinoff BE, Itsykson P, Turetsky T, Pera MF, Reinhartz E, Itzik A, et al. Neural progenitors from human embryonic stem cells. Nat Biotech. 2001;19(12):1134-40.

22. Levenberg S, Golub JS, Amit M, Itskovitz-Eldor J, Langer R. Endothelial cells derived from human embryonic stem cells. Proceedings of the National Academy of Sciences of the United States of America. 2002 April 2, 2002;99(7):4391-6.

23. Iuchi S, Dabelsteen S, Easley K, Rheinwald JG, Green H. Immortalized keratinocyte lines derived from human embryonic stem cells. Proceedings of the National Academy of Sciences of the United States of America. 2006 February 7, 2006;103(6):1792-7.

24. Hanna S, Bettina F, Anna Z, Margarita S, Joseph I-E. Differentiation of Human Embryonic Stem Cells into Insulin-Producing Clusters. Stem Cells. 2004;22(3):265-74.

25. Klug MG, Soonpaa MH, Koh GY, Field LJ. Genetically selected cardiomyocytes from differentiating embronic stem cells form stable intracardiac grafts. The Journal of Clinical Investigation. 1996;98(1):216-24.

26. Kim J-H, Auerbach JM, Rodriguez-Gomez JA, Velasco I, Gavin D, Lumelsky N, et al. Dopamine neurons derived from embryonic stem cells function in an animal model of Parkinson's disease. Nature. 2002;418(6893):50-6.

27. Lindvall O, Kokaia Z. Stem cells for the treatment of neurological disorders. Nature. 2006;441(7097):1094-6.

28. McDonald JW, Liu X-Z, Qu Y, Liu S, Mickey SK, Turetsky D, et al. Transplanted embryonic stem cells survive, differentiate and promote recovery in injured rat spinal cord. Nat Med. 1999;5(12):1410-2.

29. León-Quinto T, Jones J, Skoudy A, Burcin M, Soria B. In vitro directed differentiation of mouse embryonic stem cells into insulin-producing cells. Diabetologia. 2004;47(8):1442-51.

30. Soria B, Roche E, BernÃ¡ G, LeÃ³n-Quinto T, Reig JA, MartÃ-n F. Insulin-secreting cells derived from embryonic stem cells normalize glycemia in streptozotocin-induced diabetic mice. Diabetes. 2000 February 2000;49(2):157-62.

31. Lensch MW, Daley GQ. Scientific and clinical opportunities for modeling blood disorders with embryonic stem cells. Blood. 2006 April 1, 2006;107(7):2605-12.

32. Evans MJ, Kaufman MH. Establishment in culture of pluripotential cells from mouse embryos. Nature. 1981;292(5819):154-6.

33. Thomson JA, Itskovitz-Eldor J, Shapiro SS, Waknitz MA, Swiergiel JJ, Marshall VS, et al. Embryonic Stem Cell Lines Derived from Human Blastocysts. Science. 1998 November 6, 1998;282(5391):1145-7.

34. Xu C, Inokuma MS, Denham J, Golds K, Kundu P, Gold JD, et al. Feeder-free growth of undifferentiated human embryonic stem cells. Nat Biotech. 2001;19(10):971-4.

35. Richards M, Fong C-Y, Chan W-K, Wong P-C, Bongso A. Human feeders support prolonged undifferentiated growth of human inner cell masses and embryonic stem cells. Nat Biotech. 2002;20(9):933-6.

36. Lee JB, Lee JE, Park JH, Kim SJ, Kim MK, Roh SI, et al. Establishment and Maintenance of Human Embryonic Stem Cell Lines on Human Feeder Cells Derived from Uterine Endometrium under Serum-Free Condition. Biology of Reproduction. 2005 January 2005;72(1):42-9.

37. Amit M, Shariki C, Margulets V, Itskovitz-Eldor J. Feeder Layer- and Serum-Free Culture of Human Embryonic Stem Cells. Biology of Reproduction. 2004 March 2004;70(3):837-45.

38. Smith AG, Hooper ML. Buffalo rat liver cells produce a diffusible activity which inhibits the differentiation of murine embryonal carcinoma and embryonic stem cells. Developmental Biology. 1987;121(1):1-9.

39. Smith AG, Heath JK, Donaldson DD, Wong GG, Moreau J, Stahl M, et al. Inhibition of pluripotential embryonic stem cell differentiation by purified polypeptides. Nature. 1988;336(6200):688-90.

40. Williams RL, Hilton DJ, Pease S, Willson TA, Stewart CL, Gearing DP, et al. Myeloid leukaemia inhibitory factor maintains the developmental potential of embryonic stem cells. Nature. 1988;336(6200):684-7.

41. Gearing D.P. TCJ, VandenBos T., Gimpel S.D., Delaney P.B., King J., Price V., Cosman D., Beckman M.P. Leukemia inhibitory factor receptor is structurally related to the Il-6 signal transducer, gp130. EMBO J 1991;10:2839–48.

42. Davis S, Aldrich TH, Stahl N, Pan L, Taga T, Kishimoto T, et al. LIFR beta and gp130 as heterodimerizing signal transducers of the tripartite CNTF receptor. Science. 1993 June 18, 1993;260(5115):1805-8.

43. Minami M, Inoue M, Wei S, Takeda K, Matsumoto M, Kishimoto T, et al. STAT3 activation is a critical step in gp130-mediated terminal differentiation and growth arrest of a myeloid cell line. Proceedings of the National Academy of Sciences of the United States of America. 1996 April 30, 1996;93(9):3963-6.

44. K Nakajima YY, K Nakae, H Kojima, M Ichiba, N Kiuchi, T Kitaoka, T Fukada, M Hibi, and T Hirano. A central role for Stat3 in IL-6-induced regulation of growth and differentiation in M1 leukemia cells. EMBO J. 1996;15(14):3651–8.

45. Niwa H, Burdon T, Chambers I, Smith A. Self-renewal of pluripotent embryonic stem cells is mediated via activation ofâ€‰STAT3. Genes & Development. 1998 July 1, 1998;12(13):2048-60.

46. Raz R, Lee C-K, Cannizzaro LA, dâ€™Eustachio P, Levy DE. Essential role of STAT3 for embryonic stem cell pluripotency. Proceedings of the National Academy of Sciences of the United States of America. 1999 March 16, 1999;96(6):2846-51.

47. Scholer HR, Ruppert S, Suzuki N, Chowdhury K, Gruss P. New type of POU domain in germ line-specific protein Oct-4. Nature. 1990;344(6265):435-9.

48. Mitsui K, Tokuzawa Y, Itoh H, Segawa K, Murakami M, Takahashi K, et al. The Homeoprotein Nanog Is Required for Maintenance of Pluripotency in Mouse Epiblast and ES Cells. Cell. 2003;113(5):631-42.

49. Loh Y-H, Wu Q, Chew J-L, Vega VB, Zhang W, Chen X, et al. The Oct4 and Nanog transcription network regulates pluripotency in mouse embryonic stem cells. Nat Genet. 2006;38(4):431-40.

50. Maurizio P, Hans RS. 'Oct-4': Gatekeeper in the Beginnings of Mammalian Development. Stem Cells. 2001;19(4):271-8.

51. Zandstra PW, Le HV, Daley GQ, Griffith LG, Lauffenburger DA. Leukemia inhibitory factor (LIF) concentration modulates embryonic stem cell self-renewal and differentiation independently of proliferation. Biotechnology and Bioengineering. 2000;69(6):607-17.

52. http://stemcells.nih.gov/info/2001report/appendixB.asp.

53. Todd HDaPW. Surface morphology of trypsinized human cells in vitro. *Expetl Cell Res*. 1971;66:353-61.

54. Weinstein D. Comparison of pronase and trypsin for detachment of human cells during serial cultivation. Experimental Cell Research. 1966;43(1):234-6.

55. Waymouth C. To disaggregate or not to disaggregate, injury and cell disaggregation, transient or permanent? In Vitro Cellular & Developmental Biology - Plant. 1974;10(1):97-111.

56. Allen CSaA. The release of radioactive nucleic acids and mucoproteins by trypsin and ethylenediaminetetra-acetate treatment of baby-hamster cells in tissue culture. Biochem J. 1970;119(4):707-14.

57. Howard LH, Richard CS. Changes in ribosome-polyribosome balances in chick muscle cells during tissue dissociation, development in culture, and exposure to simplified culture-medium. Journal of Cellular Physiology. 1971;77(2):145-55.

58. Noriko Y, Teruo O, Hideaki S, Fumiko K, Yoshio S, Yasuhisa S. Thermo-responsive polymeric surfaces; control of attachment and detachment of cultured cells. Die Makromolekulare Chemie, Rapid Communications. 1990;11(11):571-6.

59. Folkman J, Moscona A. Role of cell shape in growth control. Nature. 1978;273(5661):345-9.

60. Ben-Ze'ev A, Robinson GS, Bucher NL, Farmer SR. Cell-cell and cell-matrix interactions differentially regulate the expression of hepatic and cytoskeletal genes in primary cultures of rat hepatocytes. Proceedings of the National Academy of Sciences of the United States of America. 1988 April 1988;85(7):2161-5.

61. Mitjavila-Garcia MT, Simonin C, Peschanski M. Embryonic stem cells: Meeting the needs for cell therapy. Advanced Drug Delivery Reviews. 2005;57(13):1935-43.

62. Chafika D, Pauline L, Kevin MS, Morgan RA. Comparison of Primary Rat Hepatocyte Attachment to Collagen and Plasma-Polymerised Allylamine on Glass. Plasma Processes and Polymers. 2006;3(6-7):474-84.

63. Barry JJA, Silva MMCG, Shakesheff KM, Howdle SM, Alexander MR. Using Plasma Deposits to Promote Cell Population of the Porous Interior of Three-Dimensional Poly(D,L-Lactic Acid) Tissue-Engineering Scaffolds. Advanced Functional Materials. 2005;15(7):1134-40.

64. Eves PC, Beck AJ, Shard AG, Mac Neil S. A chemically defined surface for the co-culture of melanocytes and keratinocytes. Biomaterials. 2005;26(34):7068-81.

65. Rimmer S, Johnson C, Zhao B, Collier J, Gilmore L, Sabnis S, et al. Epithelialization of hydrogels achieved by amine functionalization and co-culture with stromal cells. Biomaterials. 2007;28(35):5319-31.

66. Zelzer M, Majani R, Bradley JW, Rose FRAJ, Davies MC, Alexander MR. Investigation of cell-surface interactions using chemical gradients formed from plasma polymers. Biomaterials. 2008;29(2):172-84.

67. Buddy DR, Thomas H, Allan SH, Stephen DH. Cell adhesion to polymeric materials: Implications with respect to biocompatibility. Journal of Biomedical Materials Research. 1975;9(5):407-22.

68. McAuslan BR, Johnson G. Cell responses to biomaterials I: Adhesion and growth of vascular endothelial cells on poly(hydroxyethyl methacrylate) following surface modification by hydrolytic etching. Journal of Biomedical Materials Research. 1987;21(7):921-35.

69. Rein V. Ulijn NB, Vineetha Jayawarna, Paul D. Thornton, Simon J. Todd, Robert J. Mart, Andrew M. Smith, and, Gough JE. Bioresponsive hydrogels. Materials today. 2007;10(4):40-8.

70. Simon J. Todd DF, Julie E. Gough and Rein V. Ulijn. Enzyme-triggered cell attachment to hydrogel surfaces. Soft Matter. 2007;3:547-50.

71. Todd SJ, Scurr DJ, Gough JE, Alexander MR, Ulijn RV. Enzyme-Activated RGD Ligands on Functionalized Poly(ethylene glycol) Monolayers: Surface Analysis and Cellular Response. Langmuir. 2009;25(13):7533-9.

72. Nakayama Y, Furumoto A, Kidoaki S, Matsuda T. Photocontrol of Cell Adhesion and Proliferation by a Photoinduced Cationic Polymer Surface. Photochemistry and Photobiology. 2003;77(5):480-6.

73. Yuichi T, Kimio S, Mitsuyoshi K, Katsuhide O, Toshiyuki T, Toshiyuki K, et al. Development of a photoresponsive cell culture surface: Regional enhancement of living-cell adhesion induced by local light irradiation. Journal of Applied Polymer Science. 2006;100(1):495-9.

74. Edahiro J-i, Sumaru K, Tada Y, Ohi K, Takagi T, Kameda M, et al. In Situ Control of Cell Adhesion Using Photoresponsive Culture Surface. Biomacromolecules. 2005;6(2):970-4.

75. Gil ES, Hudson SM. Stimuli-reponsive polymers and their bioconjugates. Progress in Polymer Science. 2004;29(12):1173-222.

76. Schild HG. Poly (N-isopropylacrylamide): experiment, theory, and application. Prog Polym Sci. 1992;17:163-249

77. Carolina de las Heras A, Sivanand P, Cameron A. Stimuli Responsive Polymers for Biomedical Applications. ChemInform. 2005;36(26).

78. Neff JA, Tresco PA, Caldwell KD. Surface modification for controlled studies of cell-ligand interactions. Biomaterials. 1999;20(23-24):2377-93.

79. Vats A, Tolley NS, Polak JM, Gough JE. Scaffolds and biomaterials for tissue engineering: a review of clinical applications. Clinical Otolaryngology & Allied Sciences. 2003;28(3):165-72.

80. Teruo O, Noriko Y, Hideaki S, Yasuhisa S. A novel recovery system for cultured cells using plasma-treated polystyrene dishes grafted with poly(N-isopropylacrylamide). Journal of Biomedical Materials Research. 1993;27(10):1243-51.

81. Ai K, Masayuki Y, Chie K, Akihiko K, Yasuhisa S, Teruo O. Decrease in culture temperature releases monolayer endothelial cell sheets together with deposited fibronectin matrix from temperature-responsive culture surfaces. Journal of Biomedical Materials Research. 1999;45(4):355-62.

82. Masami H, Masayuki Y, Motohiro H, Chie T, Yuki I, Akihiko K, et al. Novel approach for achieving double-layered cell sheets co-culture: overlaying endothelial cell sheets onto monolayer hepatocytes utilizing temperature-responsive culture dishes. Journal of Biomedical Materials Research. 2002;62(3):464-70.

83. Ista LK, López GP. Lower critical solubility temperature materials as biofouling release agents. Journal of Industrial Microbiology and Biotechnology. 1998;20(2):121-5.

84. Cunliffe D, Smart CA, Tsibouklis J, Young S, Alexander C, Vulfson EN. Bacterial adsorption to thermoresponsive polymer surfaces. Biotechnology Letters. 2000;22(2):141-5.

85. Yang J, Yamato M, Kohno C, Nishimoto A, Sekine H, Fukai F, et al. Cell sheet engineering: Recreating tissues without biodegradable scaffolds. Biomaterials. 2005;26(33):6415-22.

86. Yang J, Yamato M, Nishida K, Ohki T, Kanzaki M, Sekine H, et al. Cell delivery in regenerative medicine: The cell sheet engineering approach. Journal of Controlled Release. 2006;116(2):193-203.

87. Pellegrini G, Traverso CE, Franzi AT, Zingirian M, Cancedda R, De Luca M. Long-term restoration of damaged corneal surfaces with autologous cultivated corneal epithelium. The Lancet. 1997;349(9057):990-3.

88. Shimazaki J, Aiba M, Goto E, Kato N, Shimmura S, Tsubota K. Transplantation of human limbal epithelium cultivated on amniotic membrane for the treatment of severe ocular surface disorders. Ophthalmology. 2002;109(7):1285-90.

89. Han BDVMMS, Schwab IRMD, Madsen TKBS, Isseroff RRMD. A Fibrin-based Bioengineered Ocular Surface With Human Corneal Epithelial Stem Cells. . Cornea. 2002;21(5):505-10.

90. Nishida K, Yamato M, Hayashida Y, Watanabe K, Maeda N, Watanabe H, et al. Functional bioengineered corneal epithelial sheet grafts from corneal stem cells expanded ex vivo on a temperature-responsive cell culture surface. Transplantation. 2004;77(3):379-85.

91. Sumide T, Nishida K, Yamato M, Ide T, Hayashida Y, Watanabe K, et al. Functional human corneal endothelial cell sheets harvested from temperature-responsive culture surfaces. FASEB J. 2005 December 9, 2005:04-3035fje.

92. Shimizu T, Sekine H, Isoi Y, Yamato M, Kikuchi A, Okano T. Long-Term Survival and Growth of Pulsatile Myocardial Tissue Grafts Engineered by the Layering of Cardiomyocyte Sheets. Tissue Engineering. 2006;12(3):499-507.

93. Sumanasinghe RD, Bernacki SH, Loboa EG. Osteogenic Differentiation of Human Mesenchymal Stem Cells in Collagen Matrices: Effect of Uniaxial Cyclic Tensile Strain on Bone Morphogenetic Protein (BMP-2) mRNA Expression. Tissue Engineering. 2006;12(12):3459-65.

94. Lorenz M, Vassilis K, Sandra H, Robert F, Brian S, Chunmei L, et al. Engineering bone-like tissue <I>in vitro</I> using human bone marrow stem cells and silk scaffolds. Journal of Biomedical Materials Research Part A. 2004;71A(1):25-34.

95. Battista S, Guarnieri D, Borselli C, Zeppetelli S, Borzacchiello A, Mayol L, et al. The effect of matrix composition of 3D constructs on embryonic stem cell differentiation. Biomaterials. 2005;26(31):6194-207.

96. Liu H, Collins SF, Suggs LJ. Three-dimensional culture for expansion and differentiation of mouse embryonic stem cells. Biomaterials. 2006;27(36):6004-14.

97. Konno T, Kawazoe N, Chen G, Ito Y. Culture of Mouse Embryonic Stem Cells on Photoimmobilized Polymers. The Society for Biotechnology, Japan. 2006;102(4):304-10.

98. Harrison J, Pattanawong S, Forsythe JS, Gross KA, Nisbet DR, Beh H, et al. Colonization and maintenance of murine embryonic stem cells on poly([alpha]-hydroxy esters). Biomaterials. 2004;25(20):4963-70.

99. Sharon G-N, Smadar C, Joseph I-E. Bioreactor cultivation enhances the efficiency of human embryoid body (hEB) formation and differentiation. Biotechnology and Bioengineering. 2004;86(5):493-502.

100. Levenberg S, Huang NF, Lavik E, Rogers AB, Itskovitz-Eldor J, Langer R. Differentiation of human embryonic stem cells on three-dimensional polymer scaffolds. Proceedings of the National Academy of Sciences of the United States of America. 2003 October 28, 2003;100(22):12741-6.

101. Levenberg S, Burdick JA, Kraehenbuehl T, Langer R. Neurotrophin-Induced Differentiation of Human Embryonic Stem Cells on Three-Dimensional Polymeric Scaffolds. Tissue Engineering. 2005;11(3-4):506-12.

102. Yao S, Chen S, Clark J, Hao E, Beattie GM, Hayek A, et al. Long-term self-renewal and directed differentiation of human embryonic stem cells in chemically defined conditions. 2006 May 2, 2006;103(18):6907-12.

103. Miyazaki T, Futaki S, Hasegawa K, Kawasaki M, Sanzen N, Hayashi M, et al. Recombinant human laminin isoforms can support the undifferentiated growth of human embryonic stem cells. Biochemical and Biophysical Research Communications. 2008;375(1):27-32.

104. Stefan RB, Laura Z, Sandy L, Dorien Ward-van O, Stieneke van den B, Linda van L, et al. Recombinant Vitronectin Is a Functionally Defined Substrate That Supports Human Embryonic Stem Cell Self-Renewal via alphaVbeta5 Integrin. Stem Cells. 2008;26(9):2257-65.

105. Wondimu Z, Gorfu G, Kawataki T, Smirnov S, Yurchenco P, Tryggvason K, et al. Characterization of commercial laminin preparations from human placenta in comparison to recombinant laminins 2 ([alpha]2[beta]1[gamma]1), 8 ([alpha]4[beta]1[gamma]1), 10 ([alpha]5[beta]1[gamma]1). Matrix Biology. 2006;25(2):89-93.

106. Bigdeli N, Andersson M, Strehl R, Emanuelsson K, Kilmare E, Hyllner J, et al. Adaptation of human embryonic stem cells to feeder-free and matrix-free culture conditions directly on plastic surfaces. Journal of Biotechnology. 2008;133(1):146-53.

107. Magdalena MM, David A, James SS, Roger M, Maria DBM, Lee DB, et al. Maintenance of pluripotency in human embryonic stem cells cultured on a synthetic substrate in conditioned medium. Biotechnology and Bioengineering.105(1):130-40.

108. Kolhar P, Kotamraju VR, Hikita ST, Clegg DO, Ruoslahti E. Synthetic surfaces for human embryonic stem cell culture. Journal of Biotechnology.146(3):143-6.

109. Dang JM, Sun DDN, Shin-Ya Y, Sieber AN, Kostuik JP, Leong KW. Temperature-responsive hydroxybutyl chitosan for the culture of mesenchymal stem cells and intervertebral disk cells. Biomaterials. 2006;27(3):406-18.

110. Xian Jun L, Jiansheng G, Makoto S, Takashi K, Mingzhe L, Jun L, et al. Surface Coating with a Thermoresponsive Copolymer for the Culture and Non-Enzymatic Recovery of Mouse Embryonic Stem Cells. Macromolecular Bioscience. 2009;9(11):1069-79.

111. Wobus AM, Boheler KR. Embryonic Stem Cells: Prospects for Developmental Biology and Cell Therapy. Physiol Rev. 2005 April 1, 2005;85(2):635-78.

112. Hentze H, Graichen R, Colman A. Cell therapy and the safety of embryonic stem cell-derived grafts. Trends in Biotechnology. 2007;25(1):24-32.

113. Han S, Hagiwara M, Ishizone T. Synthesis of thermally sensitive water-soluble polymethacrylates by living anionic polymerizations of oligo(ethylene glycol) methyl ether methacrylates. Macromolecules. 2003 Nov 4;36(22):8312-9.

114. Mertoglu M, Garnier S, Laschewsky A, Skrabania K, Storsberg J. Stimuli responsive amphiphilic block copolymers for aqueous media synthesised via reversible addition fragmentation chain transfer polymerisation (RAFT). Polymer. 2005 Aug 23;46(18):7726-40.

115. Brown AA, Khan NS, Steinbock L, Huck WTS. Synthesis of oligo(ethylene glycol) methacrylate polymer brushes. European Polymer Journal. 2005 Aug;41(8):1757-65.

116. Duncan R. The dawning era of polymer therapeutics. Nature Reviews Drug Discovery. 2003 May;2(5):347-60.

117. Lutz JF, Hoth A. Preparation of ideal PEG analogues with a tunable thermosensitivity by controlled radical copolymerization of 2-(2-methoxyethoxy)ethyl methacrylate and oligo(ethylene glycol) methacrylate. Macromolecules. 2006 Jan 24;39(2):893-6.

118. Lutz JF, Akdemir O, Hoth A. Point by point comparison of two thermosensitive polymers exhibiting a similar LCST: Is the age of poly(NIPAM) over? Journal of the American Chemical Society. 2006 Oct 11;128(40):13046-7.

119. Zhou F, Huck WTS. Surface grafted polymer brushes as ideal building blocks for "smart" surfaces. Physical Chemistry Chemical Physics. 2006;8(33):3815-23.

120. Jonas AM, Glinel K, Oren R, Nysten B, Huck WTS. Thermo-responsive polymer brushes with tunable collapse temperatures in the physiological range. Macromolecules. 2007 Jun 26;40(13):4403-5.

121. Alexander MR, Whittle JD, Barton D, Short RD. Plasma polymer chemical gradients for evaluation of surface reactivity: epoxide reaction with carboxylic acid surface groups. Journal of Materials Chemistry. 2004;14(3):408-12.

122. Siow KS, Britcher L, Kumar S, Griesser HJ. Plasma methods for the generation of chemically reactive surfaces for biomolecule immobilization and cell colonization - A review. Plasma Processes and Polymers. 2006 Aug 15;3(6-7):392-418.

123. Richards. RALJaRW. Polymers at surfaces and interfaces Cambridge University Press, Cambridge; 1999.

124. G. J. Fleer MACS, J. M. H. M. Scheutjens, T. Cosgrove, B. Vincent. Polymers at interfaces: Chapman & Hall, London; 1993.

125. K. Norrman AG-SaNBL. 6 Studies of spin-coated polymer films. Annu Rep Prog Chem, Sect C: Phys Chem. 2005;101:174 - 201.

126. David B. Hall PU, John M. Torkelson. Spin coating of thin and ultrathin polymer films. Polymer engineering and science. 1998;38(12).

127. Callewaert M, Gohy J-F, Dupont-Gillain CC, Boulangé-Petermann L, Rouxhet PG. Surface morphology and wetting properties of surfaces coated with an amphiphilic diblock copolymer. Surface Science. 2005;575(1-2):125-35.

128. K. Mathauer FEaGWIGA, Editor,. Comprehensive Polymer Science. The Synthesis, Characterizations, Reactions and Applications of Polymers: Pergamon Press, Oxford 1992.

129. William JB, Sergiy M. A structural definition of polymer brushes. Journal of Polymer Science Part A: Polymer Chemistry. 2007;45(16):3505-12.

130. Milner ST. Polymer Brushes. Science. 1991 Feb 22;251(4996):905-14.

131. Ji H, De Gennes PG. Adhesion via connector molecules: the many-stitch problem. Macromolecules. 1993;26(3):520-5.

132. Raphael E, De Gennes PG. Rubber-rubber adhesion with connector molecules. The Journal of Physical Chemistry. 1992;96(10):4002-7.

133. Fournier E, Passirani C, Montero-Menei CN, Benoit JP. Biocompatibility of implantable synthetic polymeric drug carriers: focus on brain biocompatibility. Biomaterials. 2003 Aug;24(19):3311-31.

134. Petr H. Hydrophilisation of silicone rubber for medical applications. Polym Int. 2003;52:1531-9.

135. Amiji M, Park K. Surface modification of polymeric biomaterials with poly(ethylene oxide), albumin, and heparin for reduced thrombogenicity. J Biomater Sci Polym Ed. 1993;4(3):217-34.

136. Joanny JF. Lubrication by molten polymer brushes. Langmuir. 1992;8(3):989-95.

137. Roosjen A, Kaper HJ, van der Mei HC, Norde W, Busscher HJ. Inhibition of adhesion of yeasts and bacteria by poly(ethylene oxide)-brushes on glass in a parallel plate flow chamber. Microbiology. 2003 Nov;149(Pt 11):3239-46.

138. Norde W, Gage D. Interaction of bovine serum albumin and human blood plasma with PEO-tethered surfaces: influence of PEO chain length, grafting density, and temperature. Langmuir. 2004 May 11;20(10):4162-7.

139. Nejadnik MR, van der Mei HC, Norde W, Busscher HJ. Bacterial adhesion and growth on a polymer brush-coating. Biomaterials. 2008 Oct;29(30):4117-21.

140. Causa F, Netti PA, Ambrosio L. A multi-functional scaffold for tissue regeneration: The need to engineer a tissue analogue. Biomaterials. 2007;28(34):5093-9.

141. Letsche S, Steinbach A, Pluntke M, Marti O, Ignatius A, Volkmer D. Usage of polymer brushes as substrates of bone cells. Frontiers of Materials Science in China. 2009;3(2):132-44.

142. Ma PX. Biomimetic materials for tissue engineering. Adv Drug Deliv Rev. 2008 Jan 14;60(2):184-98.

143. Vats A, Tolley NS, Polak JM, Gough JE. Scaffolds and biomaterials for tissue engineering: a review of clinical applications. Clin Otolaryngol Allied Sci. 2003 Jun;28(3):165-72.

144. Neff JA, Tresco PA, Caldwell KD. Surface modification for controlled studies of cell-ligand interactions. Biomaterials. 1999 Dec;20(23-24):2377-93.

145. Hersel U, Dahmen C, Kessler H. RGD modified polymers: biomaterials for stimulated cell adhesion and beyond. Biomaterials. 2003 Nov;24(24):4385-415.

146. Noiset O, Schneider YJ, Marchand-Brynaert J. Adhesion and growth of CaCo2 cells on surface-modified PEEK substrata. J Biomater Sci Polym Ed. 2000;11(7):767-86.

147. Harris BP, Kutty JK, Fritz EW, Webb CK, Burg KJ, Metters AT. Photopatterned polymer brushes promoting cell adhesion gradients. Langmuir. 2006 May 9;22(10):4467-71.

148. Alexander C, Shakesheff KM. Responsive Polymers at the Biology/Materials Science Interface. Advanced Materials. 2006;18(24):3321 - 8.

149. Drotleff S, Lungwitz U, Breunig M, Dennis A, Blunk T, Tessmar J, et al. Biomimetic polymers in pharmaceutical and biomedical sciences. European Journal of Pharmaceutics and Biopharmaceutics. 2004;58(2):385-407.

150. Goessl A, Tirelli N, Hubbell JA. A hydrogel system for stimulus-responsive, oxygen-sensitive in situ gelation. Journal of Biomaterials Science, Polymer Edition. 2004;15:895-904.

151. Napoli A, Valentini M, Tirelli N, Muller M, Hubbell JA. Oxidation-responsive polymeric vesicles. Nat Mater. 2004;3(3):183-9.

152. de Las Heras Alarcon C, Pennadam S, Alexander C. Stimuli responsive polymers for biomedical applications. Chem Soc Rev. 2005 Mar;34(3):276-85.

153. Mendes PM. Stimuli-responsive surfaces for bio-applications. Chemical Society Reviews. 2008;37(11):2512-29.

154. El-Sayed MEH, Hoffman AS, Stayton PS. Erratum to "Rational design of composition and activity correlations for pH-sensitive and glutathione-reactive polymer therapeutics" [J. Control. Release 101 (1-3) (2005) 47-58]. Journal of Controlled Release. 2005;104(2):415-.

155. Liu S, Armes SP. Synthesis and Aqueous Solution Behavior of a pH-Responsive Schizophrenic Diblock Copolymer. Langmuir. 2003;19(10):4432-8.

156. Liu S, Weaver JVM, Save M, Armes SP. Synthesis of pH-Responsive Shell Cross-Linked Micelles and Their Use as Nanoreactors for the Preparation of Gold Nanoparticles. Langmuir. 2002;18(22):8350-7.

157. Sumaru K, Ohi K, Takagi T, Kanamori T, Shinbo T. Photoresponsive Properties of Poly(N-isopropylacrylamide) Hydrogel Partly Modified with Spirobenzopyran. Langmuir. 2006;22(9):4353-6.

158. Advincula RCB, William J. Caster, Kenneth C. Rühe, Jürgen Polymer brushes: Synthesis, Characterization, Applications: Wiley-VCH; 2004.

159. Milner ST, Witten TA, Cates ME. Theory of the grafted polymer brush. Macromolecules. 1988;21(8):2610-9.

160. Alexander S. Adsorption of chain molecules with a polar head a scaling description. J Phys France. 1977;38(8):983-7.

161. Guzonas D, Hair ML, Cosgrove T. Adsorption of block copolymers from nonselective solvent. Macromolecules. 1992;25(10):2777-9.

162. Parsonage E, Tirrell M, Watanabe H, Nuzzo RG. Adsorption of poly(2-vinylpyridine)-poly (styrene) block copolymers from toluene solutions. Macromolecules. 1987;24(8):1987-95.

163. Mansky P, Liu Y, Huang E, Russell TP, Hawker C. Controlling Polymer-Surface Interactions with Random Copolymer Brushes. Science. 1997 March 7, 1997;275(5305):1458-60.

164. Koutsos V, van der Vegte EW, Hadziioannou G. Direct View of Structural Regimes of End-Grafted Polymer Monolayers: A Scanning Force Microscopy Study. Macromolecules. 1999;32(4):1233-6.

165. Koutsos V, van der Vegte EW, Pelletier E, Stamouli A, Hadziioannou G. Structure of Chemically End-Grafted Polymer Chains Studied by Scanning Force Microscopy in Bad-Solvent Conditions. Macromolecules. 1997;30(16):4719-26.

166. Tran Y, Auroy P. Synthesis of Poly(styrene sulfonate) Brushes. Journal of the American Chemical Society. 2001;123(16):3644-54.

167. Minko S, Muller M, Motornov M, Nitschke M, Grundke K, Stamm M. Two-Level Structured Self-Adaptive Surfaces with Reversibly Tunable Properties. Journal of the American Chemical Society. 2003;125(13):3896-900.

168. Sumerlin BS, Lowe AB, Stroud PA, Zhang P, Urban MW, McCormick CL. Modification of Gold Surfaces with Water-Soluble (Co)polymers Prepared via Aqueous Reversible Additionâ^'Fragmentation Chain Transfer (RAFT) Polymerizationâ€ Langmuir. 2003;19(14):5559-62.

169. Biesalski M, Ruhe J. Synthesis of a Poly(p-styrenesulfonate) Brush via Surface-Initiated Polymerization. Macromolecules. 2003;36(4):1222-7.

170. Biesalski M, Johannsmann D, Ruhe J. Synthesis and swelling behavior of a weak polyacid brush. The Journal of Chemical Physics. 2002;117(10):4988-94.

171. Christophe D, Christine J, Michael C, Pierre L, Robert J. Combination of Electrografting and Ring-Opening Metathesis Polymerization: An Efficient Way to Prepare Polynorbornene Brushes on Conducting Substrates. Angew Chem Int Ed. 2001;40:1268-71.

172. Moon JH, Swager TM. Poly(p-phenylene ethynylene) Brushes. Macromolecules. 2002;35(16):6086-9.

173. Wieringa RH, Siesling EA, Geurts PFM, Werkman PJ, Vorenkamp EJ, Erb V, et al. Surface Grafting of Poly(l-glutamates). 1. Synthesis and Characterization. Langmuir. 2001;17(21):6477-84.

174. Baum M, Brittain WJ. Synthesis of Polymer Brushes on Silicate Substrates via Reversible Addition Fragmentation Chain Transfer Technique. Macromolecules. 2002;35(3):610-5.

175. Hu T, You Y, Pan C, Wu C. The Coil-to-Globule-to-Brush Transition of Linear Thermally Sensitive Poly(N-isopropylacrylamide) Chains Grafted on a Spherical Microgel. The Journal of Physical Chemistry B. 2002;106(26):6659-62.

176. Marion KB, Armido S. Polymer Brushes by Nitroxide-Mediated Polymerization. Macromolecular Rapid Communications. 2009;30(13):1043-57.

177. Balamurugan S, Mendez S, Balamurugan SS, O'Brie MJ, Lopez GP. Thermal Response of Poly(N-isopropylacrylamide) Brushes Probed by Surface Plasmon Resonance. Langmuir. 2003;19(7):2545-9.

178. Ejaz M, Yamamoto S, Ohno K, Tsujii Y, Fukuda T. Controlled Graft Polymerization of Methyl Methacrylate on Silicon Substrate by the Combined Use of the Langmuirâ^'Blodgett and Atom Transfer Radical Polymerization Techniques. Macromolecules. 1998;31(17):5934-6.

179. Kim J-B, Huang W, Bruening ML, Baker GL. Synthesis of Triblock Copolymer Brushes by Surface-Initiated Atom Transfer Radical Polymerization. Macromolecules. 2002;35(14):5410-6.

180. von Werne TA, Germack DS, Hagberg EC, Sheares VV, Hawker CJ, Carter KR. A Versatile Method for Tuning the Chemistry and Size of Nanoscopic Features by Living Free Radical Polymerization. Journal of the American Chemical Society. 2003;125(13):3831-8.

181. Matyjaszewski K, Qin S, Boyce JR, Shirvanyants D, Sheiko SS. Effect of Initiation Conditions on the Uniformity of Three-Arm Star Molecular Brushes. Macromolecules. 2003;36(6):1843-9.

182. Jeffrey P, Tomasz K, Krzysztof M. Synthesis of Polymer Brushes Using Atom Transfer Radical Polymerization. Macromolecular Rapid Communications. 2003;24(18):1043-59.

183. Matyjaszewski K, Dong H, Jakubowski W, Pietrasik J, Kusumo A. Grafting from Surfaces for "Everyone": ARGET ATRP in the Presence of Air. Langmuir. 2007;23(8):4528-31.

184. Matyjaszewski K. Radical Nature of Cu-Catalyzed Controlled Radical Polymerizations (Atom Transfer Radical Polymerization). Macromolecules. 1998;31(15):4710-7.

185. Xia J, Gaynor SG, Matyjaszewski K. Controlled Living Radical Polymerization. Atom Transfer Radical Polymerization of Acrylates at Ambient Temperature. Macromolecules. 1998;31(17):5958-9.

186. Veerle Coessens TPaKM. Functional polymers by atom transfer radical polymerization. Progress in Polymer Science. 2001;26(3):337-77.

187. Kurosawa S, Aizawa H, Talib ZA, Atthoff B, Hilborn J. Synthesis of tethered-polymer brush by atom transfer radical polymerization from a plasma-polymerized-film-coated quartz crystal microbalance and its application for immunosensors. Biosensors and Bioelectronics. 2004;20(6):1165-76.

188. Yasuda HK. Plasma Polymerisation Academic Press, London; 1985.

189. Beck AJ, Jones FR, Short RD. Plasma copolymerization as a route to the fabrication of new surfaces with controlled amounts of specific chemical functionality. Polymer. 1996;37(24):5537-9.

190. Ameen AP, Short RD, Ward RJ. The formation of high surface concentrations of hydroxyl groups in the plasma polymerization of allyl alcohol. Polymer. 1994;35(20):4382-91.

191. Short LOTaRD. An investigation of the mechanisms of plasma polymerisation of allyl alcohol. J Chem Soc, Faraday Trans. 1997;93(6):1141 - 5.

192. France RM, Short RD, Duval E, Jones FR, Dawson RA, MacNeil S. Plasma Copolymerization of Allyl Alcohol/1,7-Octadiene: Surface Characterization and Attachment of Human Keratinocytes. Chemistry of Materials. 1998;10(4):1176-83.

193. Seah MP, Spencer SJ. Ultrathin SiO2 on Si II. Issues in quantification of the oxide thickness. Surface and Interface Analysis. 2002;33(8):640-52.

194. Seah MP, Spencer SJ. Ultrathin SiO[sub 2] on Si. I. Quantifying and removing carbonaceous contamination. Journal of Vacuum Science & Technology A: Vacuum, Surfaces, and Films. 2003;21(2):345-52.

195. S. Tanuma CJPaDRP. Calculations of electorn inelastic mean free paths. II. Data for 27 elements over the 50-2000 eV range. Surface and Interface Analysis. 1991;17:911-26.

196. Erik W, Katja U, Andreas L, Hans GB, André L, Claus D, et al. Controlled Cell Adhesion on PEG-Based Switchable Surfaces13. Angewandte Chemie International Edition. 2008;47(30):5666-8.

197. Oran U, Swaraj S, Friedrich JF, Unger WES. Static ToF-SIMS analysis of plasma chemically deposited ethylene/allyl alcohol co-polymer films. Applied Surface Science. 2006;252(19):6588-90.

198. Tsourapas G, Rutten FJM, Briggs D, Davies MC, Shakesheff KM. Surface spectroscopic imaging of PEG-PLA tissue engineering constructs with ToF-SIMS. Applied Surface Science. 2006;252(19):6693-6.

199. Veiseh M, Wickes BT, Castner DG, Zhang M. Guided cell patterning on gold-silicon dioxide substrates by surface molecular engineering. Biomaterials. 2004;25(16):3315-24.

200. Lutz JF, Weichenhan K, Akdemir O, Hoth A. About the phase transitions in aqueous solutions of thermoresponsive copolymers and hydrogels based on 2-(2-methoxyethoxy)ethyl methacrylate and oligo(ethylene glycol) methacrylate. Macromolecules. 2007 Apr 3;40(7):2503-8.

201. Jones DM, Smith JR, Huck WTS, Alexander C. Variable adhesion of micropatterned thermoresponsive polymer brushes: AFM investigations of poly (N-isopropylacrylamide) brushes prepared by surface-initiated polymerizations. Advanced Materials. 2002 Aug 16;14(16):1130-4.

202. Kessel S, Schmidt S, Muller R, Wischerhoff E, Laschewsky A, Lutz J-F, et al. Thermoresponsive PEG-Based Polymer Layers: Surface Characterization with AFM Force Measurements. Langmuir. 2009;26(5):3462-7.

203. Agashi K, Chau DYS, Shakesheff KM. The effect of delivery via narrow-bore needles on mesenchymal cells. Regenerative Medicine. 2009;4(1):49-64.

204. Lerouge S, Fozza AC, Wertheimer MR, Marchand R, Yahia LH. Sterilization by Low-Pressure Plasma: The Role of Vacuum-Ultraviolet Radiation. Plasmas and Polymers. 2000;5(1):31-46.

205. Mata A, Fleischman A, Roy S. Characterization of Polydimethylsiloxane (PDMS) Properties for Biomedical Micro/Nanosystems. Biomedical Microdevices. 2005;7(4):281-93.

206. Tsukasa M, Kotaro H, Osamu N. WAVELENGTH DEPENDENT FORMATION OF THYMINE DIMERS AND (6-4)PHOTOPRODUCTS IN DNA BY MONOCHROMATIC ULTRAVIOLET LIGHT RANGING FROM 150 TO 365 nm. Photochemistry and Photobiology. 1991;54(3):403-10.

207. Martin TM, William MC, Irina S, Alexander G, Yuri R. Cell growth and detachment from protein-coated PNIPAAm-based copolymers. Journal of Biomedical Materials Research Part A. 2007;81A(4):870-6.

208. Takezawa T, Mori Y, Yoshizato K. Cell Culture on a Thermo-Responsive Polymer Surface. Nat Biotech. 1990;8(9):854-6.

209. Okano T, Yamada N, Okuhara M, Sakai H, Sakurai Y. Mechanism of cell detachment from temperature-modulated, hydrophilic-hydrophobic polymer surfaces. Biomaterials. 1995;16(4):297-303.

210. Canavan HE, Cheng X, Graham DJ, Ratner BD, Castner DG. Surface Characterization of the Extracellular Matrix Remaining after Cell Detachment from a Thermoresponsive Polymer. Langmuir. 2004;21(5):1949-55.

211. Khor HL, Ng KW, Schantz JT, Phan T-T, Lim TC, Teoh SH, et al. Poly(-caprolactone) films as a potential substrate for tissue engineering an epidermal equivalent. Materials Science and Engineering: C. 2002;20(1-2):71-5.

212. Serrano MC, Pagani R, Vallet-Regí M, Peña J, Rámila A, Izquierdo I, et al. In vitro biocompatibility assessment of poly([]-caprolactone) films using L929 mouse fibroblasts. Biomaterials. 2004;25(25):5603-11.

213. Mitra SK, Hanson DA, Schlaepfer DD. Focal adhesion kinase: in command and control of cell motility. Nat Rev Mol Cell Biol. 2005;6(1):56-68.

214. Wu J-Y, Liu S-Q, Heng PW-S, Yang Y-Y. Evaluating proteins release from, and their interactions with, thermosensitive poly (N-isopropylacrylamide) hydrogels. Journal of Controlled Release. 2005;102(2):361-72.

215. Bianco-Peled H, Gryc S. Binding of Amino Acids to Smart Sorbents: Where Does Hydrophobicity Come into Play? Langmuir. 2003;20(1):169-74.

216. Robertson RP. Islet transplantation: travels up the learning curve. Curr Diab Rep. 2002 Aug;2(4):365-70.

217. Lindvall O, Kokaia Z, Martinez-Serrano A. Stem cell therapy for human neurodegenerative disorders-how to make it work. Nat Med. 2004 Jul;10 Suppl:S42-50.

218. Di Campli C, Nestola M, Piscaglia AC, Santoliquido A, Gasbarrini G, Pola P, et al. Cell-based therapy for liver diseases. Eur Rev Med Pharmacol Sci. 2003 Mar-Apr;7(2):41-4.

219. Menasche P. Skeletal muscle satellite cell transplantation. Cardiovasc Res. 2003 May 1;58(2):351-7.

220. Gorba T, Allsopp TE. Pharmacological potential of embryonic stem cells. Pharmacological Research. 2003 Apr;47(4):269-78.

221. Schatten G, Smith J, Navara C, Park J-H, Pedersen R. Culture of human embryonic stem cells. Nat Meth. 2005;2(6):455-63.

222. Heng BC, Liu H, Ge Z, Cao T. Mechanical dissociation of human embryonic stem cell colonies by manual scraping after collagenase treatment is much more detrimental to cellular viability than is trypsinization with gentle pipetting. Biotechnology and Applied Biochemistry. 2007 May 1, 2007;047(1):33-7.

223. Martin MJ, Muotri A, Gage F, Varki A. Human embryonic stem cells express an immunogenic nonhuman sialic acid. Nature Medicine. 2005 Feb;11(2):228-32.

224. Alarcon CDH, Pennadam S, Alexander C. Stimuli responsive polymers for biomedical applications. Chemical Society Reviews. 2005 Mar;34(3):276-85.

225. Yamada N, Okano T, Sakai H, Karikusa F, Sawasaki Y, Sakurai Y. Thermoresponsive Polymeric Surfaces - Control of Attachment and Detachment of Cultured-Cells. Makromolekulare Chemie-Rapid Communications. 1990 Nov;11(11):571-6.

226. Okano T, Yamada N, Sakai H, Sakurai Y. A Novel Recovery-System for Cultured-Cells Using Plasma-Treated Polystyrene Dishes Grafted with Poly(N-Isopropylacrylamide). Journal of Biomedical Materials Research. 1993 Oct;27(10):1243-51.

227. Kushida A, Yamato M, Konno C, Kikuchi A, Sakurai Y, Okano T. Decrease in culture temperature releases monolayer endothelial cell sheets together with deposited fibronectin matrix from temperature-responsive culture surfaces. Journal of Biomedical Materials Research. 1999 Jun 15;45(4):355-62.

228. Takezawa T, Mori Y, Yoshizato K. Cell-Culture on a Thermoresponsive Polymer Surface. Bio-Technology. 1990 Sep;8(9):854-6.

229. Cheng XH, Wang YB, Hanein Y, Bohringer KF, Ratner BD. Novel cell patterning using microheater-controlled thermoresponsive plasma films. Journal Of Biomedical Materials Research Part A. 2004 Aug 1;70A(2):159-68.

230. Schmaljohann D, Oswald J, Jorgensen B, Nitschke M, Beyerlein D, Werner C. Thermo-Responsive Pniaam-G-Peg Films for Controlled Cell Detachment. Biomacromolecules. 2003 2003 Nov-Dec;4(6):1733-9.

231. Tsuda Y, Kikuchi A, Yamato M, Sakurai Y, Umezu M, Okano T. Control of Cell Adhesion and Detachment Using Temperature and Thermoresponsive Copolymer Grafted Culture Surfaces. Journal of Biomedical Materials Research Part a. 2004 2004 Apr 1;69A(1):70-8.

232. Liu HC, Ito Y. Cell attachment and detachment on micropattern-immobilized poly(N-isopropylacrylamide) with gelatin. Lab On A Chip. 2002;2(3):175-8.

233. Smith E, Yang J, McGann L, Sebald W, Uludag H. RGD-grafted thermoreversible polymers to facilitate attachment of BMP-2 responsive C2C12 cells. Biomaterials. 2005 Dec;26(35):7329-38.

234. Stile RA, Healy KE. Thermo-Responsive Peptide-Modified Hydrogels for Tissue Regeneration. Biomacromolecules. 2001 2001 Spr;2(1):185-94.

235. Tsuda Y, Shimizu T, Yamato M, Kikuchi A, Sasagawa T, Sekiya S, et al. Cellular control of tissue architectures using a three-dimensional tissue fabrication technique. Biomaterials. 2007;28:4939-46.

236. Kwon OH, Kikuchi A, Yamato M, Okano T. Accelerated Cell Sheet Recovery by Co-Grafting of Peg With Pipaam Onto Porous Cell Culture Membranes. Biomaterials. 2003 2003 Mar;24(7):1223-32.

237. Vihola H, Laukkanen A, Valtola L, Tenhu H, Hirvonen J. Cytotoxicity of thermosensitive polymers poly(N-isopropylacrylamide), poly(N-vinylcaprolactam) and amphiphilically modified poly(N-vinylcaprolactam). Biomaterials. 2005 Jun;26(16):3055-64.

238. Martina K, Vytautas S, Roland W, Walter R. Interplay between Hydrogen Bonding and Macromolecular Architecture Leading to Unusual Phase Behavior in Thermosensitive Microgels13. Angewandte Chemie International Edition. 2008;47(2):338-41.

239. Wischerhoff E, Uhlig K, Lankenau A, Borner HG, Laschewsky A, Duschl C, et al. Controlled cell adhesion on PEG-based switchable surfaces. Angewandte Chemie-International Edition. 2008;47(30):5666-8.

240. Nishida K, Yamato M, Hayashida Y, Watanabe K, Maeda N, Watanabe H, et al. Functional bioengineered corneal epithelial sheet grafts from corneal stem cells expanded ex vivo on a temperature-responsieve cell culture surface. Transplantation. 2004 Feb 15;77(3):379-85.

241. Prime KL, Whitesides GM. Adsorption of Proteins onto Surfaces Containing End-Attached Oligo(Ethylene Oxide) - a Model System Using Self-Assembled Monolayers. Journal of the American Chemical Society. 1993 Nov 17;115(23):10714-21.

242. Zhang M, Desai T, Ferrari M. Proteins and cells on PEG immobilized silicon surfaces. Biomaterials. 1998 May;19(10):953-60.

243. Neil PD, Jeffrey AH. Biological responses to polyethylene oxide modified polyethylene terephthalate surfaces. Journal of Biomedical Materials Research. 1991;25(7):829-43.

244. Hsiue G-H, Lee S-D, Chuen-Thuen Chang P. Platelet adhesion and cellular interaction with poly(ethylene oxide) immobilized onto silicone rubber membrane surfaces. Journal of Biomaterials Science, Polymer Edition. 1996;7:839-55.

245. Ma H, Hyun J, Stiller P, Chilkoti A. 'Non-Fouling' Oligo(ethylene glycol)-Functionalized Polymer Brushes Synthesized by Surface-Initiated Atom Transfer Radical Polymerization. Advanced Materials. 2004;16(4):338-41.

246. Li L, Chen S, Zheng J, Ratner BD, Jiang S. Protein adsorption on oligo(ethylene glycol)-terminated alkanethiolate self-assembled monolayers: The molecular basis for nonfouling behavior. J Phys Chem B. 2005 Feb 24;109(7):2934-41.

247. Feldman K, Hahner G, Spencer ND, Harder P, Grunze M. Probing resistance to protein adsorption of oligo(ethylene glycol)-terminated self-assembled monolayers by scanning force microscopy. Journal of the American Chemical Society. 1999 Nov 3;121(43):10134-41.

248. Andruzzi L, Senaratne W, Hexemer A, Sheets ED, Ilic B, Kramer EJ, et al. Oligo(ethylene glycol) Containing Polymer Brushes as Bioselective Surfaces. Langmuir. 2005;21(6):2495-504.

249. Nath N, Hyun J, Ma H, Chilkoti A. Surface engineering strategies for control of protein and cell interactions. Surface Science. 2004;570(1-2):98-110.

250. Herrwerth S, Eck W, Reinhardt S, Grunze M. Factors that Determine the Protein Resistance of Oligoether Self-Assembled Monolayers â^' Internal Hydrophilicity, Terminal Hydrophilicity, and Lateral Packing Density. Journal of the American Chemical Society. 2003;125(31):9359-66.

251. Wang RLC, Kreuzer HJ, Grunze M. Molecular Conformation and Solvation of Oligo(ethylene glycol)-Terminated Self-Assembled Monolayers and Their Resistance to Protein Adsorption. The Journal of Physical Chemistry B. 1997;101(47):9767-73.

252. Erik HJD, Kenneth MY. Fibronectin, integrins, and growth control. Journal of Cellular Physiology. 2001;189(1):1-13.

253. Hynes RO. Integrins: Versatility, modulation, and signaling in cell adhesion. Cell. 1992;69(1):11-25.

254. Hynes RO. Integrins: Bidirectional, Allosteric Signaling Machines. Cell. 2002;110(6):673-87.

255. Ramirez F, Rifkin DB. Cell signaling events: a view from the matrix. Matrix Biology. 2003;22(2):101-7.

256. Yohei H, Miho Kusuda F, Tetsuji O, Kiyoshi O, Yasufumi M, Yasuaki F, et al. Integrins Regulate Mouse Embryonic Stem Cell Self-Renewal. Stem Cells. 2007;25(12):3005-15.

257. Frederick G, Marian KF. Adsorption characteristics of plasma fibronectin in relationship to biological activity. Journal of Biomedical Materials Research. 1981;15(3):363-81.

258. Grinnell F, Feld MK. Fibronectin adsorption on hydrophilic and hydrophobic surfaces detected by antibody binding and analyzed during cell adhesion in serum-containing medium. Journal of Biological Chemistry. 1982 May 10, 1982;257(9):4888-93.

259. Thom D, Powell AJ, Rees DA. Mechanisms of cellular adhesion. IV. Role of serum glycoproteins in fibroblast spreading on glass. J Cell Sci. 1979 February 1, 1979;35(1):281-305.

260. Grinnell F, Danielli GHBaJF. Cellular Adhesiveness and Extracellular Substrata. International Review of Cytology: Academic Press; 1978. p. 65-144.

261. Humphries MJ, Akiyama SK, Komoriya A, Olden K, Yamada KM. Identification of an alternatively spliced site in human plasma fibronectin that mediates cell type-specific adhesion. J Cell Biol. 1986 December 1, 1986;103(6):2637-47.

262. Guoping C, Yukio I, Yoshihiro I. Effect of protein and cell behavior on pattern-grafted thermoresponsive polymer. Journal of Biomedical Materials Research. 1998;42(1):38-44.

263. Stephen MD, Sharon G-N, Jinny C, Joseph I-E, Peter WZ. Controlled, Scalable Embryonic Stem Cell Differentiation Culture. Stem Cells. 2004;22(3):275-82.

264. Lutz J-F, Weichenhan K, Akdemir O, Hoth A. About the Phase Transitions in Aqueous Solutions of Thermoresponsive Copolymers and Hydrogels Based on 2-(2-methoxyethoxy)ethyl Methacrylate and Oligo(ethylene glycol) Methacrylate. Macromolecules. 2007;40(7):2503-8.

265. Burdon T, Stracey C, Chambers I, Nichols J, Smith A. Suppression of SHP-2 and ERK Signalling Promotes Self-Renewal of Mouse Embryonic Stem Cells. Developmental Biology. 1999;210(1):30-43.

266. Vogel W, Gish GD, Alves F, Pawson T. The Discoidin Domain Receptor Tyrosine Kinases Are Activated by Collagen. Molecular Cell. 1997;1(1):13-23.

267. Tye CE, Hunter GK, Goldberg HA. Identification of the Type I Collagen-binding Domain of Bone Sialoprotein and Characterization of the Mechanism of Interaction. Journal of Biological Chemistry. 2005 April 8, 2005;280(14):13487-92.

268. Elbert DL, Hubbell JA. Conjugate Addition Reactions Combined with Free-Radical Cross-Linking for the Design of Materials for Tissue Engineering. Biomacromolecules. 2001;2(2):430-41.

269. Yoshihiro I, Masako K, Yukio I. Materials for enhancing cell adhesion by immobilization of cell-adhesive peptide. Journal of Biomedical Materials Research. 1991;25(11):1325-37.

270. Boxus T, Touillaux R, Dive G, Marchand-Brynaert J. Synthesis and evaluation of RGD peptidomimetics aimed at surface bioderivatization of polymer substrates. Bioorganic & Medicinal Chemistry. 1998;6(9):1577-95.

271. Neff JA, Caldwell KD, Tresco PA. A novel method for surface modification to promote cell attachment to hydrophobic substrates. Journal of Biomedical Materials Research. 1998;40(4):511-9.

272. Pierschbacher MD, Ruoslahti E. Cell attachment activity of fibronectin can be duplicated by small synthetic fragments of the molecule. Nature. 1984;309(5963):30-3.

273. Yamaoka T, Hotta Y, Kobayashi K, Kimura Y. Synthesis and properties of malic acid-containing functional polymers. International Journal of Biological Macromolecules. 1999;25(1-3):265-71.

274. Carlisle ES, Mariappan MR, Nelson KD, Thomes BE, Timmons RB, Constantinescu A, et al. Enhancing Hepatocyte Adhesion by Pulsed Plasma Deposition and Polyethylene Glycol Coupling. Tissue Engineering. 2000;6(1):45-52.

275. Patel N, Padera R, Sanders GHW, Cannizzaro SM, Davies MC, Langer R, et al. Spatially controlled cell engineering on biodegradable polymer surfaces. FASEB J. 1998 November 1, 1998;12(14):1447-54.

276. KLUIJTMANS SGJMaB, Jan Bastiaan, inventor Recombinant Gelatin Particles for Cell Adhesion. WASHINGTON, DC US 2007.

277. TODA JBBAJJVEY, inventor RGD-Enriched Gelatine-Like Proteins with enhanced cell binding. NEW YORK, NY US

278. Sobral PJA, Menegalli FC, Hubinger MD, Roques MA. Mechanical, water vapor barrier and thermal properties of gelatin based edible films. Food Hydrocolloids. 2001;15(4-6):423-32.

279. Eastoe JE. The amino acid composition of mammalian collagen and gelatin. Biochem J. 1955;61(4):589–600.

280. Nandivada H, Jiang X, Lahann J. Click Chemistry: Versatility and Control in the Hands of Materials Scientists. Advanced Materials. 2007;19(17):2197-208.

281. Hein C, Liu X-M, Wang D. Click Chemistry, A Powerful Tool for Pharmaceutical Sciences. Pharmaceutical Research. 2008;25(10):2216-30.

282. Guido WMV, Harm-Anton K. Peptide/Protein Hybrid Materials: Enhanced Control of Structure and Improved Performance through Conjugation of Biological and Synthetic Polymers. Macromolecular Bioscience. 2004;4(4):383-98.

283. Lee BS, Lee JK, Kim W-J, Jung YH, Sim SJ, Lee J, et al. Surface-Initiated, Atom Transfer Radical Polymerization of Oligo(ethylene glycol) Methyl Ether Methacrylate and Subsequent Click Chemistry for Bioconjugation. Biomacromolecules. 2007;8(2):744-9.

284. Chelsea NS, Kristi SA. The influence of the RGD peptide motif and its contextual presentation in PEG gels on human mesenchymal stem cell viability. Journal of Tissue Engineering and Regenerative Medicine. 2008;2(5):296-304.